SYNTHESIS AND STUDY OF

$\mu(1,n)$ALKANEDIYL BINUCLEAR COMPOUNDS OF IRON

TUNGSTEN AND MANGANESE

by

LOUISE G. SCOTT, B.Sc. (Hons)

Thesis submitted for the Degree of

MASTER OF SCIENCE

Department of Inorganic Chemistry

University of Cape Town

September 1984

ABSTRACT

μ(1,n)Alkanediyl compounds are binuclear metal compounds of general formula $L_xM(CH_2)_nM'L'_y$ ($n \geq 2$) in which the metal centres are bonded to the terminal carbon atoms of an alkyl chain. These compounds could serve as models for surface intermediates in metal-catalysed reactions such as the Fischer-Tropsch reaction and as such their structure, stability and reactivity are of interest.

The new (1,n)alkanediyl compounds $[Cp(CO)_2Fe]_2\{\mu\text{-}(CH_2)_n\}$ (n = 8 - 12), $[Cp(CO)_3W]_2\{\mu\text{-}(CH_2)_n\}$ (n = 3 - 5), $[Cp(CO)_3W\{\mu\text{-}(CH_2)_3\}Fe(CO)_2Cp]$ and $[(CO)_5Mn]_2\{\mu\text{-}(CH_2)_4\}$ have been synthesised. A detailed discussion of the mass spectra of $[Cp(CO)_2Fe]_2\{\mu\text{-}(CH_2)_n\}$ (n = 8 - 12) and the known $[Cp(CO)_2Fe]_2\{\mu\text{-}(CH_2)_n\}$ (n = 3 - 7) is presented and comparisons are made with the mass spectra of $[Cp(CO)_3W]_2\{\mu\text{-}(CH_2)_n\}$ (n = 3 - 5) and $[Cp(CO)_3W\{\mu\text{-}(CH_2)_3\}Fe(CO)_2Cp]$. The thermal analysis of $[Cp(CO)_2Fe]_2\{\mu\text{-}(CH_2)_n\}$ (n = 3 - 12) by Differential Scanning Calorimetry is reported. Conformational polymorphism is proposed for the compounds $[Cp(CO)_2Fe]_2\{\mu\text{-}(CH_2)_n\}$ (n = 4,8) on the basis of the DSC results. Different low-energy conformations of $[Cp(CO)_2Fe]_2\{\mu\text{-}(CH_2)_4\}$ have been identified by computer simulation of the effects of rotation on the potential energy of the molecule.

The thermal decomposition reactions of $[Cp(CO)_2Fe]_2\{\mu\text{-}(CH_2)_n\}$ (n = 3 - 8) and $[Cp(CO)_3W]_2\{\mu\text{-}(CH_2)_n\}$ (n = 3 - 5) have been investigated and mechanisms for these reactions are discussed with reference to the observed organic products.

The reactions of some μ(1,n)alkanediyl diiron and ditungsten compounds with ter iary phosphines have been studied. The main product of these reactions is the diacyl species $[Cp(CO)_x(L)M\{CO(CH_2)_nCO\}M(L)(CO)_xCp]$ (M = Fe,x = 1; M = W, x = 2; L = tertiary phosphine). Attempts to prepare phosphine substituted μ(1,n)alkanediyl compounds by photochemical decarbonylation of $[Cp(CO)(L)Fe\{CO(CH_2)_nCO\}Fe(L)(CO)Cp]$ and photo-induced reaction of $[Cp(CO)_2Fe]_2\{\mu\text{-}(CH_2)_4\}$ with PPh_3 are reported. The thermal decarbonylation of $[Cp(CO)_2(L)W\{CO(CH_2)_nCO\}$-$W(L)(CO)_2Cp]$ (L = PPh_2Me, n = 4,5; L = PPh_3, n = 4) has also been investigated. The reactions of $[Cp(CO)_2Fe]_2\{\mu\text{-}(CH_2)_n\}$ (n = 3,4) with halogen (I_2 and Br_2) are reported. The paramagnetic cationic species $[Cp(CO)_2Fe(CH_2)_4Fe(CO)_2Cp]^{+}[X_2]^{-}$ were isolated from the reactions of $[Cp(CO)_2Fe]_2\{\mu\text{-}(CH_2)_4\}$ with X_2 in addtion to the expected cleavage products. A mechanism involving a one-electron transfer from electrophile to the substrate is proposed to account for the formation of these species.

ACKNOWLEDGEMENTS

My sincere thanks go to -

Professor John R Moss for his dedicated supervision of this project,

CSIR for their financial support,

Dr Graham Jackson for his assistance with the computer studies,

My colleagues in the Department, particularly Liz Sutton, Philip Hall and Gary Watkins for their help and William Hendricks for his maintenance of the Laboratory,

Bridget Williamson and Dr E E Bartell for recording the mass spectra, Dr Mike Brown for carrying out the DSC analysis and Miss D Dawson for her assistance with the thermal decomposition studies,

Mark and Bridget for their friendship and help, particularly with proof reading,

My parents for their continued understanding and encouragement and in particular to my mother for her excellent typing of this thesis.

ABBREVIATIONS

The following abbreviations are used in this project :

Cp :	$(\eta^5\text{-}C_5H_5)$
THF :	tetrahydrofuran
DME :	1,2-dimethoxyethane
hexane :	n-hexane
pentane :	n-pentane
ether :	diethyl ether

CONTENTS

SECTION 1

1. INTRODUCTION

1.1 Definition of μ(1,n)alkanediyl compounds and general motivation for study

μ(1,n)Alkanediyl compounds are binuclear metal compounds of general formula $L_xM\text{-}(CH_2)_n\text{-}M'L'_y$ ($n \geq 2$) in which the metal centres are bonded to the two terminal carbons of an alkyl chain. Two types of μ(1,n)alkanediyl compounds are known, (I) without a metal-metal bond and (II) with a metal-metal bond (Fig. 1.1). Compounds of type (II) are dimetallocycloalkanes.

Fig. 1 Two types of μ(1,n)alkanediyl compounds

The $-(CH_2)_n-$ bridge is the formal extension of a methylene bridge, and μ(1,n)alkanediyl species, like methylene bridged species [1], are of interest as possible models for surface intermediates in various metal-catalysed reactions. In the Fischer-Tropsch reaction, for example, an ethanediyl bridged intermediate 1 has been implicated to account for the formation of ethylene [2]. Such an intermediate could be formed by dimerisation of surface methylene groups [2a] or by reduction of a CH_2CO bridge on the metal surface [2b] (Scheme 1.1).

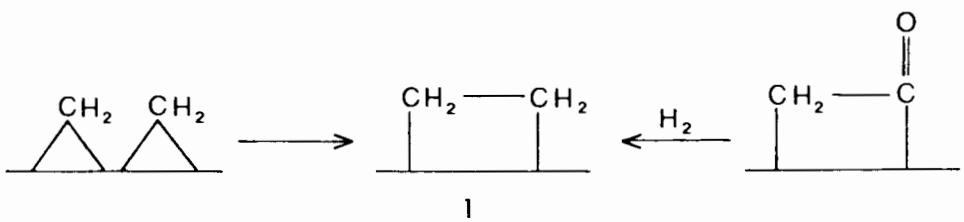

Scheme 1.1

Alkanediyl intermediates could be postulated for other metal-catalysed reactions involving the formation or rearrangement of hydrocarbons, such as the Ziegler-Natta polymerisation of ethylene [3] and platinum-catalysed hydrocarbon rearrangement [4]. Dimetallocycloalkanes have been implicated in several catalytic reactions such as olefin metathesis [5] and alkene dimerisation [6]. An example is the proposed formation of a ditungsten-cyclopentane intermediate 2 in the photo induced metathesis of *cis*- and *trans*-RCH=CHMe catalysed by $W(CO)_6/CCl_4$ [5].

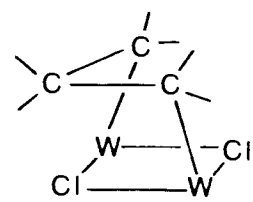

2

Discrete μ(1,n)alkanediyl bridged complexes could serve as useful models for such intermediates and as such their structure, stability and reactivity are of interest.

1.2 Review of known transition metal μ(1,n)alkanediyl compounds

The preparative routes to, and properties of, transition metal μ(1,n)alkanediyl compounds of both types are reviewed in this section according to the transition metal groups in the periodic table.

1.2.1 Titanium group

Kaminsky and Sinn [7] have isolated the type(I) μ(1,2)ethanediyl di-zirconium compound 4 from the reaction of $[Cp_2ZrCl_2]$ and triethylalane. The initial product is $[Cp_2ClZrEt]$ 3 which combines by intermolecular β-hydrogen

transfer and elimination of ethane to form 4 [8].

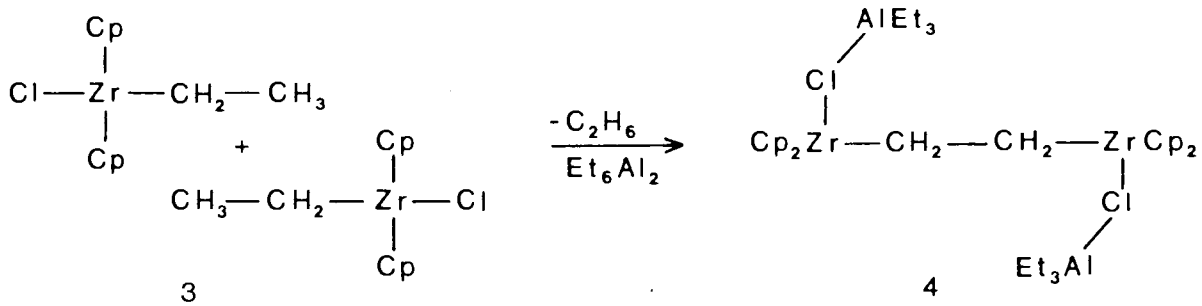

(1)

The similar compound $[Et_2Al\text{-}(\mu\text{-}Cl)_2\text{-}ZrCp_2]_2\{\mu\text{-}(CH_2)_2\}$ 5 is formed, in a parallel reaction, from 3 , while a third ethanediyl bridged species $[Cp_2ZrCl]_2\{\mu\text{-}(CH_2)_2\}$ 6 is obtained from 4 by treatment with THF. 3 also reacts with triethylalane to form a mixed metal compound $[Cp_2ClZr(CH_2CH_2)AlEt_2]$ 7 the acidic β-hydrogen cleaving an Al-Et bond to eliminate ethane [7].

The (1,2)ethanediyl bridged species are observed intermediates in a side reaction during homogeneous Ziegler-Natta polymerisation of α-olefins catalysed by bis (cyclopentadienyl) zirconium(IV) compounds and are themselves of interest as potential homogeneous catalysts for this reaction [3]. Compound 4 reacts with α-olefins and 1,3-dienes on addition of excess trimethyl- or triethylalane, especially in the presence of water. Dechlorination occurs, presumably with the formation of aluminoxanes to give an extremely active halogen-free homogeneous catalyst for polymerisation of α-olefins particularly ethylene [9].

The structural study of compound 4 [9] confirms that there is a $-(CH_2)_2-$ bridge between non-bonded zirconium atoms. The C-C bond distance in the bridge is close to that in ethane (1.53Å). An anomolous feature of this structure is the small Zr-C-C bond angle (76°). Other

structurally characterised (1,n)alkanediyl bridged compounds show much larger M-C-C bond angles For example, the Re-C-C angle in $[(CO)_5Re]_2\{\mu\text{-}(CH_2)_2\}$ is 121° [20]. The Zr-β-carbon distance in 4 is only slightly greater than the Zr-α-carbon bond distance. This suggests that the bonding of the $-(CH_2)_2-$ bridge is intermediate between a σ and a $\eta^2\text{-}(C_2H_4)$ type interaction (Fig. 1.2).

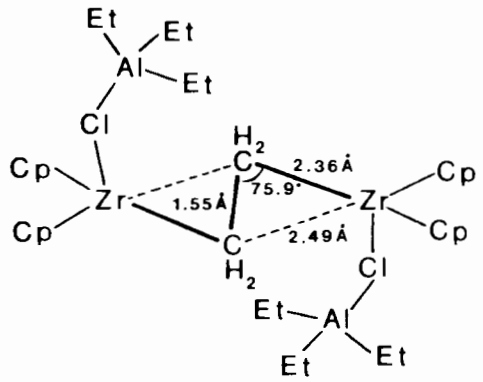

Fig. 1.2 Molecular structure of $[Et_3Al(\mu\text{-}Cl)ZrCp]_2\{\mu\text{-}(CH_2)_2\}$

Despite predictions of inherent instability for a (1,2)ethanediyl bridged species [10], the dizirconium compounds 4-6 are thermally stable, up to 96°, 110° and 180°C respectively [7]. This is in contrast to the ethyl compound [CpClZrEt] which decomposes above 0°C via β-hydrogen elimination [11]. Considering the observed proximity of the β-carbons to the metal atoms in 4 , the resistance to decomposition via β-elimination is surprising. This could be accounted for, in part, by steric factors; steric crowding in the transition state for β-elimination 8 would disfavour decomposition by this route:

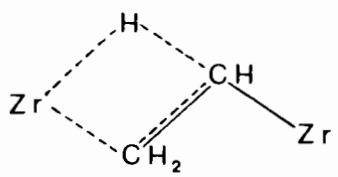

This steric effect has been observed for certain zirconium alkyl compounds; for example the bulky $[ZrCp_2Bu^n\{CH(SiMe_3)_2\}]$ is reluctant to undergo β-elimination, yielding n-butane on thermolysis at 150°C whereas $[ZrCp_2Bu^n{}_2]$ decomposes at room temperature with loss of 1-butene [12]. These $-(CH_2)_2-$ bridged compounds decompose on addition of HCl with elimination of the dimethylene bridge as ethane [7].

The analogous titanium ethanediyl bridged compounds $[Et_3Al(\mu\text{-}Cl)TiCp_2]_2\{\mu\text{-}(CH_2)_2\}$ 9 and $[Cp_2ClTi(CH_2)_2AlEt_3]$ have been detected spectroscopically during the reaction of $[Cp_2TiCl_2]$ with $AlEt_3$ [3]. However these titanium (IV) compounds could not be isolated due to the ease of reduction of titanium (IV) to the trivalent state:

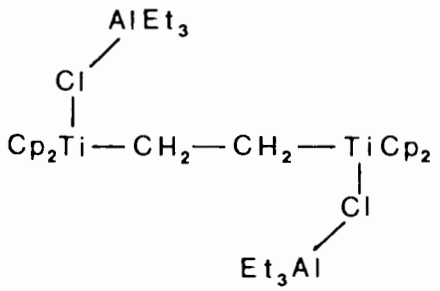

$$\longrightarrow \quad 2\ Cp_2TiCl + C_2H_4 + 2\ AlEt_3 \qquad (2)$$

9

1.2.2 Chromium Group

Beck and Olgemöller [13.14] have prepared (1,2)ethanediyl bridged complexes of molybdenum and tungsten 11-13 by nucleophilic addition of the metal anion to the ethylene complex cation 10:

$$[Cp(CO)_3M(C_2H_4)]^+ + [Cp(CO)_3M']^- \longrightarrow [Cp(CO)_3M(CH_2)_2M'(CO)_3Cp] \qquad (3)$$

10

11 M = M' = Mo

12 M = M' = W

13 M = Mo , M' = W

These compounds have low solubility and are readily isolated from solution at low temperatures. They are, however, unstable in solution, decomposing spontaneously at ambient temperatures. The mixed metal compound 13 decomposes to the (1,2)ethanediyl tungsten compound 12 and $[CpMo(CO)_3]_2$ with evolution of ethylene. Compound 11 is unstable even in the solid state above -20°C while 12 is stable at 20°C [14]. The higher stability of the tungsten compound is attributed [14] to the greater strength of the tungsten-carbon bond than the Mo-C bond [15]. This trend is also observed in the mixed metal compounds $[Cp(CO)_3M(CH_2CH_2)Re(CO)_5]$ (M = Mo,W) [14]. $[Cp(CO)_3Mo(CH_2CH_2)Re(CO)_5]$ decomposes above -15°C while $[Cp(CO)_3W(CH_2CH_2)Re(CO)_5]$ is stable at 20°C. The rhenium-carbon σ-bond is known to be particularly strong [16]; the difference in the stability of these compounds can thus be attributed to the differing strengths of the Mo-C and W-C bonds.

The triphenyl phosphine substituted tungsten compound $[CpW(CO)_2(PPh_3)]_2\{\mu\text{-}(CH_2)_2\}$ is produced in the reaction of $[CpW(CO)_2)PPh_3)]$ with $[CpW(CO)_2(PPh_3)(C_2H_4)]^+$ [13]. The infrared and ^1H NMR data for this compound indicate a *trans* arrangement of CO groups in the tetragonal pyramidal configuration of ligands around the metal atom (Cp at the apical position) (Fig. 1.3) [17]. This compound is extremely light sensitive and decomposes rapidly with evolution of ethylene in solution at room temperature.

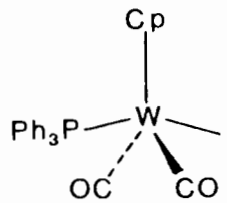

Fig. 1.3 Configuration of ligands at the metal centres in $[Cp(CO)_2(PPh_3)W]_2\{\mu\text{-}(CH_2)_2\}$

Longer chain (1,n)alkanediyl bridged molybdenum and tungsten compounds are also known. The stable compound $[Cp(CO)_3Mo]_2\{\mu\text{-}(CH_2)_4\}$ 14 (decomposition above 150°C) is obtained from the reaction of $[Cp(CO)_3Mo]^-$ with $I(CH_2)_4I$ [18]. The crystallographic study of this compound [19] shows that it has a structure similar to that of the butanediyl bridged diiron compound (see Section 1.4) having a *trans* conformation with approximate inversion symmetry.

The reaction of $[Cp(CO)_3Mo]^-$ with $I(CH_2)_3I$ does not give the corresponding propanediyl bridged compound. Only one halide atom is replaced giving $[Cp(CO)_3Mo\{(CH_2)_3I\}]$ which reacts further, on heating, to give the 2-oxacyclopentylidene complex 15 [18].

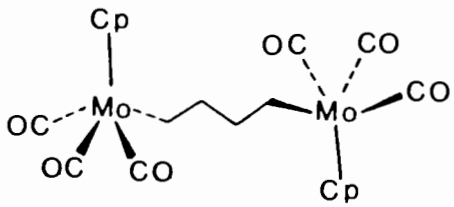

14

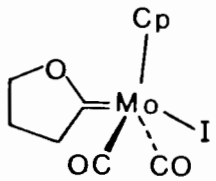

15

The reactions of $[Cp(CO)_3Mo]^-$ with $Br(CH_2)_nBr$ (n = 3,4) also produce the monohaloalkyl compounds $[Cp(CO)_3Mo\{(CH_2)_nBr\}]$ (n = 3,4) [21]. $[Cp(CO)_3Mo\{(CH_2)_3Br\}]$ does not give the bromo analogue of 15 on heating but reaction with I^- yields 15 [18]. A 2-oxacyclopentylidene is also produced on reaction of $[Cp(CO)_3Mo\{(CH_2)_3Br\}]$ with the anions CN^- and SPH^- or PPh_3 [20].

Winter *et al.* have recently reported the isolation of a second product of the reaction of $[Cp(CO)_3Mo]^-$ with $Br(CH_2)_3Br$, the unstable dimolybdenum carbene species 16 [19]. The reaction of $[Cp(CO)_3Mo\{(CH_2)_3Br\}]$ with

$[Cp(CO)_3W]^-$ produces the analogous mixed metal compound $[Cp(CO)_3MoW(\overline{COCH_2CH_2CH_2})(CO)_2Cp]$

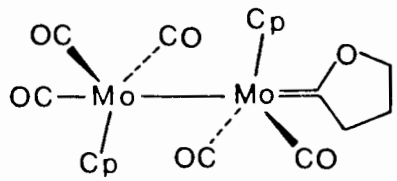

16

King and Bisnette [22] have isolated the perfluoro (1,3)propanediyl bridged species $[Cp(CO)_3Mo]_2\{\mu\text{-}(CF_2)_3\}$ by thermolysis of $[Cp(CO)_3Mo\{CO(CF_2)_3CO\}Mo(CO)_3Cp]$. This diacyl compound is formed in the reaction of $[CpMo(CO)_3]^-$ with $ClCO(CF_2)_3COCl$.

$[CpMo(CO)_3]_2\{\mu\text{-}(CH_2)_{10}\}$ has been reported [23], as the product of the reaction of $[CpMo(CO)_3]^-$ with $[CpMo(CO)_3\{(CH_2)_{10}X\}]$ (X = halogen).

The mixed metal compound $[Cp(CO)_3Mo\{\mu\text{-}(CH_2)_3\}Fe(CO)_2Cp]$ is formed on addition of $[CpMo(CO)_3]^-$ to $[CpFe(CO)_2\{(CH_2)_3Br\}]$ [24]. However in the reaction of $[CpMo(CO)_3\{(CH_2)_nBr\}]$ (n = 3,4) with $[CpFe(CO)_2]$ both the bromine atom and the $CpMo(CO)_3$ group are replaced by $[CpFe(CO)_2]$ to give $[CpFe(CO)_2]_2\{\mu\text{-}(CH_2)_n\}$ (n = 3,4) [21].

No polymethylene bridged chromium compounds have been prepared although compounds with unsaturated hydrocarbon bridges between chromium atoms are known, e.g. $[(CpCr)_2(\mu\text{-}C_8H_8)]$ 17 [25].

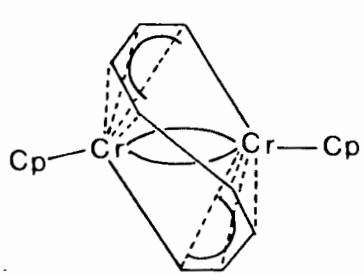

17

1.2.3 Manganese Group

The reaction of $[Mn(CO)_5]^-$ with 1,3-dibromopropane or $ClCO(CH_2)_3Cl$ yields a yellow crystalline compound which was originally thought [26] to be the μ(1,3)-propanediyl species, $[Mn(CO)_5]_2\{\mu\text{-}(CH_2)_3\}$. To explain the ^1H NMR spectrum of this compound which shows three CH_2 proton signals, the unusual structure 18 with manganese-hydrogen bonding was proposed [26]. Casey [27] subsequently showed by means of deuterium labelling and exchange experiments that this compound is in fact the cyclic carbene species 19 .

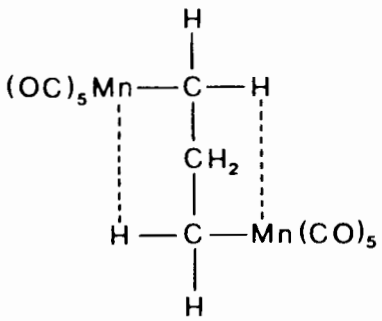

18

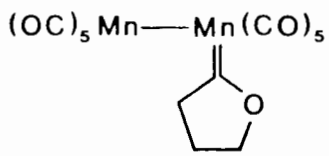

19

From observations made by King [26] it appears that the reaction of $[Mn(CO)_5]^-$ with 1,4-dibromobutane yields the analogous six membered cyclic carbene species, and possibly some of the $-(CH_2)_4-$ bridged compound. These products could not be separated from $Mn_2(CO)_{10}$ also produced in the reaction.

The only alkanediyl bridged manganese compound isolated is the perfluoro propanediyl bridged derivative $[(CO)_5Mn]_2\{\mu\text{-}(CF_2)_3\}$ [26]. This is readily obtained by thermal decarbonylation of the perfluoroacyl compound

$[(CO)_5Mn\{CO(CF_2)_3OC\}Mn(CO)_5]$ which is produced in the reaction of $[Mn(CO)_5]^-$ with perfluoroglutaryl dichloride. The ^{19}F NMR spectrum of this compound exhibits two resonances in a 2:1 ratio, as expected, for the perfluoroalkyl bridge.

The attempt [21] to prepare a mixed metal manganese compound by addition of $[Mn(CO)_5]^-$ to $[CpMo(CO)_3\{(CH_2)_3Br\}]$ leads only to the cyclic carbene compound 19 .

The only other alkanediyl bridged metal compound of this group known is the $\mu(1,2)$-ethanediyl rhenium species $[(CO)_5Re(CH_2CH_2)Re(CO)_5]$ 21 [13] . This has been prepared by two routes: (i) addition of two equivalents of $[Re(CO)_5]^-$ to $[Cp(CO)_3M(C_2H_4)]^+$ (M = Mo or W) [13], and (ii) reaction of $[Re(CO)_5]^-$ with $[(CO)_5Re(C_2H_4)]^+$ [28] (Scheme 1.2).

i) $[Cp(CO)_3M(C_2H_4)]^+ + [Re(CO)_5]^- \longrightarrow [Cp(CO)_3M(CH_2CH_2)Re(CO)_5]$

M = Mo 20b M = W

$\downarrow [Re(CO)_5]^-$

ii) $[(CO)_5Re(C_2H_4)]^+ + [Re(CO)_5]^- \longrightarrow [(CO)_5Re]_2\{\mu\text{-}(CH_2)_2\}$

21

Scheme 1.2

The mixed metal intermediates 20a and 20b have been isolated at low temperature.

$[(CO)_5Re]_2\{\mu\text{-}(CH_2)_2\}$ is considerably more stable than the $\mu(1,2)$-ethanediyl molybdenum and tungsten compounds discussed previously; it is stable in solution at 20°C and in the solid state decomposes with elimination

of ethylene at 138°C [14]. This is reasonable since rhenium alkyls are known to be particularly stable [16].

In compound 21 , the $Re(CO)_5$ groups are *trans* with respect to the C-C bond of the $-(CH_2)_2-$ bridge with Re -C-C angles of 121°. The three equatorial carbonyl ligands on each Re atom are approximately in the plane of the bridge carbons. The C-C bond of the bridge is considerably shorter than that in ethane (1.53 Å) (Fig.1.4) [14].

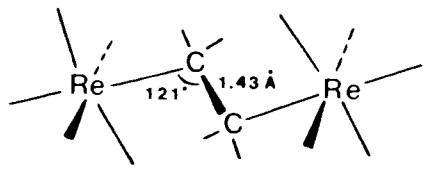

Fig. 1.4 Structure of $[(CO)_5Re]_2\{\mu-(CH_2)_2\}$

1.2.4 Iron Group

The compounds $[Cp(CO)_2Fe]_2\{\mu-(CH_2)_n\}$ (n = 3-6), prepared by King [28] from $[Cp(CO)_2Fe]^-$ and $Br(CH_2)_nBr$, were the first alkanediyl bridged species of type (I) known. These compounds have also been synthesised by other routes. For example the addition of $[Cp(CO)_2Fe]^-$ to the monohalo-alkyl compounds $[Cp(CO)_3M\{(CH_2)_nBr\}]$ (M = Mo or W; n = 3,4) [21] or $[Cp(CO)_2Fe\{(CH_2)_nBr\}]$ (n = 3-5) [24] and photochemical decarbonylation of the diacyl species $[Cp(CO)_2Fe\{CO(CH_2)_4CO\}Fe(CO)_2Cp]$ to give $[Cp(CO)_2Fe]_2\{\mu-(CH_2)_4\}$ [30].

The structural study of the propanediyl and butanediyl bridged compounds [31] confirms that the Fe atoms are linked by a $-(CH_2)_n-$ chain with the carbons of the α-methylene groups σ-bonded to the iron atoms ($Fe-CH_2$ 2.08 Å)

as postulated by King [29]. A constant C-C bond distance of 1.55 Å and C-C-C bond angle of 111° are observed in the alkanediyl bridges (Fig. 1.5).

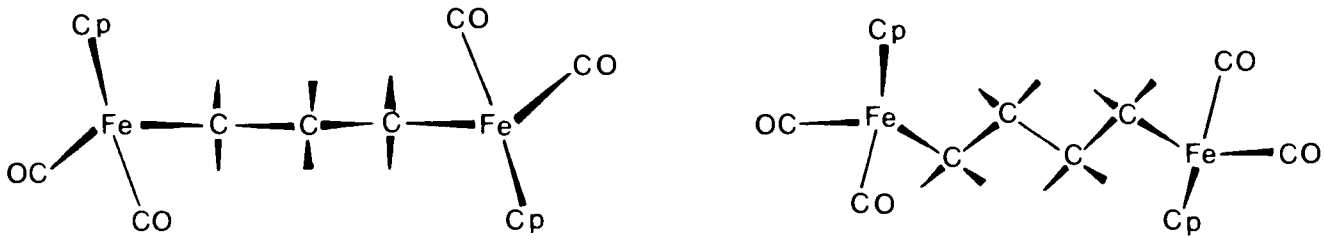

Fig. 1.5 Structures of $[Cp(CO)_2Fe]_2\{\mu\text{-}(CH_2)_3\}$ (left) and $[Cp(CO)_2Fe]_2\{\mu\text{-}(CH_2)_4\}$ (right)

^1H NMR (270 MHz) and $^{13}C\{^1H\}$ NMR spectra are consistent with the crystallographic results each showing two resonances for the methylene groups in the alkanediyl bridges [31].

Attempts to prepare the ethanediyl bridged compound have failed [21,30]. The only known two-carbon bridged iron compounds is the perfluoro-ethanediyl bridged species 22 , isolated from the photo-induced reaction of C_2F_4 with $[(CO)_3Fe]_2\{(\mu\text{-}SCH_3)_2\}$ [32].

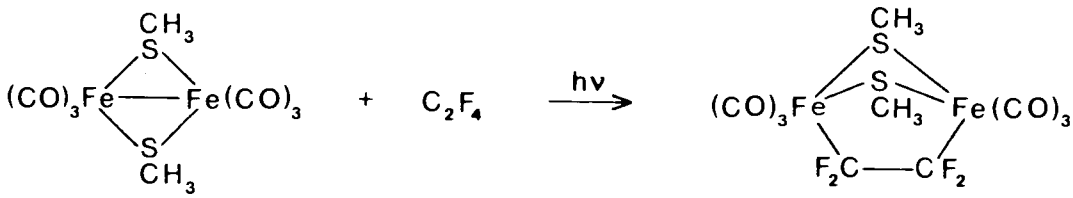

(4)

22

In this compound the iron atoms are held in a *cis* arrangement with respect to the C-C bond in the C_2F_4 bridge by the bridging methylthiolato groups. The C_2F_4 group bridges the non-bonded iron atoms through two σ C-Fe bonds

(2.02 Å) with the C-C bond parallel to the Fe-Fe axis. The trimethylphosphine substituted compound $[(CO)_2(PMe_3)Fe]_2\{\mu(CF_2)_2\}\{(\mu\text{-}SCH_3)_2\}$ has also been isolated by addition of PMe_3 to 21 in solution. These C_2F_4 bridged compounds are stable in solid form but rearrange readily in solution to the $>CFCF_3$ carbene bridged species [33].

The alkanediyl bridged iron compounds, $[Cp(CO)_2Fe]_2\{\mu\text{-}(CH_2)_n\}$ ($n = 3\text{-}12$) undergo various reactions, wellknown for mononuclear alkyl compounds. The thermally-induced reaction with CO leads to effective CO insertion into the Fe-C bonds to form the diacyl species 23; [30]

$$[Cp(CO)_2Fe]_2\{\mu\text{-}(CH_2)_n\} \xrightarrow[\Delta,\,THF]{CO\ pressure} [Cp(CO)_2Fe\overset{O}{\overset{\|}{C}}(CH_2)_n\overset{O}{\overset{\|}{C}}Fe(CO)_2Cp] \qquad (5)$$

($n = 3,4$) — 23

The CO insertion is reversible; photolysis of the diacyl species $[Cp(CO)_2Fe\{CO(CH_2)_4CO\}Fe(CO)_2Cp]$ for example produces $[Cp(CO)_2Fe]_2\{\mu\text{-}(CH_2)_4\}$ in 40 % yield [30].

As observed with mononuclear iron alkyl compounds [34], β-hydride abstraction from the hydrocarbon chain in $[Cp(CO)_2Fe]_2\{\mu\text{-}(CH_2)_n\}$ ($n = 4\text{-}6$) leads to formation of a cationic olefin species [35]. These cationic species are assigned structure 24 in which one iron atom is π-bonded and the other σ-bonded to the alkenyl chain, on the basis of ^1H NMR data:

$$[Cp(CO)_2Fe]_2\{\mu\text{-}(CH_2)_n\} + Ph_3C^+PF_6^- \qquad (6)$$

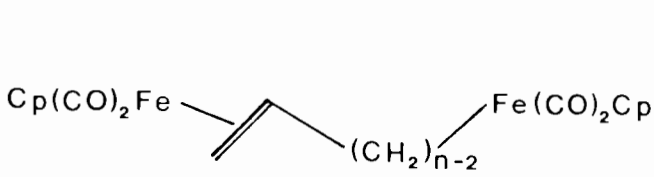

24

The analogous reaction of $[Cp(CO)_2Fe]_2\{\mu\text{-}(CH_2)_3\}$ produces a symmetrical cationic complex $[Cp(CO)_2Fe(CH_2CHCH_2)Fe(CO)_2Cp]^+$ [21,36]. This was first thought [21] to be a carbonium iron complex 26 which exists in dynamic equilibrium with the stable olefinic complexes 25 and 27 (Scheme 1.3).

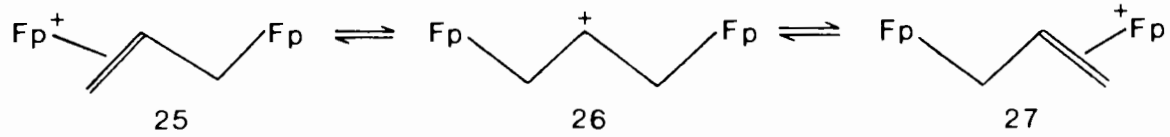

25 26 27

(Fp = $Cp(CO)_2Fe$)

Scheme 1.3

Subsequent dynamic ^1H NMR studies have revealed that the compound is fluxional rather than in dynamic equilibrium [37]. The crystallographic study of the cation [36] suggests that the positive charge is isolated on the β-carbon and is stabilised by weak Fe-CH interactions. The cation is approximately symmetric with Fe-CH separations of 2.59 and 2.72 Å, and $Fe\text{-}CH_2\text{-}CH$ bond angles of 91° and 98° respectively (Fig. 1.6). The fluxional behaviour is attributed to the restricted rotation about the $CH_2\text{-}CH$ bonds in solution [36,38].

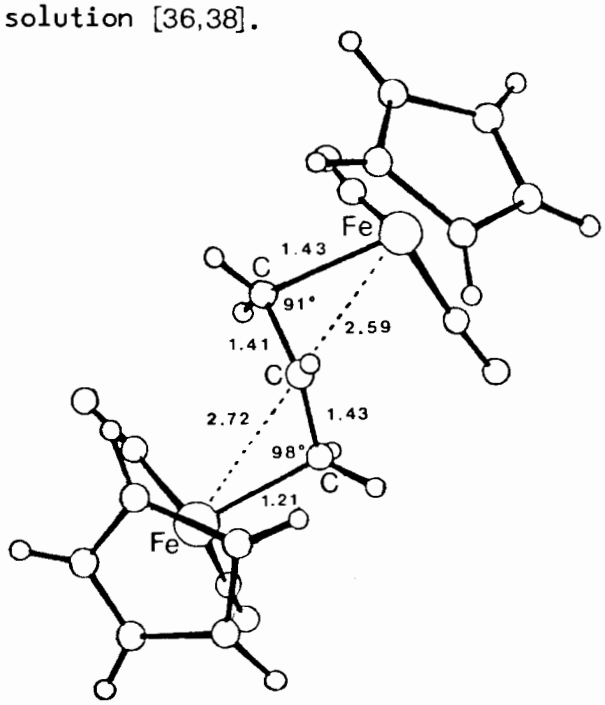

Fig. 1.6 Molecular structure of the cation $[Cp(CO)_2Fe(CH_2CHCH_2)Fe(CO)_2Cp]^+$

Several workers have studied the thermal and photochemical decomposition of $[Cp(CO)_2Fe]_2\{\mu\text{-}(CH_2)_n\}$ (n = 3-5) in solution and in the solid state [30,39,40,41]. The decomposition gives $[Cp(CO)_2Fe]_2$ with loss of the alkanediyl bridge as C_n alkane or alkene. For example, thermolysis and photolysis of $[Cp(CO)_2Fe]_2\{\mu\text{-}(CH_2)_3\}$ yields cyclopropane and propane [30,40,41] and $[Cp(CO)_2Fe]_2\{\mu\text{-}(CH_2)_4\}$ evolves mainly butenes on decomposition [41]. A mechanism involving β-hydride elimination or reductive elimination from a dimetallocyclic intermediate 28 has been proposed to account for the decomposition products of $[Cp(CO)_2Fe]_2\{\mu\text{-}(CH_2)_n\}$ (n = 3,4) [30,41].

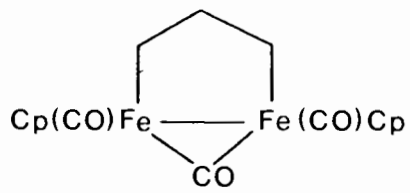

28

Knox *et al.*[40,41] have also studied the thermal decomposition of the analogous ruthenium compounds $[Cp(CO)_2Ru]_2\{\mu\text{-}(CH_2)_n\}$ (n = 3,4) and the mixed metal compound $[Cp(CO)_2Fe(CH_2)_3Ru(CO)_2Cp]$. These compounds are prepared by addition of $[CpRu(CO)_2]^-$ to $(X = I, Br)$ [40,41,42] and $[Cp(CO)_2Fe\{(CH_2)_3I\}]$ respectively. Comparison of the decompositions of the propanediyl bridge iron and ruthenium compounds reveals that the nature of the metal affects the ratio of the organic decomposition products, propene and cyclopropane. The mixed metal compound shows a product ratio intermediate between those of $[Cp(CO)_2Fe]_2\text{-}\{\mu\text{-}(CH_2)_3\}$ and $[Cp(CO)_2Ru]_2\{\mu\text{-}(CH_2)_3\}$ as would be expected. Wreford *et al.* [42] have observed the production of $Cp(CO)_2RuH$ and $Cp(CO)_2Ru(\eta^2\text{-}C_3H_5)$ in equimolar ratio in photolysis of

$[Cp(CO)_2Ru]_2\{\mu\text{-}(CH_2)_3\}$. This clearly provides evidence for the role of β-hydride elimination in the decomposition of this μ(1,3) propanediyl species.

Wreford *et al.* have also synthesised the (1,2)ethanediyl bridged ruthenium compound from 1,2-dichloroethane and $[Cp(CO)_2Ru]^-$. Thermolysis and photolysis of $[Cp(CO)_2Ru]_2\{\mu\text{-}(CH_2)_2\}$ produces ethylene [42].

A mechanism involving β-hydride elimination from a dimetallocycle has also been postulated to account for the formation of propene in the reaction of the methylene bridged iron compounds $[(CO)_3Fe]_2(\mu\text{-}CO)_2(\mu\text{-}CH_2)$ and $[Cp(CO)Fe]_2(\mu\text{-}CO)(\mu\text{-}CH_2)$ with ethylene [33]. (Scheme 1.4).

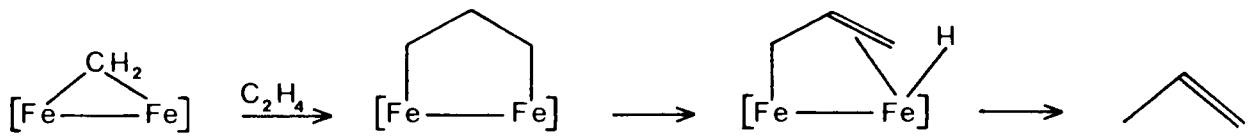

$[Fe—Fe] = [Cp(CO)Fe]_2(\mu\text{-}CO)$ or $[(CO)_3Fe]_2(\mu\text{-}CO)_2$

Scheme 1.4

The reaction of $[Fe_2(CO)_8]^{2-}$ with 1,3-diiodopropane also produces propane presumably via formation of a diferra-cyclopentane intermediate. The recent isolation [43] of the diosmacyclopentane 29 from the analogous reactions of $[(CO)_4Os]_2\{\mu\text{-}(CH_2)\}$ and $[Os_2(CO)_8]^{2-}$ provides direct evidence in support of this mechanism.

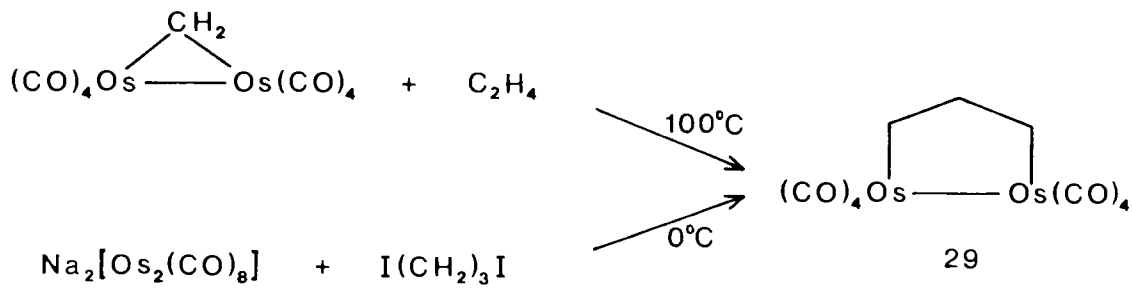

(7)

$Na_2[Os_2(CO)_8]$ + $I(CH_2)_3I$ (8)

Reaction (7) is reversible; heating 29 in toluene solution to 130°C produces 30 and a mixture of organic products.

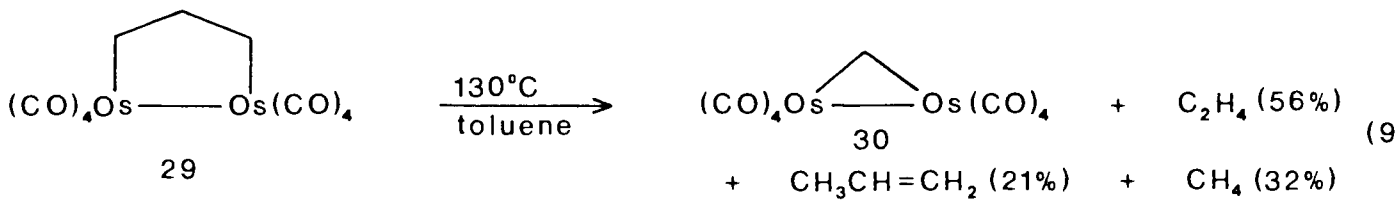

29 30 (9)

The diosmacyclobutane 31 was also prepared from the reaction of $[Os_2(CO)_8]^{2-}$ and $TsO(CH_2)_2OTs$:

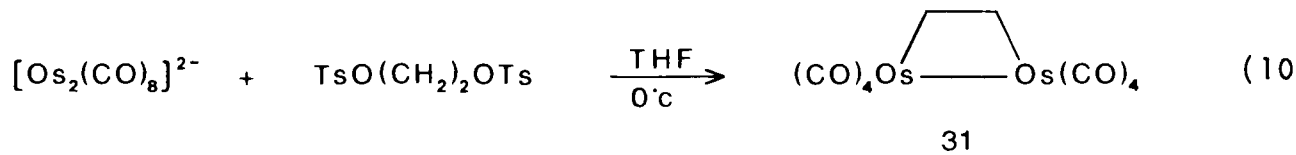

31 (10)

The crystallographic study of 31 reveals that the cyclobutane ring is bent and the Os-C-C angles slightly compressed (105°) so that the $Os(CO)_4$ units are twisted out of the unfavourable eclipsed arrangement (by 27°). The $-(CH_2)_2-$ bridge is σ-bonded to the Os atoms (Os-C 2.22 Å) and the C-C bond in the bridge is the length of a normal single bond (Fig.1.7)

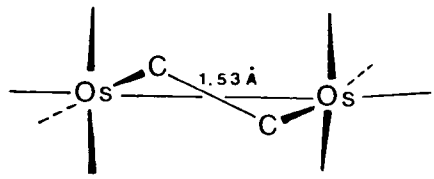

Fig.1.7. Molecular structure of compound 31 showing the bent diosmacyclobutane ring. [43]

The substituted diosmacyclobutane 32 has also been reported recently [44] as a product of the photochemical reaction of $Os_3(CO)_{12}$ with methylacrylate.

$$Os_3(CO)_{12} + CH_2CHCO_2CH_3 \xrightarrow{h\nu} (CO)_4Os(CH_2CHCO_2CH_3) + \text{32} \qquad (11)$$

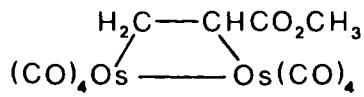

32

The structure of 32 closely resembles that of 31 . The four membered ring is also puckered and the twist angle about the Os-Os bond is similar to that in 31 (21°).

1.2.5 Cobalt Group

The first type (II) (1,n)alkanediyl bridged compound (with a metal-metal bond) reported was the five-membered ring metallocycle containing two cobalt atoms 33 , which is obtained by dialkylation of $[(CpCo)_2(\mu\text{-}CO)_2]^-$ with 1,3-diiodopropane [45].

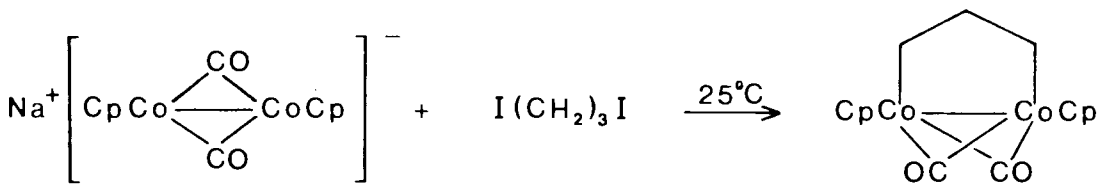

$$+ \quad I(CH_2)_3I \xrightarrow{25°C} \qquad (12)$$

33

It is not possible to isolate 33 from the reaction of the methylene bridged dimer $[Cp(CO)Co]_2(\mu\text{-}CH_2)$ with C_2H_4 although a coordinatively

unsaturated dimetallocyclopentane intermediate 34 has been implicated to explain the formation of propene in this reaction [46].

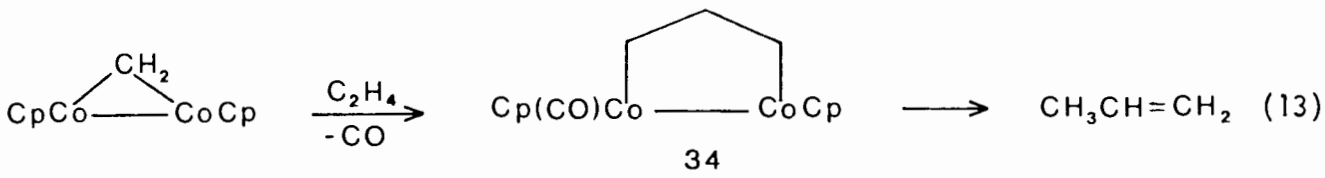

Compound 33 is considerably more stable than acylic dialkyl cobalt species; the dimethyl compound $[CpCoMe]_2(\mu\text{-}CO)_2$ for example, decomposes in solution at room temperature, whereas 33 only undergoes slow thermolysis in benzene at 100°C. Such resistance to decomposition by β-elimination has also been observed for mononuclear five-membered metallocycles [33]. The decomposition of 33 in solution produces propene (73%), cyclopropane (18%) and propane (1%) with $CpCo(CO)_2$ and $Cp_4Co_4(CO)_2$ as the main organometallic products [46]. Labelling experiments indicate that the decomposition process is predominantly intramolecular. In the presence of I_2, reductive elimination of cyclopropane is favoured and decomposition produces mainly cyclopropane (71%), propene (9%) and the diiodide $[Cp(CO)CoI_2]$ [45] (Scheme 1.5).

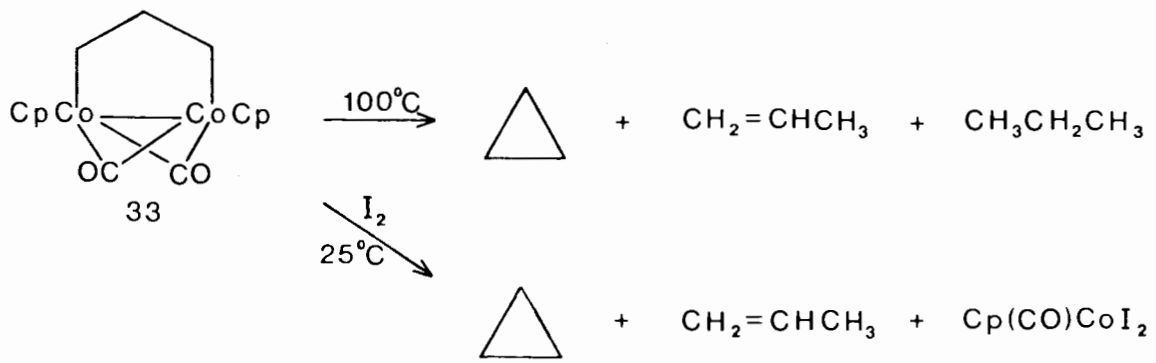

Scheme 1.5

Theopold and Bergman [48] have investigated the reactionsof the metallocycle 33 with CO and tertiary phosphines. At high concentrations of ligand, the reaction occurs rapidly at 56°C producing the mononuclear metallocycle 35 and Cp(CO)CoL. Lowering the ligand concentration causes a decrease in the reaction rate and increasing amounts of cyclopropane and propane are produced (Scheme 1.6)

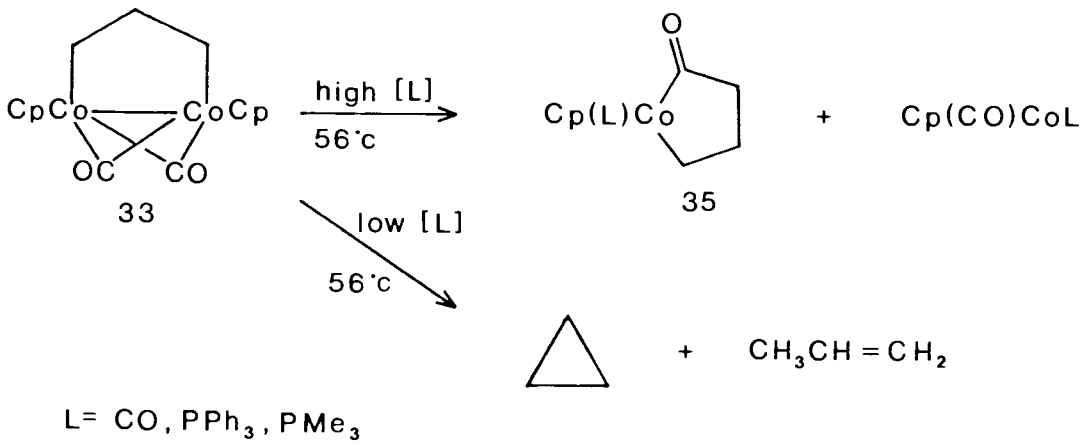

Scheme 1.6

To explain these observations, a mechanism was postulated [48] in which a ligand independent route to cyclopropane competes with ligand attack on a metallocyclobutane intermediate 36 to form cobalt cyclopentanone 35 (Scheme 1.7)

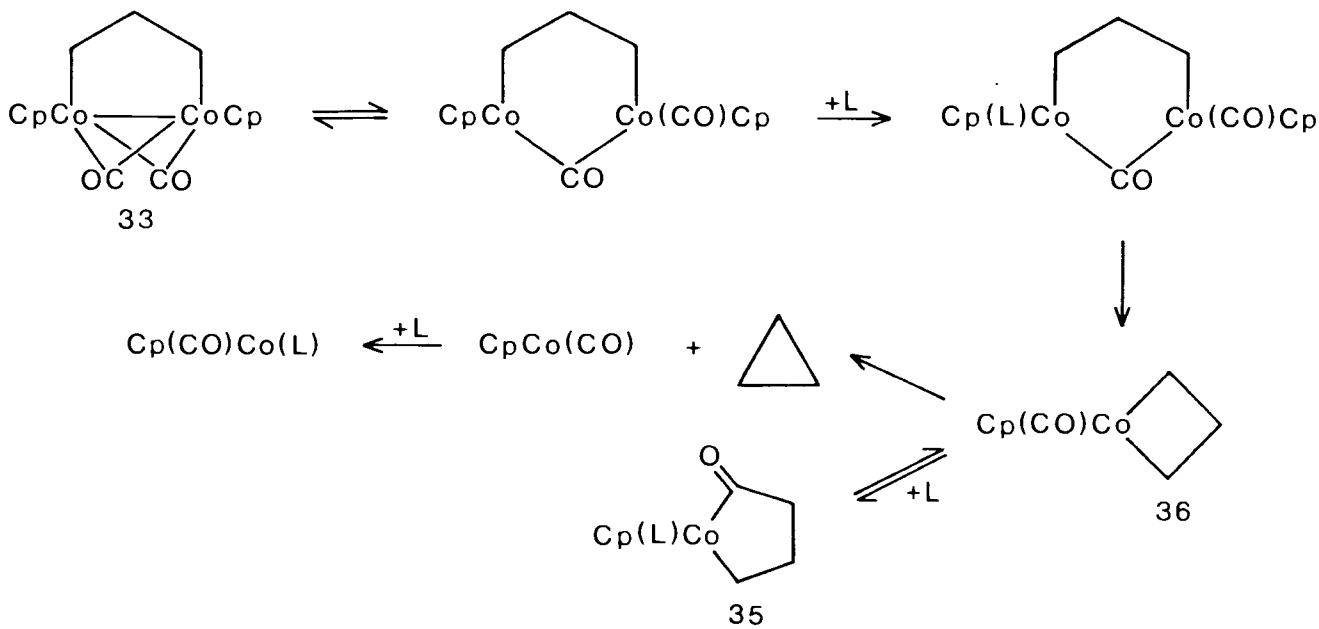

Scheme 1.7

Parallel reactions involving the migration of an alkyl group from one metal to the other are known for dialkyl dicobalt systems e.g. the generation of acetone from $[(CpCoMe)_2\{\mu\text{-}(CO)_2\}]$ via a mononuclear dimethyl cobalt intermediate [49]. Reactions of both systems lead to the formation of new carbon-carbon bonds. The structure of 33 has been reported recently (Fig. 1.8) [48]. The two Co-C bond lengths and Co-Co-C bond angles for the propanediyl bridge are the same (Co-C 2.04 Å, Co-Co-C 94.5°). However the bridge is not symmetrical; the C_1-C_2 bond is longer than the C_2-C_3 bond and the Co-C_1-C_2 angle greater than the Co-C_3-C_2 angle. The dihedral angle for the five membered ring Co-C_1-C_2-C_3 is 32.9°. The CO ligands are bent slightly towards the propanediyl bridge.

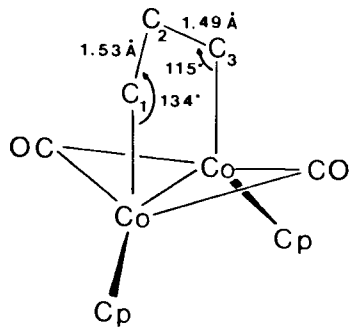

Fig. 1.8 Molecular structure of compound 33

Theopold and Bergman also report [48] the synthesis of the six-membered metallocycle 37 by reaction of $I(CH_2)_4I$ with $[(CpCo)_2(\mu\text{-}CO)_2]^-$. This compound is considerably less stable than 33 , decomposing rapidly at room temperature in solution. In the solid state 37 decomposes above 100°C whereas 33 is stable up to 170°C. Treatment of $[(CpCo)_2(\mu\text{-}CO)_2]^-$ with 1,2-diiodoethane does not yield the four-membered metallocycle 38 .

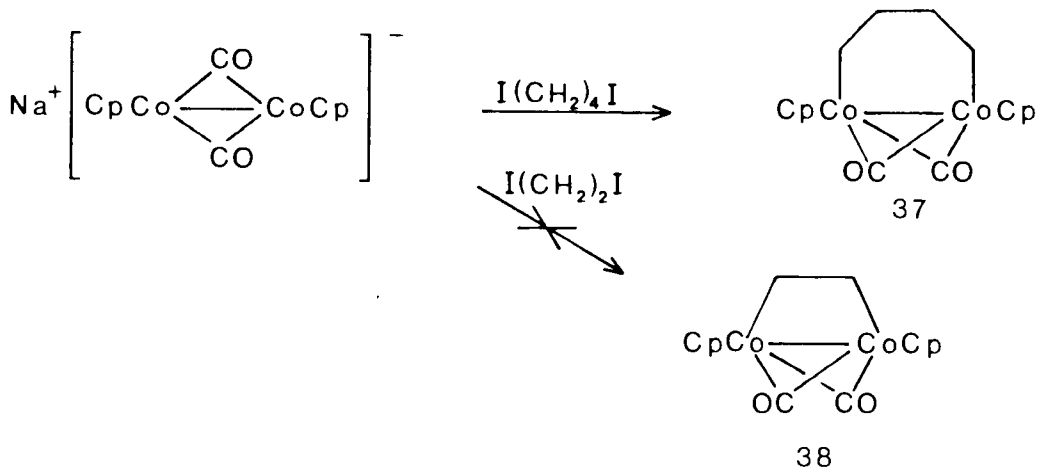

(14)

The only type (I) (1,n)alkanediyl bridged cobalt compounds known are the perfluoroalkyl derivatives $[(CO)_4Co(CF_2)_nCo(CO)_4]$ (n = 2,3) [49,51] and $K_6[(NC)_5Co(CF_2)_2Co(CN)_5]$ [52]. $[(CO)_4Co(CF_2)_2Co(CO)_4]$ [50] and $[(NC)_5Co(CF_2)_2Co(CN)_5]^{6-}$ [52] are produced by reaction of C_2F_4 with $Co_2(CO)_8$ and $[(CN)_5Co]^{3-}$ respectively. $[(CO)_4Co]_2\{\mu\text{-}(CF_2)_4\}$ is formed by addition of $[(CO)_4Co]^-$ to $ClCO(CF_2)_4COCl$ [51].

No polymethylene bridged rhodium or iridium compounds are known.

1.2.6 Nickel Group

Monaghan and Puddephatt have recently reported the synthesis of alkanediyl bridged platinum complexes 41a-d by oxidative addition of $I(CH_2)_nI$ (n = 2-5) to dimethyl (1,10-phenanthroline) platinum(II) 39 [53].

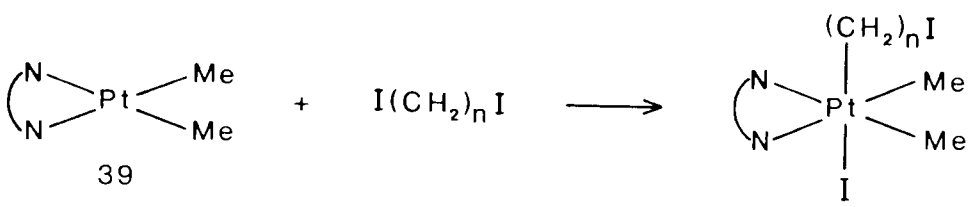

(N N = 1,10-phenanthroline)

40 a n=2
b n=3
c n=4
d n=5
e n=0

(15)

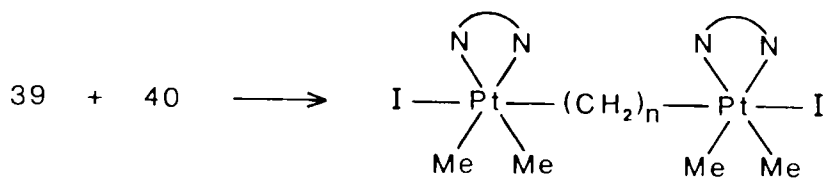

41 a n=2
b n=3
c n=4
d n=5

(16)

The reactions of 39 with $I(CH_2)_nI$ (n = 3-5) produce mixtures of compounds 40 and 41 but with a large excess of $I(CH_2)_nI$, 40 is the only product (reaction (15)) and this can be isolated and reacted with 39 to give the bridged compound 41 in high yield (reaction (16)). The reaction with $I(CH_2)_2I$ produces a mixture of 41a , ethylene, and 40e (rather than 40a). The ^1H NMR and $^{13}C\{^1H\}$NMR spectra of 41d show three resonances, two with ^{195}Pt coupling for the hydrogen and carbon nuclei in the $-(CH_2)_5-$ chain respectively, as expected for a (1,5)pentanediyl bridge between two Pt atoms. The low solubility of the compounds with n = 2-4 prevents NMR study.

Investigation of the kinetics of reactions (15) and (16) reveals that the rates of these reactions follow the order n 2 >> 3 > 4 ≃ 5. A small neighbouring atom effect by the metal atom on the C-X bond in $M(CH_2)_nX$ is observed for n = 3-5; the C-X bond is activated to further oxidative addition. For example, the second order rate constant for reaction of 39 with 40c is three times greater than that for the reaction of 39 with $I(CH_2)_3I$. This may be attributed to the lowering of the energy of the transition state of the reaction by contribution of the resonance terms :

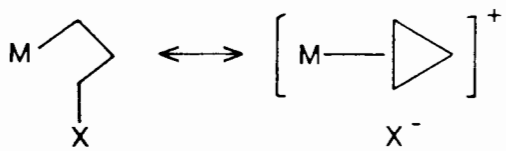

which would facilitate halide displacement.

Palladium (1,n)alkanediyl bridged species have been implicated as intermediates in the catalytic dimerisation of ethylene by bis-(η-arene)di-palladium 42

but have not been isolated [54] (Scheme 1.8).

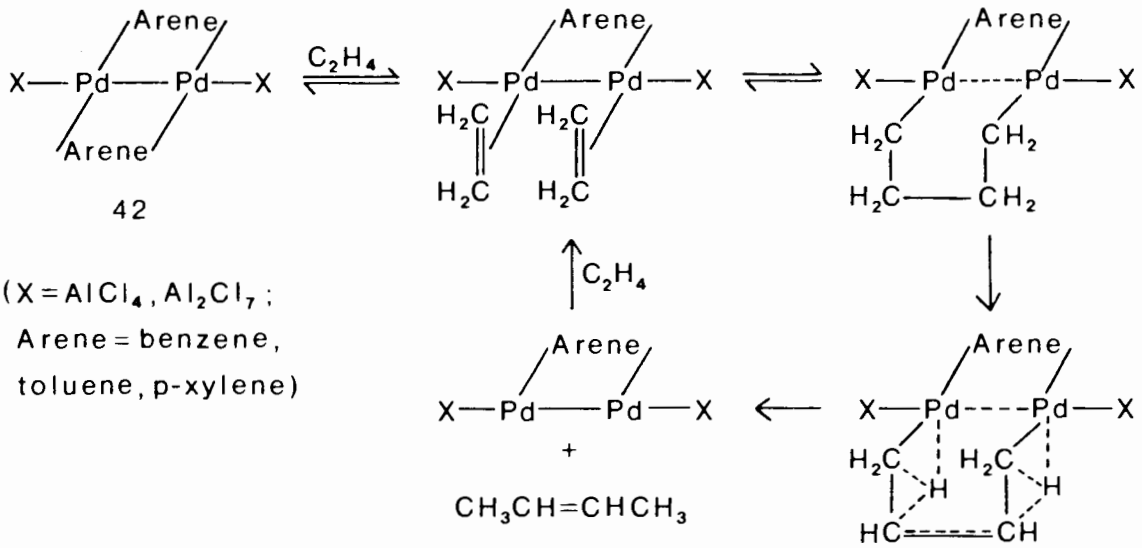

Scheme 1.8

These Pd(II) complexes also catalyse the dimerisation of propene.

1.3 Scope of this work

In this study we have prepared and characterised new alkanediyl bridge compounds of iron, tungsten and manganese. A detailed investigation of the mass spectra of μ(1,n)alkanediyl iron and tungsten compounds has been carried out. The series of diiron compounds $[Cp(CO)_2Fe]_2\{\mu\text{-}(CH_2)_n\}$ (n = 3-12) were analysed by Differential Scanning Calorimetry and the polymorphism of $[Cp(CO)_2Fe]_2\{\mu\text{-}(CH_2)_n\}$ (n = 4, 8) investigated. The thermal decomposition of $[Cp(CO)_2Fe]_2\{\mu\text{-}(CH_2)_n\}$ (n = 3-8) and $[Cp(CO)_3W]_2\{\mu\text{-}(CH_2)_n\}$ (n = 3-5) was also studied using gas chromatography to analyse the gaseous organic products. The reactions of some μ(1,n)alkanediyl diiron and ditungsten compounds with tertiary phosphines and halogens were investigated.

SECTION 2

2. SYNTHESIS AND CHARACTERISATION OF μ(1,n)ALKANEDIYL COMPOUNDS OF IRON, TUNGSTEN AND MANGANESE

2.1 General synthetic routes to μ(1,n)alkanediyl compounds

A general preparative route to mononuclear metal alkyl compounds is by reaction of a metal complex anion with an alkyl halide [55] .

$$L_nM^- + R\text{-}X \longrightarrow RML_n + X^- \qquad (17)$$

The analogous reaction of a metal anion with a dihaloalkane (in 2:1 molar ratio) can lead to either the mononuclear haloalkyl compound $L_nM(CH_2)_nX$ or the alkanediyl bridged species 43 (equation (18)).

$$2L_nM^- + X(CH_2)_nX \longrightarrow L_nM\text{-}(CH_2)_n\text{-}ML_n + 2\ X^- \qquad (18)$$

43

The product of the reaction is found to depend on the nucleophilicity of the metal anion and on the reactivity of the dihaloalkane. For example the highly nucleophilic anion † $[Cp(CO)_2Fe]^-$ reacts with $Br(CH_2)_nBr$ (n =3-6) to produce the μ(1,n)alkanediyl species $[Cp(CO)_2Fe]_2\{\mu\text{-}(CH_2)_n\}$ (n = 3-6) [29] while the reaction of the molybdenum anion $[Cp(CO)_3Mo]^-$, which is considerably less nucleophilic [56], with $Br(CH_2)_nBr$ (n = 3,4) gives only $[Cp(CO)_3Mo\{(CH_2)_nBr\}]$ [21]. However the μ(1,n)alkanediyl compound $[Cp(CO)_3Mo]_2\{\mu\text{-}(CH_2)_4\}$ is obtained from the reaction of $[Cp(CO)_3Mo]^-$ with the more reactive diiodoalkane, $I(CH_2)_4I$ [18] .

Reaction (18) can also be carried out as a two-step synthesis with

---

† This refers to the data of King *et al.* [56] on the relative nucleophilicity of various metal anions, established on the basis of their rates of reaction with an alkyl halide.

intermediate isolation of the mononuclear haloalkyl species which is then reacted with further anion to give the bridged product. This is a route to mixed metal compounds. For example [41] :

$$[Cp(CO)_2Fe]^- + I(CH_2)_3I \longrightarrow [Cp(CO)_2Fe\{(CH_2)_3I\}] \xrightarrow{[Cp(CO)_2Ru]^-} [Cp(CO)_2Fe\{\mu\text{-}(CH_2)_3\}Ru(CO)_2Cp] \quad (19)$$

Another route to alkanediyl bridged compounds is by decarbonylation of the diacyl species $[L_nM\{CO(CH_2)_nCO\}ML_n]$ which can be obtained from the reaction of the metal anion with a diacyl halide (equation (20)).

$$2\,L_nM^- + ClCO(CH_2)_nCOCl \longrightarrow L_nM\{CO(CH_2)_nCO\}ML_n + 2\,Cl^- \quad (20)$$

The perfluoroalkyl compounds $[Cp(CO)_2Fe]_2\{\mu\text{-}(CF_2)_3\}$ and $[Cp(CO)_3Mo]_2\text{-}\{\mu\text{-}(CF_2)_3\}$ have, for example, been synthesised by photochemical and thermal decarbonylation of the corresponding diacyl species respectively. [22]

In this work these routes have been applied to the synthesis of new μ(1,n)alkanediyl compounds of iron, tungsten and manganese.

2.2 Results and Discussion

2.2.1 Synthesis of iron compounds

The new μ(1,n)alkanediyl diiron compounds $[Cp(CO)_2Fe]_2\{\mu\text{-}(CH_2)_n\}$ (n = 8-12) (VIII) - (XII) have been synthesised by reaction of the

metal anion $[Cp(CO)_2Fe]^-$ with $Br(CH_2)_nBr$ (n = 8-12) in 2:1 molar ratio, following the method of King [29] (equation (21)) :

$$2Na[Cp(CO)_2Fe] + Br(CH_2)_nBr \xrightarrow[70°C,\ 12hrs]{THF} [Cp(CO)_2Fe]_2\{\mu\text{-}(CH_2)_n\} + 2NaBr \quad (21)$$

All compounds were obtained in good yield (47 - 64%) and the iron dimer $[Cp(CO)_2Fe]_2$ was the only other product of the reactions. Compounds (VIII) - (XII) are yellow crystalline solids with well defined melting points. They are stable in solid form but decompose rapidly in solution on exposure to air to a brown non-carbonyl product, at ambient temperatures. Under nitrogen, solutions of these compounds are stable even at elevated temperatures. (VIII) - (XII) have been characterised fully by IR, ^1H NMR and mass spectrometry and elemental analysis. A detailed study of the mass spectra of these compounds and those of the known $[Cp(CO)_2Fe]_2\{\mu\text{-}(CH_2)_n\}$ (n = 3-7) [29,57] (IV) - (VII) has been made and is reported in Section 3.1. The IR and ^1H NMR spectra of these compounds closely resemble those reported for the shorter chain compounds $[Cp(CO)_2Fe]_2\{\mu\text{-}(CH_2)_n\}$ (n = 3-7).

The compounds $[Cp(CO)_2Fe]_2\{\mu\text{-}(CH_2)_n\}$ (n = 3-7) were prepared for the mass spectral study by an adaptation [58] of the method of King [29]. The reaction between $[Cp(CO)_2Fe]^-$ and $Br(CH_2)_nBr$ (n = 3-7) was carried out at room temperature for 1-2 hrs. and the product extracted with n-pentane. This gives the required products in 60-70% yield compared with the yields of 15-47% reported by King [29].

The series of compounds (IV) - (XII) has been analysed by Differential Scanning Calorimetry and a study of their thermal decomposition carried out.

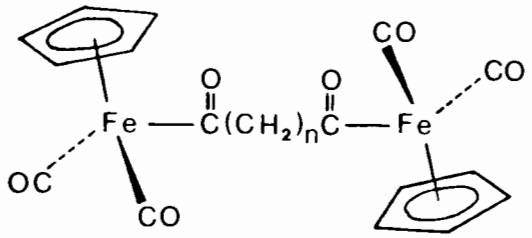

(I) n = 3
(II) n = 4

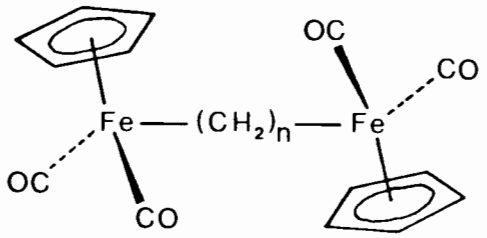

(III) n = 3
(IV) n = 4
(V) n = 5
(VI) n = 6
(VII) n = 7
(VIII) n = 8
(IX) n = 9
(X) n = 10
(XI) n = 11
(XII) n = 12

The results of this thermal analysis are presented in Section 4.

The synthesis of μ(1,n)alkanediyl diiron compounds by decarbonylation of the corresponding diacyl species has also been investigated. The diacyl compounds $[Cp(CO)_2Fe\{CO(CH_2)_nCO\}Fe(CO)_2Cp]$ (n = 3,4) (I), (II) are, like mononuclear iron acyl species, resistant to thermal decarbonylation [59]. The photolysis of (II) has been found [30] to give the decarbonylated product (IV) in low yield but (I) decomposes, on irradiation, to $[Cp(CO)_2Fe]_2$. In this work, the decarbonylation was effected under mild conditions by reaction of (I) and (II) with $RhCl(PPh_3)_3$ (equation (22)). This method of chemical decarbonylation has previously been used successfully for the conversion of several $Cp(CO)_2FeCOR$ compounds to the corresponding alkyl compounds [60].

$[Cp(CO)_2Fe\{CO(CH_2)_nCO\}Fe(CO)_2Cp]$ (n = 3,4) were synthesised by reaction of $[Cp(CO)_2Fe]^-$ with $ClCO(CH_2)_nCOCl$.

$$[Cp(CO)_2Fe\overset{O}{\overset{\|}{C}}(CH_2)_n\overset{O}{\overset{\|}{C}}Fe(CO)_2Cp] + 2RhCl(PPh_3)_3$$

(I) n = 3

(II) n = 4

$$\xrightarrow{\text{benzene, 20 °C, 6 hrs.}} \quad (22)$$

$$[Cp(CO)_2Fe]_2\{\mu\text{-}(CH_2)_n\} + 2RhCl(CO)(PPh_3)_2 + 2PPh_3$$

(III) n = 3

(IV) n = 4

The decarbonylated products (III) and (IV) were obtained in fairly good yield from these reactions (45 and 58% respectively). Some of the starting diacyl compound was recovered from the reaction of (II) with $RhCl(PPh_3)_3$ while a small amount of the monoacyl species $[Cp(CO)_2Fe\{CO(CH_2)_3\}Fe(CO)_2Cp]$

was isolated from the analogous reaction of (I). The formation of this species indicates that the decarbonylation of the diacyl species (I) proceeds in a stepwise fashion. This process could involve conversion of all the starting diacyl to the monoacyl species as the first step. However reaction of (I) with $RhCl(PPh_3)_3$ in equimolar ratio produced the μ(1,3)propanediyl species in ca. 30% yield and no monoacyl species; the diacyl starting material was recovered in 50% yield. Thus it appears that although the monoacyl species is formed as an intermediate in the decarbonylation of (I), the formation of the alkanediyl bridged product is favoured. This suggests that decarbonylation of the monoacyl intermediate occurs more readily than the initial CO abstraction from the diacyl substrate.

The infrared and ^1H NMR spectra of the product mixtures from reaction (22) also showed the presence of a PPh_3 substituted product. The reaction of $RhCl(PPh_3)_3$ with some mononuclear iron alkyl species, $Cp(CO)_2FeCOR$ (R = alkyl), has been found [60] to produce significant amounts of the PPh_3 substituted product $Cp(CO)(PPh_3)FeCOR$. It is thought that the decarbonylation reaction involves the abstraction of a terminal CO group by $RhCl(PPh_3)_3$ to give a coordinatively unsaturated intermediate [44]. Attack by PPh_3 at the vacant coordination site in this intermediate would account for the formation of a PPh_3 substituted product. The alkyl product could be formed from such an intermediate by alkyl migration to the vacant site (Scheme 2.1).

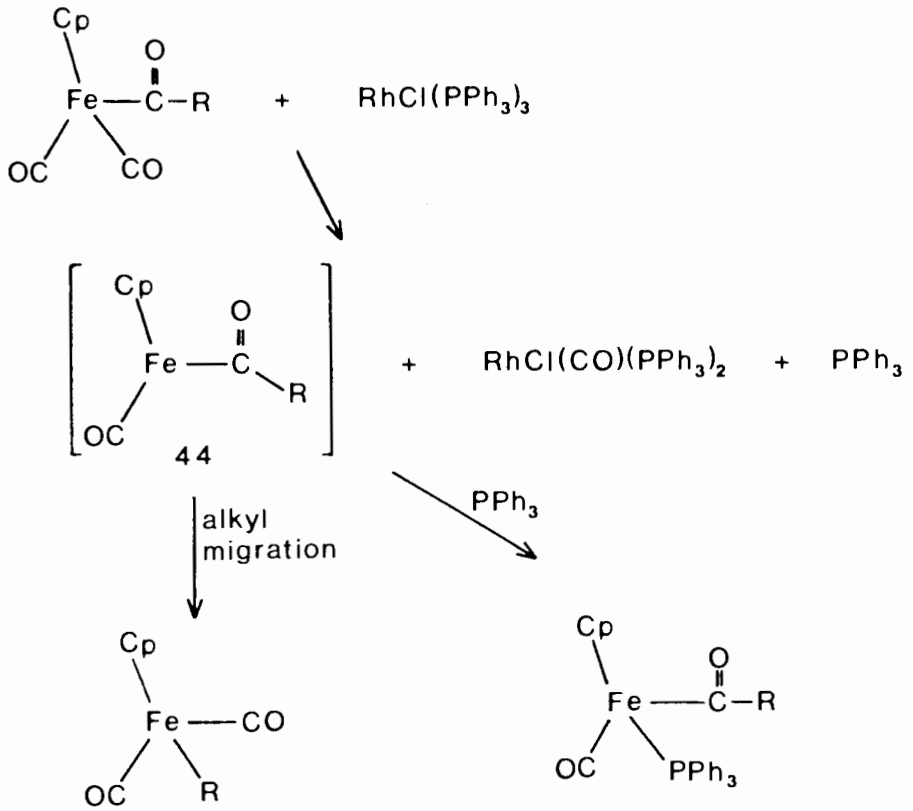

(Scheme 2.1)

In this work, several attempts have been made to isolate the μ(1,2)ethanediyl diiron compound $[Cp(CO)_2Fe]_2\{\mu\text{-}(CH_2)_2\}$. In contrast to the compounds $[Cp(CO)_2Fe]_2\{\mu\text{-}(CH_2)_n\}$ $(n \geqslant 3)$ the ethanediyl bridged species is not obtained from the reaction of $[Cp(CO)_2Fe]^-$ with the appropriate dihaloalkane. King has reported [29] that the reaction of the iron anion with dibromo- or diiodo-ethane produced only $[Cp(CO)_2Fe]_2$ and the desired product cannot be detected even at low temperature. Another route to this compound could be via reaction of the cationic ethylene complex $[Cp(CO)_2Fe(C_2H_4)]^+PF_6^-$ with $[Cp(CO)_2Fe]^-$, the analogous method to that used in the synthesis of the compounds $[Cp(CO)_3M]_2\{\mu\text{-}(CH_2)_2\}$ (M = Mo,W) [14]. A rapid reaction between $[Cp(CO)_2Fe(C_2H_4)]^+PF_6^-$

and $[CpFe(CO)_2]^-$ was observed, indicated by a sudden colour change in the reaction mixture, even at low temperature (0°C). However the only detectable reaction products were $[Cp(CO)_2Fe]_2$ and $[Cp_2Fe]$. The formation of ferrocene, under the mild reaction conditions used, could be attributed to the decomposition of an unstable reaction product, possibly the ethanediyl bridged species.

Evidence for the formation of the μ(1,2) ethanediyl compound was provided, in this study, by the observation that ethylene is produced on reaction of $[Cp(CO)_2Fe\{CO(CH_2)_2CO\}Fe(CO)_2Cp]$ with $RhCl(PPh_3)_3$. The organometallic product is again $[Cp(CO)_2Fe]_2$ (equation (23)).

$$[Cp(CO)_2Fe\overset{O}{\overset{\|}{C}}(CH_2)_2\overset{O}{\overset{\|}{C}}Fe(CO)_2Cp] + 2RhCl(PPh_3)_3 \xrightarrow{\text{benzene, 20°C}} [Cp(CO)_2Fe]_2 + C_2H_4 + 2\,RhCl(CO)(PPh_3)_2 \qquad (23)$$

These results suggest that $[Cp(CO)_2Fe]_2\{\mu\text{-}(CH_2)_2\}$ is formed on decarbonylation of the diacyl species but under the reaction conditions decomposes to $[Cp(CO)_2Fe]_2$ and ethylene. This has precedent among known ethanediyl bridged species; the analogous compounds $[Cp(CO)_3M]_2\{\mu\text{-}(CH)_2)_2\}$ (M = Mo,W) decompose with evolution of ethylene to the corresponding dimer [13]. Pettit *et al.* [30] have recently reported similar results on photolysis of $[Cp(CO)_2Fe\{CO(CH_2)_2CO\}Fe(CO)_2Cp]$.

2.2.2 Synthesis of tungsten compounds

The new compounds $[Cp(CO)_3W]_2\{\mu\text{-}(CH_2)_n\}$ (n = 3-5) (XIII) - (XV), $[Cp(CO)_2IW(\overline{COCH_2CH_2CH_2})]$ (XVI), $[Cp(CO)_3W\{(CH_2)_nI\}]$ (n = 4,5)

(XVII), (XVIII) and $[Cp(CO)_3W\{\mu\text{-}(CH_2)_3\}Fe(CO)_2Cp]$ (XIX) have been synthesised. Since the completion of this work, Winter *et al.* [19] have reported the preparation of compounds (XIII), (XIV) and (XVI) by methods entirely analogous to those used in this study.

The tungsten anion $[Cp(CO)_3W]^-$ was found to be considerably less reactive than the iron anion, in agreement with the report of King [56]. $[Cp(CO)_3W]^-$ does react with $Br(CH_2)_3Br$ to yield the μ(1,3)propanediyl compound, contrary to previous observations [21], but only in low yield after prolonged heating (equation (24)).

$$2\,[Cp(CO)_3W]^- + Br(CH_2)_3Br \xrightarrow[75°C,\,36\,hrs]{THF} \underset{11\%}{[Cp(CO)_3W]_2\{\mu\text{-}(CH_2)_3\}} + \underset{35\%}{[Cp(CO)_3WBr]} + \underset{28\%}{[Cp(CO)_3W]_2} \qquad (24)$$

(XIII) is obtained in good yield (61%) from the reaction of $[Cp(CO)_3W]^-$ with $I(CH_2)_3I$. The 2-oxacyclopentylidene compound $[Cp(CO)_2IW(\overline{COCH_2CH_2CH_2})]$ (XVII) was also isolated from this reaction (equation (25)).

$$2[Cp(CO)_3W]^- + I(CH_2)_3I \xrightarrow[95°C,\,12hrs]{DME} \underset{(XIII)}{[Cp(CO)_3W]_2\{\mu\text{-}(CH_2)_3\}} + [Cp(CO)_3WI] + \underset{(XVII)}{[Cp(CO)_2IW(\overline{COCH_2CH_2CH_2})]} \qquad (25)$$

The reaction of $[Cp(CO)_3W]^-$ with excess $I(CH_2)_3I$ gives exclusively the 2-oxacyclopentylidene product. (XVII) was also obtained in good yield from the reaction of $[Cp(CO)_3W\{(CH_2)_3Br\}]$ with $LiI\cdot 3H_2O$ (equation (26)).

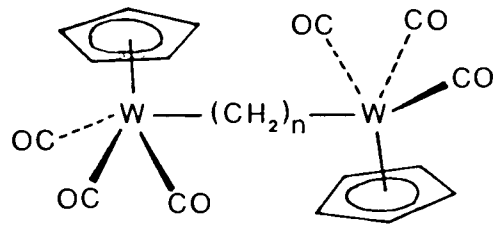

(XIII) n = 3
(XIV) n = 4
(XV) n = 5

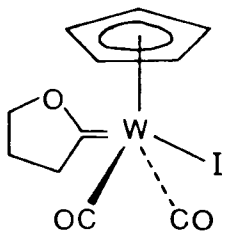

(XVI)

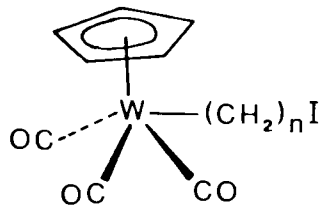

(XVII) n = 4
(XVIII) n = 5

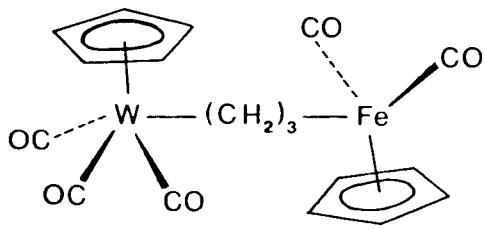

(XIX)

$$[Cp(CO)_3W\{(CH_2)_3Br\}] + LiI\cdot 3H_2O \xrightarrow[95°C,\ 28\,hrs]{DME} [Cp(CO)_2IW(\overline{COCH_2CH_2CH_2})] + [Cp(CO)_3WI] \quad (26)$$

59%

28%

(XVII) was isolated as a red crystalline solid showing one medium and one strong band in the carbonyl region of the infrared spectrum (at 1981 and 1900cm^{-1} respectively). The observed intensity ratio of these bands, which can be assigned to the asymmetric and symmetric CO stretching vibrations respectively, indicates that (XVII) has a *trans* arrangement of CO groups in the tetragonal pyramidal configuration about the tungsten atom [17].

In their recent paper [19], Winter *et al.* reported the preparation of *trans*-$[Cp(CO)_2IW(\overline{COCH_2CH_2CH_2}]$ by identical methods. They have also obtained the molybdenum species $[Cp(CO)_2IMo(\overline{COCH_2CH_2CH_2})]$ from analogous reactions [18,20]. It has been suggested [18,20] that the formation of a cyclopentylidene species in the reaction of $[Cp(CO)_3Mo]^-$ with $I(CH_2)_3I$ can be attributed to nucleophilic attack of I^- on $[Cp(CO)_3Mo\{(CH_2)_3I\}]$. The formation of (XIII) and (XVII) in reaction (25) suggests that there is competing nucleophilic attack of I^- and $[Cp(CO)_3W]^-$ on the mononuclear haloalkyl species 45 (Scheme 2.2). Attack of $[Cp(CO)_3W]^-$ on the $(CH_2)_3I$ ligand would result in the formation of the μ(1,3)propanediyl species. Competing attack of I^- would lead to the anionic acyl species 46 after migration of the alkyl group to an adjacent carbonyl group and coordination of the nucleophile to the metal atom [20]. A *cis* cyclic carbene species 47 would result from cyclisation of the acyl ligand with elimination of I^- and could undergo rapid *cis* ⟶ *trans* isomerisation to give the observed *trans* product. Alternatively 46

could undergo a *cis-trans* isomerisation prior to ring closure.

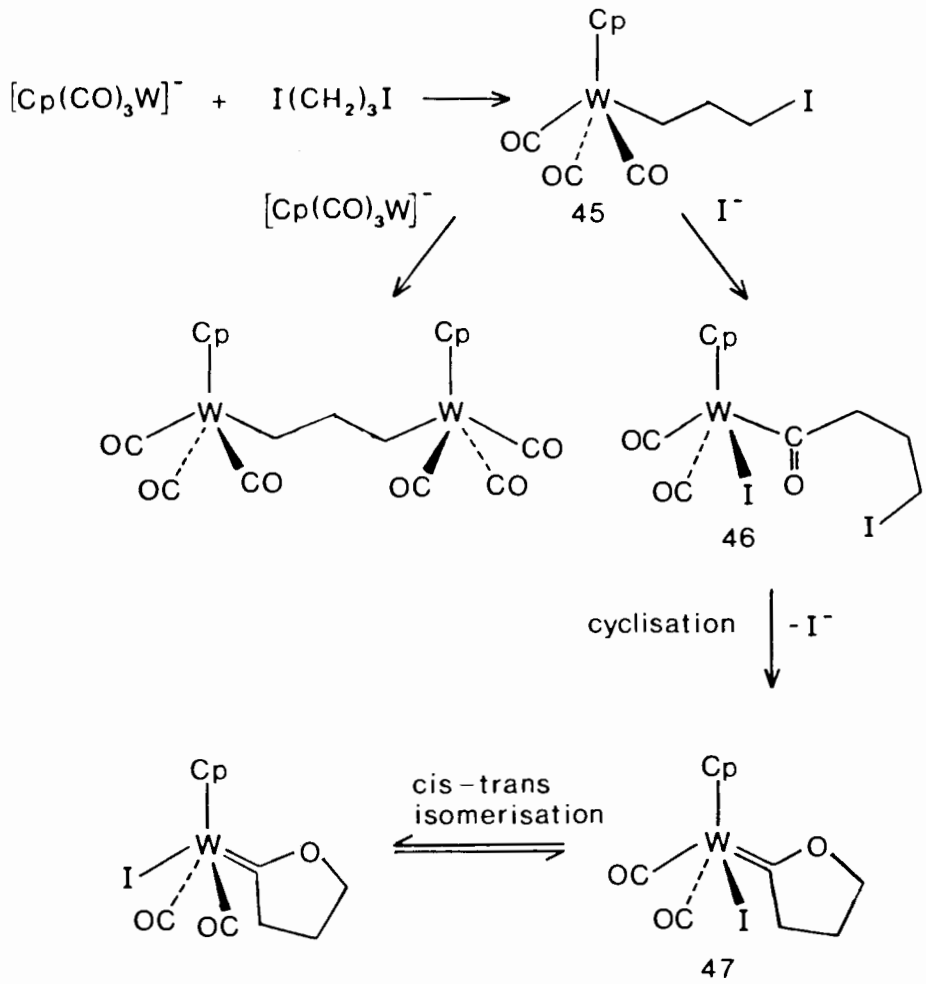

Scheme 2.2

In comparison with the molybdenum system, the formation of $[Cp(CO)_2IW(\overline{COCH_2CH_2CH_2})]$ is slow. For example, $[Cp(CO)_3Mo\{(CH_2)_3Br\}]$ reacts with LiI in THF to give $[Cp(CO)_2IMo(\overline{COCH_2CH_2CH_2})]$ in 90% yield after only 1hr. at 70°C [20] (c.f. reaction (9)). This could be attributed to the resistance of $[Cp(CO)_3W\{(CH_2)_3I\}]$ to metal-carbon bond cleavage and alkyl migration to give the acyl species 46 .

The reactions of $[Cp(CO)_3W]^-$ with $I(CH_2)_nI$ (n = 4,5) (equation (27)) produced $[Cp(CO)_3W]_2\{\mu\text{-}(CH_2)_n\}$ (n = 4,5) (XIV), (XV) respectively

in high yield.

$$[Cp(CO)_3W]^- + I(CH_2)_nI \xrightarrow[95°C,\ 12\,hrs]{DME} [Cp(CO)_3W]_2\{\mu\text{-}(CH_2)_n\} \quad (27)$$

(XIV) n = 4

(XV) n = 5

The only side product of these reactions was $[Cp(CO)_3WI]$. (XIV) and (XV) were also prepared in a two -step synthesis via the intermediate iodoalkyl species $[Cp(CO)_3W\{(CH_2)_nI\}]$ (n = 4,5) (XVII), (XVIII) (equation (28))

$$[Cp(CO)_3W]^- + I(CH_2)_nI \text{ excess} \longrightarrow [Cp(CO)_3W\{(CH_2)_nI\}] + I^- \quad (28)$$

$$(n = 4,5)$$

$$[Cp(CO)_3W\{(CH_2)_nI\}] \xrightarrow{[Cp(CO)_3W]^-} [Cp(CO)_3W]_2\{\mu\text{-}(CH_2)_n\} + I^-$$

The alkanediyl species $[Cp(CO)_3W]_2\{\mu\text{-}(CH_2)_n\}$ (n = 3 - 5) were isolated as yellow microcrystalline solids and fully characterised by IR , ^1H NMR, mass spectrometry and microanalysis. A discussion of the mass spectra of (XIII) - (XV) is presented in Section 3.2. These compounds are very insoluble , in contrast to the analogous diiron compounds. They are thermally stable, unlike the known ethanediyl bridged species $[Cp(CO)_3W]_2\{\mu\text{-}(CH_2)_2\}$ [13] but are also light sensitive in the solid state. Solutions of (XIII) - (XV) are sensitive to aerial oxidation and decompose rapidly to a black insoluble non-carbonyl compound. The IR spectra of these compounds (XIII) - (XV) resemble those of mononuclear tungsten alkyl compounds [34], showing two strong carbonyl bands (Table 6.7). In their ^1H NMR spectra, one broad singlet is observed for the methylene protons, as is found for the analogous diiron compounds.

The properties observed and characterisation data obtained for $[Cp(CO)_3W]_2\{\mu\text{-}(CH_2)_n\}$ (n = 3) agree well with those reported by Winter *et al.* [19]. However we have found that the decomposition temperature of $[Cp(CO)_3W]_2\{\mu\text{-}(CH_2)_4\}$ is considerably higher (195°C) than that noted by these workers (164°C). The reason for this discrepancy is not clear.

The mixed metal compound, $[Cp(CO)_3W\{(CH_2)_3\}Fe(CO)_2Cp]$ (XIX) was obtained in low yield from the reaction of $[Cp(CO)_2Fe\{(CH_2)_3Br\}]$ with excess $[Cp(CO)_3W]^-$. The μ(1,3)propanediyl ditungsten compound (XIII) was also isolated from the reaction. (equation (29)).

$$[Cp(CO)_3W]^- + [Cp(CO)_2Fe\{(CH_2)_3Br\}] \xrightarrow{\text{THF, 75°C, 48hrs}} [Cp(CO)_3W\{\mu\text{-}(CH_2)_3\}Fe(CO)_2Cp] + [Cp(CO)_3W]_2\{\mu\text{-}(CH_2)_3\} \quad (29)$$

(XIX) 14%

(XIII) 13%

(XIX) was isolated as an orange crystalline solid and characterised by IR, ^1H NMR, mass spectrometry and microanalysis. The properties of this compound, such as solubility and thermal stability, are intermediate between those of the diiron and ditungsten propanediyl bridged species (III) and (XIII), as might be expected. The IR spectrum of (XIX) shows four carbonyl bands which correspond in position and intensity to those observed for (III) and (XIII). In the ^1H NMR spectrum two singlets are observed for the CpFe and CpW protons and the signal for the methylene protons is again a broad unresolved singlet.

2.2.3 Synthesis of manganese compounds

The new compounds $[(CO)_5Mn\{CO(CH_2)_4CO\}Mn(CO)_5]$ (XX) and $[(CO)_5Mn]_2\{\mu\text{-}(CH_2)_4\}$ (XXI) have been synthesised.

Initially attempts were made to prepare the butanediyl bridged species (XXI) by reaction of $[(CO)_5Mn]^-$ with $I(CH_2)_4I$. The infrared spectrum of the reaction mixture showed bands in the carbonyl region, that could be attributed to an alkyl manganese product (2012 (s) 1990 (m) cm^{-1}). However this product could not be separated from the other products of the reaction, $[(CO)_5MnI]$, $[(CO)_4MnI]_2$ and $[(CO)_5Mn]_2$.

A general synthetic route to mononuclear manganese alkyl compound is via thermal decarbonylation of the corresponding acyl species [61,62]. Similarly, decarbonylation of $[(CO)_5Mn\{CO(CH_2)_4CO\}Mn(CO)_5]$ (XX) has been found to give the μ(1,4)butanediyl compound $[(CO)_5Mn]_2\{\mu\text{-}(CH_2)_4\}$. The diacyl species (XX) was prepared by reaction of $[(CO)_5Mn]^-$ with adipoyl dichloride (equation (30)).

$$2[(CO)_5Mn] + ClCO(CH_2)_4COCl \longrightarrow \underset{(XX)\quad 48\%}{[(CO)_5Mn\{CO(CH_2)_4CO\}Mn(CO)_5]} + [(CO)_5Mn]_2 \qquad (30)$$

(XX) is thermally stable at ambient temperatures, but like many mononuclear manganese acyl species [61] undergoes rapid decarbonylation on heating. $[(CO)_5Mn]_2\{\mu\text{-}(CH_2)_4\}$ was prepared in good yield (53%) by heating (XX) at 110°C until disappearance of the acyl band in the infrared spectrum of the sample. (XX) and (XXI) were isolated as white crystalline solids and fully

characterised by IR, ^{1}H NMR, mass spectrometry and microanalysis. The IR spectra of these compounds closely resemble those reported for mononuclear acyl and alkyl manganese compounds [61], in the carbonyl region. The appearance of six carbonyl bands in the region 2120 - 1900 cm^{-1} in the spectrum of (XX) indicates that the $Mn(CO)_5$ groups are distorted by the acyl substituent from the expected C_{4v} symmetry †. Two acyl bands are also observed for (XX) and these could be attributed to two rotational isomers of this compound. This has been previously shown for the haloacyl species $[(CO)_5MnCOCH_2X]$ (X = Cl, F) [64]. Three carbonyl bands are observed in the spectrum of (XXI) suggesting that the linear alkyl substituent does not cause significant distortion of the C_{4v} symmetry of the $Mn(CO)_5$ groups.

The ^{1}H NMR spectra of (XX) and (XXI) show the expected signals for the inequivalent αCH_2 and βCH_2 protons. For (XXI) two broad multiplets are observed for the methylene protons; this is in contrast to the diiron and ditungsten butanediyl bridged compounds which show an unresolved singlet for the methylene protons at 100 MHz .

(XXI) is thermally stable up to 130°C, decomposing above this temperature according to equation (31).

$$[(CO)_5Mn]_2\{\mu\text{-}(CH_2)_4\} \longrightarrow [(CO)_5Mn]_2 + \underset{91\%}{\text{but-1-ene}} + \underset{6\%}{cis\text{-but-2-ene}} + \underset{3\%}{trans\text{-but-2-ene}} \qquad (31)$$

† A compound of type $(CO)_5MnL$ with C_{4v} symmetry would display three infrared active carbonyl stretching modes as observed for $[(CO)_5Mn]_2$ [63].

(XXI) is also kinetically stable with respect to conversion into the acyl species (XX). This is in contrast to mononuclear manganese compounds with alkyl ligands which are generally kinetically unstable. For example $[(CO)_5Mn(C_2H_5)]$ decomposes even at -10°C under N_2 and the decomposition products are reported to contain the acyl complex $[(CO)_5MnCOEt]$ [34].

SECTION 3

3. MASS SPECTROMETRY OF μ(1,n)ALKANEDIYL COMPOUNDS

3.1 Mass Spectra of $[Cp(CO)_2Fe]_2\{\mu\text{-}(CH_2)_n\}$ (n = 3 - 12) (III) - (XII)

3.1.1 General

In this work, a comprehensive study of the mass spectra of the compounds $[Cp(CO)_2Fe]_2\{\mu\text{-}(CH_2)_n\}$ (n = 3-12) has been carried out. The only previous report of a mass spectral study of alkanediyl bridged compounds is that of Beck and Olgemöller [13] on the mass spectra of the ethanediyl bridged species, $[Cp(CO)_3M]_2\{\mu\text{-}(CH_2)_2\}$ (M = W,Mo), $[Cp(CO)_3W\{(CH_2)_2\}Re(CO)_5]$ and $[(CO)_5Re]_2\{\mu\text{-}(CH_2)_2\}$. In the mass spectrum of the dirhenium compound, they observed competitive loss of CO and C_2H_4 from the parent ion, indicated by the occurrence of the ions $[(CO)_9Re_2(C_2H_4)]^+$ and $[(CO)_{10}Re_2]^+$ in approximately equal abundance. Loss of $[(CO)_5Re]$ from the parent ion to give $[(CO)_5Re(C_2H_4)]^+$ also occurred. For the less stable ditungsten and dimolybdenum compounds, rapid loss of C_2H_4 occurred and the mass spectrum observed was that of the corresponding dimer, $[Cp(CO)_3M]_2$. The mixed metal compound $[Cp(CO)_3W\{\mu\text{-}(CH_2)_2\}Re(CO)_5]$ was found to decompose thermally to $[(CO)_5Re]_2\{\mu\text{-}(CH_2)_2\}$, $[Cp(CO)_3W]_2$ and ethylene in the mass spectrometer. Apart from this study, the mass spectra of μ(1,n)alkanediyl compounds have only been reported as part of their characterisation [41].

The compounds $[Cp(CO)_2Fe]_2\{\mu\text{-}(CH_2)_n\}$ (n = 3-12) are well suited to mass spectral study. They are thermally stable and reasonably volatile so only moderate source temperatures were required. In addition a large number of metastable ions are observed in the spectra of these compounds

which facilitates the interpretation of the fragmentation patterns. However, in order to establish decomposition pathways for these compounds, high resolution mass determinations were required to differentiate between losses of CO (27.995 mass units) and C_2H_4 (28.031 mass units) in the fragmentations.

3.1.2 Results and Discussion

The low resolution mass spectra of $[Cp(CO)_2Fe]_2\{\mu-(CH_2)_n\}$ (n = 3-12) (III) - (XII) are shown in Figs. 3.1 - 3.10. The mass spectrum of $[Cp(CO)_2Fe]_2$ is also included for comparison (Fig. 3.11). The intensities and probable assignments of the high mass peaks in these spectra are given in Tables 3.2 and 3.3. Fragmentation schemes for (III) and (VIII) are shown in Figs. 3.12 and 3.13. In these figures, a broken arrow indicates that no metastable ion was observed for their fragmentation.

Molecular ion peaks are observed in the mass spectra of all the compounds but are generally of low intensity. All spectra exhibit several peaks characteristic of compounds containing the $Cp(CO)_2Fe$ group [65-67], which can be assigned to the ions $[Cp(CO)_2Fe]^+$ ($^m/e$ 177), $[Cp(CO)Fe]^+$ ($^m/e$ 149), $[CpFe]^+$ ($^m/e$ 121), $[(C_3H_3)Fe]^+$ ($^m/e$ 95), $[Cp]^+$ ($^m/e$ 65) and $[Fe]^+$ ($^m/e$ 56). The relative intensities of these peaks in the mass spectra of (III) - (XII) and $[Cp(CO)_2Fe]_2$ are given in Table 3.1.

An intense peak at $^m/e$ 186, from the ion $[Cp_2Fe]^+$, is observed in the spectra of (III) - (XII). This ion is also significant in the mass spectra of mononuclear cyclopentadienyl dicarbonyl iron compounds and is thought

Table 3.1 Intensities of characteristic peaks in the mass spectra of compounds (III) - (XII)

m/e	Peak intensity [a] (%)									
	(III)	(IV)	(V)	(VI)	(VII)	(VIII)	(IX)	(X)	(XI)	(XII)
242	22	13	19	13	11	21	20	21	17	15
186	58	44	63	62	64	73	68	68	62	53
177	63	62	23	18	17	18	21	19	20	19
149	31	37	24	25	29	26	28	29	31	28
134	4	2	3	4	3	4	5	4	6	5
121	100	100	100	100	100	100	100	100	100	100
112	5	3	4	6	6	7	6	5	6	4
95	8	8	8	9	9	10	9	9	8	9
65	2	2	2	2	2	3	3	4	4	4
56	25	33	28	37	43	49	45	38	42	44

a : percentage of base peak m/e 121 in low resolution mass spectra.

Table 3.2 Peak intensities and assignment in the mass spectra of compounds (III) - (VII)

Ion [a]	Relative Peak intensity (%) [b]				
	(III)	(IV)	(V)	(VI)	(VII)
$[P]^+$	3	0.5	2	1	2
$[P-CO]^+$	1	0.5	1	1	5
$[P-2CO]^+, [P-CO-C_2H_4]^+$	1	1	3	2	5
$[P-3CO]^+, [P-2CO-C_2H_4]^+$	0.5	1	2	3	7
$[P-4CO]^+, [P-3CO-C_2H_4]^+$	1	2	2	2	4
$[P-4CO,H_2]^+$	1	1	2	3	7
$[P-C_nH_{2n}]^+$	3	-	0.5	-	-
$[P-CO-C_nH_{2n}]^+$	7	1	1	-	2
$[P-2CO-C_nH_{2n}]^+$	8	2	3	3	5
$[P-3CO-C_nH_{2n}]^+$	7	5	8	6	3
$[P-4CO-C_nH_{2n}]^+$	22	13	19	13	11
$[P-CO-Cp(CO)_2Fe]^+$	21	64	44	48	34
$[P-2CO-Cp(CO)_2Fe]^+$	29	62	18	16	14
$[P-CO-C_5H_6]^+$	-	-	2	2	5
$[P-2CO-C_5H_6]^+$	-	2	17	31	100
$[P-3CO-C_5H_6]^+$	4	7	18	30	17
$[P-4CO-C_5H_6]^+$	12	29	50	23	31
$[P-4CO-C_5H_6-H_2]^+$	3	-	10	-	14
$[CpFe_2H]^+$	5	15	16	29	27
$[Fe(C_nH_{2n-2})]^+$	1	1	2	8	19
$[C_nH_{2n}]^+$	3	4	2	2	3
$[C_5H_6]^+$	2	2	2	3	3

a : P is the parent ion $Cp_2(CO)_4Fe_2(C_nH_{2n})$

b : percentage of the base peak $^m/e$ 121 in the low resolution mass spectra.

Table 3.3 Peak intensities and assignments for the mass spectra of compounds (VIII) - (XII)

Ion [a]	Relative Peak intensity [b] (%)				
	(VIII)	(IX)	(X)[c]	(XI)[c]	(XII)[c]
$[P]^+$	2	0.5	0.5	0.5	>0.2
$[P-CO]^+$	3	1	3	1	1
$[P-2CO]^+$	3	1	4	0.5	3
$[P-3CO]^+$	5	3	13	5	5
$[P-4CO]^+$	3	2	10	4	4
$[P-4CO-H_2]^+$	4	2	13	4	4
$[P-CO-C_nH_{2n}]^+$	3	2	6	14	3
$[P-2CO-C_nH_{2n}]^+$	8	14	24	17	14
$[P-3CO-C_nH_{2n}]^+$	16	14	38	26	21
$[P-4CO-C_nH_{2n}]^+$	21	14	58	15	14
$[P-CO-Cp(CO)_2Fe]^+$	49	28	17	27	19
$[P-2CO-Cp(CO)_2Fe]^+$	14	8	10	6	5
$[P-CO-C_5H_6]^+$	4	2	4	0.5	3
$[P-2CO-C_5H_6]^+$	55	22	42	13	9
$[P-3CO-C_5H_6]^+$	22	9	10	6	5
$[P-4CO-C_5H_6]^+$	39	11	14	5	4
$[P-4CO-C_5H_6-H_2]^+$	21	10	-	10	9
$[CpFe_2H]^+$	31	31	28	26	23
$[Fe(C_nH_{2n-2})]^+$	55	87	>100	>100	>100
$[C_nH_{2n}]^+$	3	2	3	3	2
$[C_5H_6]^+$	5	5	5	5	7

a : P is the parent ion $Cp_2(CO)_4Fe_2(C_nH_{2n})$.

b : percentage of base peak $^m/_e$ 121 in the low resolution mass spectra.

c : $[Fe(C_nH_{2n-2})]^+$ is the most abundant ion in the spectrum so is off scale when intensities are measured relative to $^m/_e$ 121.

[65] to arise from the ionisation of ferrocene formed by thermal decomposition of these compounds in the ion source. In this study, the ion source temperatures used are considerably lower than the decomposition temperatures of the compounds in the series (see Tables 4.1 and 6.1) so the contribution of pyrolysis products should be small. Samples were purified by recrystallisation immediately prior to recording of the mass spectra, in order to eliminate any impurities formed by sample decomposition. The formation of $[Cp_2Fe]^+$ may thus be attributed mainly to the fragmentation and rearrangement of the sample compound.

A dominant feature of the mass spectra of the alkanediyl bridged compounds is a stepwise loss of 28 mass units from the molecular ion which could be attributed to the elimination of either CO or C_2H_4. High resolution mass determinations have shown that a major decomposition pathway for all the compounds is via stepwise CO loss from the molecular ion, as is characteristically observed for metal carbonyl-containing compounds [72]. The ions $[Cp_2(CO)_{4-x}Fe_2(C_nH_{2n})]^+$ (x = 1-4) are fairly significant in the spectra of all compounds and elimination of the fourth CO group as COH_2 is also observed †. The resulting ion is probably the alkenyl species $[Cp_2Fe_2(C_nH_{2n-2})]^+$ (since loss of H_2 from the cyclopentadienyl group is not generally observed in cyclopentadienyl iron compounds). The ions $[Cp_2Fe_2(C_nH_{2n})]^+$ and $[Cp_2Fe_2(C_nH_{2n-2})]^+$ generally decompose by elimination of the whole hydrocarbon chain, to $[Cp_2Fe_2]$ ($^m/e$ 242) but with some compounds, e.g. (V) and (VII), intermediate species such as $[Cp_2Fe_2(C_2H_4)]^+$, resulting from stepwise elimination of hydrocarbon fragments from the bridge, are observed. The ion $[Cp_2Fe_2]^+$ fragments

---

† This is apparently loss of formaldehyde in a single step but it has been suggested [66] that the losses of CO and H_2 occur consecutively during the time of flight of the ion through the field-free region of the spectrometer.

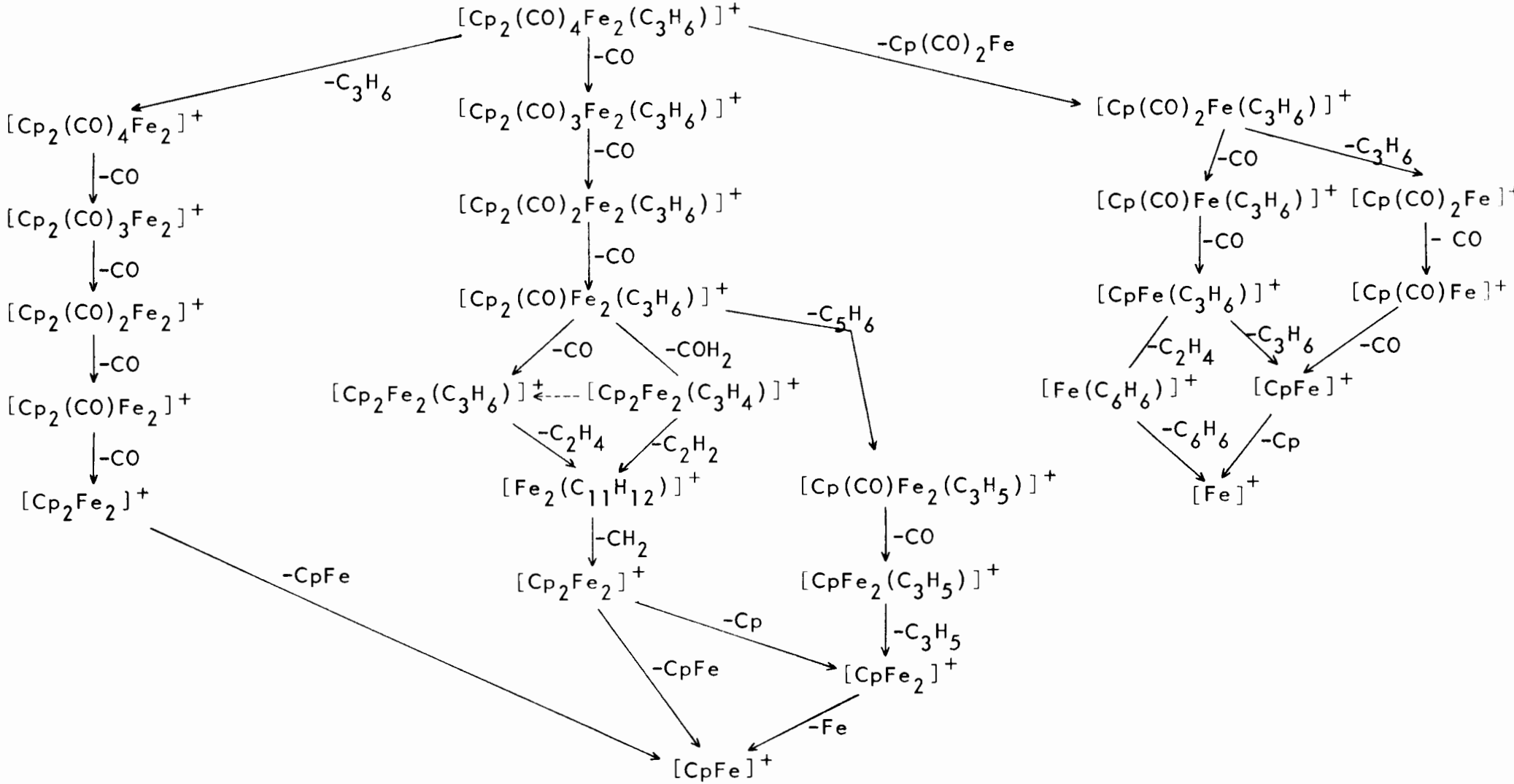

Fig. 3.12 Fragmentation scheme for $[Cp(CO)_2Fe]_2\{\mu\text{-}(CH_2)_3\}$ (III)

by loss of Fe or Cp to give $[Cp_2Fe]^+$ ($^m/e$ 186) or $[CpFe_2]^+$ ($^m/e$ 177) respectively.

For the propanediyl bridged compound, two other decomposition routes for the molecular ion, competing with CO loss, have been established on the basis of observed metastable peaks (Fig. 3.12). The major competing route involves elimination of the C_3H_6 bridge to give $[Cp_2(CO)_4Fe_2]^+$. The fragmentation of this ion is identical to that observed in the mass spectrum of $[Cp(CO)_2Fe]_2$.

The other route commences with loss of a $Cp(CO)_2Fe$ fragment. Elimination of this type of fragment from the parent ion has previously been reported for dimanganese and dirhenium cyclopentadienyl dicarbonyl compounds containing bridging vinylidene ligands [68]. The resulting ion $[Cp(CO)_2Fe(C_3H_6)]^+$ fragments by either loss of CO or C_3H_6. Elimination of CO leads to $[CpFe(C_3H_6)]^+$ which decomposes via loss of C_2H_4 or C_3H_6 to $[Fe(C_6H_6)]^+$ ($^m/e$ 134) or $[CpFe]^+$ ($^m/e$ 121). Elimination of C_3H_6 from $[Cp(CO)_2Fe(C_3H_6)]^+$ gives the ion $[Cp(CO)_2Fe]^+$ ($^m/e$ 177) which loses CO in a stepwise fashion to give $[CpFe]^+$.

These three decomposition pathways for $[Cp(CO)_2Fe]_2\{\mu\text{-}(CH_2)_3\}$ parallel those reported for $[(CO)_5Re]_2\{\mu\text{-}(CH_2)_2\}$ [13]. A fourth, much less significant decomposition route involving elimination of a C_5H_6 fragment from $[Cp_2(CO)Fe_2(C_3H_6)]^+$ is also observed for (III). This route is more significant for the longer chain compounds and is discussed in detail later.

For compounds (IV) - (XII), only one decomposition of the parent ions, i.e.

via CO loss, can be established on the basis of the observed metastable peaks. However, several decomposition routes for the $[Cp_2(CO)_3Fe_2(C_nH_{2n})]^+$ ion of these compounds, have been identified. These involve elimination of the fragments C_nH_{2n}, C_2H_4, $Cp(CO)_2Fe$ and C_5H_6 from this ion in competition with further CO loss. (See Tables 3.2 and 3.3 and for example the fragmentation scheme for $[Cp(CO)_2Fe]_2\{\mu\text{-}(CH_2)_8\}$, (Fig. 3.14)).

Loss of C_nH_{2n} : Elimination of the entire alkanediyl bridge C_nH_{2n} from $[P\text{-}CO]^+$, gives the ion $[Cp_2(CO)_3Fe_2]^+$ (^{m}/e 326). The intensity of the peak for this ion is generally low and this route is the least significant of the competing pathways (see Tables 3.2 and 3.3). $[Cp_2(CO)_3Fe_2]^+$ decomposes as in the spectrum of $[Cp(CO)_2Fe]_2$, by stepwise elimination of CO to $[Cp_2Fe_2]^+$ (^{m}/e 242).

Loss of C_2H_4 : Elimination of C_2H_4 from $[Cp_2(CO)_3Fe_2(C_nH_{2n})]^+$ in competition with CO loss, is only observed for compounds (IV) - (VII). The resulting ion $[Cp_2(CO)_3Fe_2(C_{n-2}H_{2n-4})]^+$ decomposes by elimination of CO and C_2H_4 or C_3H_6 fragments to $[Cp_2Fe_2]^+$ (^{m}/e 242). Competing elimination of CO and C_2H_4 from the ions $[Cp_2(CO)_{4-x}Fe_2(C_nH_{2n})]^+$ (x = 2,3) is also observed for (V) and (VII).

Loss of $Cp(CO)_2Fe$: The elimination of the $Cp(CO)_2Fe$ fragment from the $[Cp_2(CO)_3Fe_2(C_nH_{2n})]^+$ ion occurs in a single step as indicated by the presence of a metastable ion for this process in the mass spectra of several compounds. The resulting ion $[Cp(CO)Fe(C_nH_{2n})]^+$ loses CO to give $[CpFe(C_nH_{2n})]^+$. This ion decomposes either by consecutive loss of H_2 molecules or by elimination of the hydrocarbon chain to give $[CpFe]^+$.

Loss of up to four molecules of hydrogen from the $[CpFe(C_nH_{2n})]^+$ ion is observed, the number of molecules lost increasing with increasing length of the hydrocarbon chain. Such successive elimination of H_2 molecules is unprecedented in organic mass spectrometry. The mass spectra of n-alkanes and dihaloalkanes, for example, show the loss of at most two molecules of H_2 from the parent or fragment ions of these compounds [67]. The loss of hydrogen subsequent to elimination of carbonyl groups has been reported for various iron carbonyl derivatives containing hydrocarbon ligands [66,69]. Stone *et al.* [66] in their mass spectral study of mononuclear iron alkyl compounds of the type $[Cp(CO)_2FeR]$, observed loss of one, two or three molecules of hydrogen from the $[CpFeR]^+$ ions in the mass spectra of these compounds, depending on the length of the alkyl chain. They suggested that the hydrogen loss from the alkyl group results in the formation of a η^3-allyl or η^5-pentadienyl species (after double bond migration). It is thought [69] that after elimination of one or more carbonyl groups from an iron carbonyl ion, the iron becomes electron deficient and the formation of a π-bonded species would serve to stabilise the ion by increased electron donation to the metal.

By analogy, the loss of one molecule of H_2 from the $[CpFe(C_nH_{2n})]^+$ ion, observed for compounds (IV) - (VI) could result in the formation of a η^3-allylic species of the type shown below 48 .

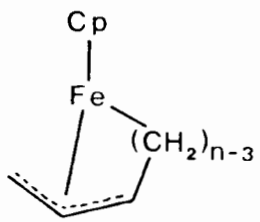

48

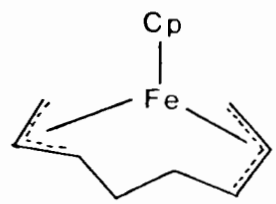

49

Elimination of further molecules of H_2, as occurs for compounds (VII) - XII), presumably gives species with more extensive π-bonding such as 49 formed from $[CpFe(C_8H_{16})]^+$ by loss of $2H_2$.

Loss of C_5H_6 : The elimination of a C_5H_6 fragment from the $[Cp_2(CO)_3Fe_2(C_nH_{2n})]^+$ ion gives an ion of the formula $[Fe_2O_3(C_{n+9}H_{2n+4})]^+$. This is most likely the alkenyl species $[Cp(CO)_3Fe_2(C_nH_{2n-1})]^+$ which would be formed by loss of one cyclopentadienyl group and a hydrogen from the alkanediyl bridge. Such an elimination of a cyclopentadienyl group from a metal carbonyl ion is unprecedented. In all previous studies of cyclopentadienyl carbonyl compounds [65-67,70-72], preferential loss of CO over C_5H_5 was observed. The only carbonyl containing fragment without a cyclopentadienyl group, which occurs in the mass spectra of some metal carbonyl cyclopentadienyl compounds, is $[M-CO]^+$ (M = metal) but this is not generally observed for iron compounds [72].

The elimination of a C_5H_6 fragment could be rationalised in terms of a β-hydrogen transfer from the alkanediyl bridge to the vacant site on one iron atom in $[Cp_2(CO)_3Fe_2(C_nH_{2n})]^+$:

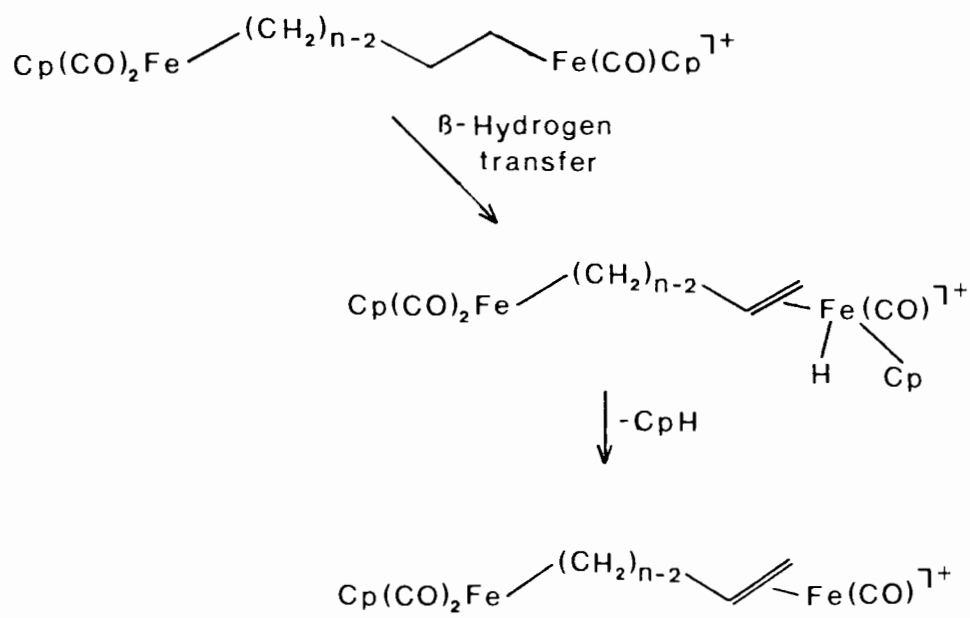

The alkenyl ion 50 loses one CO group to give $[Cp(CO)_2Fe_2(C_nH_{2n-1})]^+$ which fragments either by further CO loss to give $[CpFe_2(C_nH_{2n-1})]^+$ or by elimination of a $Cp(CO)_2FeH$ fragment to give $[Fe(C_nH_{2n-2})]^+$. The elimination of the $Cp(CO)_2FeH$ fragment is unusual in that it apparently involves a H transfer from the alkanediyl bridge to a coordinatively saturated iron atom. Stone *et al.* [66] observed an analogous mode of elimination of alkene from the parent ions of mononuclear iron alkyl compounds. The loss of the alkyl group as alkene is accompanied by H transfer to the iron atom giving $[Cp(CO)_2FeH]^+$ ($^m/e$ 178).†

The ions $[CpFe_2(C_nH_{2n-1})]^+$ and $[Fe(C_nH_{2n-2})]^+$ decompose by stepwise loss of H_2 and hydrocarbon fragments to $[CpFe_2H]^+$ and $[Fe]^+$ respectively. (See for example, the fragmentation of the $[CpFe_2(C_8H_{15})]^+$ ion in Fig. 3.13). As observed for the $[CpFe(C_nH_{2n})]^+$ ion, the $[CpFe_2(C_nH_{2n-1})]^+$ loses up to four molecules of hydrogen and the number lost increases with increasing n. The ions formed by hydrogen elimination from this ion could be π-bonded species such as 51 and 52 .

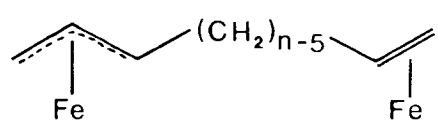

51

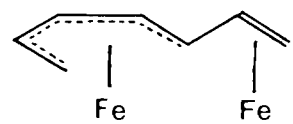

52

In the series of alkanediyl bridged compounds studied the decomposition routes established vary in significance with the length of the alkanediyl bridge. Decomposition via elimination of a C_5H_6 fragment becomes more significant

† This is in contrast to the mode of elimination of alkene on thermal decomposition of iron alkyl derivatives such as $[Cp(CO)(PPh_3)FeR]$ which involves dissociation of PPh_3 prior to β-hydrogen transfer [73].

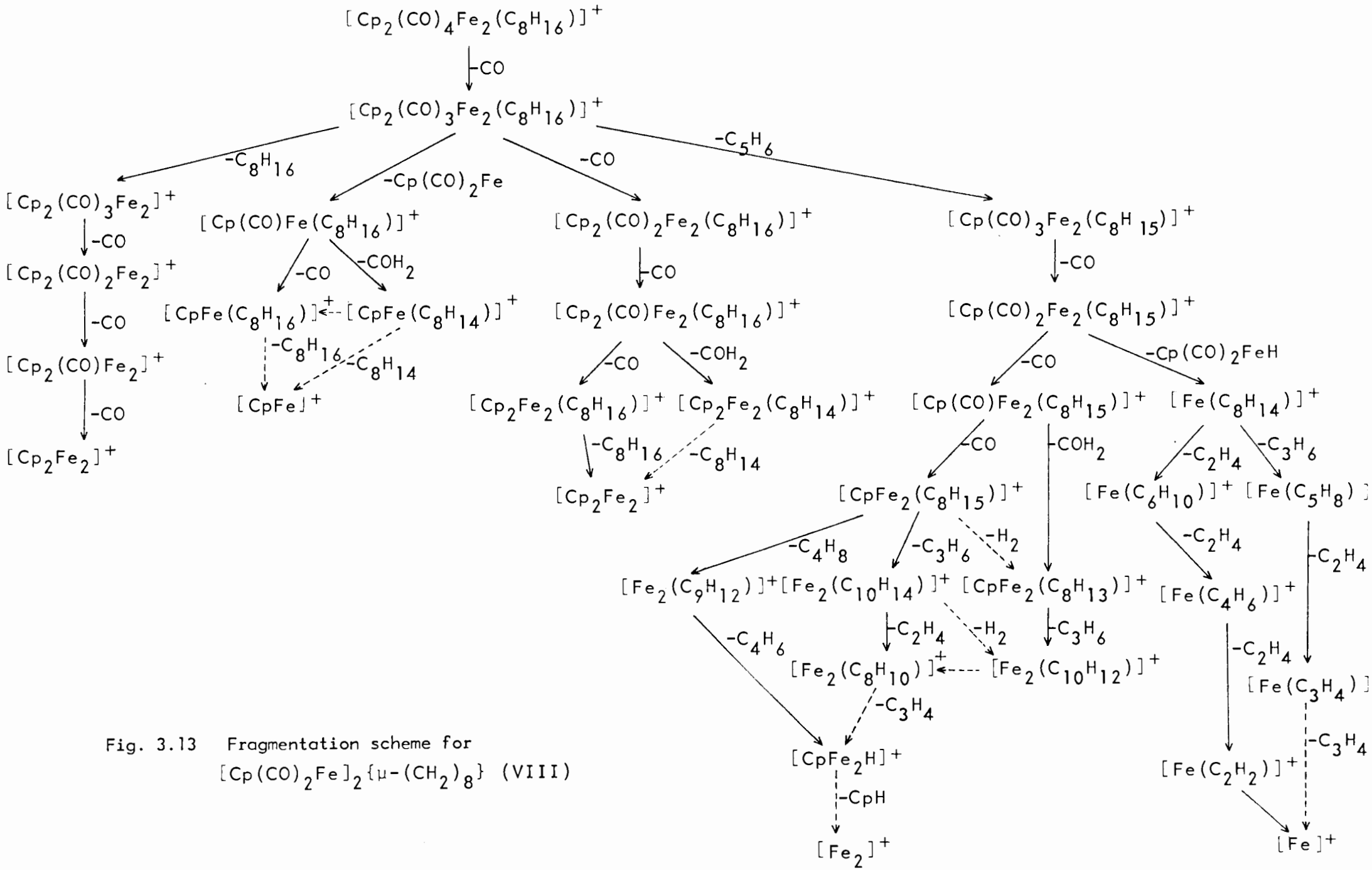

Fig. 3.13 Fragmentation scheme for $[Cp(CO)_2Fe]_2\{\mu\text{-}(CH_2)_8\}$ (VIII)

as the length of the bridge increases. This is reflected by the increasing abundance of the ions $[Fe(C_nH_{2n-2})]^+$ and $[CpFe_2H]^+$ ($^m/e$ 178) in the mass spectra of these compounds with increasing n (See Tables 3.1 - 3.3). For compounds (X) - (XII) $[Fe(C_nH_{2n-2})]^+$ is in fact the most abundant ion in the mass spectrum. This trend could reflect the effect of chain length on the stability of the transition state for the β-hydrogen transfer 53 :

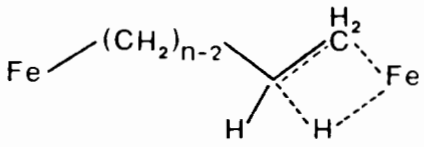

53

Steric crowding in this transition state for the shorter chain compounds could disfavour fragmentation by this route. The reverse trend is observed for the decomposition route involving elimination of C_2H_4 or C_3H_6 fragments from the alkanediyl bridge in competition with further CO loss from the $[Cp_2(CO)_{4-x}Fe_2(C_nH_{2n})]^+$ (x = 0-3) ions.

A large number of organic fragments are also observed in the mass spectra of these compounds. $[C_nH_{2n}]^+$ ions arising from the alkanediyl bridge occur as well as the ions $[C_nH_{2n-x}]^+$ (x = 1,3,5...n) formed by successive dehydrogenation of these ions. Lower carbon fragments are also observed and may be formed either by fragmentation of the $[C_nH_{2n}]^+$ ion or by decomposition of iron-containing ions such as those formed in the fragmentation of $[Fe(C_nH_{2n-2})]^+$.

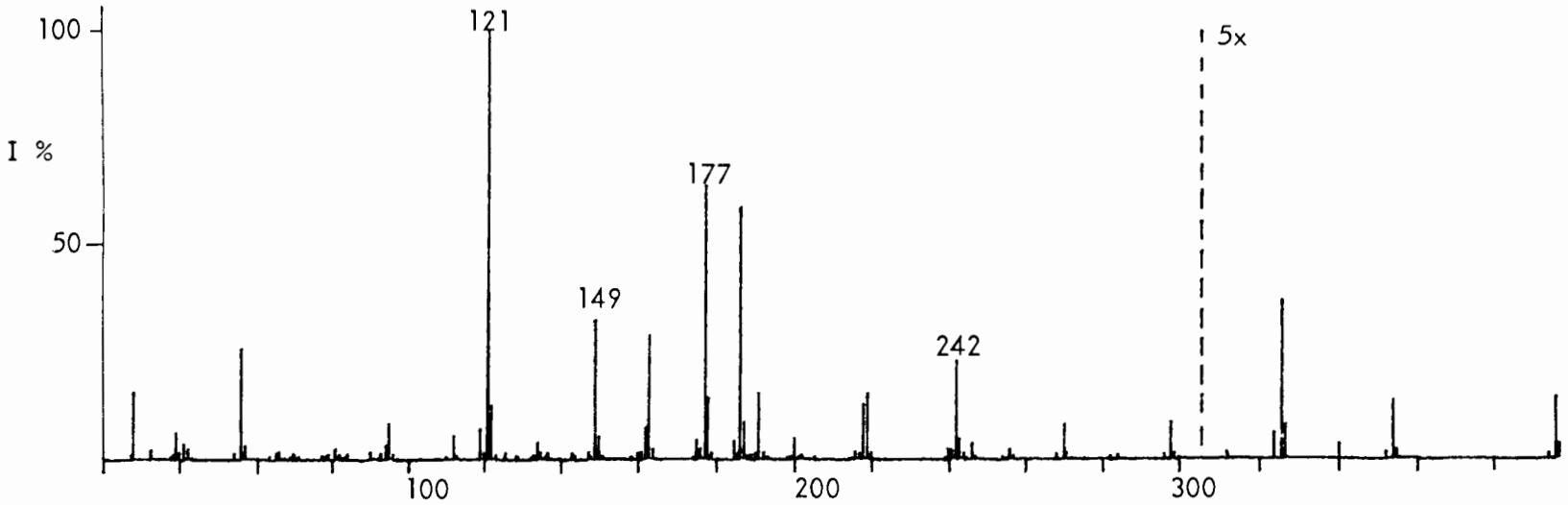

Fig. 3.1 Mass spectrum of $[Cp(CO)_2Fe]_2\{\mu-(CH_2)_3\}$ (III)

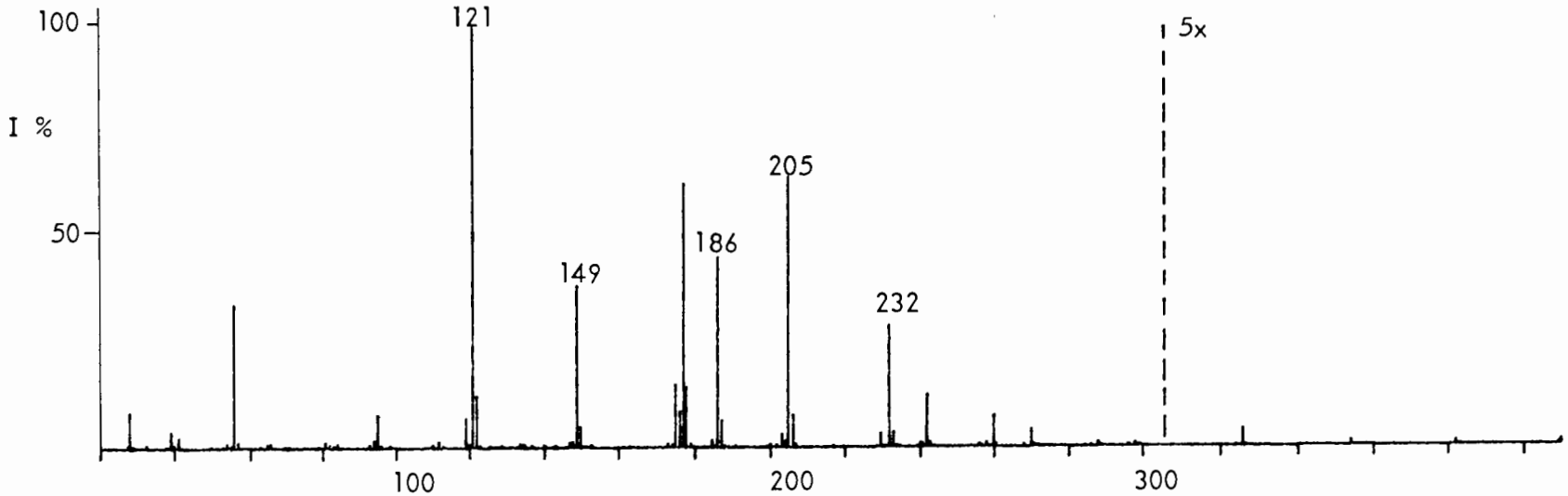

Fig. 3.2 Mass spectrum of $[Cp(CO)_2Fe]_2\{\mu-(CH_2)_4\}$ (IV)

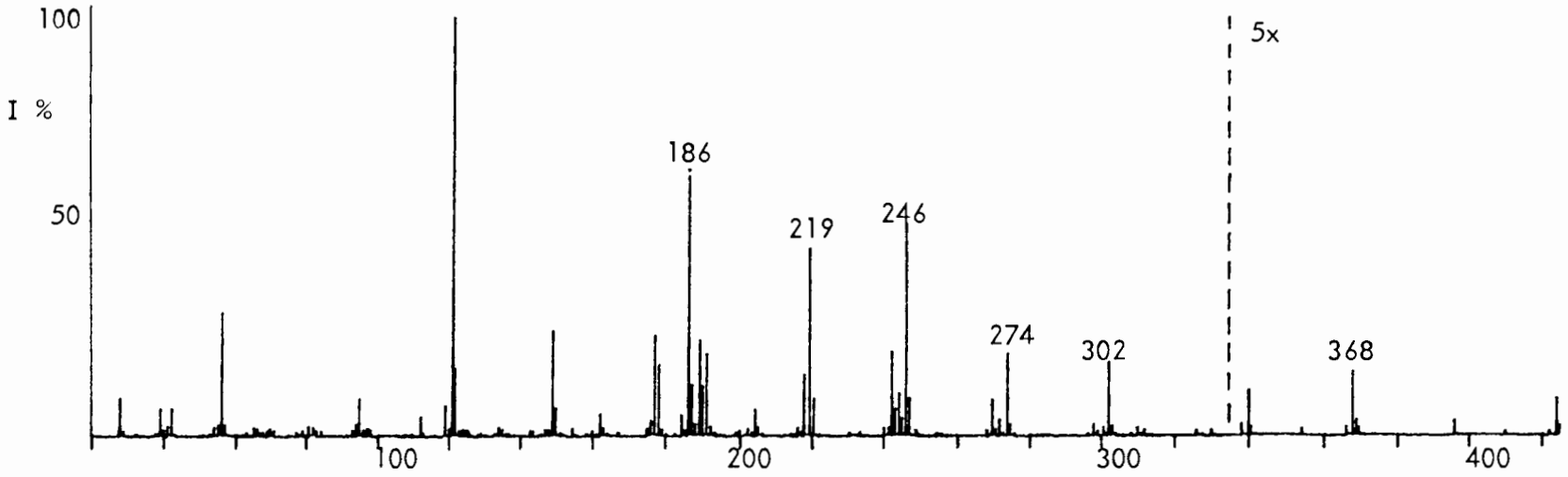

Fig. 3.3 Mass spectrum of $[Cp(CO)_2Fe]_2\{\mu\text{-}(CH_2)_5\}$ (V)

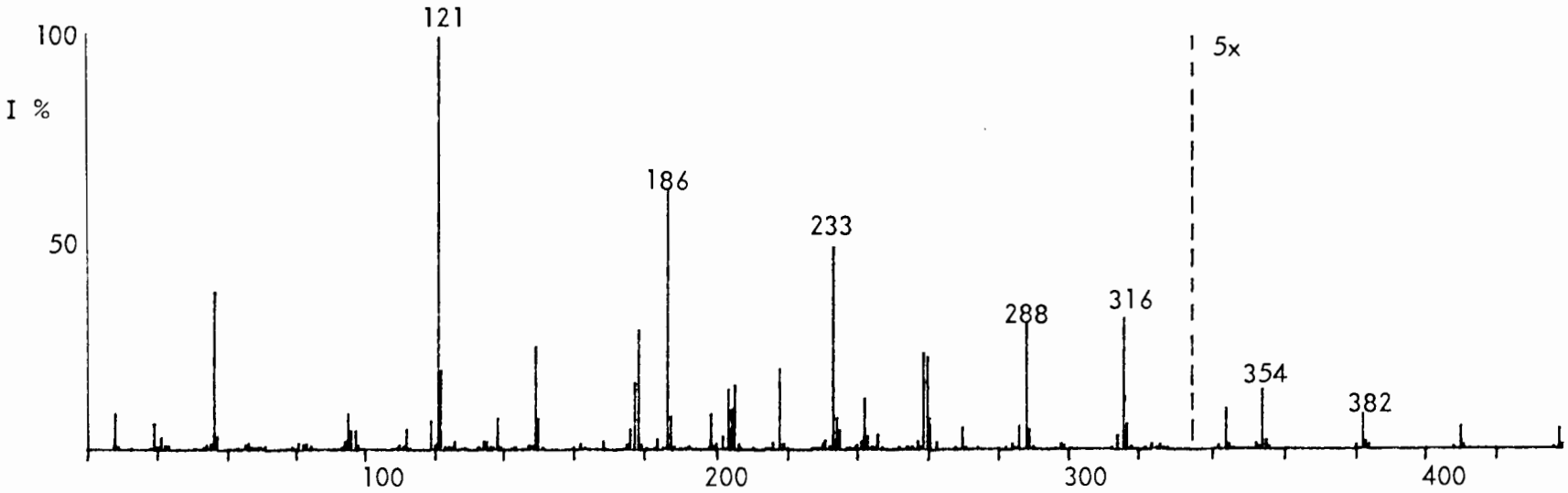

Fig. 3.4 Mass spectrum of $[Cp(CO)_2Fe]_2\{\mu\text{-}(CH_2)_6\}$ (VI)

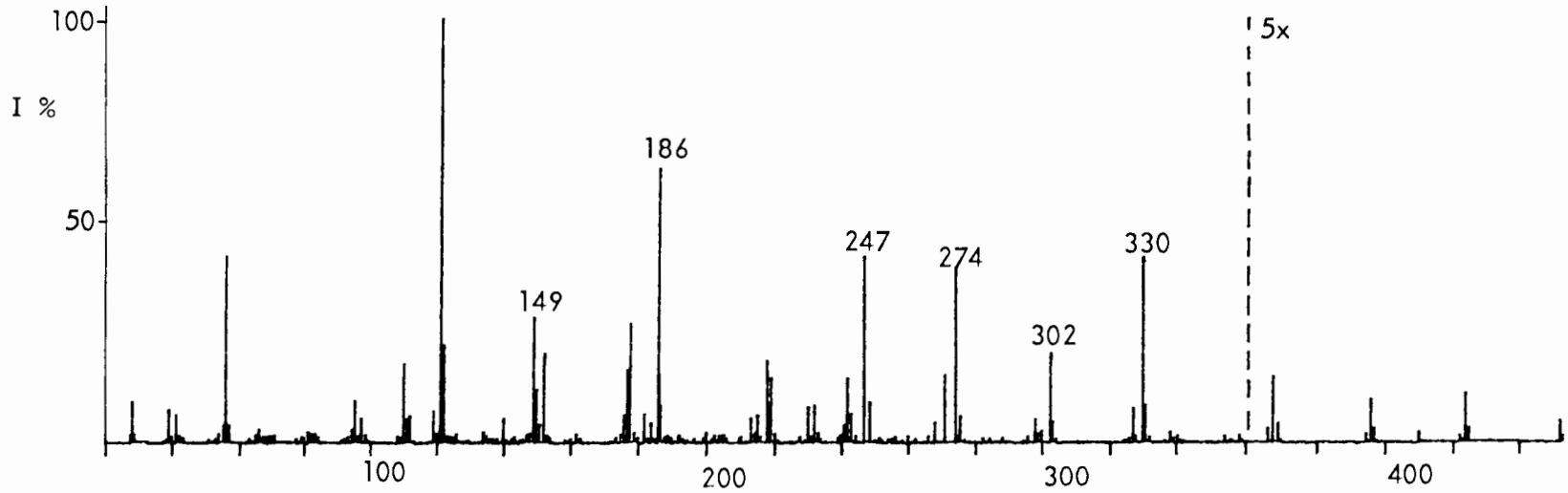

Fig. 3.5 Mass spectrum of $[Cp(CO)_2Fe]_2\{\mu\text{-}(CH_2)_7\}$ (VII)

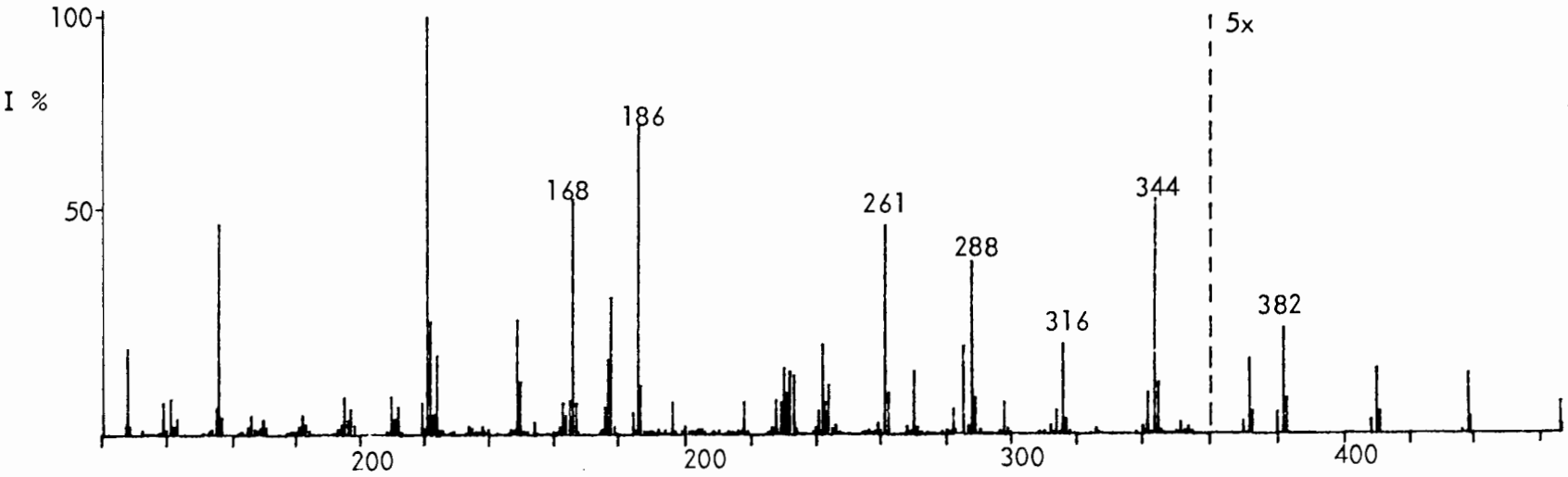

Fig. 3.6 Mass spectrum of $[Cp(CO)_2Fe]_2\{\mu\text{-}(CH_2)_8\}$ (VIII)

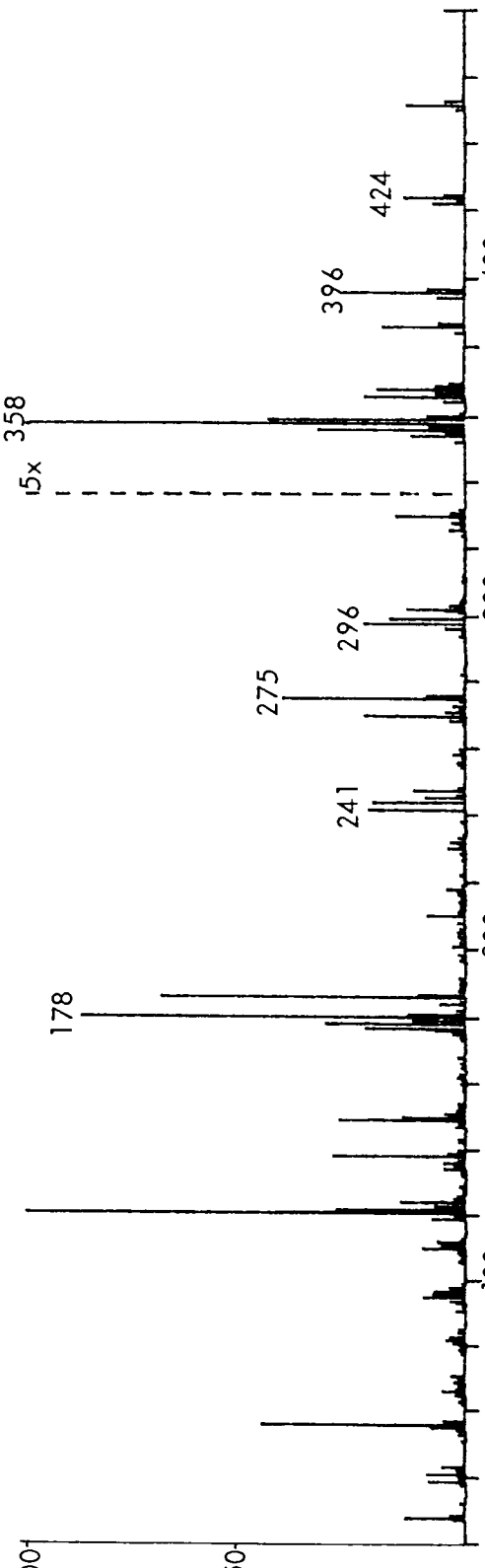

Fig. 3.7 Mass spectrum of $[Cp(CO)_2Fe]_2\{\mu-(CH_2)_9\}$ (IX)

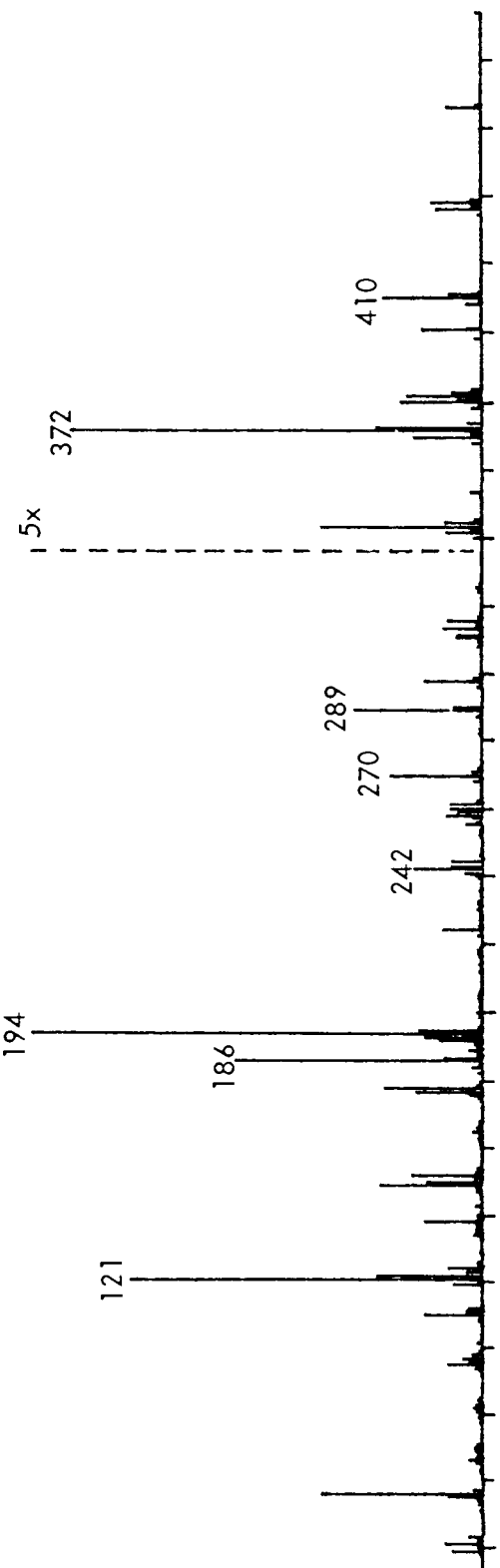

Fig. 3.8 Mass spectrum of $[Cp(CO)_2Fe]_2\{\mu-(CH_2)_{10}\}$ (X)

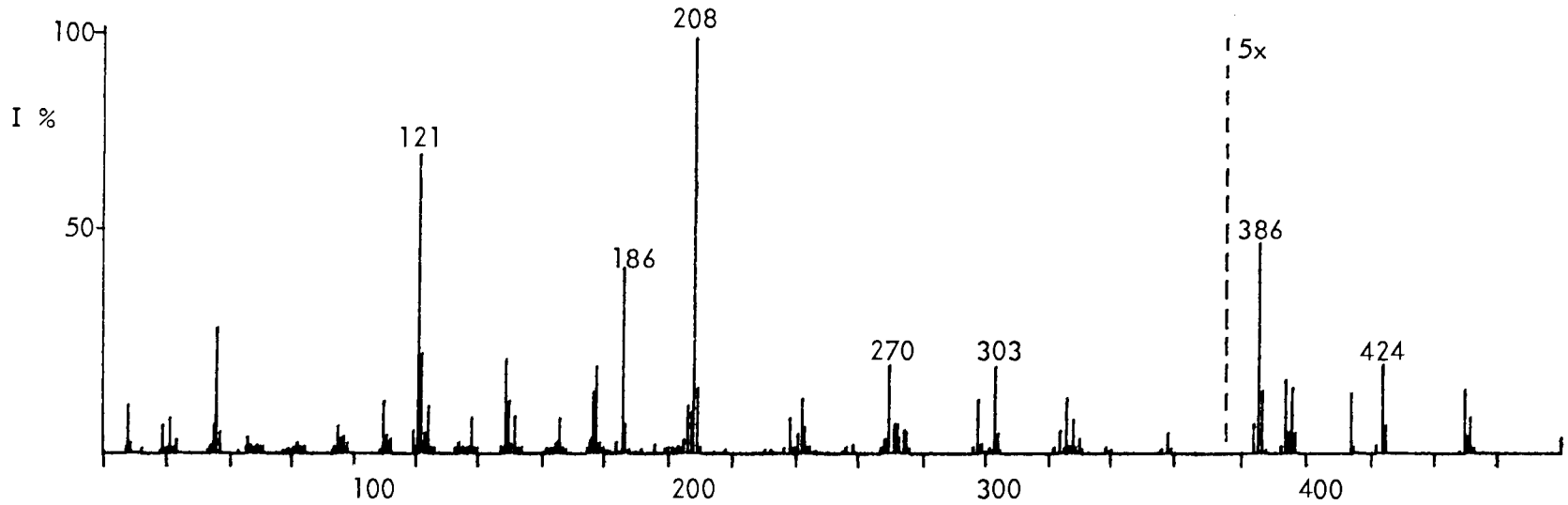

Fig. 3.9 Mass spectrum of $[Cp(CO)_2Fe]_2\{\mu-(CH_2)_{11}\}$ (XI)

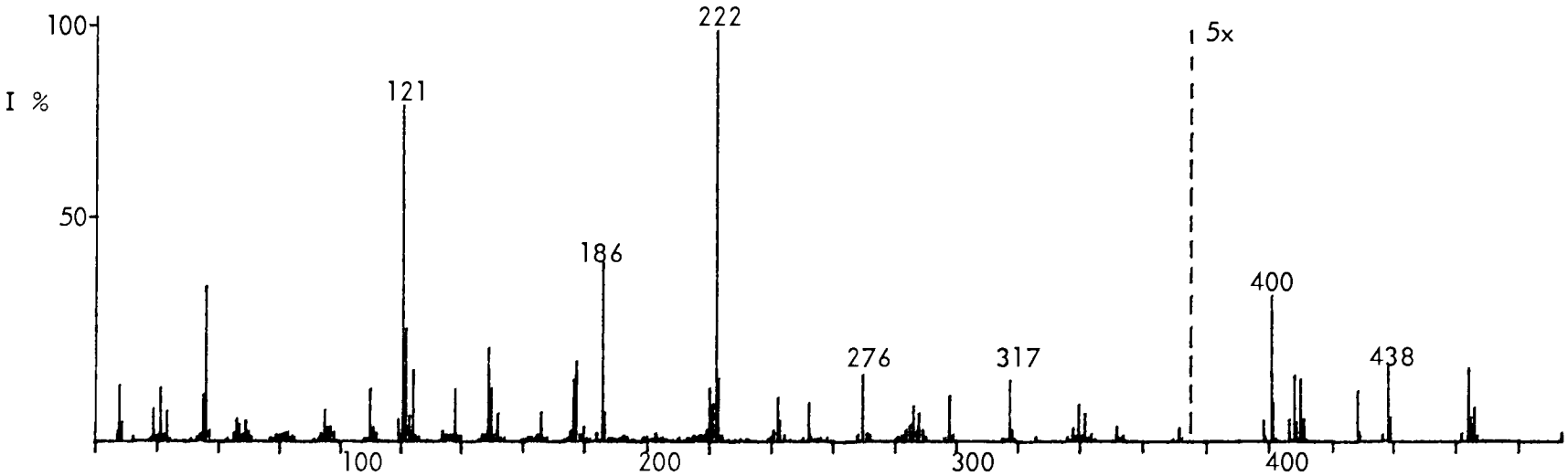

Fig. 3.10 Mass spectrum of $[Cp(CO)_2Fe]_2\{\mu-(CH_2)_{12}\}$ (XII)

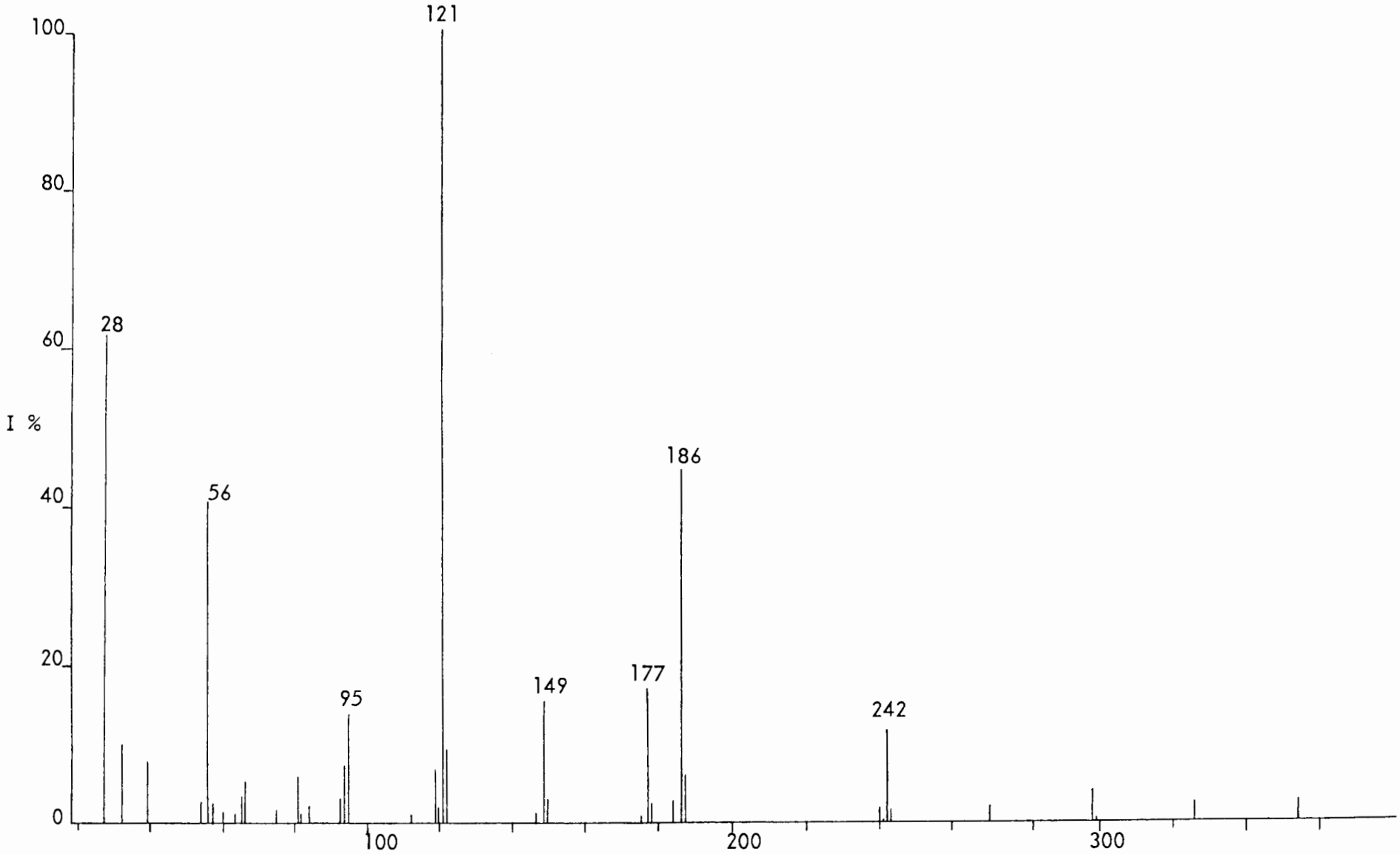

Fig. 3.11 Mass spectrum of $[Cp(CO)_2Fe]_2$

3.2 Mass Spectra of $[Cp(CO)_3W]_2\{\mu\text{-}(CH_2)_n\}$ (n = 3-5) (XIII) - (XV) and $[Cp(CO)_3W\{\mu\text{-}(CH_2)_3\}Fe(CO)_2Cp]$ (XIX)

3.2.1 General

The low resolution mass spectra of (XIII) - (XV) and (XIX) recorded as part of their characterisation are reported and discussed in this section.

The μ(1,n)alkanediyl ditungsten compounds are not very volatile and high source temperatures were required for these samples (220-245°C). Under these conditions, fragmentation of the compounds is extensive and a very low abundance of binuclear ions is observed (ca 2% of the total ion current). Parent ions were detected for (XIII) and (XV), but only in the unprocessed mass spectrum recorded as a U.V. trace. Other high mass peaks were also below the detection limit of the data system so do not appear in the mass spectra included in this work. These peaks are given in the tabulated mass spectral data for each compound.

The mass spectra of the more volatile mixed metal compound (XIX) was obtained readily at a lower source temperature (see Table 6.1).

The assignment of peaks in the mass spectra of these tungsten compounds is complicated by the extensive isotope patterns of tungsten-containing ions. To resolve the complex patterns formed by the superposition of peaks due to different ions, comparison was made with calculated isotope combination patterns. By adding the isotope patterns for the different ions in varying ratios a close match of the calculated pattern to the observed pattern was achieved. This was particularly useful for ions resulting from successive

dehydrogenations of other fragments.

3.2.2 Results and Discussion

3.2.2.1 Mass spectra of (XIII) - (XV)

The mass spectra of (XIII) - (XV) are shown in Figs. 3.14 - 3.16 respectively. The spectrum of $[Cp(CO)_3W]_2$ is included for comparison (Fig. 3.17). Peaks in the mass spectra of (XIII) - (XV) in common with the spectrum of $[Cp(CO)_3W]_2$ are listed in Table 3.4. In this study, marked differences between the relative intensities of these peaks in the mass spectra of the alkanediyl bridged compounds and those in the spectrum of the dimer, are attributed to the contribution of another sample fragment ion of the same mass (see for example the assignments for the peaks at $^m/e$ 333, 305 and 275 in the mass spectrum of (XIV)). Tables 3.5 - 3.7 give the intensities and assignments of the other major peaks in the spectra of (XIII) - (XV) respectively. The $^m/e$ values given are for the ions containing ^{184}W. Calculated isotope combination patterns for various ions are shown in Figs. 3.18, 3.19.

The fragmentation patterns of (XIII) - (XV) resemble those of the μ(1,n)alkanediyl diiron compounds. A regular loss of 28 mass units from the parent and fragment ions is observed. By analogy with the diiron compounds, this is attributable mainly to the successive elimination of CO groups. In addition, many of the tungsten-containing ions exhibit successive loss of hydrogen subsequent to CO loss. The source of the hydrogen atoms could be either the hydrocarbon bridge or the cyclopentadienyl groups. In contrast to $[CpFe]^+$, the $[CpW]^+$ ion does eliminate hydrogen. Loss of H_2 from the cyclopentadienyl group is also observed in the mass spectra of rhenium

Table 3.4 Intensities and assignments of common peaks in the mass spectra of (XIII) - (XV) and $[Cp(CO)_3W]_2$.

m/e	Ion	Relative Peak intensity (%)[a]			
		$[Cp(CO)_3W]_2$	(XIII)[b]	(XIV)[c]	(XV)[b]
498	$[Cp_2W_2]^+$	71	7	8	10
496	$[(C_5H_3)CpW_2]^+$	70	8	9	8
472	$[(C_3H_3)CpW_2]^+$	13	2	-	3
333	$[Cp(CO)_3W]^+$	47	67	97	57
305	$[Cp(CO)_2W]^+$	56	40	71	41
277	$[Cp(CO)W]^+$	55	37	45	33
249	$[CpW]^+$	100	37	33	38
247	$[(C_5H_3)W]^+$	91	30	27	34
234	$[(C_4H_2)W]^+$	10	2	2	3
221	$[(C_3H)W]^+$	36	6	8	11
209	$[(C_2H)W]^+$	5	2	1	2
152.5	$[Cp(CO)_2W]^{2+}$	1	-	2	-
138.5	$[Cp(CO)W]^{2+}$	2	-	-	-
124.5	$[CpW]^{2+}$	13	5	3	2
66	$[C_5H_6]^+$	3	5	3	2
65	$[C_5H_5]^+$	1	2	1	-
39	$[C_3H_3]^+$	5	8	5	-

a : percentage of base peak

b : base peak m/e 317

c : base peak m/e 331

Table 3.5 Peak intensities and assignments in the mass spectrum of $[Cp(CO)_3W]_2\{\mu\text{-}(CH_2)_3\}$ (XIII)

m/e	Ion [a]	Relative Peak intensity (%) [b]
708	$[P]^+$	>0.2 [c]
666	$[P\text{-}C_3H_6]^+$	>0.2 [c]
638	$[P\text{-}C_3H_6\text{-}CO]^+$	>0.2 [c]
610	$[P\text{-}C_3H_6\text{-}2CO]^+$	8
582	$[P\text{-}C_3H_6\text{-}3CO]^+$	3
566	$[P\text{-}5CO\text{-}H_2]^+$	1
554	$[P\text{-}C_3H_6\text{-}4CO]^+$	2
536	$[P\text{-}6CO\text{-}2H_2]^+$	7
526	$[P\text{-}C_3H_6\text{-}5CO]^+$	1
508	$[P\text{-}6CO\text{-}C_2H_2\text{-}2H_2]^+$	7
375	$[Cp(CO)_3W(C_3H_6]^+$	6
345	$[Cp(CO)_2W(C_3H_4)]^+$	61
317	$[Cp(CO)W(C_3H_4)]^+$	100
289	$[CpW(C_3H_4)]^+$	58
287	$[CpW(C_3H_2)]^+$	44
158.5	$[Cp(CO)W(C_3H_4)]^{2+}$	1
144.5	$[CpW(C_3H_4)]^{2+}$	2
42	$[C_3H_6]^+$	10

a : P = $Cp_2(CO)_6W_2(C_3H_6)$

b : percentage of base peak m/e 317

c : peak below detection limit of data system.

Table 3.6 Peak intensities and assignments for the mass spectrum of $[Cp(CO)_3W]_2\{\mu\text{-}(CH_2)_4\}$ (XIV)

m/e	Ion [a]	Relative Peak intensity [b] (%)
694	$[P\text{-}CO]^+$	> 1
610	$[P\text{-}4CO]^+$	2
582	$[P\text{-}5CO]^+$	2
550	$[P\text{-}6CO\text{-}2H_2]^+$	4
522	$[P\text{-}6CO\text{-}2H_2\text{-}C_2H_4]^+$	3
498	$[P\text{-}6CO\text{-}C_4H_8]^+$	8
389	$[Cp(CO)_3W(C_4H_8)]^+$	17
361	$[Cp(CO)_2W(C_4H_8)]^+$	27
333	$[Cp(CO)W(C_4H_8)]^+$, $[Cp(CO)_3W]^+$	95
331	$[Cp(CO)W(C_4H_6)]^+$	100
305	$[CpW(C_4H_8)]^+$, $[Cp(CO)_2W]^+$	70
303	$[CpW(C_4H_6)]^+$	90
301	$[CpW(C_4H_4)]^+$	75
275	$[CpW(C_2H_2)]^+$	45
55	$[C_4H_7]^+$	3
41	$[C_3H_5]^+$	4

a : P = $Cp_2(CO)_6W_2(C_4H_8)$

b : Percentage of base peak m/e 331

Table 3.7 Peak intensities and assignments for the mass spectrum of $[Cp(CO)_3W]_2\{\mu\text{-}(CH_2)_5\}$ (XV)

m/e	Ion [a]	Relative Peak Intensity (%)
736	$[P]^+$	1
708	$[P\text{-}CO]^+$	4
680	$[P\text{-}2CO]^+$	1
622	$[P\text{-}4CO\text{-}H_2]^+$	1
610	$[P\text{-}C_5H_{10}\text{-}2CO]^+$	3
594	$[P\text{-}5CO\text{-}2H_2]^+$	3
582	$[P\text{-}C_5H_{10}\text{-}3CO]^+$	2
562	$[P\text{-}6CO\text{-}4H_2]^+$	5
554	$[P\text{-}C_5H_{10}\text{-}4CO]^+$	3
536	$[P\text{-}6CO\text{-}4H_2\text{-}C_2H_2]^+$	5
526	$[P\text{-}C_5H_{10}\text{-}5CO]^+$	3
508	$[P\text{-}6CO\text{-}4H_2\text{-}2C_2H_2]^+$	5
456	$[P\text{-}6CO\text{-}4H_2\text{-}3C_2H_2]^+$	1
430	$[P\text{-}6CO\text{-}4H_2\text{-}4C_2H_2]^+$	1
375	$[Cp(CO)_2W(C_5H_{10})]^+$	36
345	$[Cp(CO)W(C_5H_8]^+$	83
317	$[CpW(C_5H_8)]^+$	100
315	$[CpW(C_5H_6)]^+$	95
289	$[CpW(C_3H_4)]^+$	27
158.5	$[CpW(C_5H_6)]^{2+}$	2
144.5	$[CpW(C_3H_4)]^{2+}$	2
70	$[C_5H_{10}]^+$	3

a : P = $Cp_2(CO)_6W_2(C_5H_{10})$

b : Percentage of base peak m/e 317

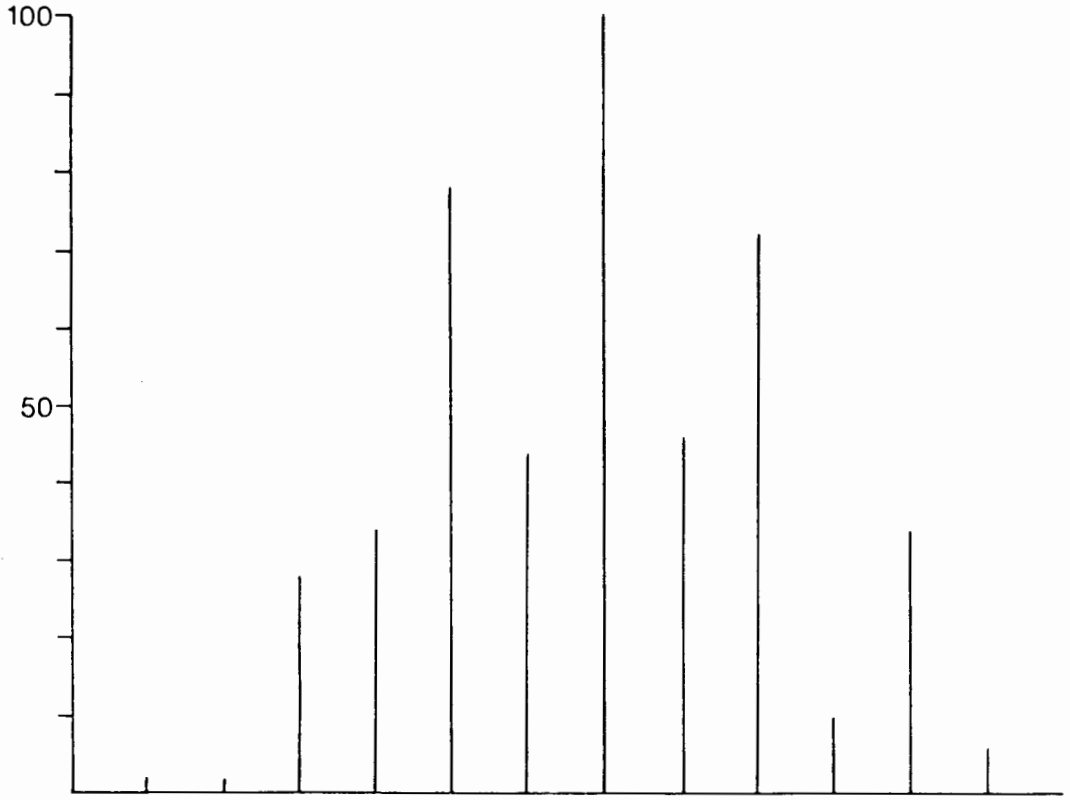

(a) Approximate isotope pattern for ditungsten ions

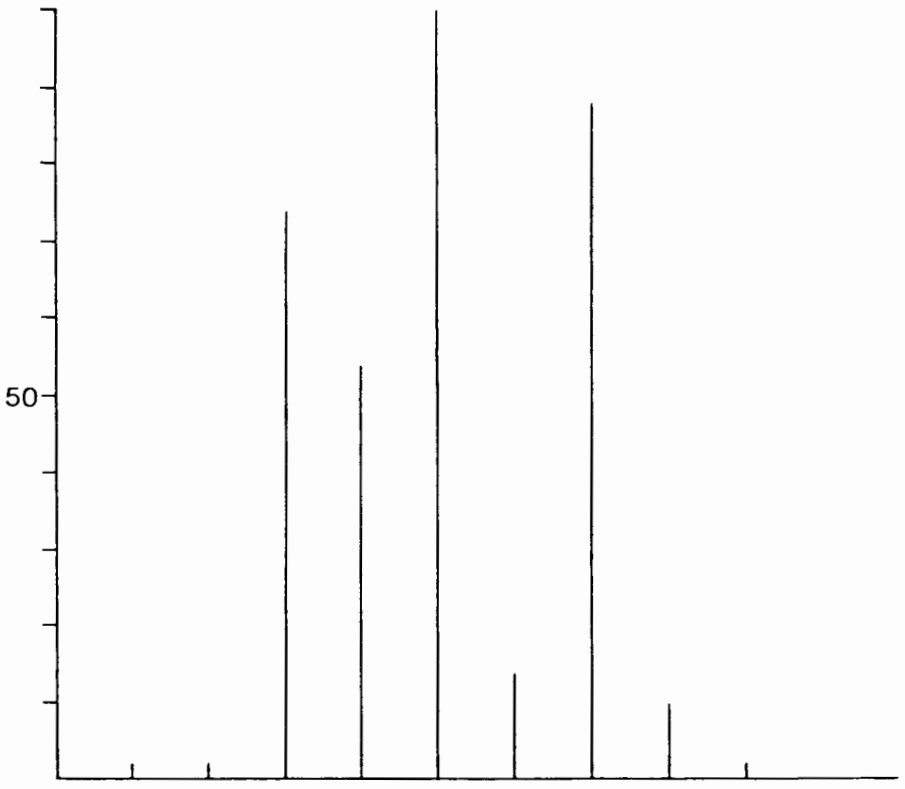

(b) Approximate isotope pattern for monotungsten ions

Fig. 3.18 Calculated isotope patterns

(a) Isotope combination pattern for the ions $[CpW]^+$ and $[(C_5H_3)W]^+$

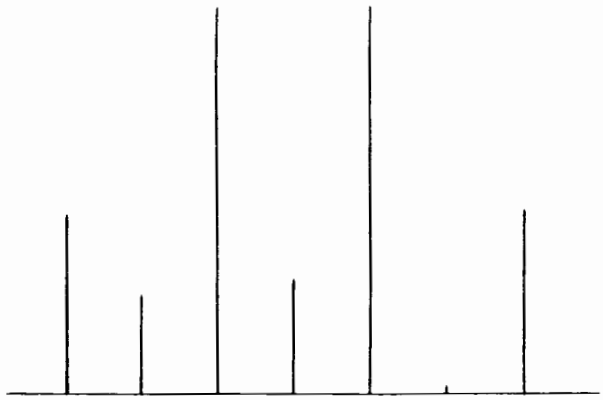

(b) Isotope combination pattern for the ions $[CpW(C_4H_8)]^+$, $[CpW(C_4H_6)]^+$ and $[CpW(C_4H_4)]^+$

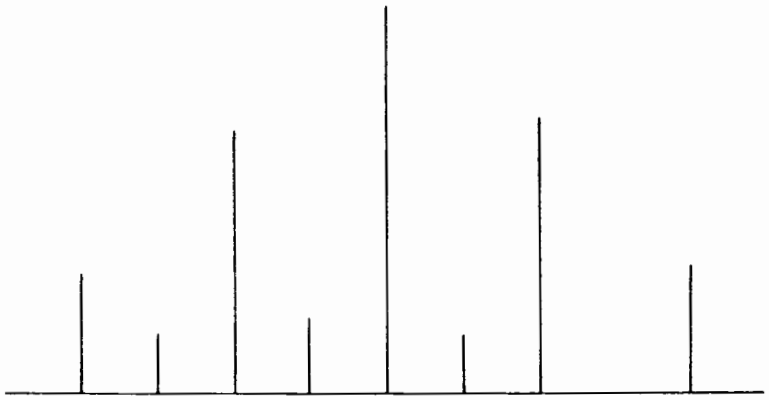

(c) Isotope combination pattern for the ions $[Cp_2W_2]^+$ and $[Cp(C_5H_3)W_2]^+$

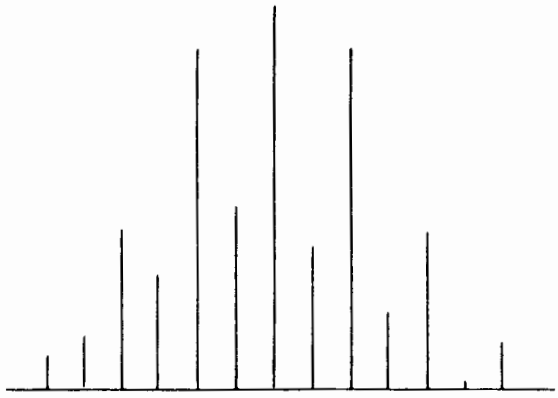

(d) Isotope combination pattern for the ions $[Cp_2W_2(C_nH_{2n})]^+$, $[Cp_2W_2(C_nH_{2n-2})]^+$ & $[Cp_2W_2(C_nH_{2n-4})]^+$

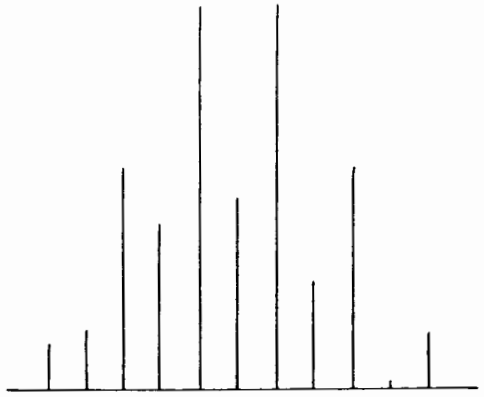

Fig. 3.19 Calculated isotope patterns

cyclopentadienyl compounds, [68] and it is suggested that the metal atom serves to catalyse the dehydrogenation. Differences in the catalytic effects of iron and tungsten could account for the observed difference in the fragmentation of the metal cyclopentadienyl moiety. The loss of one molecule of hydrogen from both $[CpW]^+$ and $[Cp_2W_2]^+$ is observed in the spectrum of $[Cp(CO)_3W]_2$. This suggests that elimination of more than one molecule of hydrogen from ions in the mass spectra of (XIII) - (XV) is attributable to dehydrogenation of the hydrocarbon chain. Consecutive loss of up to four molecules of H_2 from the $[P-x(CO)]^+$ (x = 4-6) ions is observed for compounds (XIII) - (XV). As suggested for the iron compounds this dehydrogenation probably results in the formation of species with a π-bonded hydrocarbon ligand. These ions decompose further by elimination of hydrocarbon fragments; for example, $[W_2(C_{15}H_{14})]^+$ formed by elimination of 3 H_2 molecules from $[Cp_2W_2(C_5H_{10})]^+$ in the spectrum of (XV) decomposes by successive elimination of five neutral acetylene molecules (C_2H_2).

Two other decomposition pathways, competing with stepwise CO loss, can be identified for (XIII) - (XV). These are analogous to those observed for the corresponding diiron compounds, involving elimination of the fragments C_nH_{2n} and $Cp(CO)_3W$ from the ions $[P-x(CO)]^+$(x = 0 or 1). The elimination of $Cp(CO)_3W$ from these compounds supports the assumption that they, like the diiron and dimolybdenum compounds [31,19], contain no metal-metal bond.

For (XIII), as for $[Cp(CO)_2Fe]_2\{\mu-(CH_2)_3\}$, elimination of C_3H_6 and $Cp(CO)_3W$, in competition with CO loss, from the parent ion is observed. The loss of C_3H_6 is followed by successive loss of CO to give $[Cp_2W_2]^+$. Elimination of $Cp(CO)_3W$ from the parent ion produces $[Cp(CO)_3W(C_3H_6)]^+$. This loses CO and H_2 to give an ion which could be formulated as the

η^3-allyl species 54 .

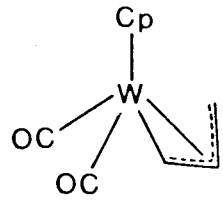

54

This ion and the ions $[Cp(CO)_{3-x}W(C_3H_4)]^+$ (x = 2,3) are the most abundant in the mass spectrum of (XIII). The dipositive ions $[Cp(CO)_{3-x}W(C_3H_4)]^{2+}$ (x = 2,3) are also observed, reflecting the stability of these species.

For (XIV) and (XV), metastable peaks indicate that the $Cp(CO)_3W$ fragment is lost from the $[P-CO]^+$ ion as observed in the parallel decomposition route for $[Cp(CO)_2Fe]_2\{\mu-(CH_2)_n\}$. The resulting ion $[Cp(CO)_2W(C_nH_{2n})]^+$ loses CO and H_2 to give the presumably η^3allyl species $[Cp(CO)W(C_nH_{2n-2})]^+$.

Decomposition via elimination of C_nH_{2n} is less significant for the longer chain compounds than for (XIII), only occurring from the ions $[P-xCO]^+$ (x = 4-5). Elimination of a C_5H_6 fragment is not observed for any of the ditungsten compounds.

3.2.2.2 Mass Spectrum of $[Cp(CO)_3W\{\mu-(CH_2)_3\}Fe(CO)_2Cp]$ (XIX)

The mass spectrum of (XIX) is shown in Fig. 3.20 and Table 3.8 gives the intensities and assignments of the major peaks in the spectrum. Isotope combination patterns calculated to match the observed patterns centred at $^m/e$ 372, 346, 317 and 289 are shown in Fig. 3.21. On the basis of the computer matching, these complex patterns could be resolved into the

Table 3.8 Peak intensities and assignments for the mass spectrum of $[Cp(CO)_3W\{\mu\text{-}(CH_2)_3\}Fe(CO)_2Cp]$

m/e [a]	Ion [b]	Relative Peak intensity (%) [c]
552	$[P]^+$	> 0.2
524	$[P\text{-}CO]^+$	> 0.2
508	$[P\text{-}C_3H_6]^+$	> 0.2
496	$[P\text{-}2CO]^+$	1
482	$[P\text{-}C_3H_6\text{-}CO]^+$	0.5
468	$[P\text{-}3CO]^+$	1
454	$[P\text{-}C_3H_6\text{-}2CO]^+$	4
440	$[P\text{-}4CO]^+$	1
438	$[P\text{-}4CO\text{-}H_2]^+$	1
426	$[P\text{-}C_3H_6\text{-}3CO]^+$	6
408	$[P\text{-}5CO\text{-}2H_2]^+$	4
402	$[P\text{-}3CO\text{-}C_5H_6]^+$	6
398	$[P\text{-}C_3H_6\text{-}4CO]^+$	5
384	$[CpW(CH_2)FeCp]^+$	4
375	$[Cp(CO)_3W(C_3H_6)]^+$	10
374	$[CpW(C_3H_5)Fe(CO)]^+$	11
370	$[CpWFeCp]^+$	14
347	$[Cp(CO)_2W(C_3H_6)]^+$	7
346	$[CpW(C_3H_5)Fe]^+$	7
344	$[(C_3H_3)WFeCp]+$	7
333	$[Cp(CO)_3W]^+$	17
319	$[Cp(CO)W(C_3H_6)]^+$	14
317	$[Cp(CO)W(C_3H_4)]^+$	16
305	$[Cp(CO)_2W]^+$, $[WFeCp]^+$	8
289	$[CpW(C_3H_4)]^+$	13
277	$[Cp(CO)W]^+$, $[WFe(C_3H)]^+$	6
249	$[CpW]^+$	8
219	$[Cp(CO)_2Fe(C_3H_6)]^+$	3
191	$[Cp(CO)Fe(C_3H_6)]^+$	36
186	$[Cp_2Fe]^+$	28
177	$[Cp(CO)_2Fe]^+$	28

/ Table 3.8 contd.

Table 3.8 (contd.)

$^{m}/_{e}$ [a]	Ion [b]	Relative Peak intensity (%) [c]
163	$[CpFe(C_3H_6)]^+$	33
149	$[Cp(CO)Fe]^+$	29
134	$[Fe(C_6H_6)]^+$	2
121	$[CpFe]^+$	100
95	$[Fe(C_3H_3)]^+$	12
81	$[Fe(C_2H_2)]^+$	4
66	$[C_5H_6]^+$	5
65	$[C_5H_5]^+$	3
56	$[Fe]^+$	31
41	$[C_3H_5]^+$	7

a : $^{m}/_{e}$ value given for ion containing ^{184}W and/or ^{56}Fe

b : P = $Cp_2(CO)_5WFe(C_3H_6)$

c : percentage of base peak $^{m}/_{e}$ 121

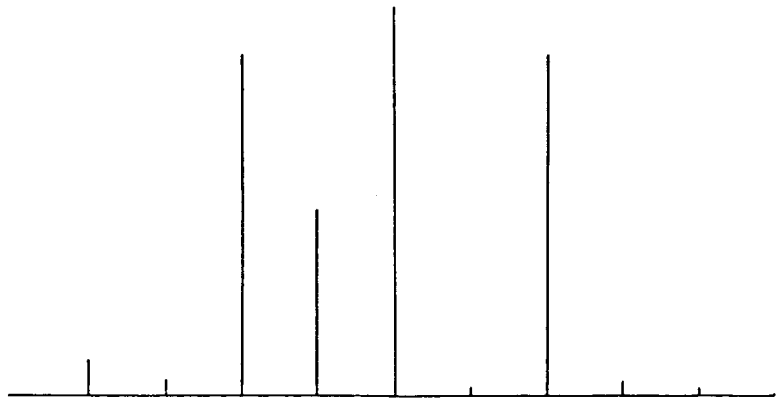

(a) Calculated isotope pattern for ions containing an iron and a tungsten atom

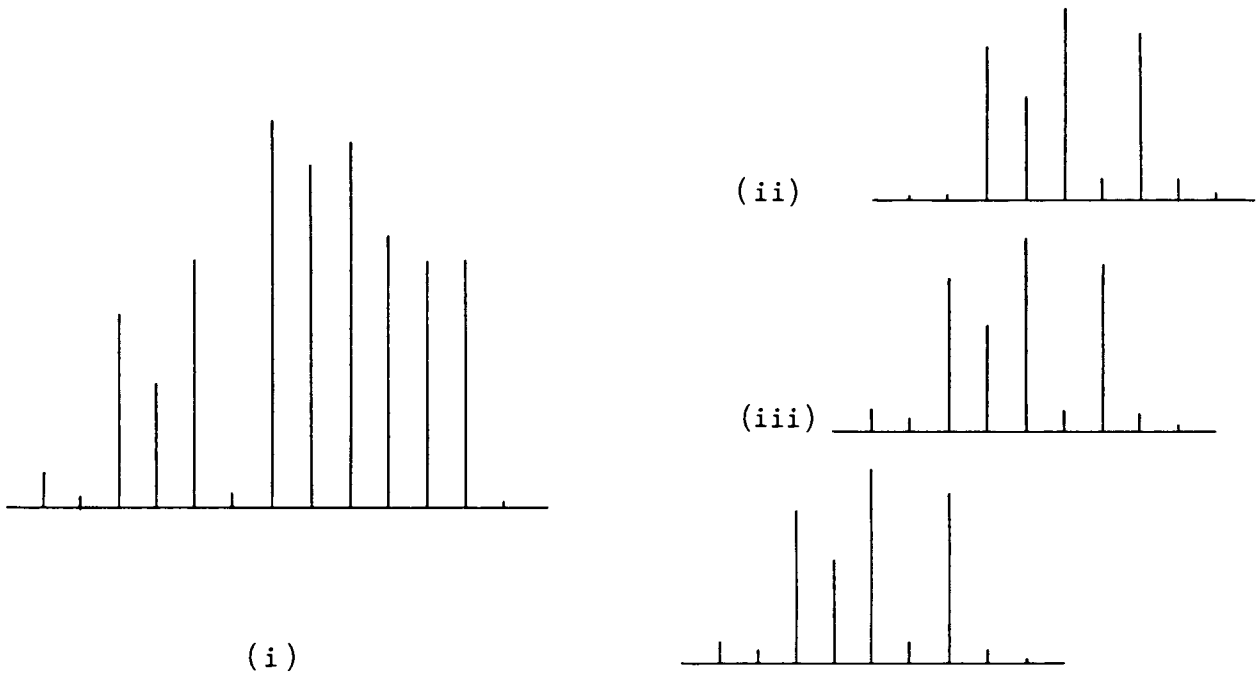

(b) (i) Calculated isotope combination pattern matching the observed pattern centered at $^{m}/e$ 372. The component isotope patterns (ii) - (iv) contributing to the combination pattern (i) are for the ions $[Cp(CO)_3W(C_3H_6)]^+$ ($^{m}/e$ 375), $[CpW(C_3H_5)Fe(CO)]^+$ ($^{m}/e$ 374), and $[CpWFeCp]$ ($^{m}/e$ 370)

Fig. 3.21 Calculated isotope patterns

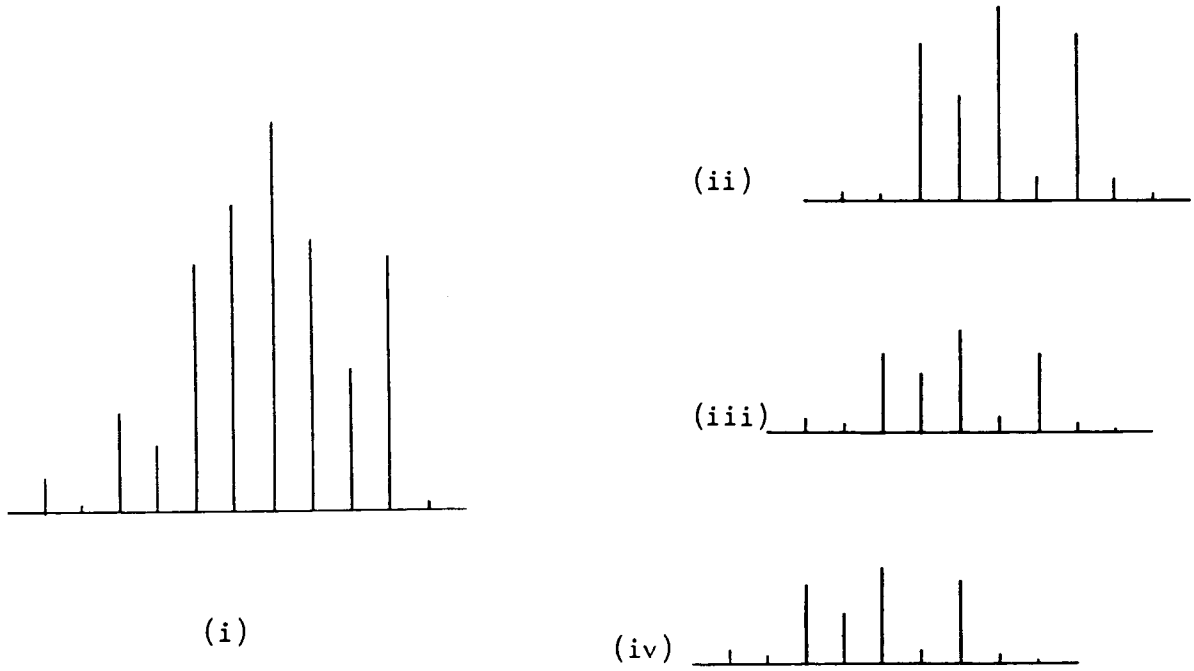

(c) (i) Calculated isotope combination pattern matching the observed pattern centred at $^{m}/e$ 346. The component isotope patterns (ii) - (iv) are for the ions $[Cp(CO)_2W(C_3H_6)]^+$ ($^{m}/e$ 347), $[CpW(C_3H_5)Fe]^+$ ($^{m}/e$ 346) and $[(C_3H_3)WFeCp]^+$ ($^{m}/e$ 344).

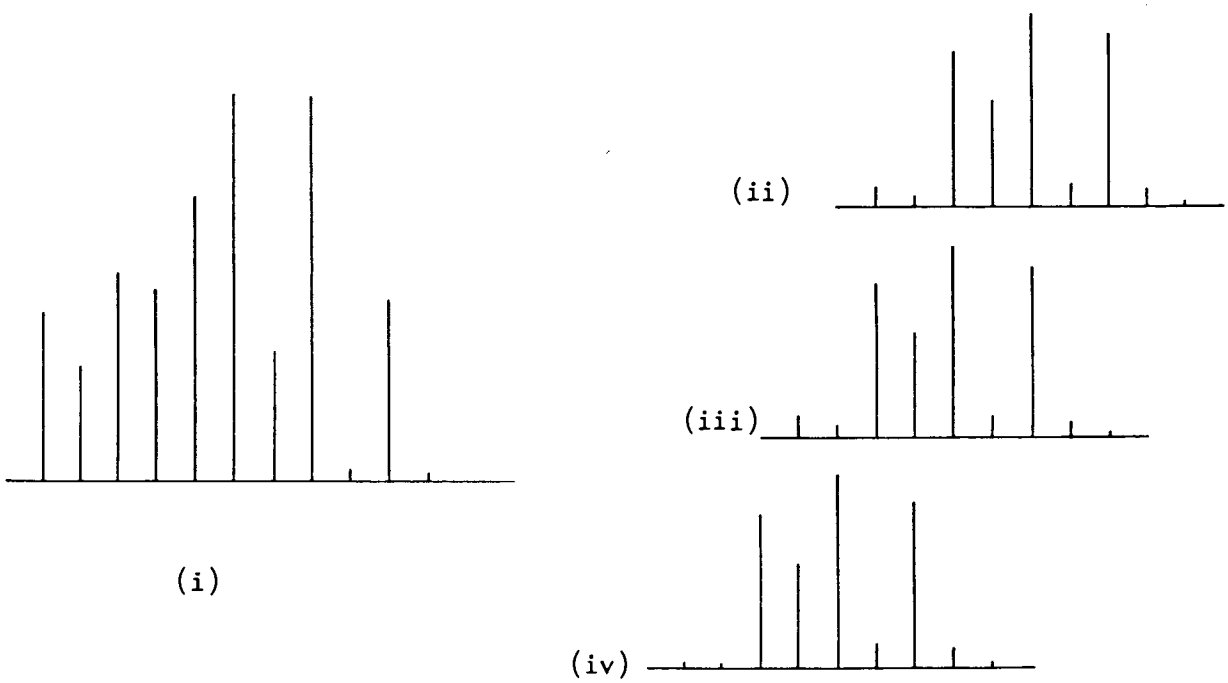

(d) (i) Calculated isotope combination pattern matching the observed pattern centred at $^{m}/e$ 317. The component patterns (ii) - (iv) are for the ions $[Cp(CO)W(C_3H_6)]$ ($^{m}/e$ 319), $[Cp(CO)W(C_3H_4)]$ ($^{m}/e$ 317) and an unidentified ion of $^{m}/e$ 314.

Fig. 3.21 (continued)

component patterns due to different fragment ions, and assignment of these ions made.

The fragmentation patterns in the mass spectrum of (XIX) can be interpreted in terms of decomposition pathways analogous to those of both the diiron and ditungsten propanediyl bridged compounds. Competing elimination of the four fragments, CO, C_3H_6, $Cp(CO)_3W$ and $Cp(CO)_2Fe$ from the parent ion of (XIX) is observed. In addition decomposition of the $[P-3CO]^+$ ion via elimination of a C_5H_6 fragment is observed as in the mass spectrum of $[Cp(CO)_2Fe]_2\{\mu-(CH_2)_3\}$. By analogy, the elimination of this fragment can be attributed to a β-hydrogen transfer from the alkanediyl bridge to the iron atom in $[Cp(CO)W(C_3H_6)Fe(CO)Cp]^+$. The resulting alkenyl species $[Cp(CO)W(C_3H_5)Fe(CO)]^+$ decomposes by successive loss of CO and C_3H_5 to $[CpWFe]^+$.

It is interesting to note that a peak at $^m/_e$ 186 due to $[Cp_2Fe]^+$ occurs in the mass spectrum of (XIX). This could be attributed to a rearrangement of the $[CpWFeCp]^+$ ion formed by successive loss of C_3H_6 and five CO groups from the parent ion.

3.3 Mass spectra of $[(CO)_5Mn\{CO(CH_2)_4CO\}Mn(CO)_5]$ (XX) and $[(CO)_5Mn]_2\{\mu-(CH_2)_4\}$ (XXI).

The low resolution mass spectra of compounds(XX) and (XXI) were recorded as part of their characterisation and are shown in Figs. 3.22 and 3.23 respectively. These compounds are volatile and so low sources temperatures were required for the samples (See Table 6.1). Molecular ions were detected in the mass spectra of both (XX) and (XXI).

The fragmentation patterns of (XX) and (XXI) are characterised by a stepwise loss of 28 mass units from the parent ions, as observed in the mass spectra of all manganese carbonyl compounds. For compounds (XX) and (XXI) this could be attributed to the elimination of either CO or C_2H_4 from the $(CH_2)_4$ bridge. As a result no assignment of the fragment ions can be made for these compounds on the basis of the low resolution mass data.

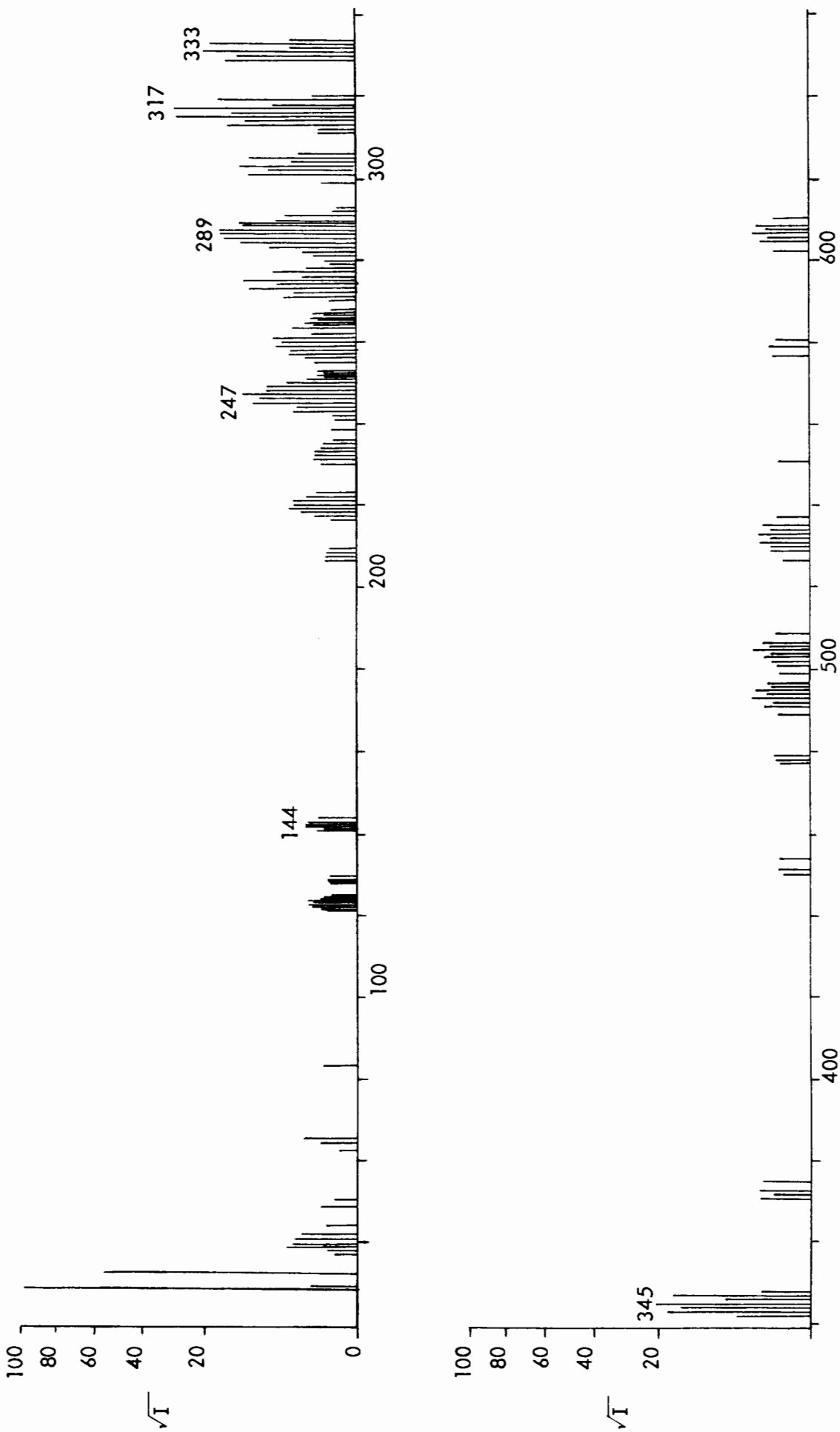

Fig. 3.14 Mass spectrum of $[Cp(CO)_3W]_2\{\mu-(CH_2)_3\}$ (XIII)

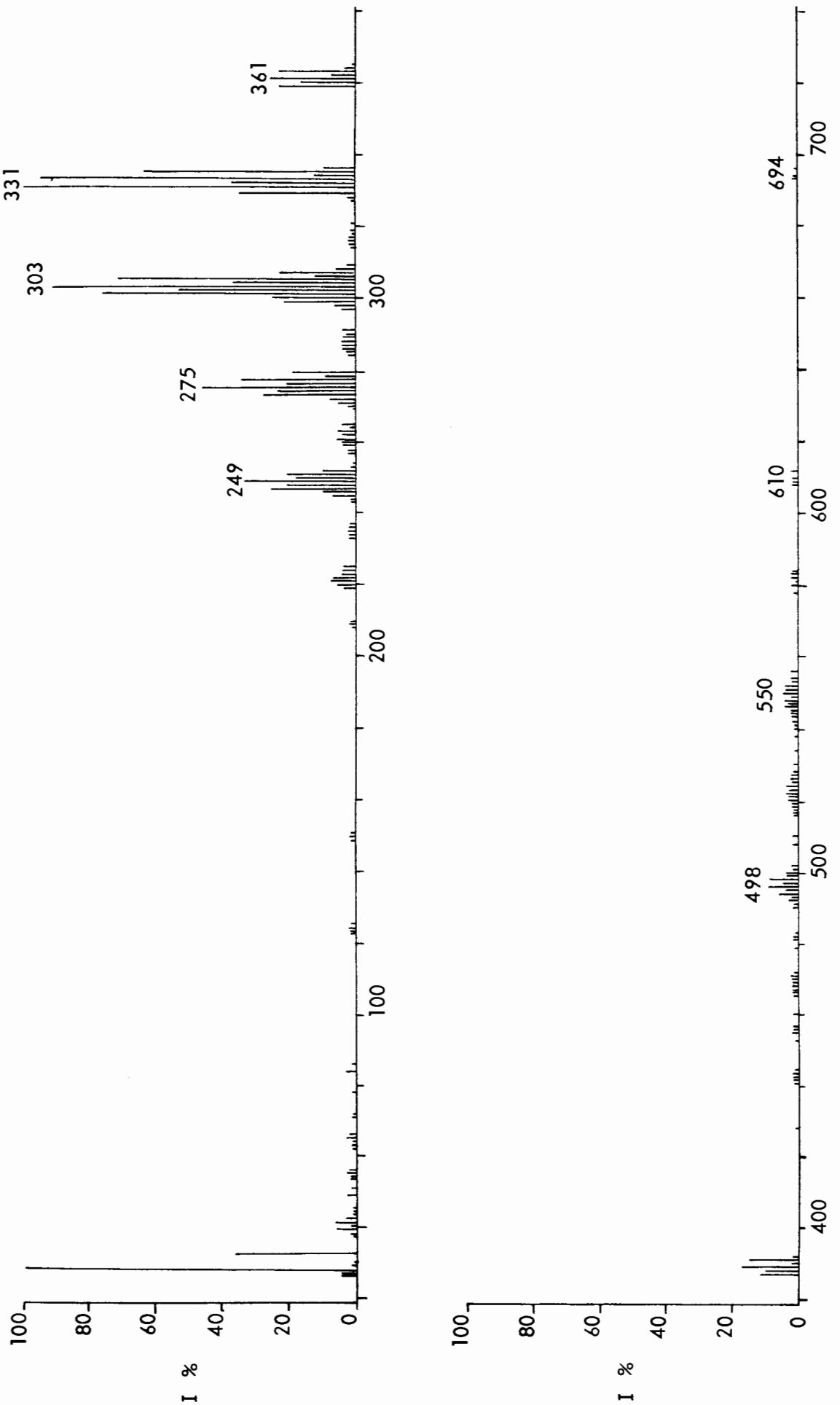

Fig. 3.15 Mass spectrum of $[Cp(CO)_3W]_2\{\mu\text{-}(CH_2)_4\}$ (XIV)

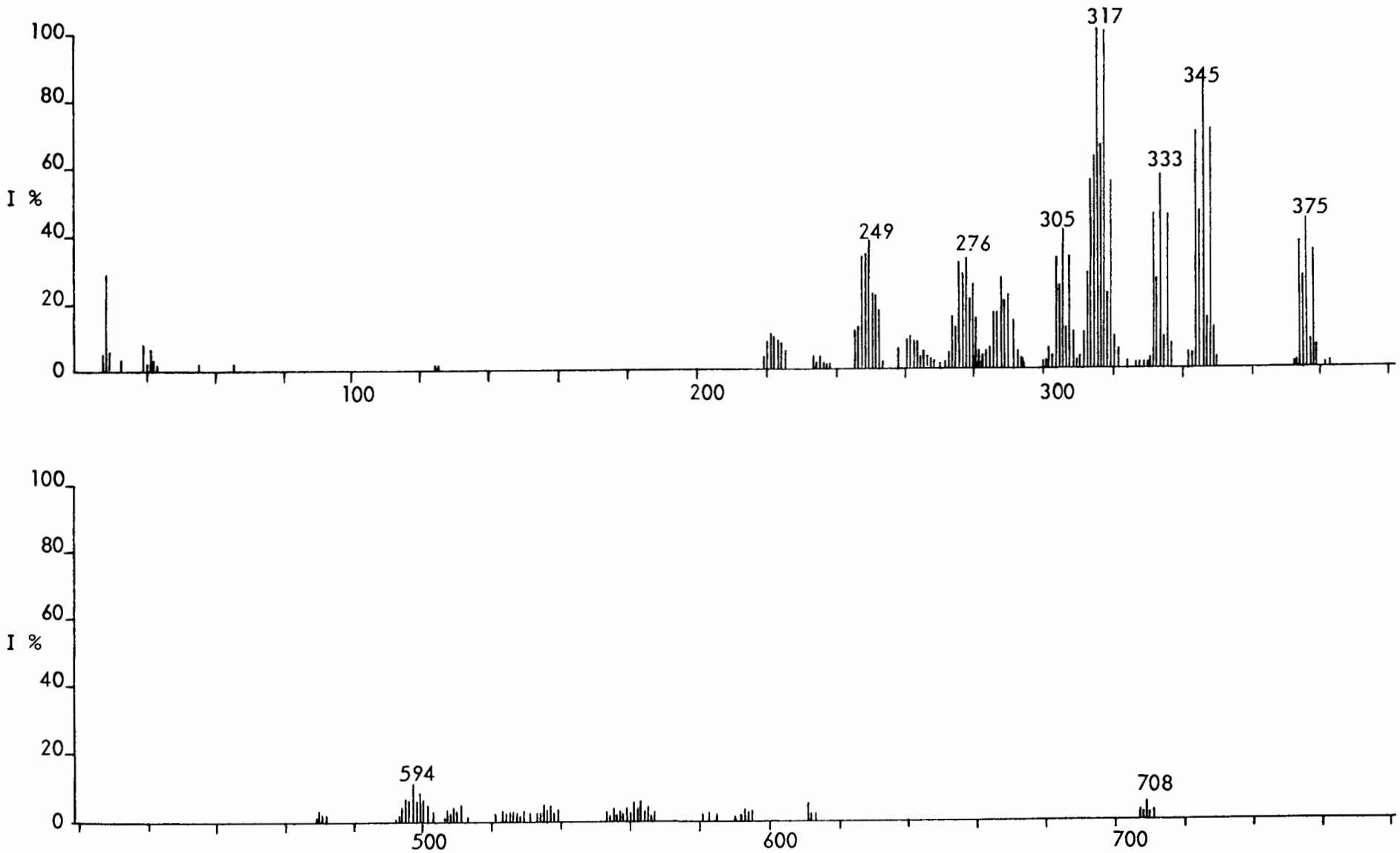

Fig. 3.16 Mass spectrum of $[Cp(CO)_3W]_2\{\mu\text{-}(CH_2)_5\}$ (XV)

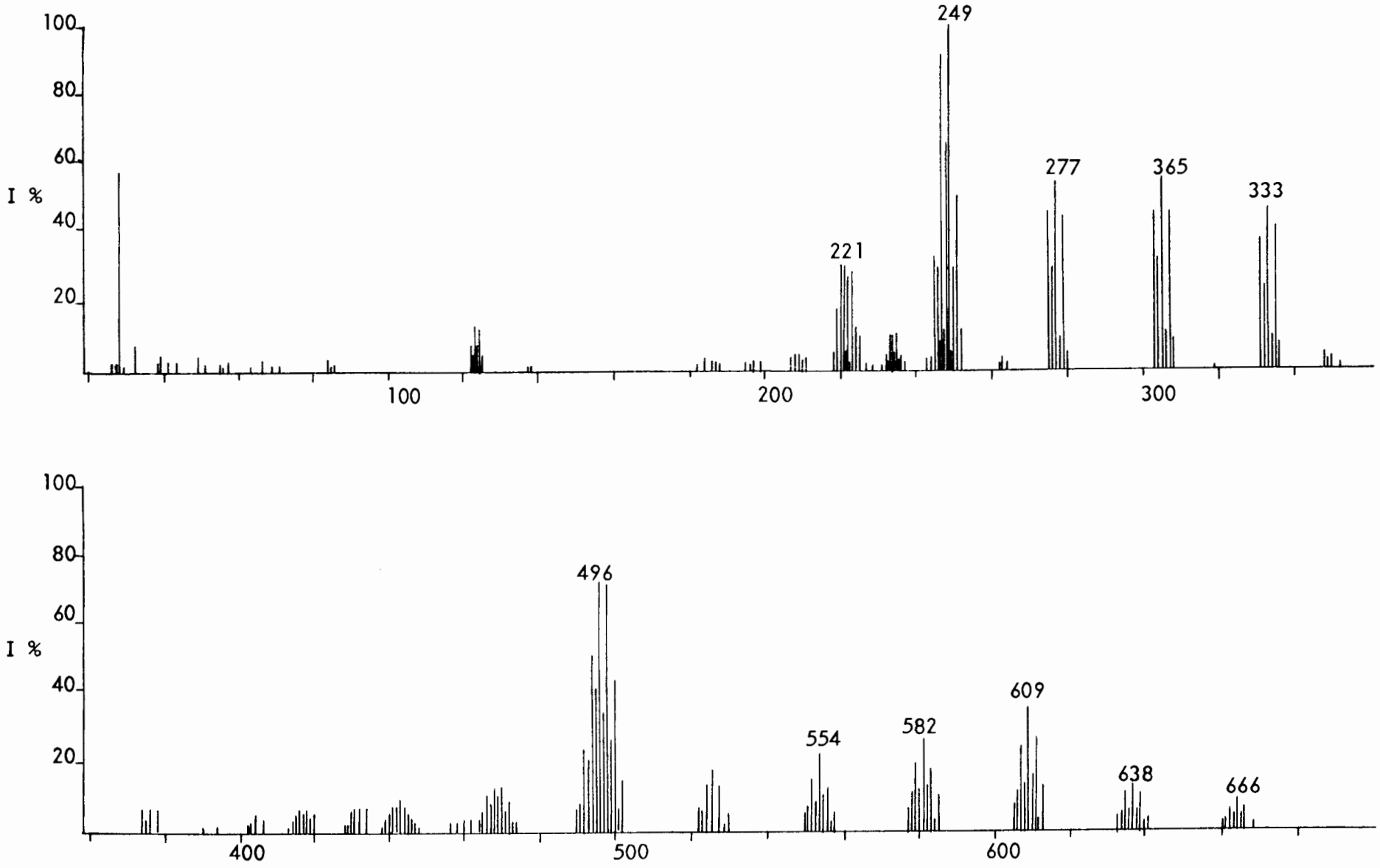

Fig. 3.17 Mass spectrum of $[Cp(CO)_3W]_2$

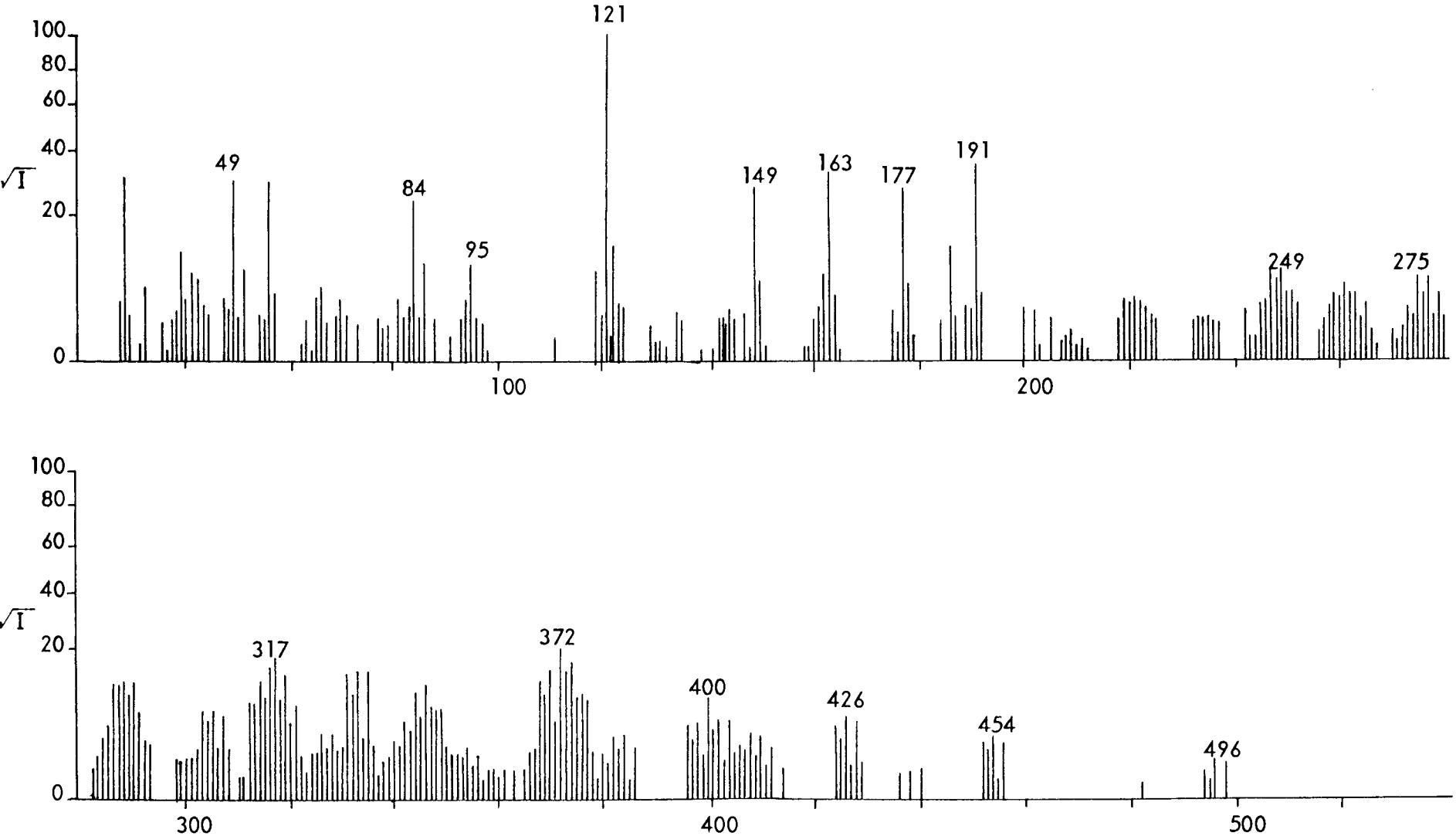

Fig 3.20 Mass spectrum of $[Cp(CO)_3W\{\mu\text{-}(CH_2)_3\}Fe(CO)_2Cp]$ (XIX)

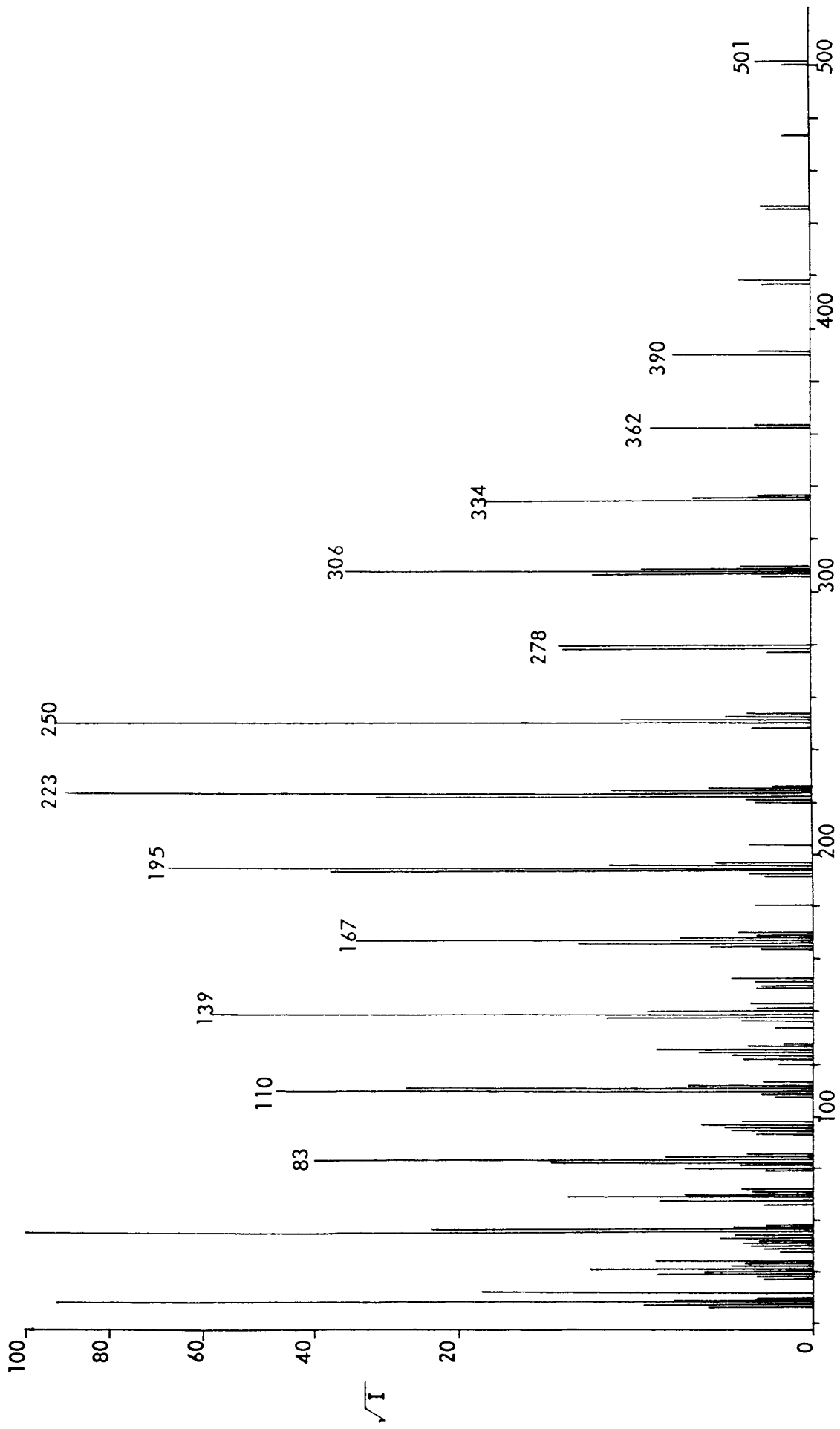

Fig. 3.22 Mass spectrum of $[(CO)_5Mn\{CO(CH_2)_4CO\}Mn(CO)_5]$ (XX)

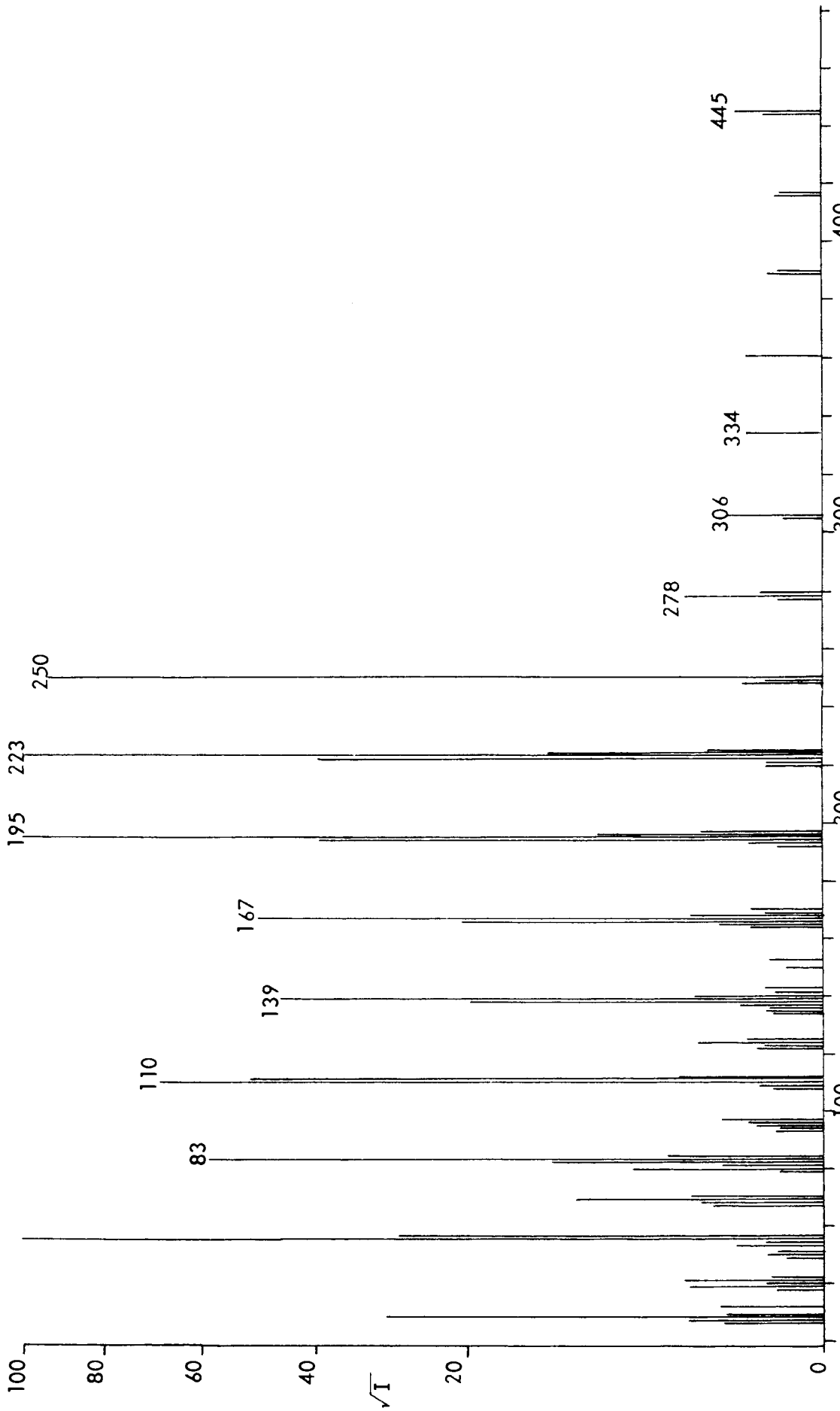

Fig. 3.23 Mass spectrum of $[(CO)_5Mn]_2\{\mu-(CH_2)_4\}$ (XXI)

SECTION 4

4. THERMAL ANALYSIS OF μ(1,n)ALKANEDIYL DIIRON AND DITUNGSTEN COMPOUNDS

4.1 Introduction

The thermal stability and decomposition products of μ(1,n)alkanediyl compounds are of interest particularly in view of the possible role of these compounds as models for catalytic intermediates. In this work the melting points and decomposition temperatures of $[Cp(CO)_2Fe]_2\{\mu\text{-}(CH_2)_n\}$ (n = 3-12) have been determined by Differential Scanning Calorimetry.† From the DSC results estimates for the enthalpies of melting and of the decomposition reactions have been made. The decomposition reactions of $[Cp(CO)_2Fe]_2\{\mu\text{-}(CH_2)_n\}$ (n = 3-8) and $[Cp(CO)_3W]_2\{\mu\text{-}(CH_2)_n\}$ (n = 3-5) have been investigated using Gas Chromatography to analyse the organic products.

4.2 DSC study of $[Cp(CO)_2Fe]_2\{\mu\text{-}(CH_2)_n\}$ (n = 3-12)

4.2.1 General remarks

Thermal analysis of the alkanediyl bridged iron compounds (III)-(XII) has been carried out by Differential Scanning Calorimetry (DSC). In this method, the sample and a reference are heated simultaneously and an equal rate of heating of sample and reference is maintained by adjustment of the heat input to the sample. The difference between heat input to the sample and that to the reference is measured and recorded as a function of temperature. Any endothermic or exothermic change in the sample will thus

---

† This technique has similarly been used in the study of mononuclear rhodium and iridium (III) metallacycles [74].

produce a peak in the DSC trace. If the calorimeter has been calibrated, the area under a peak in the trace will give a quantitative measure of the enthalpy of the change occurring in the sample.

To calibrate a DSC instrument, the DSC trace of a calibration standard with a known heat of fusion (ΔH_c) is recorded at a selected heating rate, instrument sensitivity and recorder chart speed. A calibration constant, k, is then determined from the relationship :

$$k = \frac{\Delta H_c \times m_c}{A_c} \qquad (32)$$

where m_c is the mass of calibrant used in recording the thermogram and A_c the peak area of the melting thermogram of the calibrant.

The enthalpy for any endo- or exo-thermic change in a sample, is ΔH_s , is then given by :

$$\Delta H_s = k \frac{M \times A_s}{m_s} \qquad (33)$$

where M is the molecular mass of the sample, m_s the mass of sample used and A_s the peak area of the sample thermogram recorded under the same conditions as the calibrant thermogram. In this experiment a calibration constant of 3.53 mJ(unit area)$^{-1}$ was determined based on the heat of fusion of indium metal.

4.2.2 DSC Results and Discussion

The DSC traces for compounds (III)-(XII) recorded over the range of 35-225°C are shown in Fig. 4.1. All traces show two peaks, a sharp endothermic peak and a broad exothermic peak at higher temperature. A second endothermic peak close to the first is observed in the traces for compounds (IV) and

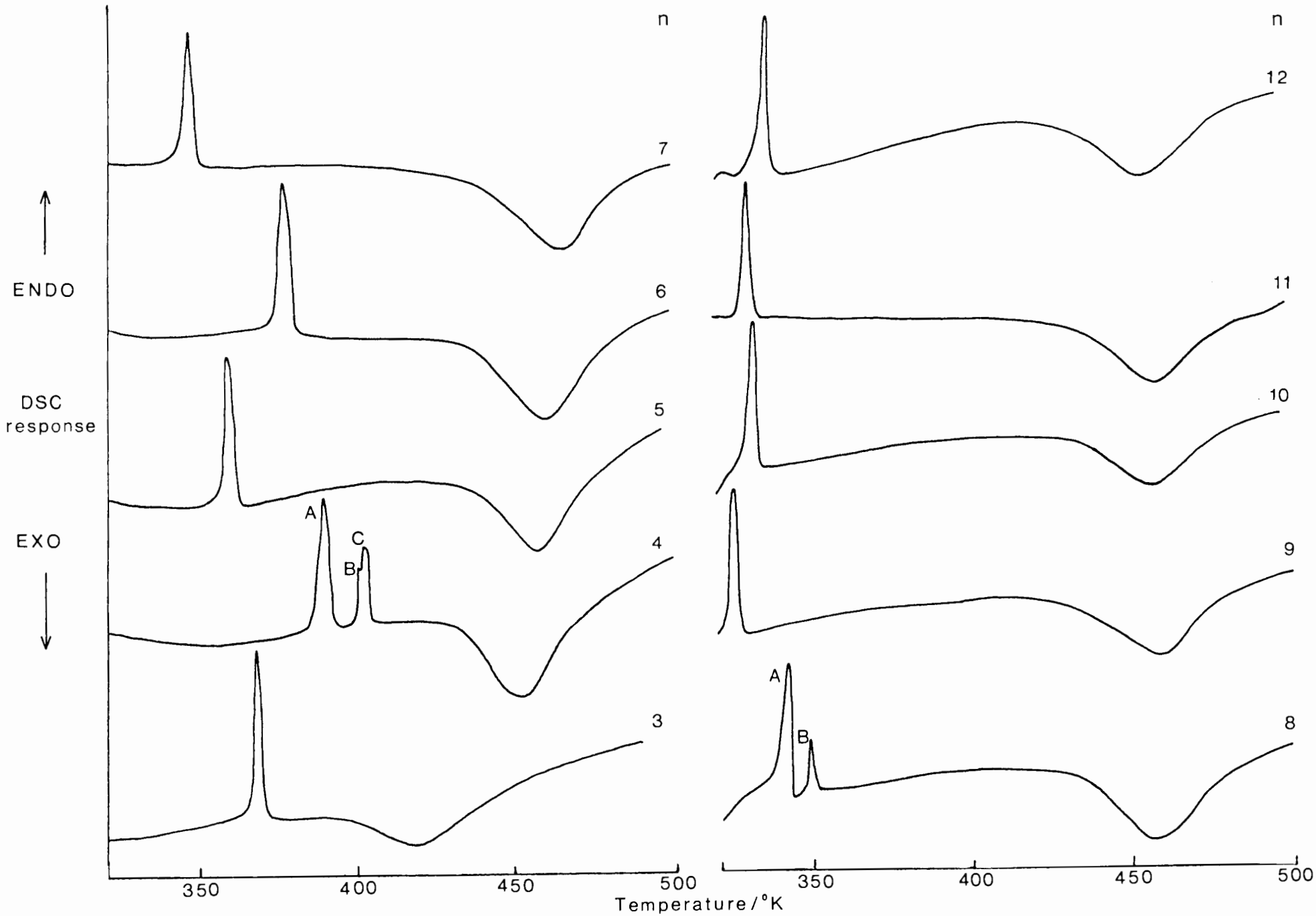

Fig. 4.1 DSC traces for compounds (III) - (XII)

(VIII). This has a shoulder on the low temperature side in the trace for (IV).

Table 4.1 lists the onset and peak temperatures, T_i and T_{max}, for the thermograms of each sample compound. These values were measured from the DSC traces as shown in Fig. 4.2. The enthalpy, ΔH_{endo} and ΔH_{exo}, calculated from equation (33), for the endotherms and exotherms respectively, are also given in Table 4.1. These are averages of values determined from several scans. The major sources of error in the determination of enthalpy values from a DSC thermogram are in the interpolation of the base line and peak integration. Errors of ±2-3 units in peak areas were observed in this experiment.

The endotherms observed for (III), (V)-(VII) and (IX)-(XII) and the higher temperature endotherms for (IV) and (VIII) occur in temperature ranges which coincide with the melting ranges measured for (III)-(XII) by conventional methods (Table 4.1), so these endotherms may be attributed to melting of the crystalline samples. The peak temperatures T_{max} are taken as the melting points of the compounds.

The appearance of two endotherms for (VIII) and three for (IV) suggests that these compounds are polymorphic,existing in several different crystalline forms or phases. The lower temperature endotherms correspond to phase transitions from one form to another. Observing a sample of compound (IV) or (VIII) during heating on a hotstage microscope, the phase transition can be clearly seen as a darkening of a portion of the crystals in the sample. This indicates that samples of these compounds, crystallised from solution comprise a mixture of the different crystalline forms.

Table 4.1 : Melting Ranges and DSC Results for the compounds $[CpFe(CO)_2]_2\{\mu-(CH_2)_n\}$

Compound	melting range/°C[a]	T(endo)/°C		ΔH_{endo}	T(exo)/°C		ΔH_{exo}
		T_i[b]	T_{max}[c]	kJ mol^{-1}	T_i[b]	T_{max}[c]	kJ mol^{-1}
(III)	104 - 105	104	107	33 ± 2	127	158	-53 ± 2
(IV)		A 114	117	-	159	178	-130 ± 2
	125 - 126	B 125	128	12 ± 1			
		C -	131	-			
(V)	83 - 85	84	87	38 ± 1	161	182	-134 ± 2
(VI)	100 - 103	103	105	54 ± 2	163	187	-137 ± 2
(VII)	66 - 68	67	73	38 ± 2	163	186	-136 ± 2
(VIII)		A 65	68	-	161	183	-153 ± 1
	73 - 75	B 74	76	10 ± 2			
(IX)	45 - 48	46	51	41 ± 2	159	182	-159 ± 1
(X)	56 - 58	57	59	46 ± 1	163	185	-149 ± 1
(XI)	52 - 54	53	58	45	162	187	-140 ± 2
(XII)	59 - 62	61	63	39	158	185	-146 ± 3

a determined on a Kofler hot stage microscope
b temperature corresponding to onset of peak
c temperature at peak maximum

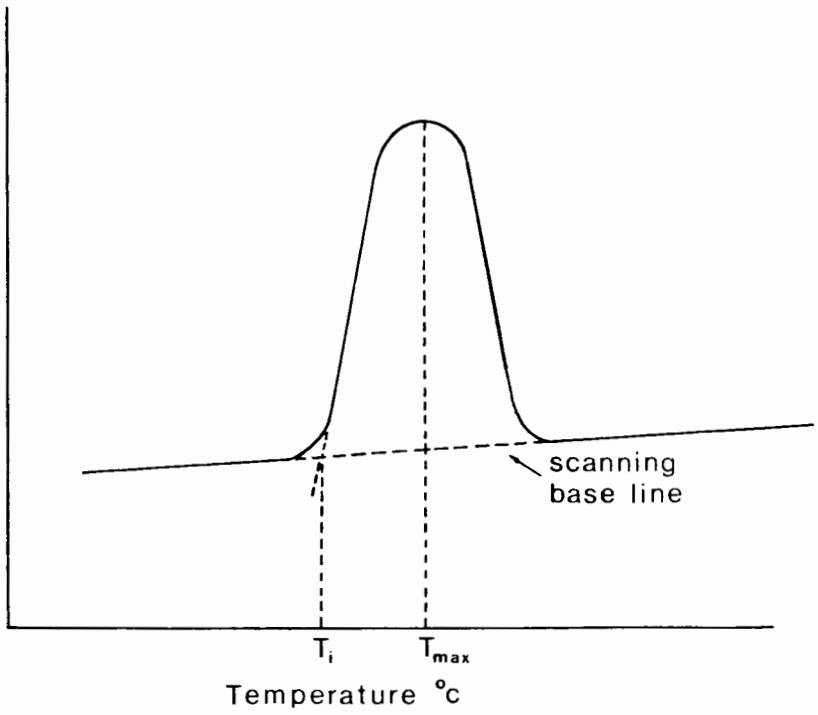

Fig. 4.2 Method used to measure the onset and peak maximum temperatures from the DSC trace

Several DSC experiments were carried out on compound (IV) to investigate the reversibility of the three endothermic processes, represented by endotherms A, B and C in the DSC trace. The series of traces recorded are shown in Fig. 4.3. Firstly, a sample of (IV) was heated to beyond the melting point of the compound (410 K), then allowed to cool. The DSC trace of this melt-recrystallised sample recorded in the range 350-410 K (Fig.4.3 1(b)) shows only two endotherms, which correspond to endotherms A and B in the original trace, with the area of the second endotherm increased relative to the first. Repeat scans of the sample over this range exhibit a decreasing area of endotherm B relative to A but endotherm C did not reappear. The temperature ranges of endotherms A and B were well reproduced in the first few repeat scans but in later scans significant broadening of the peaks with lowering of the onset temperatures was observed. This is probably due to partial decomposition of the sample during the experiment.

Secondly, a sample of (IV) was heated to beyond the first endotherm (A) (400 K) then allowed to cool. The trace of this sample over the range 320-410 K (Fig. 4.3 2(b)) shows only the two higher temperature endotherms, B and C, with the area of endotherm B considerably increased relative to C. A repeat scan of this sample after recrystallisation from the melt shows only endotherms A and B as observed in the first experiment.

The results of the first experiment suggest that the endothermic processes represented by endotherms A and B are respectively reversible and partially reversible under conditions of complete melting and rapid cooling. The fact that endotherm C does not reappear after recrystallisation from the melt suggests that this endotherm corresponds to the melting of a third crystalline form of (IV) which is formed on crystallisation from solution

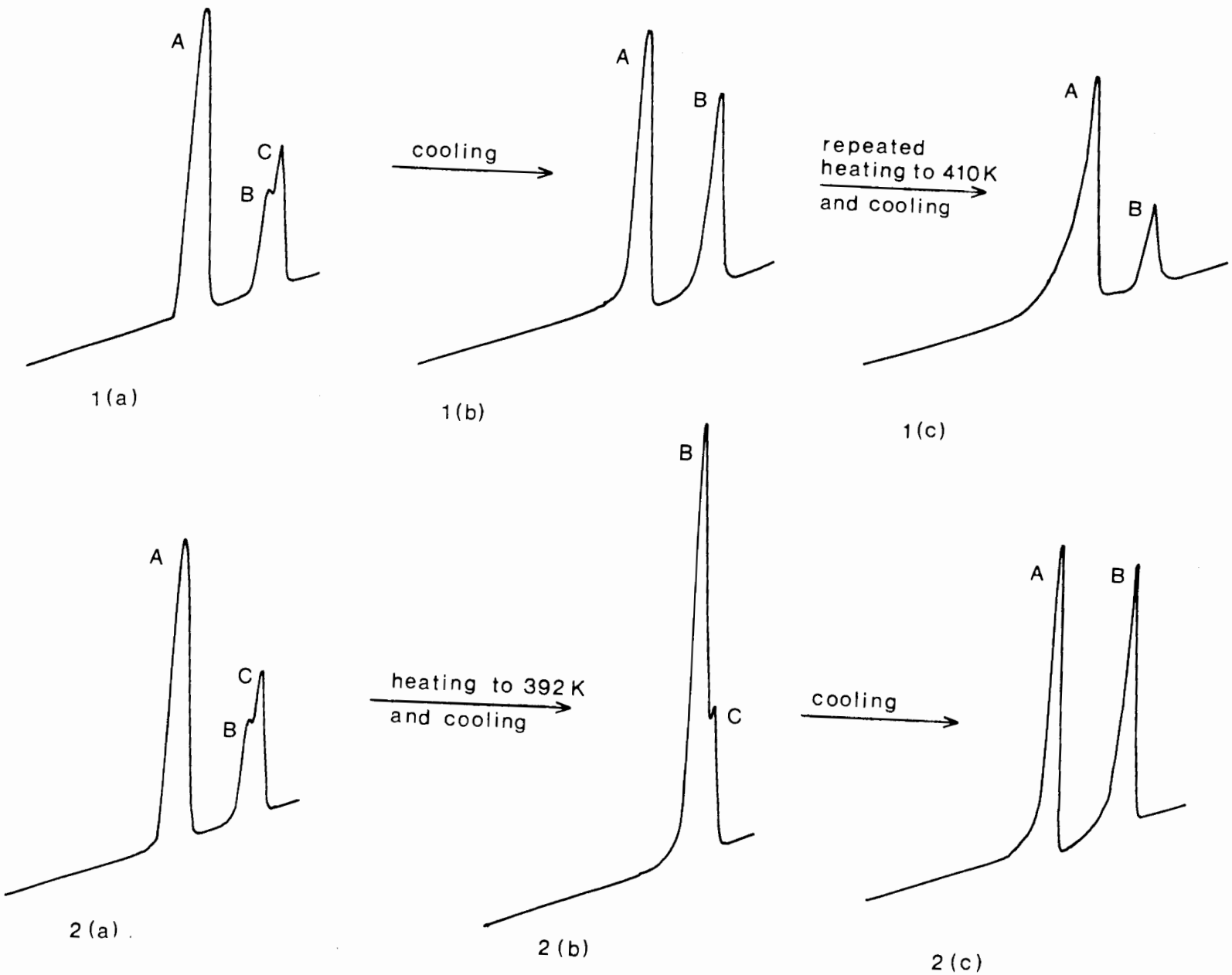

Fig. 4.3 DSC experiments: repeat scans of compound (IV) over the range 350 - 410 K with intermediate heating and/or rapid cooling.

but is unstable in the temperature range under observation. The preferential crystallisation of this portion of the sample in the second crystalline form would account for the initial increase in the area of endotherm B.

The second experiment indicates that in the temperature range below the melting point of the compound, the solid phase transition,

$$\text{Form (I)} \xrightarrow{\text{endotherm A}} \text{Form (II)}$$

is irreversible (monotropic). By combining the two heating exponents, i.e. heating a sample of (IV) to 410 K, cooling, then reheating to beyond endotherm A, the second crystalline form (Form II) can be isolated. The fact that one of the forms can be isolated simply by varying the temperature of the sample suggest that this form is significantly more stable i.e. has a lower free energy than the other forms of this compound.

For compound (VIII), the solid phase transition corresponding to endotherm A is also irreversible and the second crystalline form (Form II) can be isolated by heating a sample to beyond this phase transition.

Possible structures for the different crystalline forms of compounds (IV) and (VIII) are discussed in Section 4.3.

Trends in the melting points for the series (III)-(XII) are shown in the plot of melting point against n, the number of carbon atoms in the alkanediyl bridge (Fig. 4.4). A regular alternation of melting point between the compounds with n even and those with n odd, is observed. The melting points of the n odd compounds of the series lie on a smooth curve which is below the curve formed by the melting points of compounds (IV), (VI), (VIII) and (X).

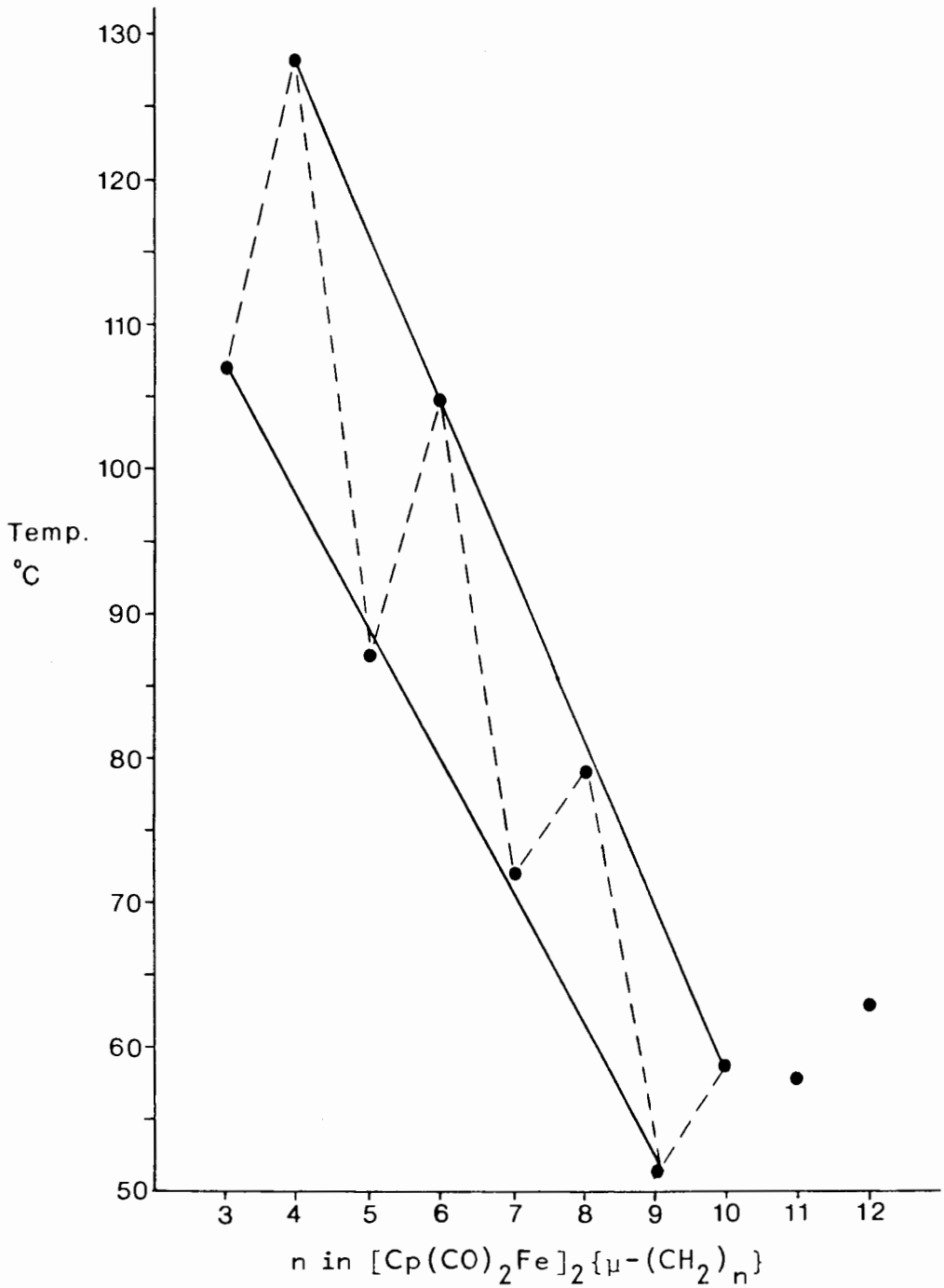

Fig. 4.4 Plot of melting point against n for $[Cp(CO)_2Fe]_2\{\mu\text{-}(CH_2)_n\}$ (n = 3-12)

Similar variations in melting point are observed in homologous series of aliphatic compounds for example the series of n-paraffins [75]. The regular alternation of melting point arises from differences in structural types between the n odd and n even members of the series. The higher melting points of the n even compounds than their odd homologous, indicates that these compounds have structures with closer packing of the molecules than the compounds with n odd.

The smooth variation of melting point in the two series n odd and n even, shows that in each series the compounds are of the same structural type [76]. On the basis of the structural study of (III) [31], compounds (V), (VII) and (IX) will thus be expected to have a structure with an imposed 2-fold symmetry axis in the crystal. It is interesting that some series of aliphatic compounds with n odd, e.g. those of fatty acids and dicarboxylic acids [76], show the same imposed symmetry. A possible structural type for the even homologues in the series (IV)-(X) would be one with symmetry 1 (centrosymmetry) as observed for the series of n even fatty acids [76]. The sudden deviation of melting points for compounds (XI) and (XII) from the two melting point curves, possibly reflects a change in structural type at this point in the series. These compounds may for example be adopting a confirmation of lower symmetry in favour of increased packing density. A similar sudden increase in melting point is observed in the series of dibromoalkanes $Br(CH_2)_nBr$ with n odd above n = 9.

Enthalpies of melting in the range 33 to 45 kJ mol^{-1} were measured for the compounds in the series with n odd (see Table 4.1), while enthalpy values of 54(±2), 46(±1) and 39 kJ mol^{-1} were determined for compounds (VI), (X) and (XII) respectively. Significantly lower enthalpies of melting were

found for the two polymorphic compounds (IV) and (VIII) (12 (±1) and 10 (±2) kJ mol respectively). Relatively low enthalpies of melting are commonly observed for compounds undergoing a solid phase transition prior to melting [75].

Enthalpy values for the phase transitions of these compounds could not be determined since the proportion of the lower temperature form in the sample is not known. However comparison of the peak areas of endotherms A and B in the traces of (IV) and (VIII) indicates that the enthalpy of the phase transition is considerably higher than the enthalpy of melting ; the ratios, area of A : area of B, for compounds (IV) and (VIII) are 2:1 and 3:1 respectively. This is generally observed for compounds undergoing a polymorphic transition into a different conformational state [76].

The exotherms in the DSC traces of (III) - (XII) correspond to the thermal decomposition of these compounds. The decomposition temperature varies little in the series (IV) - (XII) while the propanediyl bridged compound,(III), decomposes at a significantly lower temperature. Greater steric interference between the bulky metal residues on the propanediyl chain could contribute to the lower stability of (III).

Studies of the thermal decomposition of compounds (III) - (IV) involving analysis of the organic themolysis products [30,39-41] have shown that the decomposition reaction is the formation of $[Cp(CO)_2Fe]_2$ by elimination of the alkanediyl bridge as alkane or alkene. The nature and proportion of the organic products of the decomposition reaction vary depending on the length of the alkanediyl bridge. A discussion of possible decomposition mechanisms is presented in Section 4.4.

Enthalpies for the decomposition reaction, determined from the DSC traces, are in the range -130 to -159 kJ mol^{-1} for compounds (IV) - (VII). The decomposition enthalpy of (III) is considerably lower (-53±2 kJ mol^{-1}). Estimates of the activation energies for the decomposition reactions of these compounds have been made from the DSC traces, using the method of Rogers and Morris [77]. The Arrhenius plots constructed are shown in Fig.4.5. The slope of line for each compound gives the activation energy of the decomposition reaction in kcal mol^{-1} . All the compounds exhibit similar activation energies (Table 4.2) which suggests that all the decomposition reactions involve the same rate determining step.

Table 4.2 Estimated activation energies for the decomposition reactions of (III) - (XII)

Compound	Activation Energy, E_a (kcal mol^{-1})
(III)	25
(IV)	38
(V)	39
(VI)	42
(VII)	41
(VIII)	48
(IX)	32
(X)	41
(XI)	37
(XII)	31

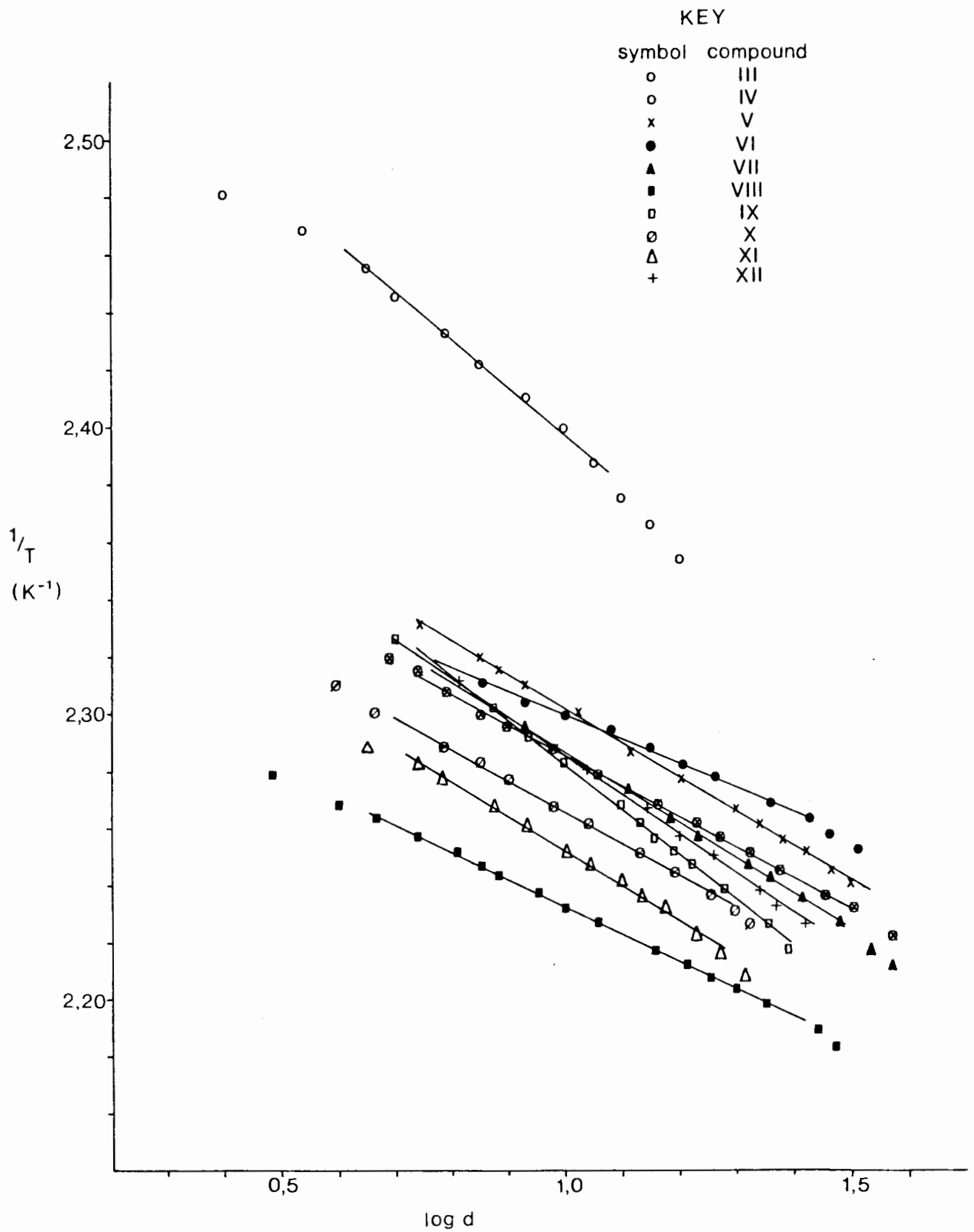

Fig. 4.5 Arrhenius plots of log d, where d is the displacement of the DSC trace from the scanning base line, against (Temperature)$^{-1}$

4.3 Discussion of the polymorphism of $[Cp(CO)_2Fe]_2\{\mu\text{-}(CH_2)_n\}$ (n = 4,8)

Polymorphism is the ability of a compound to exist in several distinct crystalline forms. These forms display differing physical properties (e.g. melting point) as a result of differences in their internal crystal structure, i.e. in the arrangement of the molecules in the crystal. On crystallisation, molecules become aligned so as to give a minimum energy arrangement. This is generally one with the maximum packing density or closest packing in the crystal [78]. Polymorphism may arise where there are two or more similar arrangements of the molecules that have comparable low energies.

The polymorphism of compounds (IV) and (VIII) is probably conformational in type, that is, the various forms differ in the rotational conformation of the molecules in the crystal lattice. Conformational polymorphism is well known among both organic and organometallic compounds. Many aliphatic compounds such as fatty acids [79] and n-alkanes [80], exhibit conformational dimorphism. Examples of transition metal compounds showing conformational polymorphism include $[Pt(bipy)Cl_2]$ [81] (bipy = 2,2'- bipyridyl), $[Ni(NCS)_2(P\{CH_2CH_2CN\}_3)_2]$ [82] and $[Co(py)_2Cl_2]$ [83] (py = pyridine).

The molecular conformations in the different polymorphs of compounds (IV) and (VIII) must represent low energy conformations of the molecules. One probable low energy conformation for these compounds would be a centrosymmetric one since this would have a *trans* configuration of the ligands on the two metal atoms and hence maximum separation between the bulky cyclopentadiene groups. The crystallographic study of (IV) [31] has shown that one crystalline form of this compound actually has a structure in which the molecules closely approximate centrosymmetry (Fig. 4.6).

The slight distortion from centrosymmetry (by bending of, and rotation about C-C bonds in, the alkanediyl bridge) arises because it allows a reduction in effective molecular volume and hence closer packing in the crystal.

In an attempt to identify other low-energy conformations of (IV) the computer program EENY [84] was used to study the effects of rotation on the non-bonded potential energy of the molecule. This program computes the non-bonded energy of a molecule by calculating the interactional energy U(r) as defined by the empirical equation (34) :

$$U(r) = ae^{-br}/r^{d} - c/r^{6} \qquad (34)$$

where r is the interatomic distance, for every pair of non-bonded atoms and summing the values of U for all the non-bonded atom pairs in the molecule. The interatomic distances are determined from the input atomic coordinates for the molecule.

From the input coordinates, the program can also calculate the atomic coordinates of other molecular conformations having varying degrees of rotation about specified bonds and hence their non-bonded potential energy. In this way the changes in non-bonded potential energy during rotation of the molecule can be determined and minima on the potential energy surface located.†

The atomic coordinates determined crystallographically for the distorted centrosymmetric conformation of (IV) [31] served as input data for the

---

† A discussion of Potential Energy surfaces of crystals is presented in ref. 75 pgs. 161-192.

(a) Input conformation

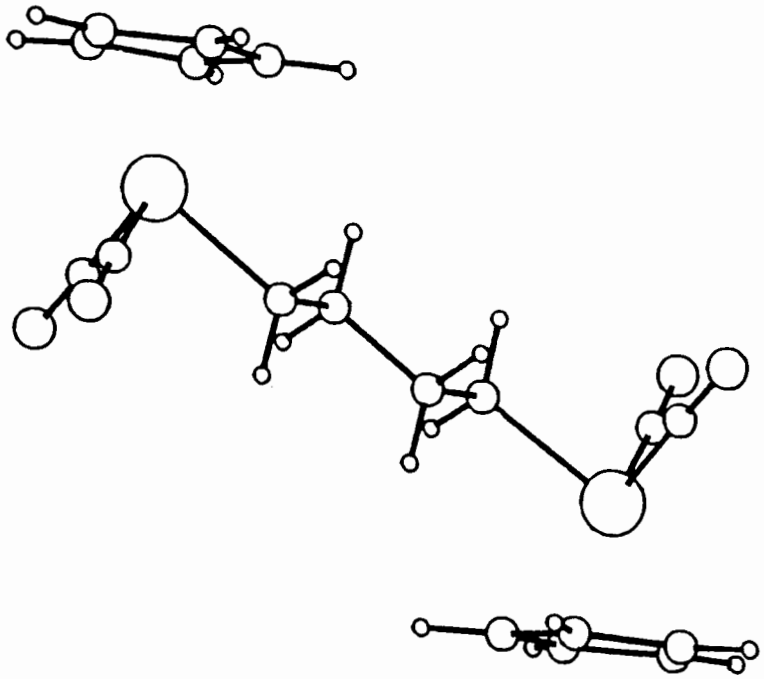

(b) Conformation with τ_1 164°, τ_2 178°, τ_3 183°, τ_4 202°, τ_5 25°

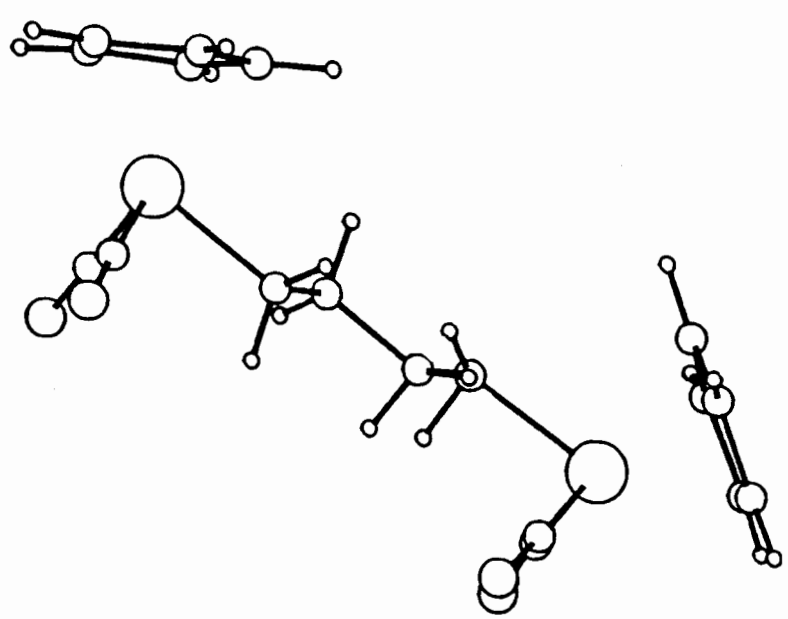

(c) Conformation with τ_1 165°, τ_2 172°, τ_3 177°, τ_4 135°, τ_5 48°

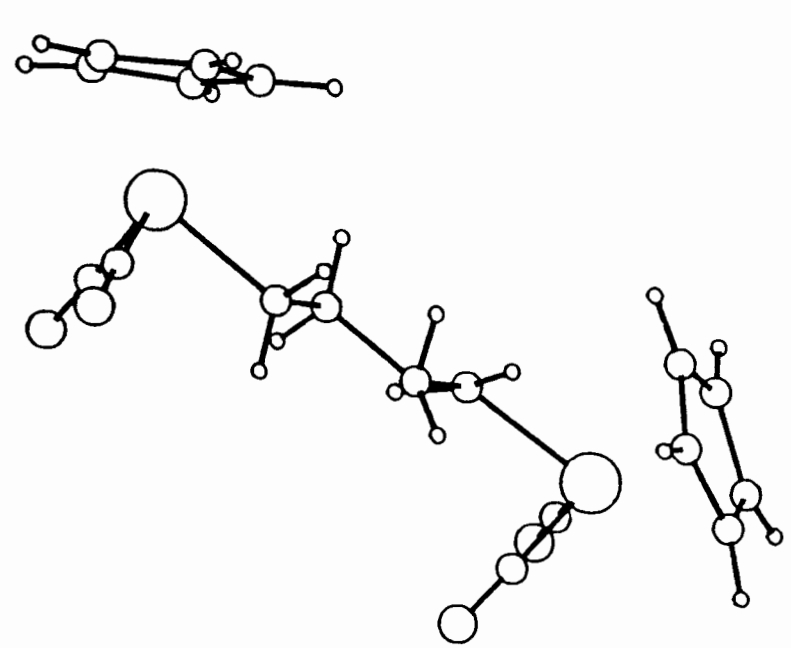

Fig. 4.6 Three low energy conformations of (IV)

computation. The values of the empirical constants a, b, c and d in equation (34) used were those derived by Giglio [85]. In the energy minimisation, all five torsion angles in the butanediyl bridge ($\tau_1 - \tau_5$ in Fig. 4.7) were allowed to vary, so that minima on the five dimensional energy surface could be located.

In an initial potential energy calculation for the input molecular conformation, the molecule was found to have a potential energy of -1.87 kJ mol^{-1} with torsion angle $\tau_1 - \tau_5$ equal to 162.5°, 179.4°, 180.1°, 178.9° and 200.1° respectively. Application of the energy minimisation procedure to the input conformation, showed that the molecule is indeed located at a potential energy minimum in this conformation.

The energy minimisation was then performed for a range of different torsion angle values. It was found that during simultaneous rotation about the Fe_1-C_1 and C_5-Fe_2 bonds, the other torsion angles ($\tau_2 - \tau_4$) did not vary significantly from 180° and a second potential energy minimum was located on the two dimensional cross section of the energy surface, describing the variation of potential energy as a function of τ_1 and τ_5. A three dimensional projection of this cross section is shown in Fig.4.8. At the second energy minimum, the molecule has a potential energy of 2.45 kJ mol^{-1} and torsion angles $\tau_1 - \tau_5$ of 164.0°, 177.7°, 183.1°, 202.2° and 25.0°.

A third potential energy minimum of 2.29 kJ mol^{-1} was located by observing the energy variation during simultaneous rotation about τ_1, τ_4 and τ_5. As before, τ_2 and τ_3 did not vary significantly from 180° during the rotation. At this minimum, the torsion angle values, $\tau_1 - \tau_5$, are 164.7°, 172.4°, 175.6°, 134.7° and 48.3° respectively.

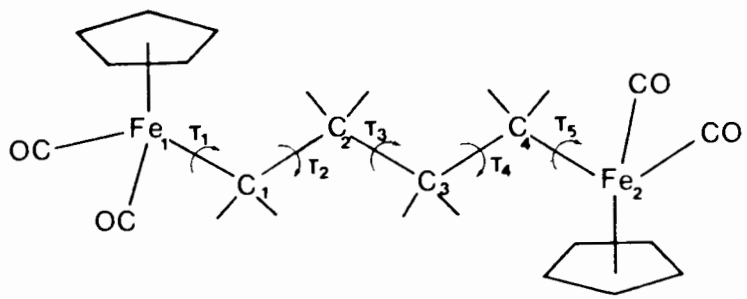

Fig. 4.7 Diagram showing the labelling of the iron and carbon atoms and the torsion angles in the alkanediyl bridge in $[Cp(CO)_2Fe]_2\{\mu\text{-}(CH_2)_4\}$

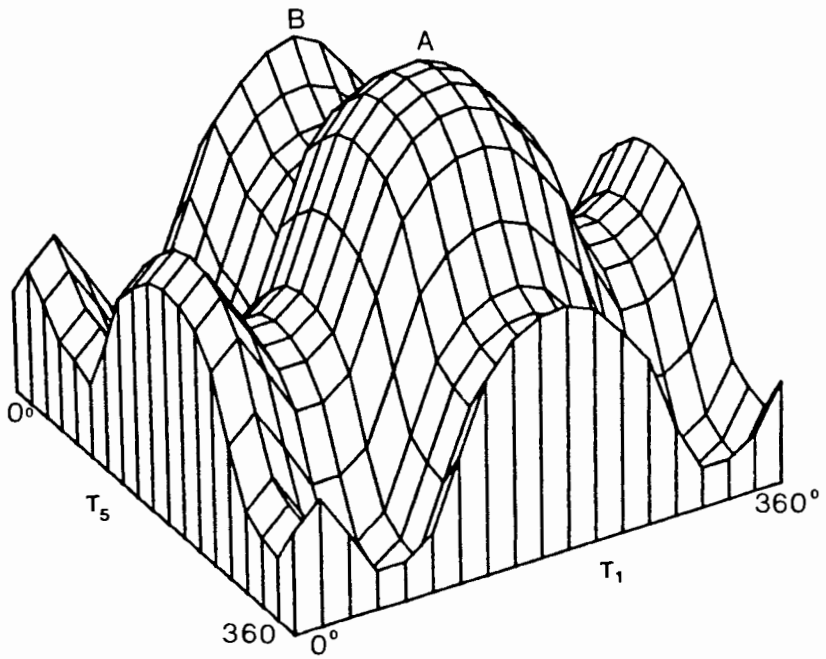

Fig. 4.8 Three-dimensional projection of the variation in the non-bonded potential energy of compound (IV) during simultaneous rotation about the Fe_1 - C_1 and Fe_2 - C_4 bonds. A and B are two energy minima on this surface.

The three different low energy conformations identified in this study are represented in Fig. 4.6. Comparison of these different forms suggests that the bulky cyclopentadiene groups are important in determining the conformation of the molecule since these conformations differ principally in the relative conformation of these groups. In the three different conformations the molecule has differing geometry and effective molecular volume. These properties will largely determine the packing of the molecules in the crystal and hence the packing density of the structure, which is the principal factor determining the free energy of the crystal. As a result structures involving the different molecular conformations could show differing physical properties.

It is not possible however to assign the different molecular conformation to the physically identified crystalline forms on the basis of the potential energy calculations. Factors such as intermolecular interactions and symmetry also contribute to determining the free energy of a structure and these are not taken into account in the calculation. Hence the calculated energies do not represent absolute values and the deepest minimum will not necessarily correspond to the lowest free energy.[†]

In an attempt to obtain information about the symmetries of the molecules in the different crystalline forms of (IV), an infrared study of this compound was carried out. The infrared spectrum of (IV) in solution (hexane) shows two strong bands in the carbonyl region at 2006 and 1953 cm^{-1}. In the infrared spectrum of this compound as a Nujol mull , these bands are resolved into several component bands which could be due to the presence of the different crystalline forms (see Fig. 4.9 (a)). In order to isolate the bands attributable to each different form, the heating procedure, used

---

[†] A discussion of this problem is presented in ref. 76.

in the DSC experiment on this compound (see Section 4.2) was followed; one sample of (IV) was heated to beyond the melting point (140°C) and cooled rapidly before the IR spectrum was recorded. Another sample was heated to 123°C (beyond the solid phase transition) and cooled rapidly, and a third sample was heated to 140°C, cooled, reheated to 123°C and finally allowed to cool. The IR spectra of these samples in the region 2100 - 1750 cm^{-1} are shown in Fig. 4.9 (b),(c) and (d) respectively.

The IR spectrum of the first sample is found to be very similar to the spectrum of the original sample although a slight change in the relative intensities of the different bands is observed. However the IR of the second sample is considerably different, the bands at 2004, 1957, 1950 and 1912 cm^{-1} having disappeared. On the basis of the DSC study, these bands can thus be assigned to Form (I), the first crystalline form. The spectrum of the third sample closely resembles that of the second sample, showing only two strong bands at 1995 and 1938 and a weak band at 1901. These bands can be attributed to the second crystalline form (Form(II)). No assignment of bands could be made for a third crystalline form from this study.

The number of carbonyl bands in the spectrum of a metal carbonyl compound is generally dependant on the symmetry of the arrangement of the carbonyl groups in the compound. (IV) would be expected to exhibit two carbonyl bands when in a centrosymmetric conformation and four bands, in a non-symmetric arrangement. On this basis, the results of the infrared study would suggest that Form (II) has the approximately centrosymmetric structure, while the Form (I) corresponds to one of the unsymmetrical conformations identified in the potential energy calculation.

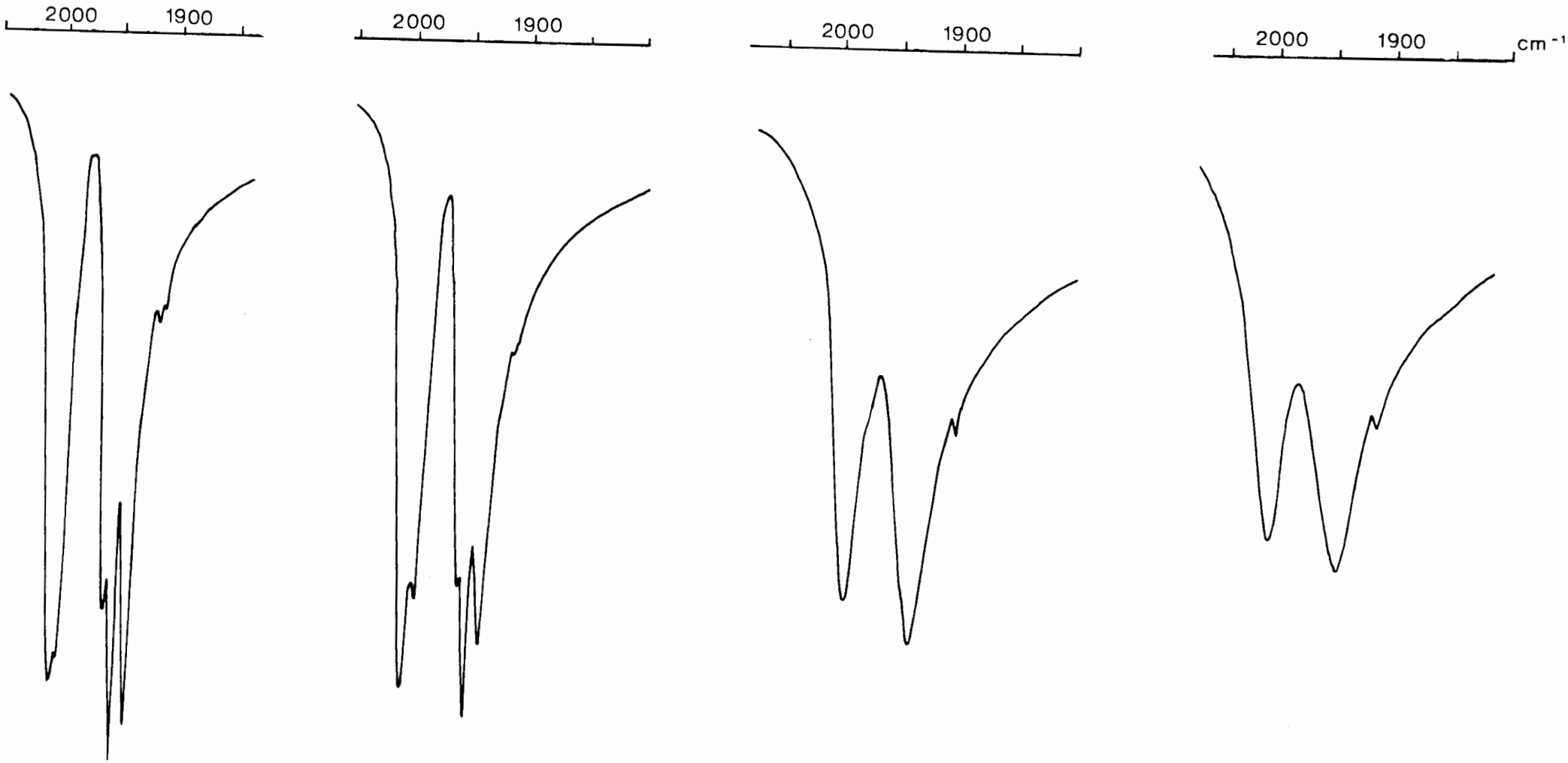

(a) solution recrystallised sample

(b) melt recrystallised sample

(c) sample heated to 123°C then cooled rapidly

(d) sample heated to 140°C cooled, reheated to 123°C and cooled again

Fig. 4.9 Infrared spectra of samples of compound (IV) treated as described above, as Nujol mulls

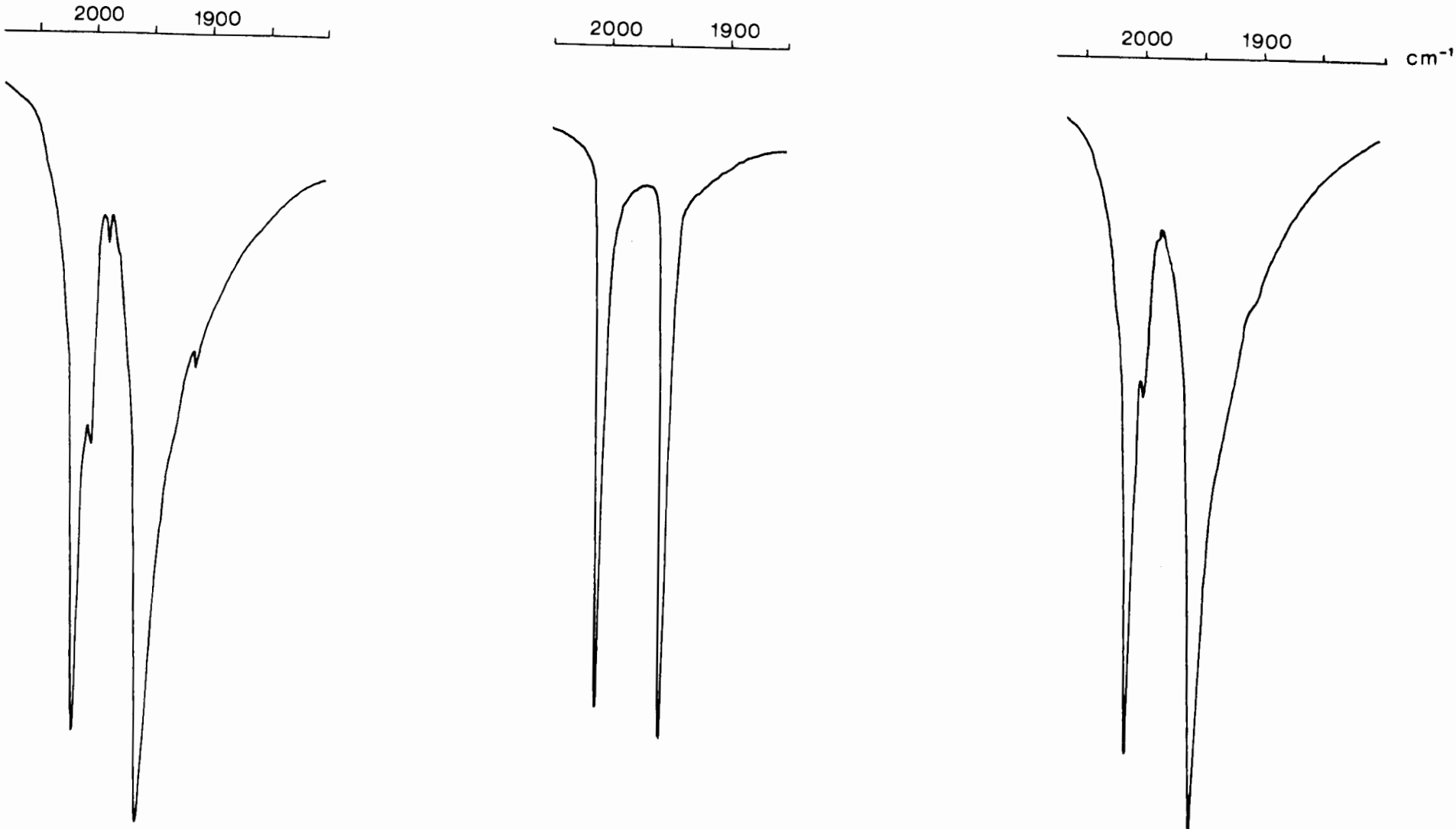

(a) solution recrystallised sample

(b) sample heated to 73 C and cooled rapidly

(c) melt recrystallised sample

Fig. 4.10 Infrared spectra of samples of compound (VIII), treated as described above, as Nujol mulls.

Assignment of carbonyl stretching bands to the two crystalline forms of (VIII) has also been made. The infrared spectrum of (VIII) in Nujol, shows six carbonyl bands in the region 2050 - 1900 cm^{-1} (Fig. 4.10 (a)); 2006 (s) 1994 (m) 1980 (w) 1951 (vs) ~1930 (sh) and 1902 (m). A sample of (VIII) was heated to beyond the phase transition (73°C) and cooled rapidly, before the infrared spectrum was recorded. The spectrum of this sample shows only two strong carbonyl bands in the same region (Fig. 4.10 (b)). The bands at 1994, 1980, 1925 and 1902 cm^{-1} disappeared on heating and can thus be assigned to the lower temperature crystalline form (Form(I)). The bands at 2006 and 1951 cm are attributable to Form (II). According to the number of carbonyl bands observed for the two different forms, it appears that, as in (IV), Form (II) has the more symmetric structure. The infrared spectrum of a sample of (VIII) heated to beyond its melting point and cooled, is very similar to the spectrum of the original sample. This indicates that as in (IV), both forms of the compound crystallise from the melt.

4.4 Thermolysis of μ(1,n)alkanediyl) diiron and ditungsten compounds.

4.4.1 Introduction

Recently there has been considerable interest in the thermal decomposition reaction of alkanediyl bridged compounds principally as a result of the significance of these compounds as models for catalytic intermediates. Detailed studies of the thermolyses and photolyses of $[Cp(CO)_2Fe]_2$-$\{\mu-(CH_2)_n\}$ (n = 3-5) both in solid state and solution have been reported [30,39-41]. These studies have shown that the decomposition reaction is the formation of $[Cp(CO)_2Fe]_2$ by elimination of the alkanediyl bridge as alkane or alkene (equation (35)), and that the proportions of saturated and unsaturated organic products produced in the reaction vary

with the length of the alkanediyl bridge. Knox *et al.*[40,41] have reported that the major product of the decomposition of $[Cp(CO)_2Fe]_2\{\mu\text{-}(CH_2)_5\}$ is pentane whereas no n-propane and n-butane are evolved by the propanediyl and butanediyl bridge species respectively. This was taken as evidence that the mechanism for the decomposition reaction of $[Cp(CO)_2Fe]_2\{\mu\text{-}(CH_2)_5\}$ differs from that of $[Cp(CO)_2Fe]_2\{\mu\text{-}(CH_2)_n\}$ (n =3,4).

$$[Cp(CO)_2Fe]_2\{\mu\text{-}(CH_2)_n\} \longrightarrow [Cp(CO)_2Fe]_2 + C_n \text{ alkane, alkenes} \qquad (35)$$

The ratio of organic products formed in this decomposition reaction is also found to depend on the conditions under which the compound is decomposed. For example, Wegner *et al.*[39], observed pent-1-ene as the major product on thermal decomposition of $[Cp(CO)_2Fe]_2\{\mu\text{-}(CH_2)_5\}$ in Nujol solution in contrast to the results of Knox *et al.*[41].

In the studies on the thermal decomposition of mononuclear iron alkyl compounds such as $[Cp(CO)(PPh_3)FeR]$ [73], a β-hydride elimination mechanism has been invoked to account for the observed production of alkane from these compounds. For the alkanediyl bridged species, metal carbon bond cleavage via simple β-hydride elimination would lead to a diene product. The fact that such products have not been detected on decomposition of $[Cp(CO)_2Fe]_2\text{-}\{\mu\text{-}(CH_2)_n\}$ (n = 4,5), together with the considerably greater thermal stability of the alkanediyl bridged compounds compared with mononuclear alkyl species, suggests that a more complex mechanism is operative. Pettit *et al.* [30] and Knox *et al.*[41] have postulated a mechanism involving β-hydride elimination or reductive elimination from a dimetallocyclic intermediate 55 to account for the decomposition products of $[Cp(CO)_2Fe]_2\{\mu\text{-}(CH_2)_n\}$ (n = 3,4) (Scheme 4.1).

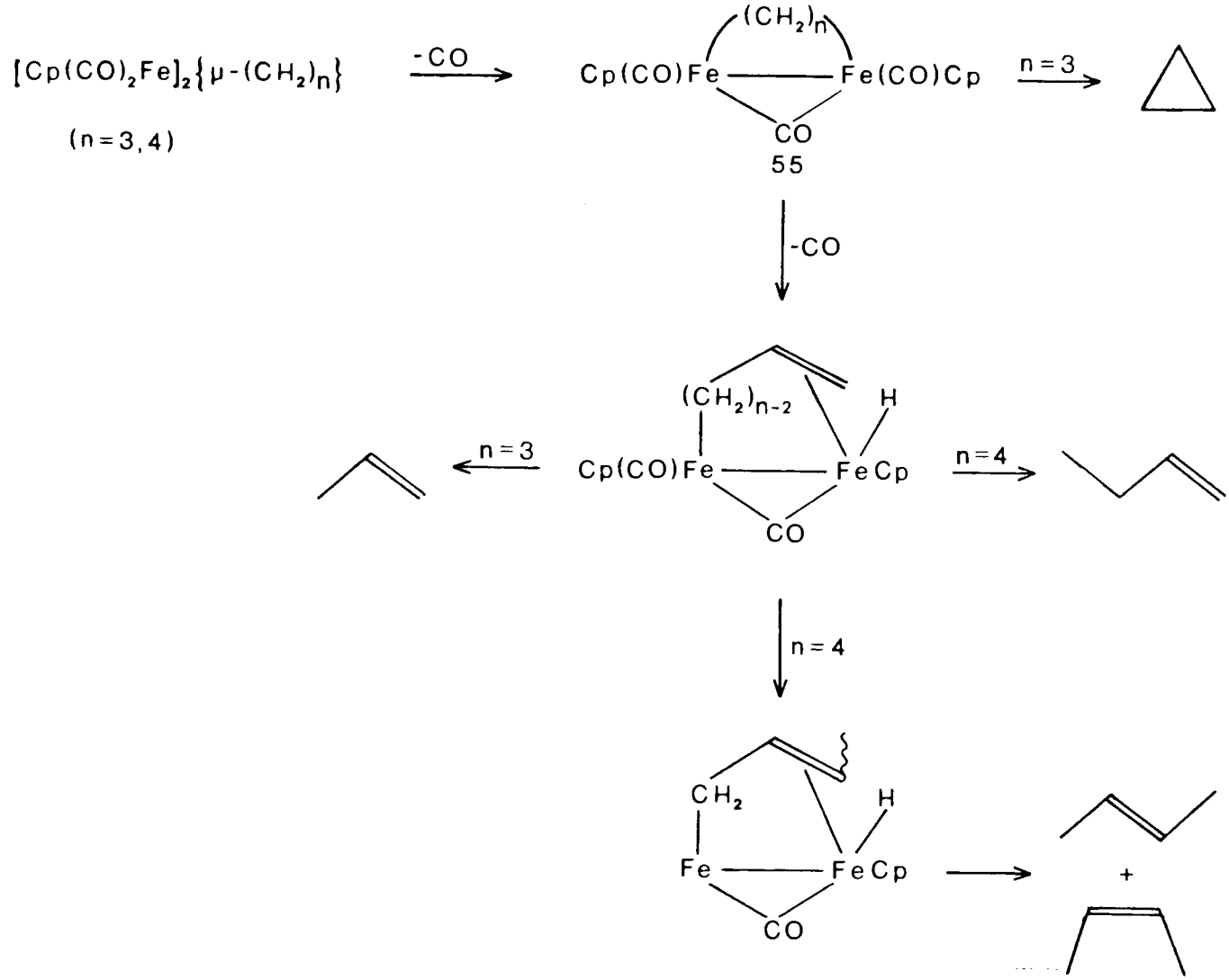

Scheme 4.1

In this mechanism, the alkene products are generated from the dimetallocyclic intermediate by intramolecular β-hydride abstraction followed by hydride migration to the other metal and reductive elimination. Reductive elimination of the $-(CH_2)_3-$ bridge with C-C bond formation from the dimetallocyclopentane intermediate would produce cyclopropane. Evidence in support of this mechanism has been provided by Knox *et al.* [41] in their observation that *trans*-but-2-ene is the major product of the decomposition of the compound $[Cp(CO)_2Fe\{\mu-(CH(Me)CH_2CH_2)\}Fe(CO)_2Cp]$. This was accounted for by steric effects in a dimetallocyclic intermediate favouring the *anti*-

configuration of the methyl group relative to the cyclopentadienyl groups which leads to a *trans*-carbon skeleton 56 .

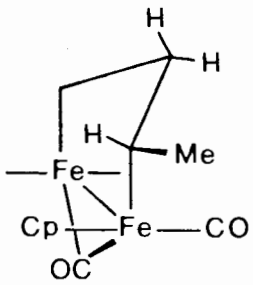

56

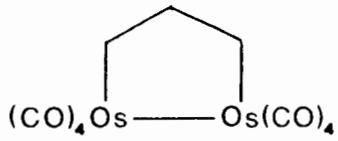

57

The reported formation of propane on decomposition of the diosmacyclopentane 57 also provides support for the mechanism of Pettit [30] and Knox [41].

The results of Knox *et al.* [41] for the decompositions of compound $[Cp(CO)_2Fe]_2\{\mu\text{-}(CH_2)_n\}$ (n=3-5) suggest that a change in the decomposition mechanism occurs at n = 5 in this series of compounds. On this basis, the longer chain compounds $[Cp(CO)_2Fe]_2\{\mu\text{-}(CH_2)_n\}$ (n = 6-12) may be expected to decompose in the same way as (V) to give mainly alkane products. To test this, we have investigated the thermolyses of $[Cp(CO)_2Fe]_2\{\mu\text{-}(CH_2)_n\}$ (n = 3-8) using gas chromatography to analyse the organic products. In addition, the thermal decompositions of the analogous ditungsten compounds $[Cp(CO)_3W]_2\{\mu\text{-}(CH_2)_n]$ (n = 3-5) have been studied and comparisons made with the diiron system.

4.4.2. Results and Discussion

4.4.2.1 Thermolyses of $[Cp(CO)_2Fe]_2\{\mu\text{-}(CH_2)_n\}$ (n = 3-8) (III)-(VIII)

The solid state thermolyses of compounds (III) - (VIII) were carried out

under vacuum (0.1mmHg) by heating over the range 100 - 220°C. The gaseous organic products were analysed by gas chromatography and the results of this analysis are presented in Table 4.3. The hydrocarbon products were identified by comparison of their retention times with those of standard samples and for (IV) and (V) from their mass spectra. The organometallic decomposition products were identified on the basis of their IR and ^1H NMR spectra by comparison with literature spectral data.

The results obtained in this study were generally consistent with those reported for μ(1,n)alkanediyl compounds by other workers [30,39-41]. The organometallic product of the decomposition reactions of $[Cp(CO)_2Fe]_2$-$\{\mu\text{-}(CH_2)_n\}$ (n = 3-8) was found to be $[Cp(CO)_2Fe]_2$ and the major organic products were Cn hydrocarbons . $[Cp_2Fe]$ and the tetramer $[Cp_4Fe_4(CO)_4]$ were also detected in the solid decomposition products, but these can be attributed to the decomposition of $[Cp(CO)_2Fe]_2$ under the thermolysis conditions [86]. Traces of C_1 and C_2 compounds were observed in the gaseous organic products.

The hydrocarbon product ratio determined for (III) and (IV) in this study, agreed fairly well with those of Knox *et al.* [41] although we detected a small amount of butane on decomposition of (IV) in contrast to the report of Knox [41]. (See Table 4.4). However we have found that pent-1-ene is the major organic product of the solid state thermolysis of (V). This is consistent with the report of Wegner and Sterling [39] for the decomposition of (V) in Nujol solution. The reason for this discrepancy with the results of Knox *et al.* [41] is not clear.

Table 4.3 Organic products of solid state thermolyses of compounds (III) - (VIII)

Compound	T/°C[a]	Hydrocarbon product	mole % [b]	alkene : alkane [b] ratio
(III)	105-198	propene	24 ± 1.5	
		cyclopropane	75 ± 1	1 : 3.1 ± 0.2
		propane	0.9 ± 0.1	
(IV)	128-220	but-1-ene	56 ± 5	
		c-but-2-ene	24 ± 3	15 ± 2 : 1
		t-but-2-ene	13 ± 4	
		n-butane	6 ± 2	
(V)	130-220	pent-1-ene	62 ± 1.5	
		t-pent-2-ene	23 ± 1	28 ± 1 : 1
		c-pent-2-ene	11.5 ± 0.5	
		n-pentane	3.5 ± 0.1	
(VI)	130-228	hex-1-ene	30 ± 7	
		t-hex-2-ene	23 ± 6	1.5 ± 0.4 : 1
		c-hex-2-ene	7 ± 2	
		n-hexane	40 ± 8	
(VII)	165-220	heptenes	30	1 :2.3
		n-heptane	70	
(VIII)	165-220	octenes	25	1 : 3.3
		n-octane	75	

a Heating range for thermolysis
b average of 2-4 experiments

Table 4.4 Comparison of results for the thermolysis of $[Cp(CO)_2Fe]_2\{\mu\text{-}(CH_2)_n\}$ (n = 3-5)

Compound	Product ratio	Results Found[a]	literature[b]
(III)	Cyclopropane : propene	3.1 ± 0.2 : 1	2.3 ± 0.3 : 1
(IV)	but-2-ene : but-1-ene	1 : 1.5 ± 0.6	1 : 1.5 ± 0.4
(V)	pentane : pentene	1 : 28 ± 1	3.2 : 1

a ; results of this study
b ; results of Knox *et al.* [41]

Decomposition of $[Cp(CO)_2Fe]_2\{\mu\text{-}(CH_2)_6\}$ produced significant amounts of hexane and hexene while the longer chain compounds (VII) and (VIII) produced mainly alkane. These results suggest that there is a change in the decomposition mechanism at (VI) rather than (V) in the series of μ(1,n)alkanediyl diiron compounds. This apparent change in the predominant decomposition mechanism could be rationalised on the basis of the mechanism of Pettit[30] and Knox [41]. With increasing length of the alkanediyl chain, decomposition via a dimetallocyclic intermediate may be expected to become less favourable due to the lower stability of the larger ring dimetallocyclic species. The alternative decomposition mechanism dominant for the longer chain compounds could be a radical process involving iron - carbon bond fission followed by hydrogen abstraction.

Attempts to detect a metallocyclic intermediate in the decomposition of the μ(1,n)alkanediyl diiron compounds have failed. Pettit *et al.*[30] have reported that (III) is stable in refluxing THF and in the presence of trimethylamine oxide, an effective CO- abstraction agent. We have found that on heating (III) in THF with Me_3NO, extensive decomposition to

$[Cp(CO)_2Fe]_2$ occurs. This seems to indicate that CO dissociation may indeed be the initial step in the decomposition reaction. Knox *et al.* [41] have reported that the reaction of $[Cp(CO)_2Ru]_2\{\mu\text{-}(CH_2)_3\}$ with Me_3NO in refluxing THF produces a small yield of the methylene complex $[Cp(CO)_2Ru]_2(\mu\text{-}CO)(\mu\text{-}CH_2)$. This could be attributed to the elimination of ethylene from a dimetallocyclic intermediate formed by CO abstraction from the propanediyl bridged species. Consistent with this was the observation that C_2H_4 was produced in small amounts on decomposition of $[Cp(CO)_2Ru]_2\{\mu\text{-}(CH_2)_3\}$ [41].

4.4.2.2 Thermolyses of $[Cp(CO)_3W]_2\{\mu\text{-}(CH_2)_n\}$ (n = 3-5) (XIII) - (XV)

The ditungsten compounds (XIII) - (XV) were decomposed under the same conditions as those used in the thermolysis of the analogous diiron compounds. The gaseous reaction products were similarly analysed by gas chromatography and the hydrocarbon components identified by their mass spectra and/or by comparison of their retention times with those of standard samples. The results of the analyses are given in Table 4.5. The organometallic products of the decompositions were identified by their IR and ^1H NMR spectra in comparison with reported spectra [87]. A control experiment, in which $[Cp(CO)_3W]_2$ was heated under identical conditions to those used in the sample thermolysis, was carried out for comparison.

The ditungsten compounds $[Cp(CO)_3W]_2\{\mu\text{-}(CH_2)_n\}$ (n = 3-5) were found to be considerably more stable than the analogous diiron compounds; decomposition temperatures of 150°, 195° and 180°C were measured for (XIII) - (XV) respectively, whereas the diiron compounds (III) - (V) decompose at 127°, 159° and 161°C respectively. However the decomposition reactions of compounds (XIII) - (XV) are analogous to those of the corresponding diiron species. The major

Table 4.5 Organic products of the solid state thermolyses of compounds (XIII) - (XV)

Compound	T/°C[a]	Hydrocarbon product	mole %[b]	alkene : alkane[b]
(XIII)	120-220	propane	65 ± 8[c]	1.9 ± 0.5 : 1
		cyclopropane	35 ± 8[c]	
(XIV)	140-220	but-1-ene	56 ± 1	19.5 ± 1 : 1
		c-but-2-ene	24 ± 1	
		t-but-2-ene	13.5 ± 0.5	
		n-butane	4.8 ± 0.1	
		unidentified product	2 ± 0.2	
(XV)	120-220	pent-1-ene	63.0 ± 0.2	13 ± 0.1 : 1
		c-pent-2-ene	11.7 ± 0.2	
		t-pent-2-ene	14 } 18.2	
		pentadiene	4.2 }	
		n-pentane	7.0	

a Heating range for decomposition
b average of 2-4 experiments
c the large error in these results is due to the overlap of the component peaks in the GLC trace

organometallic product of the reactions is $[Cp(CO)_3W]_2$ and the $-(CH_2)_n-$ bridge is eliminated as alkane or alkene (equation 36).

$$[Cp(CO)_3W]_2\{\mu-(CH_2)_n\} \xrightarrow{\Delta} [Cp(CO)_3W]_2 + C_n \text{ hydrocarbons} \qquad (36)$$

$[Cp(CO)_3WH]$ and $[(CO)_6W]$ (identified by their IR spectra) [87] were also formed in the decomposition reactions. However since the same species were produced on heating $[Cp(CO)_3W]_2$ under the same conditions, no conclusions about the source of these species can be made. The decomposition of $[Cp(CO)_3W]_2$ also produced traces of C_1, C_2 and C_6 compounds † but no C_3 - C_5 products so the organic products of the sample decomposition must derive from the alkanediyl bridges of the compounds.

$[Cp(CO)_3W]_2\{\mu-(CH_2)_n\}$ (n = 3-5) yield the same hydrocarbon products on decomposition as the analogous diiron compounds. The product ratios for the ditungsten and diiron compounds are compared in Table 4.6. $[Cp(CO)_3W]_2\{\mu-(CH_2)_3\}$ is found to favour the formation of propene over cyclopropane whereas the $\mu(1,3)$ propanediyl diiron compound yields mainly cyclopropane. This effect of the nature of the metal on the propene: cyclopropane ratio has been observed previously by Knox *et al.* [41] in their study of the decompositions of $[Cp(CO)_2M]_2\{\mu-(CH_2)_3\}$ (M = Ru and Fe).

In the decomposition of $[Cp(CO)_3W]_2\{\mu-(CH_2)_4\}$, the proportion of butenes produced is similarly greater than that evolved by the butanediyl bridged diiron compound. In contrast, $[Cp(CO)_3W]_2\{\mu-(CH_2)_5\}$ yields slightly more n-pentane than the corresponding diiron compound.

---

† These compounds were also produced in sample decompositions. The C_6 hydrocarbons probably originate from the solvent of crystallisation, hexane.

Table 4.6 Comparison of organic product ratio from decomposition of $[Cp(CO)_3W]_2\{\mu\text{-}(CH_2)_n\}$ (n = 3-5) and $[Cp(CO)_2Fe]_2\{\mu\text{-}(CH_2)_n\}$ (n = 3-5)

Compound	Product ratio	Results	
		Fe compound	W compound
3	propene : cyclopropane	1 : 3.1 ± 0.2	1.9 ± 0.5 : 1
4	butene : butane	15 ± 2 : 1	19.5 ± 1 : 1
	but-1-ene : but-2-ene	1.5 ± 0.6 : 1	1.5 ± 0.3 : 1
5	pentene : pentane	28 ± 1 : 1	13 ± 0.1 : 1

Analysis of the hydrocarbon products of the decomposition of $[Cp(CO)_3W]_2\{\mu\text{-}(CH_2)_5\}$ by GLC - mass spectrometry revealed the presence of another product which was identified from its mass spectrum as 1,4-pentadiene. This compound was not separated from *cis*- and *trans*-pent-2-ene by gas chromatography, but on estimate of the proportion of the dienyl product in the mixture was made by comparison of the total ion currents for the molecular ions of 1,4-pentadiene (M^+ m/e 68) and the pentenes (M^+ m/e 70). This is illustrated in Fig. 4.11.

The results of this study can be explained on the basis of the mechanism postulated by Knox *et al.* [41] and Pettit *et al.*[30]. The observation that the hydrocarbon products of the decompositions are predominantly the same suggests that a similar mechanism is operative in both systems. The relative strength of the tungsten-carbon bond compared with the Fe-C bond would account for the greater thermal stability of the ditungsten compounds. As proposed for the diiron and diruthenium systems, propene and cyclopropane could be formed from $[Cp(CO)_3W]_2\{\mu\text{-}(CH_2)_3\}$ via β-hydride elimination

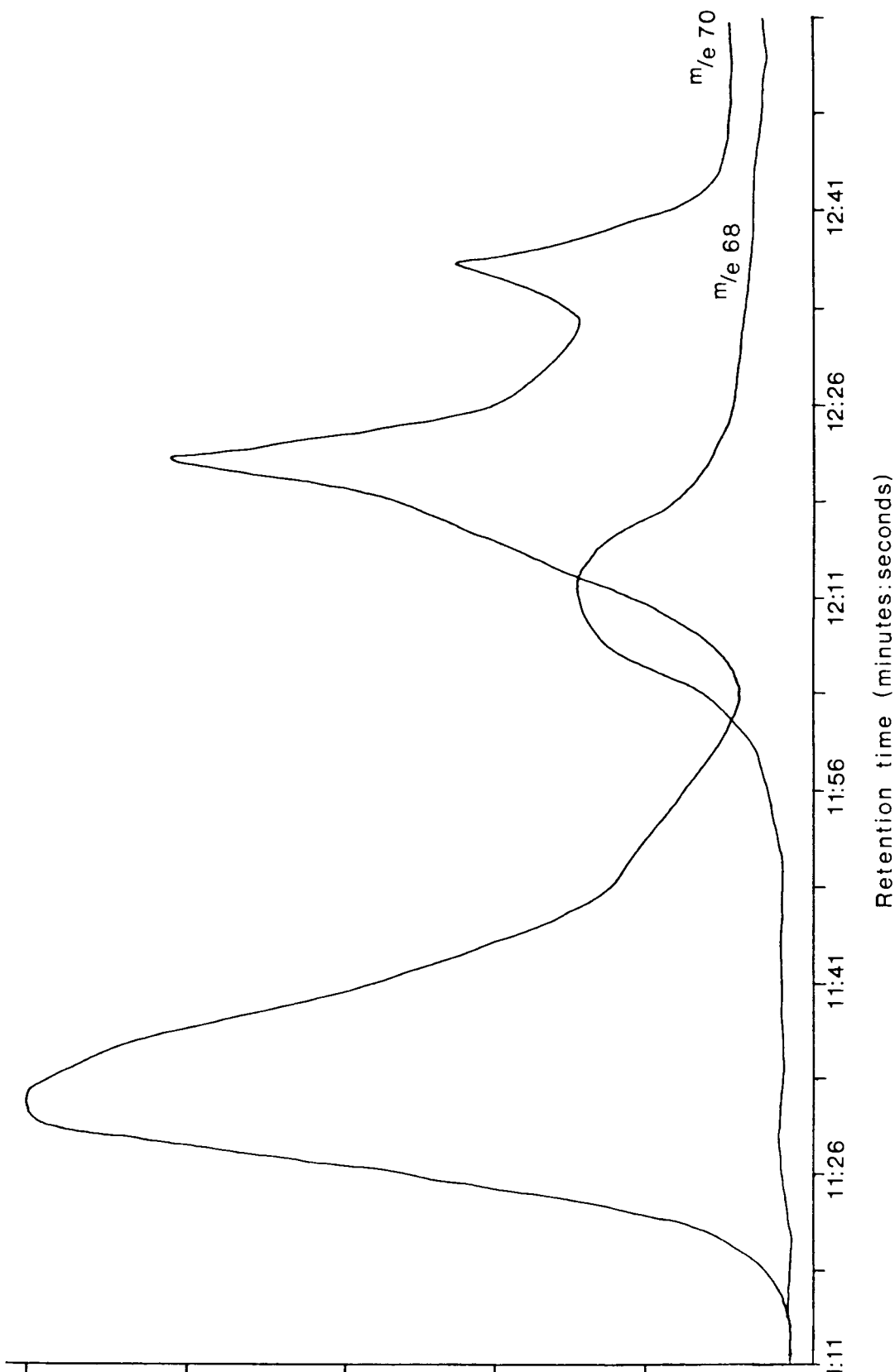

Fig. 4.11 Plot of relative ion current for the ions of $^{m}/_{e}$ 70 and $^{m}/_{e}$ 68 against retention time

and reductive elimination respectively from the intermediate dimetallocycle 58 .

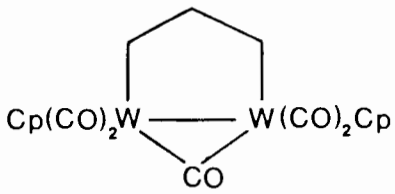

58

The preferential formation of propene from the ditungsten compound could be attributed to the resistance of 58 to reductive elimination of the $-(CH_2)_3-$ bridge, due to the strength of the tungsten-carbon bonds. Knox *et al.* [41], have also noted for the compounds $[Cp(CO)_2Fe]_2\{\mu-(CH_2)_3\}$, $[Cp(CO)_2Fe\{\mu-(CH_2)_3\}Ru(CO)_2Cp]$ and $[Cp(CO)_2Ru]_2\{\mu-(CH_2)_3\}$ that the trend of increasing propene : cyclopropane ratio corresponds to a trend of increasing metal-metal bond lengths in the order Fe-Fe < Fe-Ru < Ru-Ru. The metal-metal bond distance could also be a factor controlling dinuclear reductive elimination of cyclopropane from the dimetallocyclic intermediate 58 .

The somewhat greater proportion of butene produced on decomposition of $[Cp(CO)_3W]_2\{\mu-(CH_2)_4\}$ than evolved by $[Cp(CO)_2Fe]_2\{\mu-(CH_2)_4\}$ may also reflect a greater resistance of the ditungsten species to reductive elimination. The observation that 1,4-pentadiene is evolved from $[Cp(CO)_3W]_2\{\mu-(CH_2)_5\}$ but not from the analogous diiron compound further supports the suggestion. β-hydrogen elimination of a dienyl product rather than reductive elimination of pentene would be promoted by increased metal-carbon bond strength. Formation of a dienyl product without the intermediacy of a dimetallocyclic species could also compete with the production of alkane

by W-C bond fission. By analogy with the diiron system, longer chain alkanediyl bridged tungsten compounds may be expected to decompose mainly by metal carbon bond fission to give predominantly alkane products. Based on the precedent of the pentanediyl bridged species, it is possible that the β-hydrogen elimination of a dienyl species could be favoured over alkane production for $[Cp(CO)_3W]_2\{\mu\text{-}(CH_2)_n\}$ $(n > 5)$. This has still to be investigated.

SECTION 5

5 REACTIONS OF μ(1,n)ALKANEDIYL DIIRON AND DITUNGSTEN COMPOUNDS

5.1 Introduction

The most widely studied reactions of metal alkyl compounds are those involving cleavage of the metal-carbon σ bond [55]. These include "insertion" reactions in which a group such as CO, is effectively inserted into the bond, and electrophilic cleavage reactions in which attack by an electrophile EX results in elimination of the alkyl group R as RE (equation (37)).

$$LnMR + EX \longrightarrow LnMX + RE \qquad (37)$$

Investigations of the reactions of μ(1,n)alkanediyl compounds have shown that these compounds undergo similar cleavage reactions. Pettit *et al.* [30], have reported that the thermally induced reaction of CO with $[Cp(CO)_2Fe]_2\{\mu\text{-}(CH_2)_n\}$ (n = 3,4) leads to the diacyl species **59** (equation (38)), by apparent insertion of CO into two Fe-C bonds.

$$[Cp(CO)_2Fe]_2\{\mu\text{-}(CH_2)_n\} \xrightarrow[\Delta]{\text{CO pressure}} [Cp(CO)_2Fe\{CO(CH_2)_nCO\}Fe(CO)_2Cp] \qquad (38)$$

(n = 3,4) **59**

Similarly, the reaction of $[Cp(CO)_2Fe]_2\{\mu\text{-}(CH_2)_3\}$ with SO_2 was found [88] to produce the mono- and di-sulphinato species **60** and **61**.

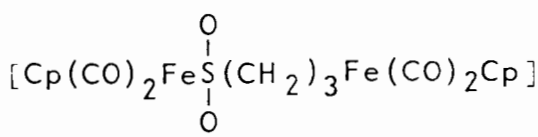

60

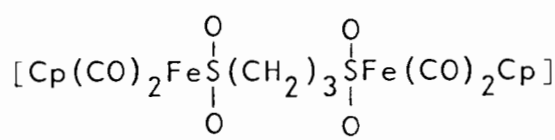

61

Electrophilic cleavage of both Zr-C bonds in $[ClCp_2Zr]_2\{\mu\text{-}(CH_2)_2\}$ on reaction with excess HCl has been reported [8] (equation (39)).

$$[ClCp_2Zr]_2\{\mu\text{-}(CH_2)_2\} \xrightarrow{HCl\ gas} 2ClCp_2ZrCl + CH_3CH_3 \qquad (39)$$

In this work, the reactions of μ(1,n)alkanediyl diiron and ditungsten compounds with a range of tertiary phosphine ligands have been investigated. Reactions of this type have only been reported previously for the dimetallocyclopentane species $[CpCo]_2\{\mu\text{-}CO\}\{\mu\text{-}(CH_2)_3\}$ (See Section 1). In addition, the cleavage of the metal-carbon bonds in $[Cp(CO)_2Fe]_2\{\mu\text{-}(CH_2)_n\}$ (n = 3 - 5) by halogens has been studied.

5.2 Results and Discussion

5.2.1 Reactions of $[Cp(CO)_2Fe]_2\{\mu\text{-}(CH_2)_n\}$ with tertiary phosphines (PPh_3, PPh_2Me, PMe_3)

As observed for mononuclear iron alkyl compounds [55], the thermally induced reactions of $[Cp(CO)_2Fe]_2\{\mu\text{-}(CH_2)_n\}$ with tertiary phosphines yield phosphine substituted acyl products. Depending on the proportion of tertiary phosphine in the reaction, either the monoacyl or the diacyl species † may be isolated as the major product. For example $[Cp(CO)_2Fe]_2\{\mu\text{-}(CH_2)_3\}$ (III) reacted with PPh_3 in equimolar ratio to give $[Cp(CO)(PPh_3)Fe\{CO(CH_2)_3\}Fe(CO)_2Cp]$ (XXII) in 64% yield (equation (40)) while in the reaction of (III) with PPh_3 in 1:2 mole ratio, the diacyl species was the major product (equation (41)).

---

† In this section mono- and di-acyl products refer to compounds containing a phosphine substituent(s) and an acyl ligand.

$$[Cp(CO)_2Fe]_2\{\mu\text{-}(CH_2)_3\} \xrightarrow[75°C,24hrs]{PPh_3\ ,\ THF} [Cp(CO)(PPh_3)Fe\overset{O}{\overset{\|}{C}}(CH_2)_3Fe(CO)_2Cp] \quad (40)$$

(XXII)

$$\xrightarrow[66hrs]{THF,75°C\ \ 2PPh_3} [Cp(CO)(PPh_3)Fe\overset{O}{\overset{\|}{C}}(CH_2)_3\overset{O}{\overset{\|}{C}}Fe(CO)(PPh_3)Cp] \quad (41)$$

(XXIII)

Similarly the reactions of $[Cp(CO)_2Fe]_2\{\mu\text{-}(CH_2)_n\}$ (n = 4 - 7) with a two mole proportion of PPh_3 in refluxing THF (36-48 hours) gave the diacyl compounds (XXIV) - (XXVII) respectively. Traces of the monoacyl products were also detected.

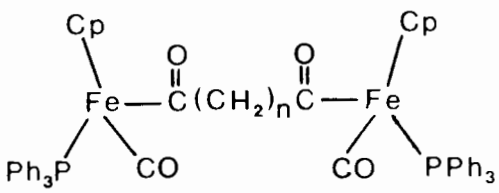

(XXIV) n = 4

(XXV) n = 5

(XXVI) n = 6

(XXVII) n = 7

The reaction of (III) with $PMePh_2$ in 1:3.5 mole ratio in refluxing THF gave $[Cp(CO)(PMePh_2)Fe\{CO(CH_2)_3CO\}Fe(CO)(PMePh_2)Cp]$ (XXVIII) in good yield after 18 hours. Under the same conditions (IV) reacted with $PMePh_2$ to give an analogous diacyl product (XXIX) in 86% yield after only 6 hours. The reaction of (III) with a large excess of PMe_3 gave $[Cp(CO)(PMe_3)Fe\{CO(CH_2)_3CO\}Fe(PMe_3)(CO)Cp]$ (XXX) in 79% yield after 42 hours in refluxing THF.

Compounds (XXII) - (XXX) were all isolated as orange microcrystalline solids and characterised by IR, ^1H NMR and microanalysis. These compounds are stable in solid form but decompose rapidly in solution, particularly in hydrocarbon solvents, on exposure to air, to non-carbonyl decomposition products.

For this reason, it proved difficult to obtain pure samples of these compounds for elemental analysis. In addition, broadening of the signals in the ^1H NMR spectra of these compounds was observed as a result of the presence of paramagnetic iron oxidation products. The IR spectra of the diacyl species (XXIII) - (XXX) resemble those of mononuclear compounds of the type $[Cp(CO)(PPh_3)FeCOR]$ [89], showing a single terminal carbonyl band in the region 1906 to 1913 cm^{-1}, the position reflecting the π-acceptor properties of the phosphine substituent, and a broad band at ~1600 cm^{-1} for the acyl groups. The monoacyl compound shows three terminal carbonyl bands of approximately equal intensity which correspond in position to those of $[Cp(CO)_2Fe]_2\{\mu\text{-}(CH_2)_3\}$ and $[Cp(CO)(PPh_3)Fe\{CO(CH_2)_3CO\}Fe(CO)(PPh_3)Cp]$

The ^1H NMR spectrum of (XXII) is as expected for the structure $[Cp(CO)(PPh_3)Fe\{CO(CH_2)_3\}Fe(CO)_2Cp]$, showing two singlet C_5H_5 proton resonances and an approximate triplet for the $\underline{CH_2}CO$ protons in the ratio 5:5:2. The signal for the remaining methylene protons is an unresolved doublet. In the ^1H NMR spectra of the diacyl species (XXIII) - (XXX) the methylene proton resonances are more complex. All the spectra show a complex multiplet for the four $\underline{CH_2}CO$ protons and two broad singlets for the other methylene protons. One possible explanation for these signals could be the existence of different methylene proton environments as a result of restricted rotation of the molecule about the C-C bonds in the bridge. However there is no evidence for this effect. In a variable temperature ^1H NMR study of (XXIII) and (XXVI) over the range -40 to 80°C no change in the methylene proton signals could be detected. However, below -20°C, some splitting of the cyclopentadienyl resonance of (XXIII) was observed. In addition, the extent of the splitting of the methylene proton signals does not vary noticeably with increasing length of the alkanediyl bridge in compounds (XXIII)

- (XXVII) or with decreasing bulk of the tertiary phosphine substituents (compounds (XXIII), (XXVIII), (XXX)) as might be expected if it were due to restricted rotation of the molecule.

Alternatively, the splitting of the methylene proton signals could arise from the diastereomeric shielding of these protons by the asymmetric Cp(CO)(L)Fe groups [17a]. In this case, the two protons in each $\underline{CH_2}CO$ group would be non-equivalent and coupling between these protons could give rise to the observed splitting. The effect of the diastereomeric shielding could also extend to the β-CH_2 protons and so account for the splitting of the other methylene proton signal. Such shielding effects have been reported for the compounds $[Cp(CO)(PPh_3)FeCOC_2H_5]$ [90] and $[Cp(CO)(PPh_3)FeCH_2Ph]$ [17a].

The fact that the mono-acyl species (XXII) can be isolated from the equimolar reaction of (III) with PPh_3 suggests that the formation of diacyl compounds may proceed in a stepwise fashion. To investigate this an infrared study of the reactions of (III) - (VII) with a two molar ratio of PPh_3 has been made. The progress of the reactions was followed by observing the disappearance of the bands at ~2000 and ~1940 cm^{-1} in the infrared spectrum of the reaction mixture, and the accompanying appearance of product bands at ~1920 and ~1610 cm^{-1}. Initially a rapid decrease in the bands at 2000 and 1940 cm^{-1} to approximately half their original intensity was observed. After this point, further decrease was slow and the rate was found to depend on the length of the alkanediyl bridge in the substrate. This is illustrated in Fig. 5.1 by the plots of I_t/I_o against time where I_o is the intensity of the band at 2000 cm^{-1} at the start of the reaction and I_t its intensity at time t.

These observations are consistent with the reactions proceeding by initial

rapid conversion of the substrate to the monoacyl species 62 . On completion of this reaction (equation (42)) i.e. the point at which there is a sudden change in reaction rate (see Fig. 5.1), the IR spectrum of the reaction mixture corresponds to that of the monoacyl product showing bands at ~2000 and ~1940 cm^{-1} for the terminal carbonyl groups on the unsubstituted iron residue and bands at ~1920 and ~1810 cm^{-1} for the terminal carbonyl group on the other iron and the acyl group respectively. The monoacyl species then reacts slowly with further PPh_3 to give the diacyl product 63 (equation (43).

$$[Cp(CO)_2Fe]_2\{\mu\text{-}(CH_2)_n\} \longrightarrow [Cp(CO)(PPh_3)Fe\overset{O}{\overset{\|}{C}}(CH_2)_nFe(CO)_2Cp] \quad (42)$$

62

$$[Cp(CO)(PPh_3)Fe\overset{O}{\overset{\|}{C}}(CH_2)_nFe(CO)_2Cp] \longrightarrow [Cp(CO)(PPh_3)Fe\overset{O}{\overset{\|}{C}}(CH_2)_n\overset{O}{\overset{\|}{C}}Fe(CO)(PPh_3)Cp] \quad (43)$$

63

Reaction (43) corresponds to the slow decrease in the bands at ~2000 and ~1940 cm^{-1} due to the monoacyl species. The reaction with a second molecule of PPh_3 would be expected to be slower as a result of the greater steric hindrance to attack by the bulky phosphine group on the mono-substituted species 62 . The dependence of the rate of this reaction on the length of the alkanediyl bridge reflects a decrease in steric hindrance with increasing distance between the metal atoms.

In this work, several attempts have been made to decarbonylate the diacyl compounds prepared (XXII) - (XXX) to form tertiary phosphine substituted $\mu(1,n)$alkanediyl species. The diacyl compounds $[Cp(CO)(L)Fe\{CO(CH_2)_nCO\}Fe(L)(CO)Cp]$ are resistant to thermal

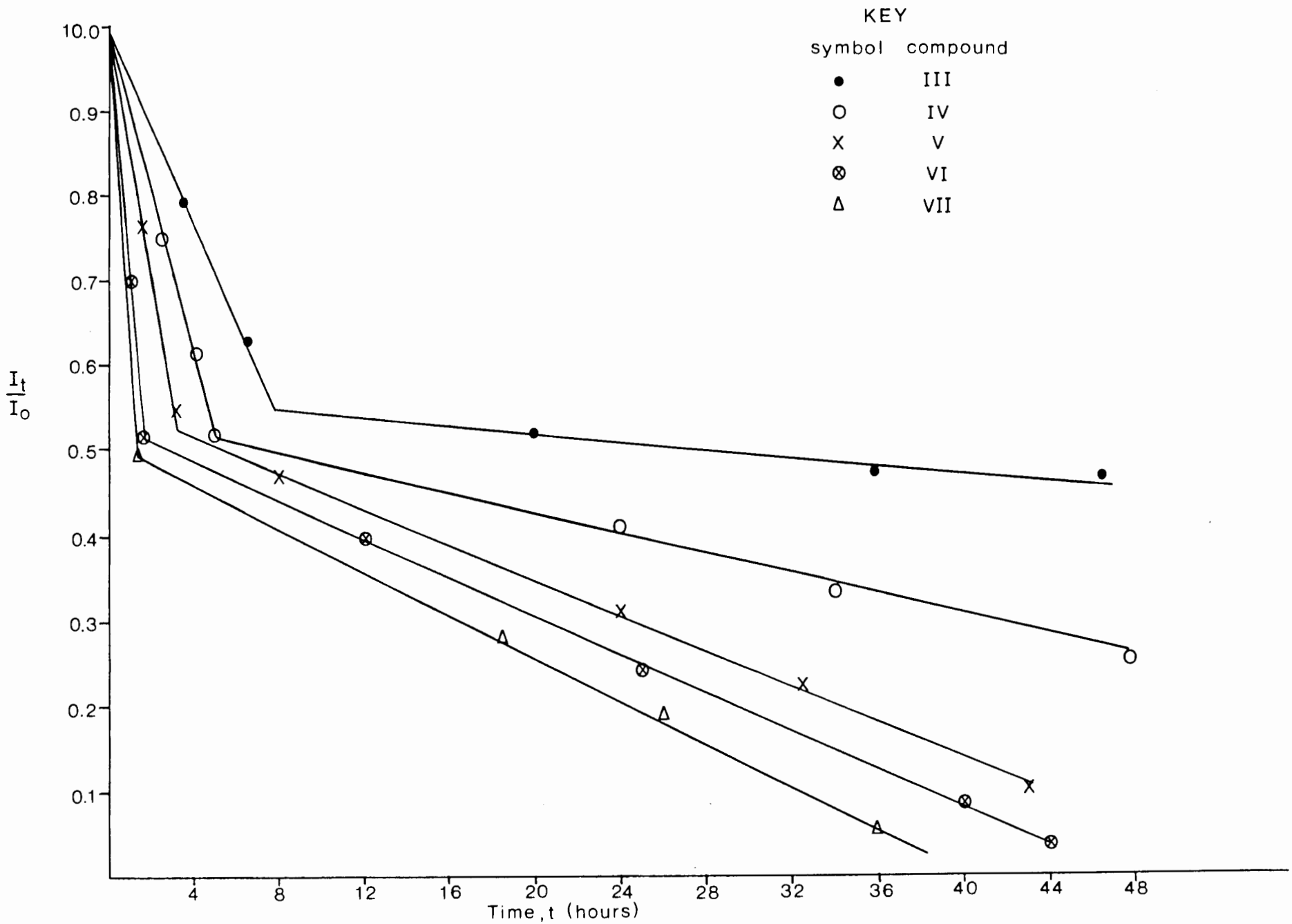

Fig. 5.1 Plots of I_t/I_o against time for the reactions of compounds (III) - (VII) with PPh_3

decarbonylation; (XXIV) was found to be stable in refluxing dimethoxyethane for prolonged periods. In refluxing petroleum ether (b.p. 130-160°C) decomposition of the diacyl compound to a non-carbonyl product was observed.

An established route to compounds of the type [Cp(CO)(L)FeR] [89,91] (L = tertiary phosphine ; R = alkyl) is via photochemical decarbonylation of the corresponding acyl species [Cp(CO)(L)FeCOR]. However photolysis of $[Cp(CO)(PPh_3)Fe\{CO(CH_2)_4CO\}Fe(CO)(PPh_3)Cp]$ in THF, was found to result in extensive decomposition of the compound and none of the desired product $[Cp(CO)(PPh_3)Fe]_2\{\mu\text{-}(CH_2)_4\}$ could be detected. During the reaction the infrared spectra of the reaction mixture, in the region 2100-1550 cm^{-1}, showed the disappearance of starting material bands and the accompanying appearance of bands at 2011, 1991, 1950, 1781 and 1732 cm^{-1}. The bands at 1991, 1950 and 1781 were attributable to $[Cp(CO)_2Fe]_2$ while the band at 2011 cm^{-1} could be due to the presence of a non-substituted acyl species (c.f. $[Cp(CO)_2Fe\{CO(CH_2)_4CO\}Fe(CO)_2Cp]$ ν(CO)(THF) 2012(s) 1950 (s) cm^{-1}). The appearance of a band at 1732 cm^{-1} suggested that an organic product with a ketonic or carboxylic CO group was formed in the reaction. The only organometallic products isolated from the reaction mixture were $[Cp(CO)_2Fe]_2$ and $[Cp_2Fe]$. The organic product was separated as an oil with an infrared spectrum very similar to that reported for $COOH(CH_2)_4COOH$. The formation of such a product could result from elimination of the $CO(CH_2)_4CO$ bridge from the starting material. It is possible that the photolysis of diacyl compounds may have a synthetic application for the preparation of bifunctional aliphatic compounds from dihaloalkanes. The synthesis of aldehydes [92a], ketones [92b] and carboxylic acids [92c] by reaction of compounds of the type $Li[(CO)_4FeR]$ (R = alkyl) with tertiary phosphines has been reported [92] (equation (44));

$$Li[(CO)_4FeR] + PR_3 \longrightarrow Li[(CO)_3(PR_3)FeCOR] \xrightarrow{AcOH} RCHO \qquad (44)$$

$$\downarrow X_2 \mid H_2O$$

$$RCOOH$$

The photolysis of (XXIV) was also carried out in the presence of free PPh_3 to inhibit the dissociation of the tertiary phosphine ligand, and in petroleum ether. Wojcicki *et al.* [89] have reported good yields of $[Cp(CO)(PPh_3)FeR]$ from the photolysis of $[Cp(CO)(PPh_3)FeCOR]$ (R = CH_3, C_2H_5) in hydrocarbon solvents. However, in this study, extensive decomposition of $[Cp(CO)(PPh_3)Fe\{CO(CH_2)_4CO\}Fe(CO)(PPh_3)Cp]$ to insoluble non-carbonyl products occurred on photolysis in petroleum ether and only a small amount of $[Cp(CO)_2Fe]_2$ was isolated from the reaction. Similar results were obtained for the irradiation of $[Cp(CO)(PPh_3)Fe\{CO(CH_2)_6CO\}Fe(CO)(PPh_3)Cp]$ in THF or petroleum ether. $[Cp(CO)_2Fe]_2$ and an organic product analogous to that observed on photolysis of (XXIV), were the only isolable products.

The attempt was made to decarbonylate (XXIV) under milder conditions by reaction with $RhCl(PPh_3)_3$ at room temperature, to limit sample and product decomposition. However, no reaction was detected after 10 hours and the starting diacyl compound was eventually recovered in 98% yield. The resistance of this compound to chemical decarbonylation can be attributed to the greater strength of the Fe-CO bond in the phosphine substituted diacyl compound compared with $[Cp(CO)_2Fe\{CO(CH_2)_nCO\}Fe(CO)_2Cp]$ (n = 3,4).

Alternative routes to phosphine-substituted alkanediyl bridged species were also investigated. Alexander [93] has reported the isolation of $[Cp(CO)(PPh_3)FeCH_3]$ in 23% yield by irradiation of $[Cp(CO)_2FeCOCH_3]$

in the presence of PPh_3. However irradiation of THF solutions of $[Cp(CO)_2Fe\{CO(CH_2)_nCO\}Fe(CO)_2Cp]$ (n = 3,4) and excess PPh_3, produced mainly $[Cp(CO)_2Fe]_2$. An organic product similar to that formed in the photolysis of (XXIV) was detected in these reactions (ν(CO)1732 cm^{-1}). A small yield of $[Cp(CO)_2Fe]_2\{\mu\text{-}(CH_2)_4\}$ (19%) was also obtained from the photolysis of $[Cp(CO)_2Fe\{CO(CH_2)_4CO\}Fe(CO)_2Cp]$ in the presence of PPh_3.

Compounds of the type $[Cp(CO)(PPh_3)FeR]$ (R =alkyl) have also been prepared by reaction of $[Cp(CO)_2FeR]$ with PPh_3 under U.V.irradiation [89]. On irradiation of $[Cp(CO)_2Fe]_2\{\mu\text{-}(CH_2)_4\}$ in the presence of excess PPh_3 in THF, $[Cp(CO)_2Fe]_2$ was again formed as the major product. In addition, a band at ~1905 cm^{-1} in the infrared spectrum of the reaction mixture, suggested the presence of the required product (c.f. ν(CO)1901 cm^{-1} for $[Cp(CO)(PPH_3)FeC_2H_5]$). In the workup of the reaction mixture $[Cp(CO)_2Fe]_2$ and $[Cp(CO)(PPh_3)Fe\{CO(CH_2)_4CO\}Fe(PPh_3)(CO)Cp]$ were isolated in 28% and 16% yield respectively. Two unstable orange solids were also isolated. One was identified as $[Cp(CO)(PPh_3)FeH]$ on the basis of its infrared spectrum and its reaction with $CHCl_3$ to give $[Cp(CO)(PPh_3)FeCl]$. The other product showed a strong carbonyl band at 1906 cm^{-1} which suggested that this was the required product. However, the compound was unstable and decomposed rapidly in solution and in the solid state to a non-carbonyl product so no satisfactory ^1H NMR spectrum or elemental analysis could be obtained. The isolation of $[Cp(CO)(PPh_3)FeH]$ from the reaction suggests that $[Cp(CO)(PPh_3)Fe]_2\{\mu\text{-}(CH_2)_4\}$ is formed but decomposes according to equation (45) under the reaction conditions.

$$[Cp(CO)(PPh_3)Fe]_2\{\mu\text{-}(CH_2)_4\} \longrightarrow 2[Cp(CO)(PPh_3)FeH] + C_4H_6 \qquad (45)$$

This type of decomposition reaction has been reported for $[Cp(CO)(PPh_3)FeC_2H_5]$. The fact that neither $[Cp(CO)(PPh_3)Fe]_2\{\mu\text{-}(CH_2)_4\}$ nor $[Cp(CO)(PPh_3)FeH]$ could be detected in the photolysis of $[Cp(CO)(PPh_3)Fe\{CO(CH_2)_4CO\}Fe(CO)(PPh_3)Cp]$ (XXIV) under the same conditions, suggests that (XXIV) is not formed as an intermediate in reaction (46),

$$[Cp(CO)_2Fe]_2\{\mu\text{-}(CH_2)_4\} \xrightarrow{PPh_3,\ h\nu} [Cp(CO)(PPh_3)Fe]_2\{\mu\text{-}(CH_2)_n\} \quad (46)$$

as concluded for the photochemical reaction of $[Cp(CO)_2Fe(C_2H_5)]$ with PPh_3 to give $[Cp(CO)(PPh_3)FeC_2H_5]$ [89].

5.2.2 Reactions of μ(1,n)alkanediyl diiron compounds with halogens.

The reactions of mononuclear iron alkyl compounds $[Cp(CO)_2FeR]$ with a wide variety of electrophilic reagents have been studied [94] and there has been much interest in the mechanism of these reactions [95-100]. However, no investigations of the analogous reactions of μ(1,n)alkanediyl diiron compounds have been reported. By analogy, with the mononuclear systems, $[Cp(CO)_2Fe]_2\{\mu\text{-}(CH_2)_n\}$ should react with a two mole proportion of an electrophile EX to give 2 $[Cp(CO)_2FeX]$ and $E(CH_2)_nE$.

In this work, the reactions of $[Cp(CO)_2Fe]_2\{\mu\text{-}(CH_2)_n\}$ (n = 3,4) (III) and (IV) with halogens (I_2 and Br_2) have been investigated. $[Cp(CO)_2Fe]_2\{\mu\text{-}(CH_2)_3\}$ reacted rapidly with I_2 and Br_2 in 1:2 mole ratio to produce the expected cleavage products (equation (47)).

$$[Cp(CO)_2Fe]_2\{\mu\text{-}(CH_2)_3\} + 2X_2 \xrightarrow[20°C]{THF/CH_2Cl_2} [Cp(CO)_2FeX] + X(CH_2)_3X \quad (47)$$
$$(X = Br, I)$$

The products were identified on the basis of their IR and mass spectra by comparison with those of authentic samples. In the analogous reaction of $[Cp(CO)_2Fe]_2\{\mu\text{-}(CH_2)_4\}$ with I_2, a third product (ν(CO)(THF): 2080 (s) 2046 (s) cm^{-1}) in addition to the expected $I(CH_2)_4I$ and $[Cp(CO)_2FeI]$ was detected in the infrared spectrum of the reaction mixture. This product was isolated as an insoluble highly unstable red solid (XXXI). The insolubility of this compound and the high frequency of the carbonyl bands in its infrared spectrum suggested it was a cationic species †. This was confirmed by the precipitation of the compound as a yellow tetraphenylborate salt on addition of $NaBPh_4$ to a solution of (XXXI) in methanol.

The ^1H NMR spectrum of (XXXI) showed two broad singlets at δ 5.96 and δ 4.04 which correspond in position to the cyclopentadienyl and methylene proton resonances observed for $[Cp(CO)_2Fe(C_2H_4)]^+$. The breadth of the signals in the ^1H NMR spectrum suggested that this compound was paramagnetic. Attempts to characterise (XXXI) further failed due to its instability particularly under vacuum. Solutions of (XXXI) in acetone and THF were found to decompose rapidly on standing and the infrared spectrum of these solutions showed new bands at 2044, 1999 and 1948 cm^{-1}. The ^1H NMR spectrum of the decomposition products showed the presence of $[Cp(CO)_2FeI]$ (δ 5.30, C_5H_5) and $[Cp(CO)_2Fe]_2\{\mu\text{-}(CH_2)_4\}$ (δ 1.26, CH_2 ; δ 5.04, C_5H_5).

The reaction of $[Cp(CO)_2Fe]_2\{\mu\text{-}(CH_2)_4\}$ with Br_2 also produced a cationic species (ν(CO) 2076 (s) 2044 (s); ^1H NMR (acetone-d^6) δ 4.08 (s,8H) δ 6.00 (s,10H)) (XXXII). This compound was isolated as a dark orange solid and was

---

† A comparison was made with the IR spectrum of the cationic species $[Cp(CO)_2Fe(C_2H_4)]$ which shows two bands at 2080 (s) and 2040 (s) cm^{-1}.

found to be more stable than (XXXI) in the solid state. As for (XXXI), broad proton resonances were observed in the ^1H NMR spectrum of (XXXII) consistent with the compounds being paramagnetic. This was confirmed by magnetic susceptibility measurements; a paramagnetic mass susceptibility (χ_m) of 6.6×10^{-7} m^3kg^{-1} (5.2×10^{-6} cgsu) was measured for (XXXII) compared with a value of $\chi_m = -0.5 \times 10^{-6}$ m^3kg^{-1} for the diamagnetic $[Cp(CO)_2Fe]_2\{\mu\text{-}(CH_2)_4\}$.

The formation of $[Cp(CO)_2FeI]$ and $[Cp(CO)_2Fe]_2\{\mu\text{-}(CH_2)_4\}$ on decomposition of (XXXI) suggests that this compound may be formed as an intermediate in the cleavage reaction of $[Cp(CO)_2Fe]_2\{\mu\text{-}(CH_2)_4\}$. Investigations of the kinetics and stereochemistry of reactions of mononuclear iron alkyl compounds with various electrophilic reagents [95-100] have indicated that these cleavage reactions may proceed either by a one electron transfer process (equation (48)) or via oxidative addition of the electrophile to the substrate molecule (equation (49)).

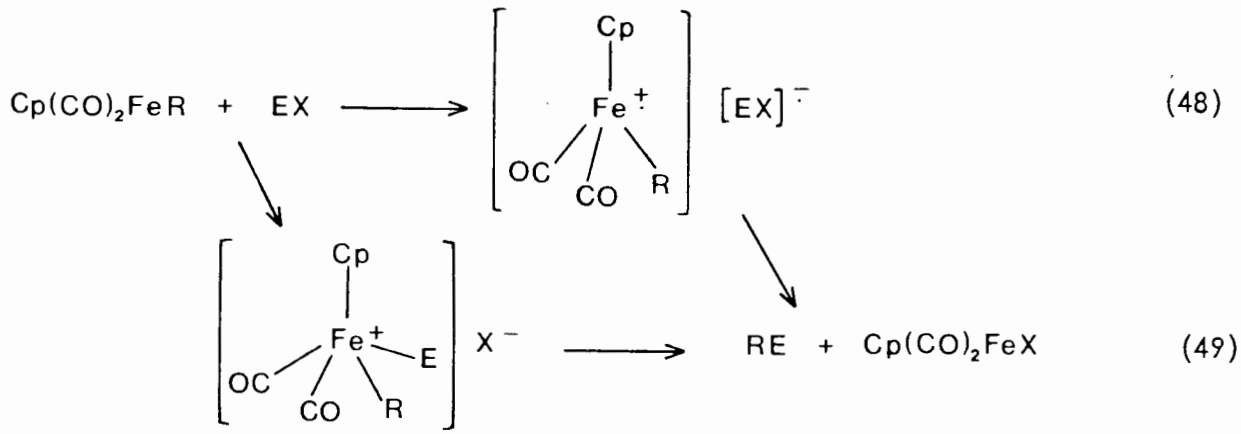

Both routes involve the formation of a cationic intermediate prior to metal-carbon bond cleavage. Since the cationic species isolated from the reactions of $[Cp(CO)_2Fe]_2\{\mu\text{-}(CH_2)_4\}$ with X_2 are paramagnetic, it appears that the

one electron transfer process (50);

$$[Cp(CO)_2Fe]_2\{\mu\text{-}(CH_2)_4\} \overset{X_2}{\rightleftharpoons} \underset{64}{[Cp(CO)_2Fe(CH_2)_4Fe(CO)_2Cp]^{+}[X_2]^{-}} \quad (50)$$

may be operative in these reactions. The formulation of (XXXI) and (XXXII) as 64 is consistent with the observed properties of these compounds. The close similarity of their spectral data to that of the cationic species $[Cp(CO)_2Fe(C_2H_4)]^+$ is suggestive of this structure rather than that of a halide containing cation. Similarly the isolation of a yellow BPh_4 salt of (XXXI) suggests that the halogen is present only as a counter ion in this species. In addition, decomposition of the BPh_4 salt of (XXXI) produces no $[Cp(CO)_2FeI]$ only $[Cp(CO)_2Fe]_2\{\mu\text{-}(CH_2)_4\}$.

The reaction products could be derived from the intermediate 64 by direct attack of X^- on the alkyl group and displacement of $Cp(CO)_2Fe\cdot$ which would combine with $X\cdot$ to form $[Cp(CO)_2FeX]$ (equation (51)). Alternatively a second one electron transfer may occur to give $[Cp(CO)_2Fe(CH_2)_4Fe(CO)_2CpX]^+[X]^-$ 65 . Attack of X^- on this species could result in displacement of $Cp(CO)_2FeX$ (equation (52)).

$$[Cp(CO)_2Fe(CH_2)_4Fe(CO)_2Cp]^{+}[X_2]^{-} \xrightarrow{X^-} [Cp(CO)_2Fe]\cdot + [X(CH_2)_4Fe(CO)_2Cp] \quad (51))$$

$$\downarrow e^- \text{ transfer}$$

$$\underset{65}{[Cp(CO)_2FeX(CH_2)_4Fe(CO)_2Cp]^{+}[X]^{-}} \xrightarrow{X^-} [Cp(CO)_2FeX] + [X(CH_2)_4Fe(CO)_2Cp] \quad (52)$$

(with $X\cdot$ ↓ connecting $[X(CH_2)_4Fe(CO)_2Cp]$ to the X^- step)

Further reaction of $[Cp(CO)_2Fe(CH_2)_4X]$ with another molecule of X_2 could result in the formation of $X(CH_2)_4X$. $[Cp(CO)_2Fe(CH_2)_4Br]$ was indeed found to react with Br_2 to give $[Cp(CO)_2FeBr]$ and $Br(CH_2)_4Br$. No intermediate species could be detected in this reaction but this is not surprising since discrete intermediates have seldom been observed in electrophilic cleavage reactions of mononuclear iron alkyls. The proposal that the cleavage of the metal-carbon bonds in $[Cp(CO)_2Fe]_2\{\mu\text{-}(CH_2)_n\}$ occurs in a stepwise fashion is supported by the observation of small amounts of $[Cp(CO)_2Fe\{(CH_2)_4X\}]$ (detected by IR and Mass spectroscopy) in the reactions of (IV) with X_2. Cleavage of the Fe-C bond in $[Cp(CO)_2Fe\{(CH_2)_4X\}]$ apparently occurs more readily than the initial bond cleavage in $[Cp(CO)_2Fe]_2\{\mu\text{-}(CH_2)_4\}$ since reaction of (IV) with a one molar proportion of X_2 produces $[Cp(CO)_2FeX]$ and $X(CH_2)_4X$, and ca. 50% of the starting material (IV) is recovered.

Subsequent to the studies of the reactions of (IV) with X_2, the reactions of (III) with I_2 and Br_2 were reinvestigated and at low temperature (0°C), a cationic species could be detected in the IR spectra of the reaction mixtures. This suggests that these reactions proceed by a similar route to those of (IV).

From this work it is apparent that further study of the electrophilic cleavage reactions of $\mu(1,n)$alkanediyl diiron compounds would be of interest since the relative stability of the reaction intermediates would aid mechanistic investigations of this type of reaction.

5.2.3 Reactions of μ(1,n)alkanediyl ditungsten compounds with tertiary phosphines

Although there has been considerable interest in the reactions of metal alkyl compounds such as $[Cp(CO)_2FeR]$ and $[Cp(CO)_3MoR]$ with tertiary phosphines few related reactions of tungsten species have been investigated [91,101]. This could be due to the relative reluctance of the tungsten compounds to undergo carbonyl insertion reactions. In this study, the μ(1,n)alkanediyl ditungsten compounds were found to be considerably less reactive than their diiron analogues. The reactions of (XIII) - (XV) with tertiary phosphines generally required higher temperatures and/or longer reaction times than those of the corresponding diiron compounds (III) - (V).

Like the diiron compounds, $[Cp(CO)_3W]_2\{\mu\text{-}(CH_2)_n\}$ react with a two molar proportion of tertiary phosphine to give phosphine-substituted diacyl products. In addition and in contrast to the reactions of (III) - (V) which yield only acyl products, these reactions also produce non-acyl substituted compounds in low yield. These species could be formulated as $[Cp(CO)_2(L)W\{\mu\text{-}(CH_2)_n\}W(CO)_3Cp]$ or $[Cp(CO)_2(L)W]_2\{\mu\text{-}(CH_2)_n\}$. Since these products could not be separated from the starting material recovered from the reactions, no definite structural assignment could be made in most cases. The formation of these compounds was indicated by the appearance of a doublet resonance at δ 4.75 in the ^1H NMR spectra of the product mixtures. This could be assigned to the C_5H_5 proton resonance of a phosphine substituted alkyl product by comparison with the ^1H NMR spectra of compounds of the type $[Cp(CO)_2(L)MCH_3]$ [102,103] (L = tertiary phosphine; M = Mo,W).

The reactions of $[Cp(CO)_3W]_2\{\mu\text{-}(CH_2)_n\}$ (n = 4,5) with tertiary phosphines

in refluxing THF are slow; after 70 hours, the diacyl species $[Cp(CO)_2(PMePh_2)W\{CO(CH_2)_nCO\}W(PMePh_2)(CO)_2Cp]$ (n = 4,5) (XXXIII) and (XXXIV) were only isolated in ca. 54% yield from the reactions of (XIV) and (XV) with $PMePh_2$ (in 1:2 mole ratio) in THF. In refluxing DME, the reaction of (XIV) with $PMePh_2$ (in 1:2 mole ratio) gave (XXXIII) in 55% yield after 38 hours.

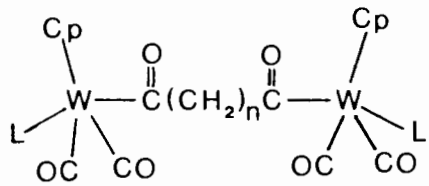

(XXXIII) L = $PMePh_2$; n = 4

(XXXIV) L = $PMePh_2$; n = 5

(XXXVI) L = PPh_3; n = 4

(XXXVII) L = PPh_3; n = 5

The reaction of $[Cp(CO)_3W]_2\{\mu\text{-}(CH_2)_4\}$ with a two molar proportion of PPh_3 in refluxing DME produced only the monoacyl species $[Cp(CO)_2(PPh_3)W\{CO(CH_2)_4\}W(CO)_3Cp]$ (XXXV) and a substituted non-acyl product, probably $[Cp(CO)_2(PPh_3)W\{(CH_2)_4\}W(CO)_3Cp]$, after 34 hours. In refluxing THF, a 37% yield of the diacyl species $[Cp(CO)_2(PPh_3)W\{CO(CH_2)_4CO\}W(PPh_3)(CO)_2Cp]$ (XXXVI) was obtained after 75 hours. $[Cp(CO)_3W]_2\{\mu\text{-}(CH_2)_5\}$ reacted with PPh_3 (in 1:2 mole ratio) in refluxing THF to give $[Cp(CO)_2(PPh_3)W\{CO(CH_2)_5CO\}W(PPh_3)(CO)_2Cp]$ (XXXVII) in 45% yield after several days.

Compounds (XXXIII) - (XXXVII) were isolated as microcrystalline yellow solids and characterised by IR, ^1H NMR and microanalysis. These compounds could exist in several different geometrical isomers with *cis* and/or *trans* configuration of the CO groups in the $Cp(CO)_2(L)W$ moieties. On the basis of their IR and ^1H NMR spectra the diacyl species can be assigned the all *trans* structure 66.

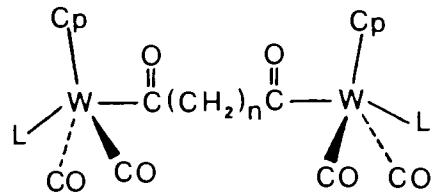

66

The IR spectra of these compounds show two terminal bands in the ranges 1932 - 1922 and 1845 cm^{-1} with the lower frequency band more intense than the higher frequency band. This intensity pattern has been shown by Manning [104] to be indicative of a *trans* geometry in compounds containing a $Cp(CO)_2(L)M$ residue (M = Mo,W) (e.g. $Cp(CO)_2(PPh_3)MoI$).

More definitive evidence [17a] for the *trans* geometry of compounds (XXXIII), (XXXIV), (XXXVI) and (XXXVII) is obtained from the ^1H NMR spectra of these compounds. All these compounds exhibit a doublet cyclopentadienyl resonance due to ^{31}P coupling ($J \simeq 1.5$ Hz) with the phosphine ligand. This splitting is reported to be characteristic of the *trans* isomer of compounds of the type $[Cp(CO)_2(L)MR]$ (L = tertiary phosphine, M = Mo,W; R = H, alkyl) [105,106] while the *cis* isomer shows a singlet resonance for the C_5H_5 protons ($J < 0.2$ Hz). In addition, the ^1H NMR spectra of the diacyl species, show a well-defined triplet for the $\underline{CH_2}CO$ protons. If the compounds contained a *cis* - $Cp(CO)_2(L)W$ residue the metal atom would be asymmetric and diastereomeric shielding of the $\underline{CH_2}CO$ protons would result in further splitting of this signal [104].

^1H NMR spectrum of the monoacyl species $[Cp(CO)_2(PPh_3)W\{CO(CH_2)_4\}W(CO)_3Cp]$ (XXXV) shows a doublet C_5H_5 resonance for the $Cp(CO)_2(PPh_3)W$ residue indicative of a *trans* geometry about this tungsten atom. In the IR spectrum

of (XXXV) the carbonyl bands from the $Cp(CO)_2(PPh_3)W$ residues are superimposed so no information about the geometry of the substituted group can be obtained.

The resistance of $[Cp(CO)_3W]_2\{\mu\text{-}(CH_2)_n\}$ (n = 3-5) to tertiary phosphine-induced CO -insertion compared with the analogous diiron compounds could reflect a difference in the metal-carbon bond strength. It is generally thought [101,107] that the rate determining step of a carbonyl insertion reaction is the migration of the alkyl group onto a terminal CO to form an unsaturated intermediate. If this is so, the slower rate of reaction of the tungsten compounds could be attributed to greater strength of the tungsten-carbon bond.

The formation of non-acyl phosphine substituted products in the reaction of $[Cp(CO)_3W]_2\{\mu\text{-}(CH_2)_n\}$ with tertiary phosphine can be attributed to the thermal decarbonylation of acyl products of these reactions (equations (53) and (54)).

$$[Cp(CO)_2(L)W\{\overset{O}{\overset{\|}{C}}(CH_2)_n\}W(CO)_3Cp] \xrightarrow{-CO} [Cp(CO)_2(L)W\{(CH_2)_n\}W(CO)_3Cp] \quad (53)$$

$$[Cp(CO)_2(L)W\{\overset{O}{\overset{\|}{C}}(CH_2)_n\overset{O}{\overset{\|}{C}}\}W(L)(CO)_2Cp]$$

$$\xrightarrow{-2CO} [Cp(CO)_2(L)W]_2\{\mu\text{-}(CH_2)_n\}$$

$$\xrightarrow{-CO} [Cp(CO)_2(L)W\{(CH_2)_n\overset{O}{\overset{\|}{C}}\}W(L)(CO)_2Cp] \xrightarrow{-CO} [Cp(CO)_2(L)W]_2\{\mu\text{-}(CH_2)_n\} \quad (54)$$

Consistent with this is the observation that the proportion of diacyl product produced in the reaction of (XIV) with $PMePh_2$ in DME, is decreased and

that of the substituted non-acyl product increased, by prolonged heating of the reaction mixture. In addition, it was found that the diacyl compounds (XXXIII), (XXXIV), (XXXVI) and (XXXVII) can be converted to non-acyl substituted products by heating in DME in the presence of an excess of free phosphine ligand. The excess of phosphine is required to inhibit the dissociation of the phosphine ligand; in the absence of free phosphine the diacyl compounds are rapidly converted to the corresponding unsubstituted μ(1,n)alkanediyl compounds (XIV) and (XV).

In comparison with compounds of the type $[Cp(CO)_2(L)MoR]$ [105] (L = tertiary phosphine; R = alkyl), the diacyl species (XXXIII), (XXXIV) and (XXXVII) are relatively resistant to thermal decarbonylation to the corresponding phosphine substituted non-acyl species. For example, decarbonylation of $[Cp(CO)_2(PPh_3)MoCOCH_3]$ proceeds readily at 65°C in acetonitrile with 50% conversion to the corresponding methyl compound after 10 hours [105] whereas only a trace of a phosphine substituted alkyl product could be detected after heating (XXXVI) in refluxing acetonitrile for 48 hours. Among the diacyl tungsten compounds, decarbonylation of the PPh_3 substituted compounds was found to occur more rapidly than that of the $PMePh_2$ substituted species. After 24 hours in refluxing DME, approximately 50% conversion of (XXXVII) to a non-acyl product was observed whereas under the same conditions, only ~10% of (XXXIV) was converted to a non-acyl product. (The percentage conversion in these reactions was determined from the relative intensities of the C_5H_5 proton resonances of the acyl starting material (~ δ 5.00) and the non-acyl product (~ δ 4.80) in the ^1H NMR spectra of the reaction mixtures). Similar ligand dependence has been reported for the decarbonylation reaction of $[Cp(CO)_2(L)MoCH_3]$ [105] (L = tertiary phosphine) and it is thought to be largely steric in origin. The increased rate of decarbonylation

with increased size of the tertiary phosphine ligand has been accounted for in terms of a dissociative mechanism in which CO is lost from the substrate to form a coordinatively unsaturated intermediate 67 (equation (55)).

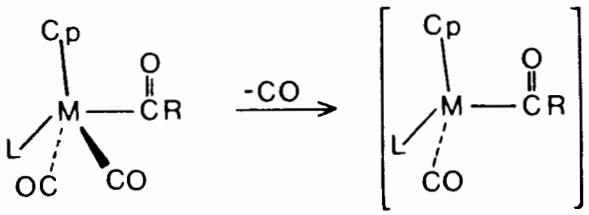

(55)

67

The dissociation of CO would be favoured by the increased size of L. This mechanism would also be consistent with the electronic effects of L, since the increased basicity of L on going from PPh_3 to PPh_2Me would inhibit dissociation of CO by forcing stronger M-CO back bonding [105].

The stereochemistry of the CO insertion reaction and the reverse decarbonylation is of interest since information can be gained about the reaction mechanisms from their stereochemical results. The exclusive formation of the *trans* diacyl product in the carbonyl insertion reactions of $[Cp(CO)_3W]_2\{\mu\text{-}(CH_2)_n\}$ is consistent with the reported steriochemistry of the reaction of $[Cp(CO)_3MCH_3]$ (M = Mo,W) with tertiary phosphines to give $[Cp(CO)_2(L)MCOCH_3]$ [105,106]. The formation of the *trans* isomer in these reactions has been attributed to rearrangement of a kinetically favoured *cis* product[91,107]. In this study, evidence in support of this mechanism was provided by the observation of an acyl product with a *cis* - $Cp(CO)_2(L)W$ configuration in the reaction of (XIV) with PPh_3 in THF. This was indicated by the presence of a singlet C_5H_5 resonance at δ 5.08 in the ^1H NMR spectrum of the reaction mixture. The detection of the

cis product suggests that the *cis* ⟶ *trans* isomerisation occurs less readily in the lower boiling solvent.

The decarbonylation reactions of $[Cp(CO)_2(L)W\{CO(CH_2)_nCO\}W(L)(CO)_2Cp]$ (L = PPh_3, PPh_2Me; n = 4,5) in refluxing DME were found to give only the *trans*-phosphine substituted product. This was indicated by the appearance of a doublet C_5H_5 resonance in the ^1H NMR spectra for these compounds. An all *trans* product is similarly observed on decarbonylation of $[Cp(CO)_2(L)MoCOCH_3]$ (L = tertiary phosphine), and has been attributed to the preferential migration of the alkyl ligand away from the bulky phosphine group in the unsaturated intermediate 68 [105].

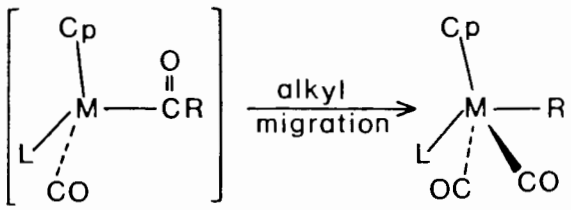

68

SECTION 6

6. EXPERIMENTAL

6.1 General

All reactions were carried out under an atmosphere of high purity nitrogen in nitrogen-saturated solvents using Schlenk tube techniques.

$[Cp(CO)_2Fe]_2$, and $[Mn_2(CO)_{10}]$ were obtained from Strem Chemicals Inc. and were used without further purification. $[Cp(CO)_3W]_2$ was prepared from $[W(CO)_6]$ and NaCp by the method of Manning *et al.* [108]. The sodium salts of the anions $[Cp(CO)_2Fe]^-$, $[Cp(CO)_3W]^-$ and $[(CO)_5Mn]^-$ were prepared by stirring the corresponding dimer with an excess of 5 % sodium mercury amalgam in THF or DME, for 1 - 2 hours at room temperature [87]. $Br(CH_2)_nBr$ (n = 3 - 12) were obtained from Aldrich Chemical Corporation and $I(CH_2)_nI$ (n = 3,4,5) from Fluka AG, Ega-chemie and Riedel-de Haën AG respectively.

$RhX(PPh_3)_3$ (X = Cl,Br) were prepared by the methods of Wilkinson *et al.* [109]. The tertiary phosphines were obtained from Strem Chemicals Inc. and Merck. PMe_3 was produced by the method of Mann and Wells [110]. All other reagents were obtained commercially and used without further purification.

Analytical grade solvents were generally used and were purified further when necessary. THF and DME were dried by distillation over $LiAlH_4$ under N_2.

Column chromatography was carried out using BDH silica gel (60 - 120 mesh) or Merck Aluminium oxide 90 (70 - 230 mesh). Merck aluminium TLC plates

precoated with silica gel 60 were used for thin layer chromatography.

^{1}H NMR spectra were recorded on a Varian XL 100 spectrometer or on a Bruker WH 90 instrument operating in the Fourier Transform mode. Tetramethylsilane was used as internal reference and chemical shifts are given in ppm downfield of TMS (δ).

IR spectra were recorded on a Perkin Elmer 983 spectrophotometer in solution using solution cells with NaCl windows and a 0.1 mm path length or as a Nujol mull on NaCl plates. In the description of IR spectra the following abbreviations are used; (w) = weak, (m) = medium, (s) = strong, (vs) = very strong and (sh) = shoulder.

Microanalyses were performed by Mr. W T Hemsted, the microanalyst of the School of Chemistry at the University of Cape Town.

Melting ranges were determined on a Kofler hotstage microscope and are uncorrected.

The low resolution electron impact mass spectra were recorded on a VG Micromass 16F spectrometer, operating at 70 eV with an accelerating voltage of 4 kV, and the data analysed on a VG 2000 data system. The unprocessed mass spectrum was also recorded, as a UV trace, on an EMI SE6150 UV Oscillograph so that metastable peaks and ions with abundances below the detection limit of the data system could be observed. The samples were introduced into the spectrometer as solids on a direct probe at room temperature. Ion source temperatures used for the various samples studied are given in Table 6.1.

High resolution mass spectra of the iron compounds $[Cp(CO)_2Fe]_2$-$\{\mu-(CH_2)_n\}$ (n = 4-12) were recorded on a Varian 311 A spectrometer coupled to a Varian 71 data system. An operating voltage of 70 eV and source temperature of 138°C were used. Samples were introduced as solids on a heated probe. The probe temperatures used for the various samples are given in Table 6.1.

Isotope combination patterns for various parent and fragment ions of the tungsten compounds studied, were calculated using a computer program prepared at the University of Alberta, Alberta, Canada, adapted by Dr.M.L.Niven and extended by Dr.G.E.Jackson of the Dept. of Inorganic Chemistry, University of Cape Town, on the Univac 1106 computer.

The DSC traces of the compounds $[Cp(CO)_2Fe]_2\{\mu-(CH_2)_n\}$(n = 3-12) were recorded on a Perkin-Elmer DSC 2 instrument. The solid crystalline samples (typically of 2-5 mg) were contained in crimped aluminium pans. The samples were heated over the range 320 - 500 K at a rate of 20 K min^{-1} under an atmosphere of nitrogen. The calorimeter was calibrated against the fusion of indium (heat of fusion of 28,5 Jg^{-1}). The curves were integrated with a planimeter.

Calculations of the potential-energy of $[CpFe(CO)_2]_2\{\mu-(CH_2)_4\}$ during rotation were performed using the program EENY [84] and the interaction coefficients of Giglio [85].

Thermolyses were performed on solid samples of ca 50 mg under vacuum using the apparatus of Hall *et al.* [111]. Gas chromatographic analysis of the organic decomposition products were carried out on a Varian 3700 instrument.

Table 6.1 Probe and Ion source temperatures used in the recording of mass spectra for (III) - (XII) and (XIII) - (XXI)

compound	Ion source temperature °C [a]	Probe temperature °C [b]
(III)	90-110	-
(IV)	140	80
(V)	130	70
(VI)	130-140	50
(VII)	140	80
(VIII)	140	90
(IX)	150	90
(X)	150	100
(XI)	180	110
(XII)	180	120
(XIII)	215-245	-
(XIV)	235	-
(XV)	235	-
(XVI)	190	-
(XVII)	190	-
(XIX)	190	-
(XX)	120-130	-
(XXI)	90-120	-

a : for low resolution mass spectra

b : for high resolution mass spectra

A 2m n-octane/poracil column was used for compounds (III) - (VI) and (XIII) - (XV) and a 2m column of 3% OV-101 on Chromasorb 100/120 mesh WIP for compounds (VII) and (VIII). Peak integration was performed on a Varian CDS 401 terminal. A GLC-mass spectrometric analysis of the organic decomposition products of (IV), (V), (XIV) and (XV) was also carried out, using a Carlo Erba 4200 gas chromatograph linked to the VG Micromass mass spectrometer. All the gas chromatographic separations were performed using the same heating program, starting at 50°C for 4 minutes followed by a temperature increase at 8 K/minute to 125°C. The separated components were identified by comparison of retention times and/or mass spectra with those of standard samples.

Magnetic susceptibility measurements were carried out by the Gouy method on a Gallencamp magnetobalance. The calibrant was $Hg[Co(CSN)_4]$ and the measurements were carried out at room temperature. The samples were finely ground prior to introduction into the Gouy tube. A diamagnetic correction of $-5,886 \times 10^{-6}$ $kgms^{-2}$ was applied for the tube .

Photochemical reactions were performed in an Hanovia photochemical reactor, in a 1 ℓ reaction vessel under nitrogen.

6.2 Experimental details of Reactions in Section 1

6.2.1 General synthetic route [29] to μ(1,n)Alkanediyl bis(dicarbonyl cyclopentadienyl iron) compounds, $[Cp(CO)_2Fe]_2\{\mu\text{-}(CH_2)_n\}$ (n = 8-12)

$Br(CH_2)_nBr$ (6 mmole) was added dropwise over 5 minutes to a stirred solution of $Na[Cp(CO)_2Fe]$ (12 mmole) in THF (20 ml). The reaction mixture was stirred for 6 hours at room temperature then heated under reflux (75°C) for a further 6-8 hours. The reaction mixture was then allowed to cool to room temperature and the solvent removed under reduced pressure. The brown oily residue was extracted with CH_2Cl_2 (3 x 20 ml) and the extract filtered under suction and evaporated under reduced pressure. Addition of n-pentane (20 ml) to the solid brown residue and cooling caused rapid precipitation of the product as a yellow solid which was filtered off and washed with pentane. Recrystallisation from pentane gave the product as yellow crystals. Yields and melting points are recorded in Table 6.2, elemental analyses in Table 6.3 and IR and ^1H NMR data in Table 6.4. Mass spectra are reported and discussed in Section 3.

$[Cp(CO)_2Fe]_2\{\mu\text{-}(CH_2)_n\}$ (n = 3-7) (III) - (VII) were prepared for the thermal analysis and mass spectral study, by an adaptation of this method [88] . The mixture of $Na[Cp(CO)_2Fe]$ and $Br(CH_2)_nBr$ was stirred at room temperature for only 1-2 hours then evaporated and the residue extracted with n-pentane instead of CH_2Cl_2. Concentration of the filtered pentane solution gave the product in high yield (see Table 6.5).

Table 6.2 Yields and melting ranges of $[Cp(CO)_2Fe]_2\{\mu-(CH_2)_n\}$ (n = 8-12) (VIII) - (XII)

Compound	yield %	melting range °C
(VIII)	53	63-65, 73-75 [a]
(IX)	48	45-48
(X)	47	56-58
(XI)	64	52-54
(XII)	53	59-62

a : for discussion of the double melting point see section 4

Table 6.3 Elemental analyses of $[Cp(CO)_2Fe]_2\{\mu-(CH_2)_n\}$ (n = 8-12)

Compound	elemental composition			
	expected		found	
	% C	% H	% C	% H
(VIII)	56.7	5.6	56.9	5.6
(IX)	57.5	5.8	57.3	5.9
(X)	58.3	6.1	58.3	6.2
(XI)	59.1	6.3	59.2	6.4
(XII)	59.8	6.5	59.9	6.7

Table 6.4 IR and ^1H NMR data for $[Cp(CO)_2Fe]_2\{\mu-(CH_2)_n\}$ (n = 8-12)

Compound	IR $\nu(CO)$ [a] cm^{-1}	^1H NMR[b,c] : chemical shift, δ Cp	$-CH_2-$	
(VIII)	2007 (s) 1952 (vs)	4.68	1.49 (8H)	1.32 (8H)
(IX)	2010 (s) 1956 (vs)	4.90	1.57 (9H)	1.40 (9H)
(X)	2008 (s) 1954 (vs)	4.85	1.55 (10H)	1.35 (10H)
(XI)	2008 (s) 1954 (vs)	4.78	1.48 (11H)	1.29 (11H)
(XII)	2008 (s) 1954 (vs)	4.84	1.54 (12H)	1.32 (12H)

a : in Hexane solution

b : in $CDCl_3$

c : signals from Cp protons sharp singlets and from $-CH_2-$ protons two broad singlets

Table 6.5 Yields of $[Cp(CO)_2Fe]\{\mu-(CH_2)_n\}$ (n = 3-7)

Compound	yield %
(III)	61
(IV)	73
(V)	68
(VI)	70
(VII)	60

6.2.2 Preparation of (III) and (IV) by chemical decarbonylation of $[Cp(CO)_2Fe\{CO(CH_2)_nCO\}Fe(CO)_2Cp]$ (n = 3,4) with $RhX(PPh_3)_3$ (X = Cl,Br)

6.2.2.1 Preparation of $[Cp(CO)_2Fe\{CO(CH_2)_nCO\}Fe(CO)_2Cp]$ (n = 3,4) (I) and (II)

$[Cp(CO)_2Fe\{CO(CH_2)_nCO\}Fe(CO)_2Cp]$ (n = 3,4) were prepared by an adaptation of the method of King [59], as follows:

$ClCO(CH_2)_nCOCl$ (5,8 mmole) was added dropwise to a stirred solution of $Na[Cp(CO)_2Fe]$ (12 mmole) in THF (20 ml). The reaction mixture was stirred at room temperature for 1 hour then evaporated under reduced pressure. The brown oily residue was extracted with CH_2Cl_2 and chromatographed on an alumina column (made up with 20 % CH_2Cl_2/hexane). A red band was eluted with 20 % CH_2Cl_2/hexane and evaporation of the solution gave $[Cp(CO)_2Fe]_2$. The product was eluted as a yellow band (n = 3) or an orange band (n = 4) which gave the required products as a yellow or orange solid respectively on evaporation; yield; (I) 1.9 g, 74 % ; (II) 1.7 g, 65 % . The product was recrystallised from CH_2Cl_2/hexane and the IR and ^1H NMR spectra were found to be identical to those reported for $[Cp(CO)_2Fe\{CO(CH_2)_nCO\}Fe(CO)_2Cp]$ (n = 3,4) [59].

6.2.2.2 Reaction of $[Cp(CO)_2Fe\{CO(CH_2)_nCO\}Fe(CO)_2Cp]$ (n = 3,4) with $RhCl(PPh_3)_3$

A mixture of $[Cp(CO)_2Fe\{CO(CH_2)_nCO\}Fe(CO)_2Cp]$ (0.1 mmole) and $RhCl(PPh_3)_3$ (0.25 mmole) in degassed benzene (5 ml) was stirred at room

temperature for 6 hrs in which time all solid dissolved and the solution became yellow in colour. The reaction was followed by infrared spectroscopy. The mixture was evaporated under reduced pressure and the residue extracted with 20 % CH_2Cl_2/hexane and chromatographed on an alumina column (made up with hexane). Elution with hexane separated two yellow bands. The first band, eluted with hexane, gave a yellow solid on evaporation, which was identified by IR and ^1H NMR spectroscopy as $[Cp(CO)_2Fe]_2\{\mu\text{-}(CH_2)_n\}$ (n = 3 or 4) yields; n = 3: 45 %, n = 4: 58 %. The ^1H NMR showed some contamination of the product with PPh_3. A second yellow band was eluted with 50 % CH_2Cl_2/hexane and evaporated to give an orange residue. IR and ^{1} H NMR spectra of this portion showed the presence of the starting diacyl compound and a trace of a PPh_3-substituted product (IR ν(CO): 1910 cm^{-1}; ^1H NMR : δ 4.3 (d, J $\simeq$ 2Hz)). In the decarbonylation of $[Cp(CO)_2Fe\{CO(CH_2)_3CO\}Fe(CO)_2Cp]$ the mono-acyl species $[Cp(CO)_2Fe\{CO(CH_2)_3\}Fe(CO)_2Cp]$ was also detected in this band: ν(CO) (CH_2Cl_2) 2014 (m), 2001 (s), 1958 (s), 1941 (vs), 1603 (w) cm^{-1} ; ^1H NMR ($CDCl_3$) δ 4.94 (s, 5H), δ 4.74 (s, 5H), δ 2.96 (t, J = 7Hz, 2H), δ 1.26 (m, 4H) (literature spectrum ref. 59).

A brown residue remained after the extraction of the reaction mixtures for chromatography. This was found to contain $RhCl(CO)(PPh_3)_2$ on the basis of its IR spectrum (ν(CO) ($CHCl_3$) 1977 cm^{-1}) (literature spectrum ref. 109).

The analogous reactions of $[Cp(CO)_2Fe\{CO(CH_2)_nCO\}Fe(CO)_2Cp]$ (n = 3,4) with $RhBr(PPh_3)_3$ also produced the decarbonylated products $[Cp(CO)_2Fe]_2\{\mu\text{-}(CH_2)_n\}$ (n = 3,4) in 52 and 57 % yield respectively.

6.2.3 Attempted preparations of $[Cp(CO)_2Fe]_2\{\mu\text{-}(CH_2)_2\}$

6.2.3.1 Reaction of $[Cp(CO)_2Fe(C_2H_4)]^+PF_6^-$ with $[Cp(CO)_2Fe]^-$

1. Preparation of $[Cp(CO)_2Fe(C_2H_4)]^+ PF_6^-$

$[Cp(CO)_2Fe(C_2H_4)]^+PF_6$ was prepared by an adaptation of the method of Green and Nagy, [34] as follows:

A solution of $Na[Cp(CO)_2Fe]$ (11.3 mmole) in THF (30 ml) was added dropwise to CH_3CH_2I (12 mmole) with stirring. The reaction mixture was stirred for 1 hour at room temperature then evaporated under reduced pressure. The oily brown residue was extracted with hexane (3 x 20 ml) and the extract filtered and evaporated to give a yellow-brown oil. This was identified as $[Cp(CO)_2Fe(C_2H_5)]$ by IR in the $\nu(CO)$ region and ^1H NMR (literature spectra ref. 34, 112) (yield 81 %). $[Cp(CO)_2Fe(C_2H_5)]$ (9.3 mmole) was dissolved in THF (20 ml) and $Ph_3C^+PF_6^-$ (3.8 g, 10 mmole) added with stirring. The reaction mixture was stirred for 1 hour at room temperature then evaporated under reduced pressure. The black oil was extracted with acetone (3 x 20 ml) and the extract filtered. Addition of ether to the brown filtrate caused precipitation of the product as a yellow solid (1.3 g, 40 %); m.p. (decomp.) 180°C; ν (CO) (Nujol) 2080 (s), 2040 (s) cm^{-1}; ^1H NMR (acetone-d^6) δ 6.0 (s, 5 H, Cp), δ 4.03 (s, 4 H, C_2H_4); Found C 30.6 % H 2.6 %, $C_9H_9F_6FeO_2P$ requires C 30.9 % H 2.6 %.

2. Reaction of $[Cp(CO)_2Fe(C_2H_4)]^+PF_6$ with $[Cp(CO)_2Fe]$

$Na[Cp(CO)_2Fe]$ (5.5 mmole) in THF (10 ml) was added dropwise with stirring to $[Cp(CO)_2Fe(C_2H_4)]^+PF_6^-$ (1,0 g, 2.9 mmole) in THF (5 ml) at 0°C.

The yellow salt dissolved during the addition and the solution became red-brown in colour. The reaction mixture was stirred at 0°C for 30 minutes then evaporated under reduced pressure. The brown residue was extracted with 10 % CH_2Cl_2/hexane and chromatographed on an alumina column (made up with hexane). Two bands were collected; a yellow band eluted with hexane gave orange crystals on evaporation, identified by ^1H NMR and mass spectrometry as $[Cp_2Fe]$ (5 %). A red band was eluted with 50 % CH_2Cl_2/hexane and yielded $[Cp(CO)_2Fe]_2$ on evaporation (84 %) (identified by IR spectroscopy).

6.2.3.2. Decarbonylation of $[Cp(CO)_2Fe\{CO(CH_2)_2CO\}Fe(CO)_2Cp]$

1. Preparation of $[Cp(CO)_2Fe\{CO(CH_2)_2CO\}Fe(CO)_2Cp]$

$ClCO(CH_2)_2COCl$ (0.7 ml, 5.8 mmole) was added dropwise over 5 minutes to a stirred solution of $Na[Cp(CO)_2Fe]$ (12 mmole) in THF (30 ml) at 0°C. The mixture was allowed to warm up to room temperature and stirred for 2 hours at room temperature. Evaporation under reduced pressure gave a red oily residue which was extracted with CH_2Cl_2 (3 x 20 ml). The extract was filtered under N_2 and evaporated. Addition of n-pentane to the brown residue caused precipitation of the product as a yellow solid. This was recrystallised from CH_2Cl_2/pentane to give $[Cp(CO)_2Fe\{CO(CH_2)_2CO\}Fe(CO)_2Cp]$ as a microcrystalline yellow solid (1.4 g, 27 %) m.p: 168 - 170°C; $\nu(CO)(CH_2Cl_2)$ 2017 (s) 1958 (s) 1640 (w,broad) cm^{-1}; ^1H NMR ($CDCl_3$) δ 4.90 (s, 10H) δ 3.00 (s, 4H); Found C 49.2 % H 3.2 %, $C_{18}H_{14}Fe_2O_4$ requires C 49.3 % H 3.2 %.

2. Reaction of $[Cp(CO)_2Fe\{CO(CH_2)_2CO\}Fe(CO)_2Cp]$ with $RhCl(PPh_3)_3$

$[Cp(CO)_2Fe\{CO(CH_2)_2CO\}Fe(CO)_2Cp]$ (0.5 g, 1.1 mmole) and $RhCl(PPh_3)_3$ (0.17 g, 0.25 mmole) in 5 ml degassed benzene were stirred in a sealed tube under N_2 for 10 hours. In this time the mixture became orange red in colour and a pale precipitate formed. The mixture was then evaporated under reduced pressure and the volatile components collected in a liquid nitrogen-cooled trap. GLC analysis of this portion revealed the presence of ethylene (identified by comparison of retention time with that of a standard sample of this gas). The inorganic reaction products were extracted with 10 % $CHCl_3$/hexane and chromatographed on an alumina column (made up with hexane). Two bands were separated by elution with $CHCl_3$/hexane. A yellow band eluted with 20 % $CHCl_3$/hexane gave the starting diacyl species in 65 % yield. A red band was eluted with 80 % $CHCl_3$/hexane and on evaporation yielded $[Cp(CO)_2Fe]_2$ (28 %). The brown residue remaining after extraction for chromatography was found to contain $RhCl(CO)(PPh_3)_2$ (identified by IR ν(CO) by comparison with the literature spectrum ref. 109) as well as unreacted $RhCl(PPh_3)_3$.

6.2.4. Synthesis of μ(1,3)propanediyl bis(tricarbonyl cyclopentadienyl tungsten), $[Cp(CO)_3W]_2\{\mu\text{-}(CH_2)_3\}$ (XIII)

6.2.4.1 Reaction of $[Cp(CO)_3W]^-$ with $Br(CH_2)_3Br$

$Br(CH_2)_3Br$ (1.4 mmole) was added dropwise to a stirred solution of $Na[Cp(CO)_3W]$ (3.0 mmole) in THF (10 ml). The reaction mixture was heated under reflux (75°C) for 18 hours then a further 2 ml of the anion solution

(0.9 mmole) was added and the mixture heated for a further 18 hours. The reaction mixture was then allowed to cool and evaporated. The brown residue was extracted with CH_2Cl_2 (3 x 20 ml) and the extract filtered and reduced in volume. Addition of hexane caused precipitation of (XIII) as a yellow solid which was recrystallised from CH_2Cl_2/hexane (0.12 g, 11 %) m.p. (decomp.) 160°C. Elemental analysis is reported in Table 6.7 and IR and ^1H NMR data in Table 6.8. The other products of the reaction, identified by IR, were $[Cp(CO)_3W]_2$ and $[Cp(CO)_3WBr]$. ^1H NMR of the reaction mixture after 18 hours showed that $[Cp(CO)_3W\{(CH_2)_3Br\}]$ was formed as an intermediate.

6.2.4.2. Reaction of $[Cp(CO)_3W]^-$ with $I(CH_2)_3I$

$I(CH_2)_3I$ (0.2 ml, 1.6 mmole) was added dropwise to a stirred solution of $Na[Cp(CO)_3W]$ (3.2 mmole) in 1,2-dimethoxyethane (15 ml). The reaction mixture was heated under reflux (95°C) for 12 hours then allowed to cool and evaporated under reduced pressure. The orange residue was extracted with CH_2Cl_2 (5 ml) and chromatographed on an alumina column (made up with hexane). Elution with hexane and CH_2Cl_2 separated three components. A yellow band eluted with hexane gave the product as a yellow solid on evaporation (0.65 g, 61 %). An orange band was eluted with 20 % CH_2Cl_2/hexane and on removal of the solvent gave an orange solid identified by IR in the ν(CO) region as $[Cp(CO)_3WI]$ (literature spectrum ref. 113). A second orange band was eluted with CH_2Cl_2 and evaporation yielded a red solid. This was recrystallised from diethyl ether and identified as the new 2-oxacyclopentylidene compound $[Cp(CO)_2IW(\overline{COCH_2CH_2CH_2})]$ (XVII) (0.15 g, 20 %) m.p.(decomp.) 164 - 168°C; ν(CO) (CH_2Cl_2) 1978 (m) 1897 (s) cm^{-1}; ^1H NMR ($CDCl_3$) δ 5.65 (s, 5H) δ 4.48 (t, J = 7.2 Hz, 2H) δ 3.40 (t, J = 7.2 Hz, 2H) δ 1.88 (quin., J = 7.2 Hz, 2H); Found C 26.4 % H 2.2 %, $C_{11}H_{11}IO_3W$ requires C 26.3 % H 2.2 %; Mass spectrum: M^{+m}/e 502.

6.2.5. Synthetic routes to the *trans*-2-oxacyclopentylidene tungsten compound $[Cp(CO)_2IW(\overline{COCH_2CH_2CH_2})]$ (XVII)

6.2.5.1. Reaction of $[Cp(CO)_3W]^-$ with $I(CH_2)_3I$ (1 : 1)

A solution of $Na[Cp(CO)_3W]$ (1.5 mmole) in 1,2-dimethoxyethane (15 ml) was added to $I(CH_2)_3I$ (1.5 mmole) with stirring, and the reaction mixture heated under reflux for 6 hours. The mixture was then allowed to cool and evaporated under reduced pressure. The orange residue was extracted with CH_2Cl_2 (2 x 10 ml) and the extract filtered. Addition of ether (20 ml) to the filtrate caused precipitation of orange crystals of (XVII) (0.67 g, 88 %) indentified by IR (ν(CO)) and ^{1}H NMR spectroscopy.

6.2.5.2. Reaction of $[Cp(CO)_3W\{(CH_2)_3Br\}]$ with LiI.

$[Cp(CO)_3W\{(CH_2)_3Br\}]$ was prepared by the method of King and Bisnette [21]. $[Cp(CO)_3W\{(CH_2)_3Br\}]$ (0.44 mmole) was dissolved in 1,2-dimethoxyethane (5 ml) and $LiI \cdot 3H_2O$ (0.1 g, 0.75 mmole) added with stirring. The mixture was heated under reflux for 26 hours then allowed to cool and evaporated under reduced pressure. The orange residue was worked up as above to give the product (XVII) in 59 % yield.

6.2.6. General synthetic route to μ(1,n)alkanediyl bis(tricarbonyl-cyclopentadienyl tungsten) compounds, $[Cp(CO)_3W]_2\{\mu\text{-}(CH_2)_n\}$ (n = 4 5) (XIV), (XV)

$I(CH_2)_nI$ (3 mmole) was added to a stirred solution of $Na[Cp(CO)_3W]$ (6 mmole) in 1,2-dimethoxyethane (30 ml). The reaction mixture was heated under reflux

(95°C) for 8 hours, then allowed to cool and evaporated under reduced pressure. The orange residue was extracted with CH_2Cl_2 (3 x 20 ml) and the extract filtered and reduced in volume. Addition of hexane (10 ml) and cooling caused precipitation of the product ((XIV) or (XV)) as a yellow solid which was filtered off and washed with hexane. The orange filtrate was evaporated to give a red solid identified by IR as $[Cp(CO)_3WI]$. Yields and melting points of (XIV) and (XV) are given in Table 6.6, elemental analyses in Table 6.7 and IR and ^1H NMR data in Table 6.8

Table 6.6 Yields and melting points of $[Cp(CO)_3W]_2\{\mu-(CH_2)_n\}$ (n = 4,5) (XIV) and (XV)

Compound	yield %	melting point/°C
(XIV)	82	195 (with decomp.)
(XV)	63	148 - 150 C

Table 6.7 Elemental analyses of $[Cp(CO)_3W]_2\{\mu-(CH_2)_n\}$ (n = 3-5)

Compound	elemental composition			
	expected		found	
	% C	% H	% C	% H
(XIII)	32.2	2.3	31.8	2.4
(XIV)	33.2	2.5	33.4	2.6
(XV)	34.2	2.7	34.2	2.8

Table 6.8 IR and ^1H NMR data of $[Cp(CO)_3W]_2\{\mu-(CH_2)_n\}$ (n = 3-5)

Compound	IR ν(CO) [a] cm^{-1}	^1H NMR; chemical shift, δ [b,c] Cp	$-CH_2-$
(XIII)	2012 (sh) 2003 (s) 1912 (vs)	5.38	1.56
(XIV)	2009 (s) 1912 (vs)	5.34	1.48
(XV)	2008 (s) 1912 (vs)	5.35	1.52

a : in CH_2Cl_2

b : in $CDCl_3$

c : signals from Cp protons sharp singlets and from $-CH_2-$ protons broad singlet.

(XIV) and (XV) are also obtained in good yield from the reactions of $Na[Cp(CO)_3W]$ with $I(CH_2)_nI$ (n =4,5) in THF or 50 % THF/dimethoxyethane although longer reaction times are required for the reactions in the lower boiling solvents. These compounds have also been prepared in a two-step synthesis with intermediate isolation of the mono-haloalkyl compounds, $[Cp(CO)_3W\{(CH_2)_nI\}]$ (n = 4,5) (XVII), (XVIII).

1. Preparation of $[Cp(CO)_3W\{(CH_2)_nI\}]$ (n = 4,5)

A solution of $Na[Cp(CO)_3W]$ (1.6 mmole) in 1,2-dimethoxyethane (10 ml) was added with stirring to $I(CH_2)_4I$ (0.2 ml , 1.6 mmole). The reaction mixture was heated under reflux for 6 hours then allowed to cool and evaporated under reduced pressure. The residue was extracted with

CH_2Cl_2 (3 x 20 ml) and the extract filtered and evaporated. Addition of n-pentane and cooling caused precipitation of a yellow solid which was recrystallised from pentane to give $[Cp(CO)_3W\{(CH_2)_4I\}]$ (XVII) as yellow crystals (86 %) m.p; 69 - 71°C; ν (CO) (CH_2Cl_2) 2010 (s) 1911 (vs) cm^{-1}; ^1H NMR (CD_2Cl_2), δ 5.4 (s, 5 H), δ 3.24 (t, J = 7 Hz, 2 H) δ 1.80 (quintet, J = 7 Hz, 4 H) δ 1,56 (s, 2 H); Found C 28.1 % H 2.6 %, $C_{12}H_{13}IO_3W$ requires C 27.9 % H 2.5 %; Mass spectrum: M^+ m/e 516

$[Cp(CO)_3W\{(CH_2)_5I\}]$ was prepared in the same way by reaction of $[Cp(CO)_3W]^-$ (0.9 mmole) with $I(CH_2)_5I$ (0.9 mmole) in refluxing DME. After 8 hours, the reation mixture was allowed to cool and work up of the mixture as described above produced (XVIII) as yellow crystals (67 %); m.p; 129 - 131°C; ν(CO) (CH_2Cl_2) 2009 (s) 1910 (vs) cm^{-1}; ^1H NMR ($CDCl_3$) δ 5.4 (s, 5 H) δ 3.20 (t, J = 7 Hz, 2 H) δ 1.86 (m, 6 H) δ 1.54 (s, 2 H) Found C 29.4 % H 2.9 %, $C_{13}H_{15}IO_3W$ requires C 29.5 % H 2.8 %.

2. Reaction of $[Cp(CO)_3W\{(CH_2)_nI\}]$ (n = 4,5) with $Na[Cp(CO)_3W]$

Reaction of $[Cp(CO)_3W\{(CH_2)_nI\}]$ (n = 4,5) with $Na[Cp(CO)_3W]$ in 50 % dimethoxylethane/ THF at reflux temperature for 6 hours gave the alkanediyl bridged compounds (XIV) and (XV) in 45 % and 43 % yield respectively after a work up procedure similar to that described above.

6.2.7. Synthesis of $[Cp(CO)_2Fe\{\mu\text{-}(CH_2)_3\}W(CO)_3Cp]$

The mixed metal compound was synthesised by reaction of $[Cp(CO)_2Fe\{(CH_2)_3Br\}]$ with $[Cp(CO)_3W]^-$ (in excess). The bromopropyl

iron compound was prepared by the method of Moss [24]. $[Cp(CO)_2Fe\{(CH_2)_3Br\}]$ (1.2 mmole) in THF 5 ml was added to a stirred solution of $Na[Cp(CO)_3W]$ (1.5 mmole) in THF (15 ml). The mixture was heated under reflux for 48 hours then allowed to cool and evaporated. The orange residue was extracted with CH_2Cl_2 (3 x 20 ml), the extract filtered and reduced in volume. On cooling orange crystals of the product (XIX) precipitated and were filtered off and washed with CH_2Cl_2 (0.09 g, 14 %). The filtrate was reduced in volume and hexane added. A yellow solid precipitated and was filtered off and washed with hexane. This was identified by IR and ^1H NMR as $[Cp(CO)_3W]_2\{\mu-(CH_2)_3\}$ (0.07 g, 13 %). The other products of the reaction identified by IR in the $\nu(CO)$ region were $[Cp(CO)_2Fe]_2$ and $[Cp(CO)_3W]_2$.

Characterisation of (XIX); m.p: 116 - 118°C; ν (CO) (CH_2Cl_2) 2008 (vs) 1998 (s) 1939 (s) 1908 (vs) cm^{-1}; ^1H NMR ($CDCl_3$) δ 5.31 (s, 5 H) δ 4.68 (s, 5 H) δ 1.59 (m, 6 H); Found C 38.9 % H 2.9 %, $C_{18}H_{16}FeO_5W$ requires C 3.91 % H 2.9 %; mass spectrum of (XIX) is reported and discussed in Section 3.

6.2.8 Synthesis of μ(1,4)butanediyl bis(pentacarbonyl manganese) $[(CO)_5Mn]_2\{\mu-(CH_2)_4\}$ (XXI)

$[(CO)_5Mn]_2\{\mu-(CH_2)_4\}$ was prepared by thermal decarbonylation of $[(CO)_5Mn\{CO(CH_2)_4CO\}Mn(CO)_5]$ (XX) which is readily obtained from the reaction of $[Mn(CO)_5]^-$ with $ClCO(CH_2)_4COCl$;

6.2.8.1. Preparation of (XX)

$ClCO(CH_2)_4COCl$ (0.4 ml, 2.8 mmole) was added dropwise to a stirred

solution of $Na[Mn(CO)_5]$ (5.8 mmole) in THF (10 ml). The mixture was stirred at room temperature for 1 hour, then evaporated under reduced pressure. The yellow solid residue was extracted with $CHCl_3$ (5 x 30 ml) and the extract filtered and reduced in volume. On cooling a white solid precipitated and was filtered off and washed with $CHCl_3$. Recrystallisation gave the product (XX) as a white microcrystalline solid (0.6 g, 38 %) m.p. (decomp.) 140°C; ν(CO) ($CHCl_3$); 2114 (w) 2051 (w) 2016 (vs) 1636 (m) (benzene) 2112 (w) 2045 (sh) 2010 (sh) 2000 (s) 1986 (vs) 1965 (sh) 1632 (w) 1625 (w) cm^{-1}; ^1H NMR ($CDCl_3$) δ 2.92 (t, J = 6.5 Hz, 4 H) δ 1.42 (m, 4 H); Found C 38.3 % H 1.60 %, $C_{16}H_8Mn_2O_{12}$ requires C 38.3 % H 1.59 % ; Mass Spectrum: M^+ $^m/_e$ 502.

6.2.8.2. Preparation of (XXI)

$[(CO)_5Mn]_2\{\mu\text{-}(CH_2)_4\}$ (XXI) was prepared by heating $[(CO)_5Mn\{CO(CH_2)_4CO\}Mn(CO)_5]$ at 110 C (at atmospheric pressure) until the acyl band in the infrared spectrum (1636 cm^{-1}) disappeared. The product was isolated by sublimation at 100°C (0.1 mmHg) onto a water- cooled probe as a white microcrystalline solid; m.p. (decomp.) 135°C; ν (CO) ($CHCl_3$) 2102 (w) 2006 (vs) 1980 (m,sh) cm^{-1}, ν (CO) (heptane) 2102 (w) 2009 (vs) 1988 (m) cm^{-1} ; ^1H NMR ($CDCl_3$) δ 1.70 (m, 4 H) δ 1.09 (m, 4 H); Found C 37.9 % H 1.9 %, $C_{14}H_8Mn_2O_{10}$ requires C 37.7 % H 1.8 %.

6.3 Experimental details of reactions in Section 5

6.3.1 Reaction of $[Cp(CO)_2Fe]_2\{\mu\text{-}(CH_2)_3\}$ with PPh_3 (1 : 1)

$[Cp(CO)_2Fe]_2\{\mu\text{-}(CH_2)_3\}$ (0.6 mmole) was dissolved in THF (10 ml) and PPh_3 (0.6 mmole) added. The reaction mixture was heated under reflux until no further change in the infrared spectrum of the mixture could be detected (in the region 2200 - 1600 cm^{-1}) then allowed to cool and evaporated under reduced pressure. The oily orange residue was extracted with CH_2Cl_2 (5 ml) and chromatographed on an alumina column (made up with 20 % ether/hexane). Elution with 20 % ether/hexane gave a yellow solution which yielded starting material, $[Cp(CO)_2Fe]_2\{\mu\text{-}(CH_2)_3\}$ (23 %), on evaporation. An orange band was eluted with 50 % ether/hexane and on evaporation under reduced pressure, an orange solid was obtained. Recrystallisation from ether/pentane gave $[Cp(CO)(PPh_3)Fe\{CO(CH_2)_3\}Fe(CO)_2Cp]$ (XXII) as a microcrystalline orange solid (64 %); m.p: 152 - 156°C; $\nu(CO)(CH_2Cl_2)$ 1999 (s) 1939 (s) 1911 (s) 1601 (w) cm^{-1}; ^1H NMR (CD_2Cl_2) δ 7.4 (m, 15 H) δ 4.68 (s, 5 H) δ 4.38 (s, 5 H) δ 2.76 (t, J = 7 Hz, 2 H) δ 1.26 (d, J = 7 Hz, 4 H); Found C 63.9 % H 4.9 %, $C_{35}H_{31}Fe_2O_4P$ requires C 63.8 % H 4.7 %.

6.3.2. Reactions of $[Cp(CO)_2Fe]_2\{\mu\text{-}(CH_2)_n\}$ (n = 3-7) with tertiary phosphine (1 : 2)

General procedure :

A mixture of $[Cp(CO)_2Fe]_2\{\mu\text{-}(CH_2)_n\}$ (0.6 mmole) and tertiary phosphine (1.2 mmole) in THF (10 ml) was heated under reflux and the course of the

reaction followed by IR spectroscopy in the region (2200 - 1600 cm^{-1}). Heating was continued until no further change in the infrared spectrum of the mixture could be detected. The reaction mixture was then allowed to cool and the solvent removed under reduced pressure. The oily orange residue was extracted with $CHCl_3$ (5 ml) and chromatographed on an alumina column (made up with 20 % ether/hexane). Any starting material was eluted with 20 % ether/hexane. Elution with 50 % ether/hexane separated two bands. An orange band eluted with 50 % ether/hexane, gave a trace of an orange solid on evaporation which was identified as the monoacyl product from its IR spectrum. A second orange band was eluted with ether, and on evaporation, an orange solid was isolated; recrystallisation from ether/pentane gave $[Cp(CO)(PPh_3)Fe\{CO(CH_2)_nCO\}Fe(CO)(PPh_3)Cp]$ as a microcrystalline orange solid.

The reaction times and product yields for the various tertiary phosphine reactions performed are listed in Table 6.8. The melting points and elemental analyses of the products are given in Table 6.9 and IR and ^1H NMR data in Table 6.10.

Table 6.8 : Reactions of $[Cp(CO)_2Fe]_2\{\mu\text{-}(CH_2)_n\}$ (n = 3 - 7) (III) - (VII) with tertiary phosphine (L) (1 : 2)

Compound	L	reaction time (hours)	products (yield)	
(III)	PPh_3	66	$[Cp(CO)(PPh_3)Fe\{CO(CH_2)_3\}Fe(CO)_2Cp]$	(12 %)
			$[Cp(CO)(PPh_3)Fe\{CO(CH_2)_3CO\}Fe(CO)(PPh_3)Cp]$	(57 %)
(IV)	PPh_3	48	$[Cp(CO)(PPh_3)Fe\{CO(CH_2)_4CO\}Fe(CO)(PPh_3)Cp]$	(69 %)
(V)	PPh_3	48	$[Cp(CO)(PPh_3)Fe\{CO(CH_2)_5CO\}Fe(CO)(PPh_3)Cp]$	(68 %)
(VI)	PPh_3	42	$[Cp(CO)(PPh_3)Fe\{CO(CH_2)_6CO\}Fe(CO)(PPh_3)Cp]$	(76 %)
(VII)	PPh_3	36	$[Cp(CO)(PPh_3)Fe\{CO(CH_2)_7CO\}Fe(CO)(PPh_3)Cp]$	(88 %)
(III)	$PMePh_2$	18	$[Cp(CO)(PMePh_2)Fe\{CO(CH_2)_3CO\}Fe(CO)(PMePh_2)Cp]$	(62 %)
(IV)	$PMePh_2$	6	$[Cp(CO)(PMePh_2)Fe\{CO(CH_2)_4CO\}Fe(CO)(PMePh_2)Cp]$	(86 %)
(III)	PMe_3	42	$[Cp(CO)(PMe_3)Fe\{CO(CH_2)_3CO\}Fe(CO)(PMe_3)Cp]$	(79 %)

Table 6. 9 : Melting points and elemental analyses of $[Cp(CO)(L)Fe\{CO(CH_2)_nCO\}Fe(CO)(L)Cp]$ (n = 3 - 7; L = tertiary phosphine) (XXIII) - (XXX)

Compound	melting point /°C	elemental composition			
		expected		found	
		% C	% H	% C	% H
(XXIII)	105 - 110	69.2	5.0	69.0	5.0
(XXIV)	100 - 104	69.3	5.1	69.6	5.1
(XXV)	64 - 68	69.6	5.3	69.9	5.4
(XXVI)	85 - 95	69.8	5.4	70.0	5.4
(XXVII)	82 - 86	70.0	5.5	69.8	5.8
(XXVIII)	65 - 68	64.8	5.3	64.6	5.3
(XXIX)	135 - 138	65.2	5.4	65.4	5.7
(XXX)	134 - 136	50.4	6.2	50.5	6.3

Table 6.10 : IR and ^1H NMR data for $[Cp(CO)(L)Fe\{CO(CH_2)_nCO\}Fe(L)(CO)Cp]$ (n = 3 - 7; L = tertiary phosphine) (XXIII) - (XXX)

Compound	IR ν(CO) cm^{-1} [a]	^1H MNR; Chemical shift, δ (ppm) [b,c]			
		$-CH_2-$ [d]	CH_2CO [e]	Cp [f]	PMe [g]
(XXIII)	1913 (s) 1604 (m)	0.89 (1 H) .26 (1 H)	2.60 (4 H)	4.35 (10 H)	-
(XXIV)	1913 (s) 1607 (m)	0.88 (2 H) 1.26 (2 H)	2.58 (4 H)	4.36 (10 H)	-
(XXV)	1912 (s) 1603 (m)	0.89 (2 H) 1.25 (4 H)	2.60 (4 H)	4.36 (10 H)	-
(XXVI)	1913 (s) 1599 (m)	0.88 (2 H) 1.26 (6 H)	2.65 (4 H)	4.36 (10 H)	-
(XXVII)	1913 (s) 1603 (m)	0.93 (2 H) 1.25 (8 H)	2.68 (4 H)	4.38 (10 H)	-
(XXVIII)	1912 (s) 1595 (m)	0.88 (1 H) 1.25 (1 H)	2.44 (4 H)	4.40 (10 H)	1.99 (6 H)
(XXIX)	1911 (s) 1595 (m)	0.90 (2 H) 1.24 (2 H)	2.46 (4 H)	4.41 (10 H)	2.00 (6 H)
(XXX)	1906 (s) 1596 (m)	1.70 (2 H)	2.78 (4 H)	4.40 (10 H)	1.34 (18 H)

a : in CH_2Cl_2 solution

b : in $CDCl_3$ solution

c : for (XXIII) - (XXIX) a multiplet at $\sim \delta$ 7.4 is observed for the phenyl protons

d : all signals broad singlets

e : all signals complex multiplets

f : all signals doublets with J $\simeq$ 1.8 Hz

g : all signals doublets with J = 9 Hz

6.3.3 Attempted decarbonylation of $[Cp(CO)(PPh_3)Fe\{CO(CH_2)_{2-n}CO\}Fe(CO)(PPh_3)Cp]$ (n = 4,6).

6.3.3.1 Photolysis of $[Cp(CO)(PPh_3)Fe\{CO(CH_2)_{2-n}CO\}Fe(PPh_3)(CO)Cp]$ (n = 4,6)

A solution of $[Cp(CO)(PPh_3)Fe\{CO(CH_2)_4CO\}Fe(PPh_3)(CO)Cp]$ (5 mmole) in THF (40 ml) was irradiated at 35°C and the reaction followed by infrared spectroscopy (in the region 2100 - 1500 cm^{-1}). The reaction was stopped when the band at 1913 cm^{-1}, due to the starting diacyl compound, had disappeared (3 hours). The reaction mixture was filtered under N_2 to remove a brown insoluble solid and the solvent removed from the filtrate under reduced pressure. The brown residue was extracted with 10 % CH_2Cl_2/hexane and chromatographed on an alumina column (made up with hexane). Three bands were separated. A yellow band eluted with hexane gave an orange solid with no carbonyl groups identified by ^1H NMR as ferrocene. A red band eluted with 30 % CH_2Cl_2/hexane gave $[Cp(CO)_2Fe]_2$ on evaporation (ν(CO) 1991 (s) 1950 (vs) 1778 (s) cm^{-1}). A second yellow band was eluted with CH_2Cl_2 and removal of the solvent under reduced pressure gave a yellow oil. The infrared spectrum of this portion showed the presence of some of the starting diacyl compound (ν(CO) (CH_2Cl_2) 1913 (s) 1602 (w) cm^{-1}). A strong band at 1732 cm^{-1} which is in the range for a C = O stretching vibration in an organic ketone or acid was also observed. The infrared spectrum of the oil in the range 3600 - 600 cm^{-1} was found to be very similar to that reported for $HOOC(CH_2)_4COOH$. [114]

Similar results were obtained for the photolysis of (XXIV) in petroleum ether and in THF in the presence of PPh_3.

Photolysis of $[Cp(CO)(PPh_3)Fe\{CO(CH_2)_6CO\}Fe(CO)(PPh_3)Cp]$ was carried out in the same way. After irradiation for 3 hours the reaction mixture was worked up as described above. A red band was eluted with 30 % CH_2Cl_2/hexane and the red solid, obtained on evaporation, identified as $[Cp(CO)_2Fe]_2$ on the basis of its infrared spectrum (38 %). A pale yellow band eluted with CH_2Cl_2, gave a yellow oil on evaporation, the infrared spectrum of which was similar to that of $HOOC(CH_2)_6COOH$ (3600 - 600 cm^{-1}) [114].

6.3.3.2. Reaction of $[Cp(CO)(PPh_3)Fe\{CO(CH_2)_4CO\}Fe(PPh_3)(CO)Cp]$ (XXIV) with $RhCl(PPh_3)_3$

A mixture of (XXIV) (0.5 mmole) and $RhCl(PPh_3)_3$ (1.0 mmole) in benzene (5 ml) was stirred at room temperature for 10 hours. The reaction mixture was then evaporated under reduced pressure and the red residue extracted with CH_2Cl_2 (5 ml) and chromatographed on an alumina column (made up with 50 % CH_2Cl_2/hexane). Only one band was collected on elution with CH_2Cl_2 and evaporation of the solution gave an orange solid identified by its infrared spectrum as starting material (XXIV) (98 % yield). The solid residue remaining after CH_2Cl_2 extraction for chromatography contained $RhCl(PPh_3)_3$.

6.3.4. Photochemical reaction of $[Cp(CO)_2Fe\{CO(CH_2)_4CO\}Fe(CO)_2Cp]$ with PPh_3.

A mixture of $[Cp(CO)_2Fe\{CO(CH_2)_4CO\}Fe(CO)_2Cp]$ (0.5 mmole) and PPh_3 (1.0 mmole) in THF was irradiated at 25°C for 3 hours. The reaction mixture was then filtered to remove a brown insoluble solid and evaporated under reduced pressure. Chromatography of the brown residue on an alumina column made up with 20 % CH_2Cl_2/hexane separated two bands. A red band was

eluted with 30 % CH_2Cl_2/hexane and, on evaporation, gave $[Cp(CO)_2Fe]_2$ (47 %). Elution with CH_2Cl_2 gave a pale yellow solution and, on evaporation, a yellow oil was isolated. The IR spectrum of this portion showed it to contain an organic product similar to that observed in the photolysis of $[Cp(CO)(PPh_3)Fe\{CO(CH_2)_4CO\}Fe(PPh_3)(CO)Cp]$.

6.3.5. Photochemical reaction of $[Cp(CO)_2Fe]_2\{\mu\text{-}(CH_2)_4\}$ with PPh_3.

A stirred solution of $[Cp(CO)_2Fe]_2\{\mu\text{-}(CH_2)_4\}$ (3.7 mmole) and PPh_3 (7.6 mmole) in THF (100 ml) was irradiated under N_2 at 30°C for 3 hours. The reaction was followed by IR spectroscopy in the region 2100 - 1500 cm^{-1} and was stopped when no further increase in the product band at 1905 cm^{-1} could be detected. The reaction mixture was evaporated under reduced pressure and the brown residue extracted with CH_2Cl_2 (5 x 20 ml) and filtered under N_2 to remove an insoluble non-carbonyl product. The resulting dark orange solution was concentrated then chromatographed on an alumina column (made up with petroleum ether (30 - 40°C)). Four bands were separated by elution with petroleum ether and CH_2Cl_2. A yellow band was eluted with petroleum ether and evaporation of the solution yielded an orange solid, the infrared spectrum of which was identical to that reported for $[Cp(CO)(PPh_3)FeH]$. The assignment of this formula to the product was confirmed by the observed reaction of the product with $CHCl_3$ to give green crystals of $[Cp(CO)(PPh_3)FeCl]$ (ν(CO); 1956 cm^{-1}) as reported for $[Cp(CO)(PPh_3)FeH]$.

A second yellow band was eluted with 10 % CH_2Cl_2/petroleum ether and evaporation gave an orange solid showing one strong carbonyl band at 1906 cm^{-1} (CH_2Cl_2). This product was unstable and decomposed rapidly both in solid

form and solution on exposure to air, so could not be characterised further. A red band eluted with 30 % CH_2Cl_2/petroleum ether, gave a red solid on evaporation, identified as $[Cp(CO)_2Fe]_2$ by IR spectroscopy (28 %). Elution with CH_2Cl_2 gave a yellow solution which yielded $[Cp(CO)(PPh_3)Fe\{CO(CH_2)_4CO\}Fe(PPh_3)(CO)Cp]$ (16 %) (IR ν(CO); 1913 (s) 1604 (w) cm^{-1}).

6.3.6. Reactions of $[Cp(CO)_2Fe]_2\{\mu-(CH_2)_n\}$ (n = 3,4) with halogens

General procedure

$[Cp(CO)_2Fe]_2\{\mu-(CH_2)_n\}$ (0.2 mmole) was dissolved in THF or CH_2Cl_2 (5 ml) and X_2 (X = I or Br) added with stirring at 20°C or 0°C. The mixture was stirred at the addition temperature for 10 minutes then evaporated under reduced pressure. The brown residue was extracted with CH_2Cl_2 and chromatographed on an alumina column (made up with hexane). Elution with CH_2Cl_2/hexane separated the reaction products. The eluted solutions were evaporated under reduced pressure and the products identified by comparison with authentic samples or with reported spectral data.

6.3.6.1. Reactions of $[Cp(CO)_2Fe]_2\{\mu-(CH_2)_3\}$ with X_2 (1 : 2)

Addition of I_2 (0.4 mmole) to a solution of $[Cp(CO)_2Fe]_2\{\mu-(CH_2)_3\}$ (0.2 mmole) in THF at 20°C gave a dark brown solution. The work up of the reaction mixture as described above separated two products. A pale yellow band eluted with 20 % CH_2Cl_2/hexane, gave a yellow oil on evaporation. The IR and mass spectra of this portion showed that it contained mainly $I(CH_2)_3I$ with a trace of starting material (IV). A brown band was eluted

with CH_2Cl_2 and evaporation of this solution produced a dark purple solid the IR and ^1H NMR spectra of which were identical to those reported for $[Cp(CO)_2FeI]$ [87] (yield; 92 %).

$[Cp(CO)_2FeI]$ and $I(CH_2)_3I$ were also isolated from the reaction of (III) with I_2 in CH_2Cl_2.

The reaction of $[Cp(CO)_2Fe]_2\{\mu\text{-}(CH_2)_3\}$ with Br_2 in THF was carried out in the same way and the work up of the reaction mixture separated two products which were identified on the basis of their IR, ^1H NMR and mass spectra as $Br(CH_2)_3Br$ and $[Cp(CO)_2FeBr]$ (yield 89 %).

The reaction of $[Cp(CO)_2Fe]_2\{\mu\text{-}(CH_2)_3\}$ with Br_2 was also performed at 0°C in THF. The infrared spectrum of this reaction mixture showed the presence of a cationic product (ν(CO) 2080 (s) 2046 (s) cm^{-1}) but this could not be isolated.

6.3.6.2. Reactions of $[Cp(CO)_2Fe]_2\{\mu\text{-}(CH_2)_4\}$ with X_2 (1 : 2)

I_2 (0.4 mmole) was added to a stirred solution of $[Cp(CO)_2Fe]_2\{\mu\text{-}(CH_2)_4\}$ in THF at 20°C. The reaction mixture was worked up as described above and three products separated. A yellow band eluted with hexane gave a yellow oil on evaporation which was found to contain $I(CH_2)_4I$ and a small amount of $[Cp(CO)_2Fe\{(CH_2)_4I\}]$ on the basis of the IR and mass spectra of this portion. A brown band was eluted with CH_2Cl_2 and the brown solid produced on evaporation identified by its IR, ^1H NMR and mass spectra as $[Cp(CO)_2FeI]$ (78 %). A brown residue remained after the extraction with CH_2Cl_2 for chromatography. This was dissolved in a minimum of THF and

CH_2Cl_2 added. A dark red solid which precipitated was filtered off under suction (0.06 g). This product (XXXI) was unstable even in solid form and could only be characterised by IR and ^1H NMR spectroscopy. The spectral data is consistent with the structure $[Cp(CO)_2Fe(CH_2)_4Fe(CO)_2Cp]^+[I_2]^-$; ν(CO) (THF) 2080 (s) 2046 (s) cm^{-1}; ^1H NMR (acetone-d^6) δ 4.04 (s, 8 H) δ 5.96 (s, 10 H).

The reaction of $[Cp(CO)_2Fe]_2\{\mu\text{-}(CH_2)_4\}$ with Br_2 was carried out in the same way. The products isolated by chromatography were identified on the basis of their IR, ^1H NMR and mass spectra as $Br(CH_2)_4Br$, $[Cp(CO)_2FeBr]$ (72 %) and $[Cp(CO)_2Fe\{(CH_2)_4Br\}]$ (trace). An orange-brown solid was isolated from the residue remaining after CH_2Cl_2 extraction for chromatography (0.08 g). This was assigned the structure $[Cp(CO)_2Fe(CH_2)_4Fe(CO)_2Cp]^+$ $[Br_2]^-$ which is consistent with its IR and ^1H NMR spectra and its measured paramagnetic suspectibility; ν(CO) (THF) 2076 (s) 2040 (s) cm^{-1}; ^1H NMR (acetone-d^6) δ 4.08 (s, 8 H), δ 6.00 (s, 10 H); χ_m = 6.6 x 10^{-7} m^3kg^{-1} at 17°C.

6.3.6.3. Reaction of $[Cp(CO)_2Fe]_2\{\mu\text{-}(CH_2)_4\}$ with X_2 (1 : 1)

I_2 (0.2 mmole) was added to a stirred solution of $[Cp(CO)_2Fe]_2\{\mu\text{-}(CH_2)_4\}$ in THF (5 ml) at 20 C. After stirring for 10 minutes, the reaction mixture was worked up as described above. A yellow band was eluted with hexane and on evaporation gave an oily yellow solid. IR and ^1H NMR spectra showed that this portion contained $I(CH_2)_4I$ and the starting material. The solid was dissolved in a minimum of hexane and on cooling, yellow crystals of (IV) precipitated from the solution (yield : 47 %). A brown band was eluted with CH_2Cl_2 and removal of the solvent gave a dark purple solid identified on the basis of IR and ^1H NMR spectra as $[Cp(CO)_2FeI]$ (36 %).

6.3.7 Reactions of $[Cp(CO)_3W]_2\{\mu\text{-}(CH_2)_n\}$ (n = 3-5) with tertiary phosphines.

General procedure

$[Cp(CO)_3W]_2\{\mu\text{-}(CH_2)_n\}$ was dissolved in THF or DME (10 ml) and a two molar proportion of tertiary phosphine added. The mixture was heated under reflux and the reaction followed by IR spectroscopy in the region 2100 - 1550 cm^{-1}. The reaction was stopped when no further decrease in the carbonyl bands of the starting material could be detected. The reaction mixture was then evaporated under reduced pressure and the residue extracted with ether and chromatographed on an alumina column (made up with 20 % ether/hexane). Separation of the products was achieved by elution with an increasing concentration of ether in hexane. The eluted solutions were evaporated under reduced pressure to give the solid products.

6.3.7.1. Reaction of (XIV) with PPh_2Me

A mixture of $[Cp(CO)_3W]_2\{\mu\text{-}(CH_2)_4\}$ (0.3 mmole) and PPh_2Me (0.6 mmole) in THF was heated under reflux for 70 hours. The reaction mixture was worked up as described above. Elution with 50 % ether/hexane gave a pale yellow solution which yielded a yellow solid on evaporation. The IR and ^1H NMR spectra of this portion showed it to contain starting material (XIV) (ν (CO) 2009 (s) 1910 (vs); ^1H NMR ($CDCl_3$) δ 5.32 (s, C_5H_5) δ 1.26 (s, $(CH_2)_4$)) and a non-acyl phosphine-substituted product, possibly $[Cp(CO)_2(PPh_2Me)W]_2\{\mu\text{-}(CH_2)_4\}$ (ν(CO) (CH_2Cl_2) 1923 (m,sh) 1845 (s); ^1H NMR ($CDCl_3$), δ 4.75 (d, J $\simeq$ 2 Hz, C_5H_5) δ 2.18 (d, J = 9 Hz, PMe)) A second yellow band

was eluted with ether and evaporation gave a yellow solid which was recrystallised from ether/pentane to give yellow crystals of $[Cp(CO)_2(PMePh_2)W\{CO(CH_2)_4CO\}W(PMePh_2)(CO)_2Cp]$ (XXXIII) (0.17 g, 55 %); m.p: 175 - 179°C; ν(CO) (benzene) 1923 (m) 1840 (s) 1611 (w) cm^{-1} ^1H NMR (CD_2Cl_2) δ 1.25 (m, 4 H) δ 2.30 (d, J = 9 Hz, 6 H) δ 2.84 (t, J = 6 Hz, 4 H) δ 5.01 (d, J $\simeq$ 1.5 Hz, 10 H) δ 7.4 (m, 20 H); Found C 49.2 % H 3.9 %, $C_{46}H_{44}O_6P_2W_2$ requires C 48.9 % H 3.9 %.

The reaction of (IV) with PPh_2Me was also carried out in refluxing DME for 38 hours. Work up of the reaction mixture gave (XXXIII) in 54 % yield and a yellow solid containing a mixture of starting material and a non-acyl phosphine-substituted product. After prolonged heating of a mixture of (IV) and PPh_2Me in DME (72 hours), the ^1H NMR of the reaction mixture showed an increase in the proportion of the non-acyl product formed and the diacyl compound (XXXIII) was only isolated in 36 % yield.

6.3.7.2. Reaction of $[Cp(CO)_3W]_2\{\mu-(CH_2)_5\}$ with PPh_2Me

A mixture of $[Cp(CO)_3W]_2\{\mu-(CH_2)_5\}$ (0.35 mmole) and PPh_2Me (0.7 mmole) in THF was heated under reflux for 72 hours. On working up the reaction mixture two product bands were separated. A yellow band eluted with 50 % ether/hexane gave a yellow solid on evaporation. On the basis of the IR and ^1H NMR spectra of this portion, it was found to contain a mixture of starting material, a non-acyl phosphine substituted product and possibly the mono-acyl species $[Cp(CO)_2(PPh_2Me)W\{CO(CH_2)_5\}W(CO)_3Cp]$; ν(CO) (CH_2Cl_2) 2008 (m) 1924 (sh) 1916 (s) 1836 (vs) 1598 (w) cm^{-1}; ^1H NMR ($CDCl_3$) δ 5.32 (s, C_5H_5 in (XV)) δ 5.05 (d, J $\simeq$ 2 Hz, C_5H_5 in acyl product) δ 4.80 (d, J $\simeq$ 2 Hz, C_5H_5 in non-acyl product).

A second yellow band was eluted with ether and evaporation of the yellow solution gave $[Cp(CO)_2(PPh_2Me)W\{CO(CH_2)_5CO\}W(PPh_2Me)(CO)_2Cp]$ (XXXIV) as a yellow solid (0.16 g, 54 %); m.p : 75 - 80°C; ν(CO) (CH_2Cl_2) 1925 (m) 1838 (vs) 1596 (w) cm^{-1}; ^1H NMR ($CDCl_3$) δ 1.25 (m, 6 H) δ 2.34 (d, J = 9 Hz, 6 H) δ 2.9 (t, J = 7 Hz, 4 H) δ 5.04 (d, J $\simeq$ 1.8 Hz, 10 H) δ 7.5 (m, 20 H); Found C 49.7 % H 4.1 %, $C_{47}H_{46}O_6P_2W_2$ requires C 50.2 % H 4.3 %.

6.3.7.3. Reaction of $[Cp(CO)_3W]_2\{\mu-(CH_2)_4\}$ with PPh_3.

A mixture of $[Cp(CO)_3W]_2\{\mu-(CH_2)_4\}$ (0.3 mmole) and PPh_3 (0.6 mmole) in DME was heated under reflux for 34 hours. Two product bands were isolated on working up the reaction. A yellow band eluted with 50 % ether/hexane gave a yellow solid on evaporation which was found to contain a mixture of (XIV) and a non-acyl substituted product on the basis of the IR and ^1H NMR spectra; ν(CO) (CH_2Cl_2) 2008 (s), 1924 (sh) 1911 (vs) 1842 (m) cm^{-1}; The ^1H NMR spectrum shows a singlet at δ 5.32 (C_5H_5 of (XIV) and a doublet at δ 4.80 (J $\simeq$ 1,5 Hz, C_5H_5 for non-acyl product). A second yellow band was eluted with 80 % ether/hexane and on evaporation a yellow solid was isolated. This was formulated as $[Cp(CO)_2(PPh_3)W\{CO(CH_2)_4\}W(CO)_3Cp]$ on the basis of IR and ^1H NMR data (28 %); ν(CO) (CH_2Cl_2) 2006 (s) 1924 (s) 1910 (vs) 1842 (s) 1595 (w) cm^{-1} ; ^1H NMR ($CDCl_3$) δ 7.4 (m, 15 H) δ 5.32 (s, 5 H) δ 5.05 (s, 5 H) δ 2.92 (t, J = 7 Hz, 2 H) δ 1.26 (s, 6 H).

The reaction of (XIV) with PPh_3 was also carried out in refluxing THF for 75 hours. The work up of the reaction mixture separated two product bands. A yellow band eluted with 50 % ether/hexane was found to contain starting material (XIV) and a trace of a substituted non-acyl product on the basis

of the IR and ^{1}H NMR data. A second yellow band was eluted with ether and on evaporation gave yellow crystals of $[Cp(CO)_2(PPh_3)W\{CO(CH_2)_4CO\}W(PPh_3)(CO)_2Cp]$ (XXXVI) (0.2 g. 37 %); ν(CO) (CH_2Cl_2) 1932 (m) 1847 (vs) 1598 (m) cm^{-1}; ^{1}H NMR (CD_2Cl_2) δ 7.4 (m, 30 H) δ 5.04 (d, J $\simeq$ 1.5 Hz, 10 H) δ 2.82 (t, J = 7 Hz, 4 H) δ 1.29 (m, 4 H); Found C 53.8 % H 4.1 %, $C_{56}H_{48}O_6P_2W_2$ requires C 53.9 % H 3.9 %.

6.3.7.4. Reaction of $[Cp(CO)_3W]_2\{\mu-(CH_2)_5\}$ with PPh_3.

A mixture of $[Cp(CO)_3W]_2\{\mu-(CH_2)_5\}$ (0.4 mmole) and PPh_3 (0.8 mmole) in THF was heated under reflux for 60 hours. The work up of the reaction mixture gave two product bands. A yellow band eluted with 50 % ether/hexane was found to contain starting material (XV) (38 %) on the basis of the IR and ^{1}H NMR spectra. A second yellow band was eluted with ether and on evaporation under reduced pressure yielded $[Cp(CO)_2(PPh_3)W\{CO(CH_2)_5CO\}W(CO)_2(PPh_3)Cp]$ (XXXVI) as a yellow solid (45 %); ν(CO) (CH_2Cl_2) 1930 (m) 1845 (vs) 1595 (m) cm^{-1}; ^{1}H NMR (CD_2Cl_2) δ 7.4 (m, 30 H) δ 5.05 (d, J $\simeq$ 1.5 Hz, 10 H) δ 2.84 (t, J = 7 Hz, 4 H) δ 1.26 (m, 6 H); Found C 54.5 % H 4.0 %, $C_{57}H_{50}O_6P_2W_2$ requires C 54.3 % H 3.9 %.

6.3.8. Thermal decarbonylation of the diacyl compounds (XXXIII), (XXXIV) and (XXXVI)

General procedure

The diacyl compound was dissolved in DME (5 ml) and an approximate 4-fold excess of tertiary phosphine added. The mixture was heated under reflux for 24 hours then allowed to cool and evaporated under reduced pressure. The ^{1}H NMR of the reaction mixture was recorded and the percentage conversion

of the starting material to a non-acyl phosphine-substituted product determined from the ratio of the C_5H_5 proton resources at ~ δ 5.00 and ~ δ 4.75 for starting material and product respectively. In each reaction, a resonance at ~ δ 5.32 was observed indicating the presence of some non-substituted μ(1,n)alkanediyl product. The results of these decarbonylation reactions are given in Table 6.11.

Table 6.11 Decarbonylation of (XXXIII) (XXXIV) and (XXXVI)

Compound	Percentage conversion to non-acyl product %
(XXXIII)	10
(XXXIV)	15
(XXXVI)	50

REFERENCES

1. W.A.Herrman, *Pure & Appl. Chem.*, 54 (1982) 65.
   W.A.Herrman, *Angew. Chem. Int. Ed. Engl.*, 21 (1982) 117.
2. a R.C.Brady and R.Pettit, *J. Am. Chem. Soc.*, 102 (1980) 6181.
   b C.Masters, *Adv. Organometal. Chem.*, 17 (1979) 61.
3. H.Sinn and W.Kaminsky, *Adv. Organometal. Chem.*, 18 (1980) 99.
4. G.A.Samorjai and S.M.Davis, *Platinum Metals Rev.*, 27 (1983) 54.
5. F.Garnier, P.Krausz and J-E. Dubois, *J. Organometal. Chem.*, 170 (1979) 195.
6. P.Pertici and G.Vitulli, *Tet. Lett.*, 21 (1979) 1897.
7. W. Kaminsky and H. Sinn, *Justus Liebigs Ann. Chem.*, (1975) 424.
8. H. Sinn and E. Kolk, *J. Organometal. Chem.*, 6 (1966) 373.
9. W.Kaminsky, J.Kopf, H.Sinn and H-J. Vollmer, *Angew. Chem. Int. Ed. Engl.*, 15 (1976) 629.
10. J.E.Ellis, *J. Organometal. Chem.*, 86 (1975) 1.
11. H.Sinn and G. Opperman, *Angew. Chem. Int. Ed. Eng.*, 5 (1966) 962
12. J.L.Atwood, G.K.Barker, J.Holton, W.E.Hunter, M.F.Lappert and R.Pearce, *J. Am. Chem. Soc.*, 99 (1977) 6645.
13. W.Beck and B. Olgemöller, *J. Organometal. Chem.*, 127 (1977) C45.
14. W.Beck and B. Olgemöller, *Chem. Ber.*, 114 (1981) 867.
15. F.A.Adedeji, J.A. Connor, H.A.Skinner, L.Galyer and G.Wilkinson, *J. Chem. Soc. Chem. Comm.*, (1967) 159.
16. H.C.Lewis Jr. and B.N.Storhoff, *J. Organometal. Chem.* 43 (1972) 1.
17. a J.W.Faller and A.S.Anderson, *J. Am. Chem. Soc.*, 91 (1969) 1550.
   b A.R.Manning, *J.Chem. Soc.*(A), (1967) 1984.
18. N.A.Bailey, P.L.Chell, A. Mukhopadhyay, H.E.Tabbron and M.J.Winter, *J. Chem. Soc. Comm.*, (1982) 251.

19. H.Adams, N.A.Bailey and M.J.Winter, *J. Chem. Soc. Dalton Trans.*, (1984) 273.

20. N.A.Bailey, P.L.Chell, C.P.Manuel, A. Mukhopadhyay, D.Rogers, H.E.Tabbron and M.J.Winter, *J. Chem. Soc. Dalton Trans.*, (1983) 2397.

21. R.B.King and M.B.Bisnette, *J. Organometal. Chem.*, 7 (1967) 311.

22. R.B.King and M.B.Bisnette, *J. Organometal. Chem.*, 2 (1964) 15.

23. W.Herrman and G.Kriechbaum, unpublished results quoted in W.A.Herrman, *Adv. Organometal. Chem.*, 20 (1982) 159.

24. J.R.Moss, *J. Organometal. Chem.*, 231 (1982) 229.

25. W.Geibel, G.Wilke, R.Goddard, C. Krüger and R. Mynott, *J.Organometal. Chem.*, 160 (1978) 139.

26. R.B. King, *J. Am. Chem. Soc.*, 85 (1963) 1922.

27. C.P.Casey, *J. Chem. Soc. Chem. Comm.*, (1970) 1220.

28. K. Raab, B. Olgemöller, K.Sclholer and W.Beck, *J. Organometal. Chem.* 241 (1981) 81.

29. R.B.King, *J. Am. Chem. Soc.*, 85 (1963) 531.

30. S.C.Kao, C.H. Thiel and R.Pettit, *Organometallics*, 2 (1983) 914.

31. L.Pope, P. Sommerville, M.Laing, K.J.Hindson and J.R.Moss, *J. Organometal. Chem.*, 112 (1976) 309.

32. J.J.Bennet, R.Mathieu, R.Poilblanc and J.A.Ibers, *J. Am. Chem. Soc.*, 101 (1979) 7487.

33. C.E.Sumner Jr., P.E.Riley, R.E.Davis and R.Pettit, *J. Am.Chem. Soc.*, 102 (1980) 1752.

34. M.L.H. Green and P.L.I. Nagy, *J.Organometal. Chem.*,1 (1963) 58.

35. J.W.Johnson and J.R.Moss, *Polyhedron*, in press.

36. M.Laing, J.R.Moss and J.W.Johnson, *J. Chem. Soc. Chem. Comm.*,(1977) 656.

37. R.C.Kerber, W.P. Giering, J. Bauch, P. Waterman and E-Hua Chou, *J. Organometal. Chem.*, 120 (1976) C31.

38. G.E.Jackson, J.R.Moss and L.G.Scott, *S. Afr. J. Chem.*, 36(2) (1982) 69.

39. P.A.Wegner and G.P.Sterling, *J.Organometal. Chem.*, 167 (1978) C31.

40. M.Cooke, N.J. Forrow and S.A.R. Knox *J.Organometal. Chem.*, 222 (1981) C21.

41. M.Cooke, N.J.Forrow and S.A.R.Knox, *J. Chem. Soc. Dalton Trans.*, (1983) 2435.

42. Y.C.Lin, J.C.Calabrese and S.S.Wreford, *J. Am. Chem. Soc.*, 105 (1983) 1679.

43. K.M.Motyl, J.R.Norton, C.K.Schauer and O.P.Anderson, *J.Am. Chem. Soc.*, 104 (1982) 7325.

44. M.R.Burke, J.Takats, F.W.Grevels and J.G.A.Reuvers, *J. Am. Chem. Soc.*, 105 (1983) 4092.

45. K.H.Theopold and R.G.Bergman, *J. Am. Chem. Soc.*, 102 (1980) 5694.

46. K.H.Theopold and R.G.Bergman, *J. Am. Chem. Soc.*, 103 (1981) 2489.

47. J.X.McDermott, J.F.White and G.M.Whitesides, *J. Am. Chem. Soc.*, 95 (1973) 4451.

48. K.H.Theopold and R.G.Bergman, *Organometallics*, 1 (1982) 1571.

49. N.E.Shore, C.Ilenda and R.G.Bergman, *J. Am. Chem. Soc.*, 98 (1976) 7436.

50. H.H.Hoehn, L.Prall, K.F.Watterson and G.Wilkinson, *J. Chem. Soc.*, (1961) 2738; B.L.Booth, R.N.Haszeldine and P.R.Mitchell, *J.Chem. Soc.* (A), (1969) 691.

51. B.L.Booth, R.N.Haszeldine and T.Inglis, *J. Chem. Soc. Dalton Trans.*, (1975) 1449.

52. M.J.Mays and G.Wilkinson, *Nature*, 203 (1964) 1167.

53. P.K.Monaghan and R.J.Puddephatt, *Inorg. Chim. Acta*, 76 (1983) L237.

54. P.Pertici and G.Vitulli, *Tet. Lett.*, 21 (1979) 1897.

55. G.W.Parshall and J.J.Mrowca, *Adv. Organometal. Chem.*, 7(1968) 157.

56. R.E.Dessy, R.L.Pohl and R.B.King, *J. Am. Chem. Soc.*, 88 (1966) 5121.

57. C.Botha and J.R.Moss, private communication of unpublished results (1982).

58. J.P.Bibler and A.Wojcicki,*J. Am. Chem. Soc.*, 88 (1966) 4862.

59. R.B.King, *J. Am. Chem. Soc.*, 85 (1963) 1918.

60. J.J.Alexander and A.Wojcicki, *Inorg. Chem.*, 12 (1973) 74.

61. K.Noack, U.Schaever and F.Calderazzo, *J.Organometal. Chem.*, 8 (1967) 517.

62. R.D.Closson, J.Kozikowski and T.H.Coffield, *J. Org. Chem.*, 22 (1957) 598.

63. J.B.Wilford and F.G.A.Stone, *Inorg. Chem.*, 4 (1965) 389.

64. F.Calderazzo, K.Noack and U.Schaever, *J.Organometal. Chem.*, 6 (1966) 265.

65. R.B.King, *J. Am. Chem. Soc.*, 90 (1968) 1417.

66. J.A.Stone, D.E.Laycock, M.Lin and M.C.Baird, *J. Chem. Soc. Dalton Trans.*, (1980) 2488.

67. D.H.Williams and I. Howe , "Principles of Organic Mass Spectrometry" McGraw-Hill, London (1972) pgs. 109-110 and 118-120.

68. V.F.Sizoi, YU.S.Nekrasar, YU.N.Sukharer, N.E.Kolobara, O.M.Khitrova, N.S.Obezyuk and A.B.Antonova, *J.Organometal. Chem.* 162 (1978) 71.

69. M.A.Haas and J.M.Wilson, *J. Chem. Soc.* (B), (1968) 104.

70. J.Müller, *Angew. Chem. Int. Ed. Engl.*, 11 (1972) 653.

71. J.Lewis, A.R.Manning, J.R.Miller and J.M.Wilson, *J.Chem. Soc.*(A), (1966) 1663.

72. M.I.Bruce, *Adv. Organometal Chem.*, 6 (1968) 2.

73. D.L.Reger and E.C.Culbertson, *J. Am. Chem. Soc.*, 98 (1976) 2789.

74. A.Cuccuru, P.Diversi, G.Ingrosso and A.Lucherini, *J.Organometal. Chem.*, 204 (1981) 123.

75. A.I.Kitaigarodsky, "Molecular Crystals and Molecules", Academic Press, New York and London, (1973), pgs. 48-62.

76 A.I.Kitaigarodsky, "Organic Chemical Crystallography", Consultant's Bureau, New York, (1966) pgs. 177-187.

77. R.N.Rogers and E.D.Morris Jr., *Anal. Chem.*, 38 (1966) 416.

78. M.Laing, *S. Afr. J. Sci.*, 71 (1975) 171.

79. G.Nassim, S.Sarig and E.Wellner, *Thermochim. Acta.*, 37(2) (1980) 131.

80. G.Ungar, *J. Phys. Chem.*, 87 (1983) 689.

81. E.Bielli, P.M.Gidney, R.D.Gillard and B.T.Heaton, *J. Chem. Soc. Dalton Trans.*, 2 (1974) 2133.

82. H.Mazurek, *Diss. Abstr. Int. B*, 41 (1980) 1764.

83. P.J.Clarke and H.J.Milledge, *Acta. Cryst.*, B31 (1975) 1554.

84. W.D.S.Motherwell, "EENY (Potential Energy Program)", Cambridge (1974) unpublished.

85. E.Giglio, *Nature*, 222 (1969) 339.

86. P.Braunstein, J.Dehand, M.Gross and P.Lemoine, *J. Thermal Anal.*, 8 (1975) 109.

87. R.B.King, "Organometallic synthesis Vol. I : Transition metal compounds", Academic Press, New York and London, (1965).

88. J.P.Bibler and A.Wojicki, *J. Am. Chem. Soc.*, 88 (1966) 4862.

89. S.R.Su and A.Wojcicki, *J. Organometal.Chem.*, 27 (1971) 231.

90. M.Green and D.J.Westlake, *J. Chem. Soc. (A)*, (1971) 367.

91. A. Wojcicki, *Adv. Organometal. Chem.*, 11 (1973) 87.

92. a M.P.Cooke, *J. Am. Chem. Soc.*, 92 (1970) 6080.

b J.P.Collman, S.R.Winter and D.R.Clark, *J. Am. Chem. Soc.*, 94 (1972) 1788.

c J.P.Collman, S.R.Winter and R.G.Komoto, *J. Am. Chem. Soc.*, 95 (1973) 249.

93. J.J.Alexander, *J. Am. Chem. Soc.*, 97 (1957) 1729.

94. M.D.Johnson, *Acc. Chem. Res.*, 11 (1978) 57.

95. W.N.Rogers and D.L.Miles, *Inorg. Chem.*, 20 (1981) 3521.

96. T.C.Flood and D.L.Miles, *J. Organometal Chem.*, 127 (1977) 33.

97. T.G.Attig, R.G.Teller, S-M.Wu, R.Bau and A.Wojcicki, *J. Am. Chem. Soc.*, 101 (1979) 619.

98. N.Deluca and A.Wojcicki, *J.Organometal. Chem.*, 193 (1980) 359.

99. D.Dong, D.A.Slack and M.C.Baird, *Inorg. Chem.*, 18 (1979) 188.

100. D.A.Slack and M.C.Baird, *J. Am. Chem. Soc.*, 98 (1976) 5539.

101. E.J.Kuhlmann and J.J.Alexander, *Coord. Chem. Rev.*, 33 (1980) 195.

102. K.W.Barnett and D.W.Slocum, *J. Organometal. Chem.*, 44 (1972) 1.

103. K.W.Barnett and P.M.Treichel, *Inorg. Chem.*, 6 (1967) 294.

104. A.R.Manning, *J. Chem. Soc.* (A), (1967) 1984.

105. K.W.Barnett, T.G.Pollman and T.W.Soloman, *J. Organometal. Chem.*, 36 (1972) C23.

106. K.W.Barnett, D.L.Beach, S.P.Gaydos and T.G.Pollman, *J. Organometal. Chem.*, 69 (1974) 121.

107. F.Calderazzo, *Angew. Chem. Int. Ed. Engl.*, 16 (1977) 299 and references therein.

108. R.Birdwhistell, P.Hackett and A.R.Manning, *J.Organometal. Chem.*, 157 (1978) 239.

109. J.A.Osborn, F.H.Jardine, J.F.Young and G.Wilkinson, *J.Chem. Soc.* (1966) 1711.

110. F.G.Mann and A.F.Wells, *J. Chem. Soc.*, (1938) 702.

111. P.W.Hall, R.J.Puddephatt, K.R.Seddon and C.F.H.Tipper, *J. Organometal. Chem.*, 81 (1974) 423.

112. T.S.Piper and G.Wilkinson, *J. Inorg. Nucl. Chem.*, 3 (1956) 104.

113. P.Hackett and A.R.Manning, *J. Chem. Soc. Dalton Trans.*, (1972) 7434.

114. C.J.Pouchert, "The Aldrich Library of Infra-red spectra", 2nd Ed., Aldrich Chemical Co., Winsconson, (1975).